

**Intergovernmental Oceanographic Commission  
technical series**

**67**

**Interdisciplinary Geoscience Research on the  
North East Atlantic Margin, Mediterranean  
Sea and Mid-Atlantic Ridge**

Preliminary results of investigations during the TTR-12 cruise of  
*RV Professor Logachev*  
June-August, 2002

Editors: N.H. Kenyon  
M.K. Ivanov  
A.M. Akhmetzhanov  
G.G. Akhmanov

**UNESCO 2003**

The designations employed and the presentation of the material in this publication do not imply the expression of any opinion whatever on the part of the Secretariats of UNESCO and IOC concerning the legal status of any country or territory, or its authorities, or concerning the delimitation of the frontiers of any country or territory.

**For bibliographic purposes, this document should be cited as follows:**

Interdisciplinary Geoscience Research on the North East Atlantic Margin, Mediterranean Sea and Mid-Atlantic Ridge  
*IOC Technical Series No. 67, UNESCO, 2003 (English)*

Printed in 2003  
by the United Nations Educational, Scientific  
and Cultural Organisation  
7, place de Fontenoy, 75352 Paris 07 SP

Printed in UNESCO's Workshops

©UNESCO 2003  
*Printed in France*

(SC-2004/WS/3)

## TABLE OF CONTENTS

<b>ABSTRACT</b> .....	iii
<b>ACKNOWLEDGEMENTS</b> .....	iv
<b>INTRODUCTION</b> .....	1
<b>METHODS</b> .....	5
<b>1. EASTERN FAEROE MARGIN AND ROCKALL TROUGH (LEG 1)</b> .....	9
<b>1.1. Eastern Faeroe margin</b> .....	9
1.1.1. Introduction and background .....	9
1.1.2. Seabed mound field to the northeast of Fugloy Ridge .....	10
1.1.2.1. Interpretation of seismic .....	10
1.1.2.2. Interpretations of OKEAN sidescan sonar and hull-mounted subbottom profiler .....	13
1.1.2.3. Interpretation of MAK sidescan and MAK subbottom profiler .....	15
1.1.2.4. Bottom sampling .....	16
1.1.2.5. Conclusions .....	19
1.1.3. GEM Raft area at the central Faeroese slope of the Faeroe-Shetland Channel .....	19
1.1.3.1. Interpretation of MAK sidescan sonar and subbottom profiler .....	19
1.1.3.2. Bottom sampling .....	22
1.1.3.3. Conclusions .....	24
<b>1.2. Rockall Trough seabed sampling</b> .....	25
<b>2. GULF OF CADIZ (LEG 2)</b> .....	28
<b>2.1. Introduction and objectives of Leg 2</b> .....	28
<b>2.2. Geological setting</b> .....	29
<b>2.3. South Portuguese mud volcano field</b> .....	30
2.3.1. Seismic data .....	30
2.3.2. Sidescan sonar data .....	36
2.3.3. Bottom sampling .....	36
<b>2.4. Sand lobe mapping</b> .....	41
<b>2.5. El Araiche mud volcano field</b> .....	43
2.5.1. Introduction .....	43
2.5.2. Sidescan sonar data .....	45
2.5.3. Bottom sampling .....	49
2.5.4. Main results .....	50
<b>3. ALBORAN BASIN (LEG 3)</b> .....	51
<b>3.1. Introduction and objectives of Leg 3</b> .....	51
<b>3.2. Mud volcanoes in the Alboran Basin: main results</b> .....	54
3.2.1. Mud volcanoes in the northern West Alboran Basin .....	55
3.2.1.1. Airgun seismic and hull mounted profiles .....	55
3.2.1.2. Sidescan sonar data .....	58
3.2.2. Mud volcanoes in the southern West Alboran Basin .....	59
3.2.2.1. Airgun seismic and hull mounted profiles.....	59

3.2.2.2. Sidescan sonar data .....	61
<b>3.3. The Almeria margin: main results .....</b>	<b>62</b>
3.3.1. Seismic profiling and interpretation .....	62
3.3.2. Sidescan sonar data .....	65
<b>3.4. Bottom sampling .....</b>	<b>68</b>
3.4.1. Introduction .....	68
3.4.2. Location 1 .....	68
3.4.3. Location 2 .....	69
3.4.4. Location 3 .....	70
3.4.5. Pelagic cores .....	70
<b>4. TYRRHENIAN SEA (LEG 4) .....</b>	<b>72</b>
<b>4.1. Marsili Seamount .....</b>	<b>72</b>
4.1.1. Introduction and geological setting .....	72
4.1.2. Side scan sonar (MAK 1M) .....	74
4.1.3. TV seabed inspection .....	80
4.1.4. Bottom sampling .....	80
<b>4.2. Palinuro Seamount .....</b>	<b>81</b>
4.2.1. Introduction and geological setting .....	81
4.2.2. MAK sidescan sonar data .....	82
4.2.3. TV seabed inspection .....	82
4.2.4. Bottom sampling .....	83
<b>4.3. Vavilov Seamount .....</b>	<b>84</b>
4.3.1. Introduction and geological setting .....	84
4.3.2. Seismic data .....	85
4.3.3. OKEAN long range sidescan sonar mosaic .....	90
4.3.4. MAK sidescan sonar data .....	90
<b>5. AZORES MARGIN (LEG 5) .....</b>	<b>91</b>
<b>5.1. Aims and objectives .....</b>	<b>91</b>
<b>5.2. Seismic data .....</b>	<b>93</b>
5.2.1. Seismic data interpretation .....	93
5.2.2. Structure of the study area .....	97
<b>5.3. Coring of the achipelagic apron south of the Azores Plateau .....</b>	<b>100</b>
<b>5.4. Deep-towed sidescan sonar and TV survey data .....</b>	<b>102</b>
5.4.1. Eastern part of Lucky Strike Segment .....	102
5.4.2. Southern part of the Lucky Strike Segment. Menez Hom high .....	103
<b>5.5. Biology .....</b>	<b>105</b>
<b>REFERENCES .....</b>	<b>109</b>

**ANNEX I: CORE LOGS**

**ANNEX II. LIST OF TTR-RELATED REPORTS**

## ABSTRACT

The scientific programme of the 12th Training-through-Research Cruise included several interdisciplinary studies of geological processes on continental margins of Europe and North Africa. Research themes included:

1. Focused fluid escape and related mud volcanism, gas hydrates, carbonate and sulphide structures, chemosynthetic communities (Gulf of Cadiz, Western Alboran Sea)
2. Neotectonic and down-slope processes on continental margins (Faeroe-Shetland Channel, Rockall Trough, Alboran Sea, Tyrrhenian Sea)
3. Modern deep-water sand lobes (Gulf of Cadiz, Eastern Alboran Sea);
4. Underwater volcanism, hydrothermal activity and related mineralization (Tyrrhenian Sea, Azores margin);
5. Geosphere-Biosphere coupling processes manifested in specific faunal communities, chemohierms growing and deep-water coral 'reefs' (Rockall Trough, Gulf of Cadiz).

**Eastern flank of the Fugloy Ridge at the northern entrance of the Faeroe-Shetland Channel.** Seamounts of unknown origin were mapped on a basinward continuation of the Fugloy Ridge (to the east of the Faeroe Islands) using seismic and two types of sidescan sonars and samples were collected. Geophysical records indicate the presence of at least two separate groups of diapirs outcropping at the sea floor. Bottom sampling data suggest that diapirs mainly consist of semi-lithified diatom ooze of Miocene age with some admixture of glauconite and foraminifera. No evidence of coral settlements or recent fluid venting is reported.

**GEM Raft at the central Faeroese slope of the Faeroe-Shetland Channel.** A submarine slide called GEM Raft was investigated in detail in order to gain information on its most recent episode of instability. The upper part of the raft is found to be the smallest and possibly the youngest. There is no indication that sediments cover the latest slump deposits and this is confirmed by bottom sampling. Buried slump deposits indicate that this upper part was previously prone to instability. The lower part of the raft shows a variety of down-slope processes, for example detached blocks, pressure ridges, slumps and debris flows. This lower part seems to be covered by a more recent sedimentary layer, and there is no clear indication that bottom processes are still active.

**Rockall Trough.** Intensive bottom sampling was performed in the Rockall Trough area. Sampling was mainly related to environmental studies, but also to calibrate acoustic facies for interpretation of multibeam reflectivity data.

**Gulf of Cadiz.** In the Gulf of Cadiz, a broad range of investigations were carried out, resulting in the discovery of a new field of carbonate chimneys in the northern part of the Gulf. In the central part of the Gulf, two new, active mud volcanoes (named Captain Arutjunov and Tangier) were also studied in detail and heavy hydrocarbon gases and gas hydrates were sampled. On the Moroccan margin, a detailed study and sampling were performed on a mud volcanic field, which had been discovered earlier in 2002 by the Gent University (Belgium) group during the R/V Belgica cruise and was mapped by seismic and multibeam survey. The investigations also included mapping and sampling of deep-water coral settlements in different locations, the discovery of exotic blocks of sandstones, igneous and metamorphic rocks on tops of some shallow-water mud volcanoes, and the mapping of the Gil Eanes deep-water sandy system using the 100 kHz sidescan sonar and deep-towed 5 kHz profiler.

**Western Alboran Sea.** Four new mud volcanoes and large fields of pockmarks were found in the Western Alboran Sea. Two mud volcanoes, named Kalinin and Perejil, were located in the Spanish part of the basin. Both structures are covered with relatively thick hemipelagic sediments and they appear dormant at present. Samples of hydrocarbon gas and clasts of ancient rocks in mud volcanic breccia were collected and should be of value in defining the source formation of these two volcanoes.

**Eastern Alboran Sea.** Investigations in the Eastern Alboran basin focused mostly on the study of basinward continuation of the Almeria turbidite system. Its upper part was mapped ten years ago with the deep-towed sidescan sonar MAK-1M during the TTR-2 cruise. Mapping of the distal part of the system was carried out with the same instrument and revealed a very complex structure consisting of overlapping channels and sedimentary lobes.

**Tyrrhenian Sea.** In the Tyrrhenian Sea, the morphology and volcano-tectonic processes at the three biggest submarine volcanos, Marsili, Palinuro and Vavilov, were studied. Mapping of the northern side of the Marsili volcano with the deep-towed sidescan sonar yielded significant information regarding its morphology and recent activity. Many small-scale features corresponding to recent activity of the volcano are seen on acoustic records. Several areas of low-temperature hydrothermal activities are observed at the summits of the Marsili and Palinuro volcanoes using an underwater TV system.

**Sedimentary basin to the south of the Azores plateau and the Lucky Strike field.** A long seismic line was performed with two 3-litre airguns across a young sedimentary basin, which is located to the south of the Azores plateau. Seismic records demonstrate a surprisingly thick (more than 1 km) sedimentary cover. TV observations and sampling of different types of igneous rocks in the Lucky Strike segment were also carried out.

## ACKNOWLEDGEMENTS

The twelfth Training-through-Research Cruise has received financial support from a variety of sources among which were: the Intergovernmental Oceanographic Commission (IOC) of UNESCO, FOIB consortium of oil companies, Geological Survey of Denmark and Greenland, Irish Geological Survey, Instituto Geologico e Mineiro (Portugal), University of Aveiro (Portugal), Renard Center of Marine Geology of the University of Ghent (Belgium), University of Granada (Spain), University of Barcelona (Spain), Istituto di Geologia Marina of CNR (Italy), the Russian Ministry of Science and Technological Policy, the Polar Marine Geological Research Expedition (PMGRE) of the Russian Ministry of Natural Resources and Moscow State University (Russia). Logistic support was provided by the NIOZ (the Netherlands).

A number of people from different organizations supported the Training-through-Research Programme in 2002 and were involved in the cruise preparation. The editors would like to express their gratitude for the contributions made by Prof. I. F. Glumov (Ministry of Natural Resources of the Russian Federation), Dr. A. Suzyumov (UNESCO), Dr. P. Bernal (Executive Secretary, IOC), and Mr. V. Zhivago (Ministry of Science and Technological Policy of the Russian Federation).

Credits also should be given to Dr. Maarten van Arkel of the NIOZ and Prof. Dr. B. A. Sokolov (Moscow State University) for their continuous administrative and logistic support.

Thanks are due to the administration and staff of the PMGRE (St. Petersburg) for their co-operation and assistance with the cruise organization. Captain B. Dobriakov and the skilful crew of the R/V *Professor Logachev* are thanked for the successful carrying out of the operations at sea.

Staff and students of the UNESCO-MSU Marine Geosciences Centre provided valuable support in processing the acoustic data and preparation of illustrations.

## INTRODUCTION

The TTR-12 cruise was carried out from 9 June to 31 August onboard the R/V *Professor Logachev*, owned and operated by Polar Marine Geosurvey Expedition (PMGE), departing from St. Petersburg (Russia) and terminating in Ponta Delgada (Azores, Portugal). The cruise was sub-divided into five legs separated by port calls, where partial exchange of the scientific party was made: in Foynes (Ireland) on 2-3 July, in Porto (Portugal) on 6-7 July, in Cadiz (Spain) on 18 July, in Cartagena (Spain) on 28 July and in Civitavecchia (Italy) on 12 August.

An international team of 77 scientists, postgraduate and undergraduate students (in addition to a group of Russian technicians who had been working with the Logachev equipment), from 13 countries (Bangladesh, Belgium, Brazil, Denmark, Georgia, Italy, Ireland, Morocco, Portugal, Russia, Spain, Sweden and United Kingdom) participated in the cruise.

The objectives of the cruise were to conduct interdisciplinary investigations of a broad range of geological processes including focused fluid escape, neotectonics, deep-water clastic sedimentation, underwater volcanism and geosphere-biosphere coupling on continental margins of Europe and North Africa.

Another important element of the programme was to provide training-on-the-job for students specialising in marine geoscience research.

Detailed sidescan sonar investigations and gravity coring were planned at selected sites on the Faeroe margin in order to study slope instability processes and to detect possible mud volcanism.

The underwater TV survey and extensive seabed sampling programme were designed to be conducted in the Rockall Trough in order to characterize various sedimentary environments and calibrate existing acoustic datasets.

Further detailed investigations of known mud volcanoes, fluid escape features, gas hydrate accumulations and other related

phenomena were to be conducted, together with searching for as yet unknown structures of similar origin in the Gulf of Cadiz. Cold water reefs discovered in the area during the TTR-9 cruise on tops of several diapirs were a target for a detailed study. Another study was aimed at a complex sand-rich clastic depositional system developing in the area.

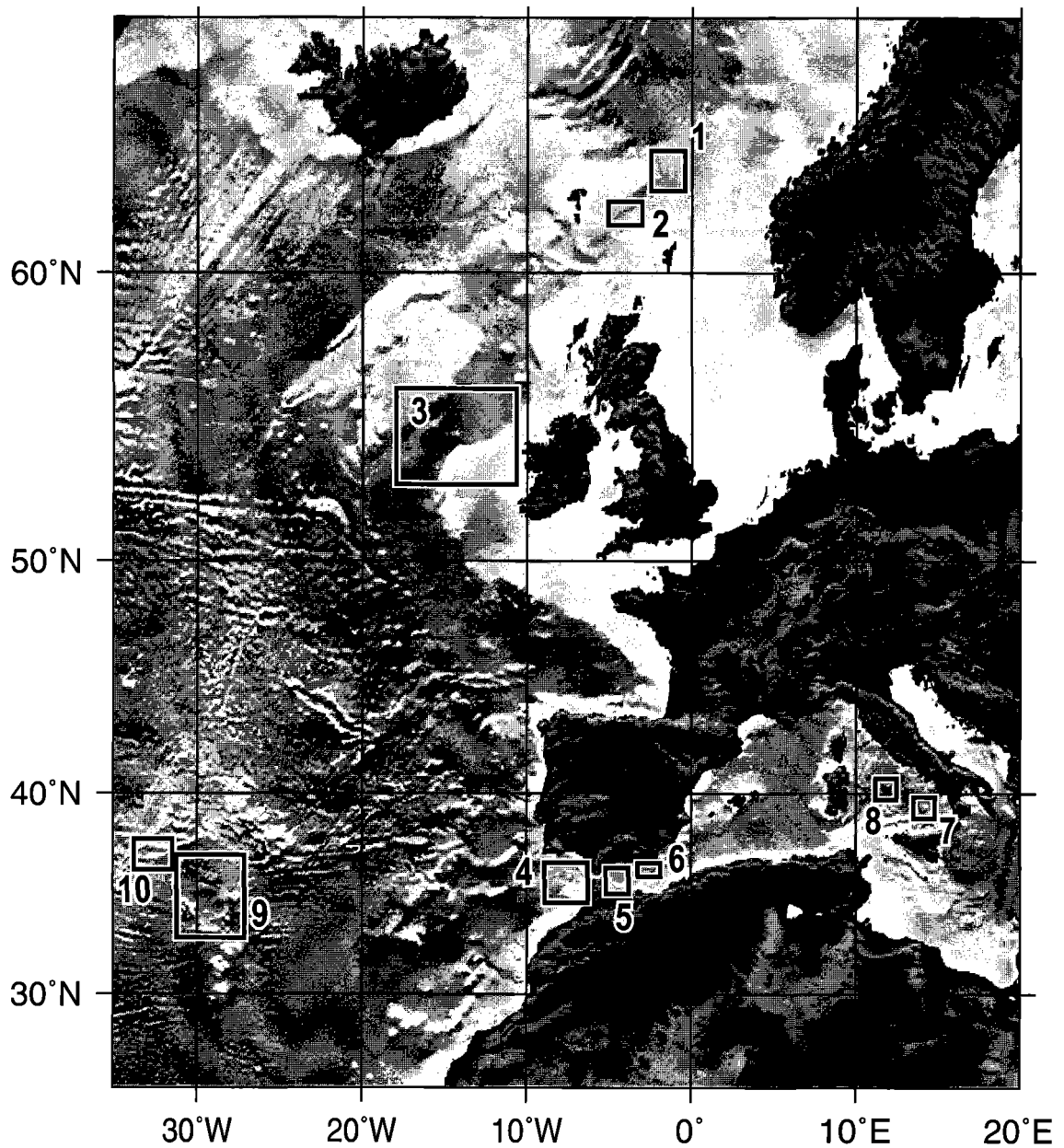
The survey in the Western Alboran Sea intended to continue previous studies of a mud diapir province. The tectonic framework of the area as well as the volcanic basement were also to be investigated.

The depositional area lying beyond the mouth of the complex channel system developing on the Almeria margin in the Eastern Alboran Sea was to be surveyed by high resolution seismic and sidescan sonar.

Another task in this area was to continue studies of pelagic sedimentation and, in particular, formation and distribution of inferred sapropel layers in the Southern Balearic Basin.

The basic objectives of the planned study in the Tyrrhenian Sea were to acquire detailed sidescan and sampling data from the major volcanoes in order to identify areas affected by recent volcanic activity hazards. This would help in planning the study of the related hazards with further high-resolution investigations. The use of the deep-towed MAK-1M and TV-controlled grab systems offer state-of-the-art data and the possibility of fulfilling these objectives.

Work on the Azores margin consisted of several studies including a seismic survey across a young sedimentary basin, located to the south of the Azores plateau, TV observations and sampling of different types of igneous rocks in the Lucky Strike segment, and bottom sampling to the north and to the south of the Azores front in order to understand the paleoceanography and paleoproductivity of the area.



**1, 2 - Faeroe margin; 3 - Rockall Trough; 4 - Gulf of Cadiz; 5, 6 - Alboran Sea;  
7, 8 - Marsili and Vavilov Basins (Tyrrhenian Sea); 9, 10 - Azores margin**

*TTR-12 cruise location map*



**LIST OF PARTICIPANTS**

TTR-12 Cruise  
9 June - 31 August 2002  
R/V *Professor Logachev*

**BANGLADESH**

Asrarur Rahaman Talukder

**BELGIUM**

Pieter Van Rensbergen  
Kasper Moureaux  
Davy Depreiter

Hendrik Gheerardun

**BRAZIL**

Crisogono Vasconcelos

**DENMARK**

Tove Nielsen (*co-chief scientist, Leg 1*)

Mette Kruse

Henrik Sulsbruck Moeller

**GEORGIA**

Nodar Usupashvili

**ITALY**

Michael Marani (*co-chief scientist, Leg 4*)

Adriano Mazzini  
Fabiano Gamberi  
Daniela Penitenti  
Alessandro Rivalta  
Alessandro Bonazzi  
Giulia Amadori  
Nico Martinelli  
Chiara Consolaro

**IRELAND**

Thomas McKenzie Furey

**MOROCCO**

Benyounes Abdellaoui  
Merouane Rachidi

**PORTUGAL**

Luis Menezes Pinheiro (*co-chief scientist,  
Leg 2*)

Jose Hipolito Monteiro (*co-chief scientist,  
Leg 5*)

Marina Ribeiro da Cunha  
Luis Serrano Pinto

Mary Torres

Ines Lampreia

Carlos Fillpe Moura

Sergey Bouriak

Celia Ribeiro

Jose Vicente

Pedro Ferreira

Filipa Marques

Silvia Nave

Cristina Roque

Nelson Ricardo Peralta

Maria do Amaral

Tiago Alves

**RUSSIA**

## Technical support staff:

Mikhail Maslov (*chief staff scientist*)

Alexander Shagin

Alexander Machulin

Eugene Samsonov

Nikolay Volkov

Gennady Antipov

Roman Safronov

Sergey Zheleznyak

Alexander Kyrilovich

Dmitry Gagarin

Irina Antipova

Maxim Kuryshkin

Victor Sheremet

Alexander Ayupov

Anatoly Chudinov

Sergey Panteleev

Alexander Plakhotnik

Sergey Lyubimov

Konstantin Plakhotik

Vladislav Malin

Alexey Ivanov

## Researchers and students:

Mikhail Ivanov (*co-chief scientist*)

Pasha Shashkin

Sergey Agibalov

Mikhail Osipenko  
Alexandra Kostinenkova  
Anna Volkonskaya  
Igor Kuvaev  
Vladimir Tarasov  
Igor Uvarov  
Ekaterina Spungina  
Grigory Akhmanov  
Igor Fedorov  
Inna Mardanyan  
Vladislav Torlov  
Alexandr Samoilov  
Eugene Sarantsev  
Elena Kozlova  
Valentina Blinova  
Elena Poludetkina  
Olga Barvalina  
Eugene Bileva  
Alexey Sadekov

**SPAIN**

Menchu Comas (*co-chief scientist, Leg 3*)  
Ferran Estrada Liacer  
Ricardo Leon-Buendia  
Maria Jose Jurado Rodriguez  
Marta Molinos Solsona  
Fermin Fernandez Ibauez  
Francisca Martinez-Ruiz  
Juan-Ignacio Soto  
Francisco J. Rodriguez-Tovar  
Francisco J. Jimenez Espejo  
Guillermo Marro  
Manuel-J. Roman-Alpiste

**SWEDEN**

Jenny Levander  
Nina Tuomikoski

**UNITED KINGDOM**

Neil Kenyon (*co-chief scientist, Leg 2*)  
Andrey Akhmetzhanov

## METHODS

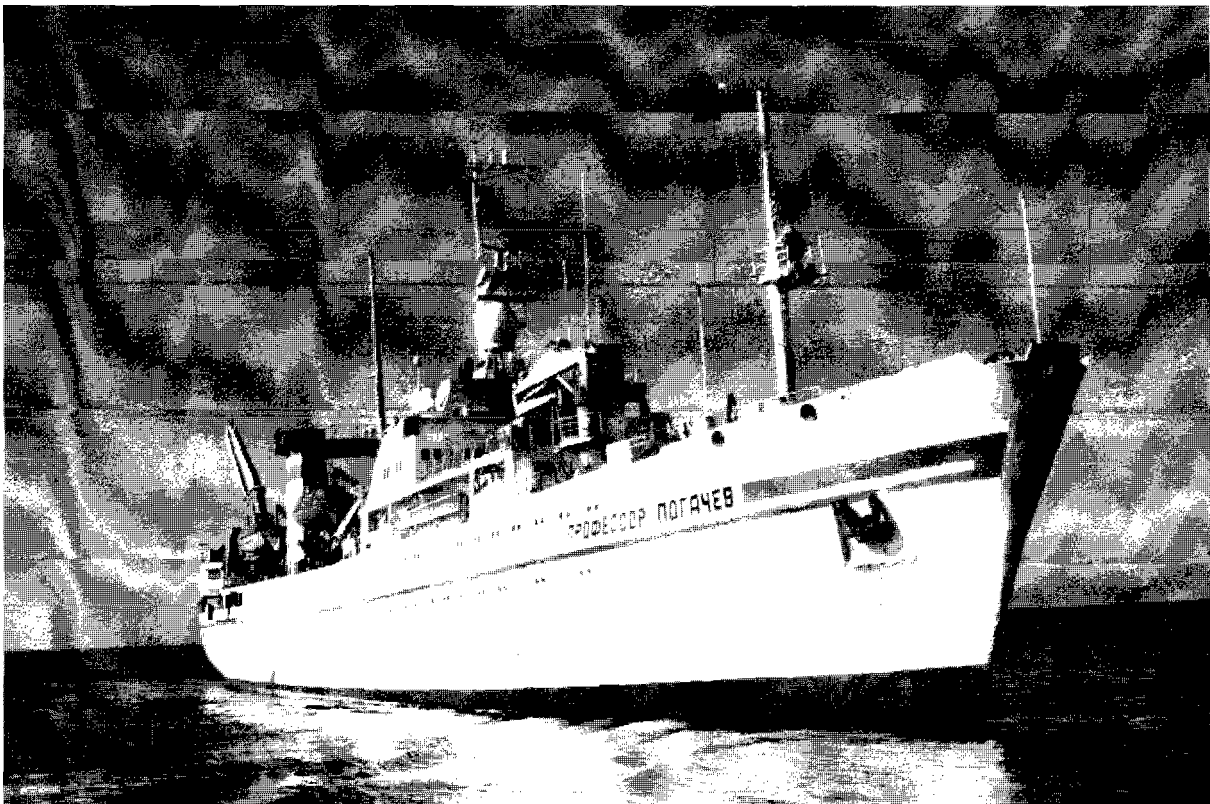
The R/V *Professor Logachev* is a Russian marine geology research and survey vessel equipped with seismic and seabed sampling equipment. She is operated by the State Enterprise "Polar Marine Geosurvey Expedition" St. Petersburg. The vessel has: a draught of 6.66 m, length of 104.5 m, width of 16 m, net tonnage of 1351 ton, displacement of 5700 ton and is powered by two 3500 hp diesel engines.

### *Navigation*

Positioning during the TTR-12 cruise was acquired using an Ashtech GG24 GPS + GLONASS receiver. The use of both GPS and GLONASS satellite configurations allows for greater accuracy than is available from conventional GPS alone, with up to 60% greater satellite availability. Positions are calculated in real-time code differential mode with 5 measurements per second and an accuracy of +/- 35 cm (75 cm at 95% confidence limits)

with optimal satellite configuration. Realistic positioning accuracy under normal satellite configuration for European waters is assumed as ca. 5 m. Positioning when the vessel is moving also utilizes Doppler velocity determinations from the differential code signal to generate a vessel speed accuracy of 0.04 knots (0.1 at 95% confidence limits) with optimum satellite configuration.

The GPS+GLONASS receiver is located centrally on the vessel with accurate levelling to sampling and equipment deployment positions on the vessel allowing precise back navigation. Seabed sampling positions with the gravity corer is normally 5% of the accuracy of the vessel position due to their rapid deployment. MAK1-M sidescan sonar and deep-towed video system are all fitted with a pinger allowing precise navigation between the vessel and sub-sea surface position. This is necessary as deep-towed equipment is subject to greater spatial differences with respect to the vessel. This underwater



*R/V Professor Logachev*

navigation is based on the Sigma-1001 hydroacoustic system. Four stationary aerials, spaced 14 m apart, are hull mounted and receive acoustic signals from pingers attached to deployed equipment in short-base mode operating between 7-15 kHz. The signal emitted by the sub-surface pinger is tracked on board and accurate x,y positioning of the device relative to the vessel is computed taking into account vessel roll, trim and ship's speed. Error positioning of this method usually does not exceed 1-2% of water depth.

#### *Seismic profiling*

The seismic source usually consisted of one 3 litre airgun, at a pressure of 120 bar (12 MPa). The airguns were towed at a depth of approximately 2-2.5 meters and were fired every 10 seconds (i.e. approximately every 30 meters). The streamer consisted of one active section, 30 meters long, with 50 hydrophones, towed at a depth of approximately 2.5-3 meters. The offset between the seismic source and the centre of the live hydrophone array was 135 meters.

The data was acquired digitally using the MSU developed software and preliminarily processed with the RadExPro software, which was provided to the UNESCO MSU Centre for Marine Geosciences by GSD Productions, Moscow. The signals were low-pass filtered analogically to 250 Hz in the acquisition stage. The sample interval was 1 ms and the record length 3 seconds.

The preliminary on board processing was carried out using the RadExPro software. The basic processing sequence consisted of definition of the acquisition geometry, static shifts correction, spiking deconvolution, amplitude recovery by spherical divergence correction and Butterworth bandpass filtering (20-60-180-240 Hz).

#### *Hull-mounted acoustic profiler*

A hull-mounted 5.1 kHz profiler was routinely used during most of the operations, with a continuous paper output and a selective recording of the digital data.

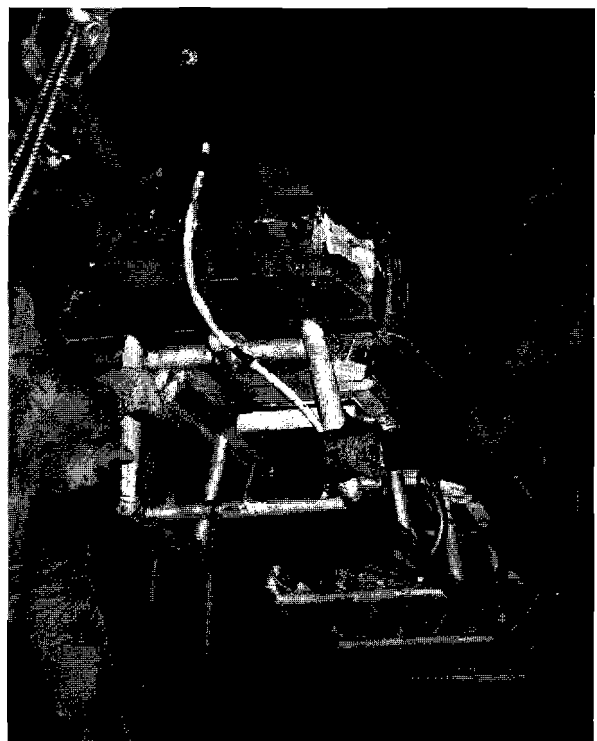
### *Sidescan sonar systems*

#### O K E A N

The OKEAN is a long-range sidescan sonar operating at a frequency of 9.5 kHz, which, with its up to 15 km swath range and 6 knots towing speed, is well suited for reconnaissance surveying of large deep-sea areas. The OKEAN vehicle is towed behind the ship at about 40-80 m below the sea surface. Depending on the waterdepth and resolution required the swath could be set to 7 or 15 km.

#### M A K - 1 M

The MAK-1M deep-towed hydroacoustic system contains a high-resolution sidescan sonar operated at frequencies of 30 and 100 kHz, with a total swath range of up to 2 km (1 km per side) and a subbottom profiler, operated at a frequency of 5 kHz. The sonar has a variable resolution of about 7 to 1 m across track (maximum range to centre) and along track (center to maximum range). During TTR-12, the fish was towed at a nearly constant altitude of about 100-150 m above



*Deployment of MAK-1M sidescan sonar fish.*

the seafloor at a speed of 1.5-2 knots for 30 kHz surveys and about 50 m above seafloor for 100 kHz ones. The positioning of the tow-fish was archived with a short-based underwater navigation system.

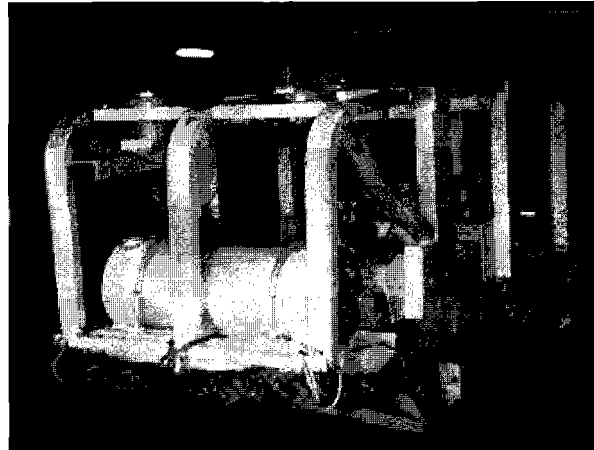
The data from the tow-fish was transmitted on board through a cable, recorded digitally, and stored in Seg-Y format, with a trace length of 4096 2-byte integer samples per side. Time-variant gain was applied to the data while recording, to compensate the recorded amplitudes for the irregularity of the directional pattern of the transducers as well as for the spherical divergence of the sonic pulse.

Onboard processing of the collected data included slant-range-to-ground-range (SLT) correction of the sonographs, geometrical correction of the profiles for recovery of the real seafloor topography, and smoothing average filtering of both types of records. Individual lines were geometrically corrected for the towing speed of the fish, converted into a standard bitmap image format. Some image processing routines, such as histogram equalization and curve adjustment, which are aimed at improving the dynamic range of the imagery were also applied before printing out. Geographic registration of the acquired images was also done onboard.

#### *Underwater photo and television system*

The television system operating onboard cruise TTR-12 is a deep towed system designed for underwater video surveys of the seabed at depths of up to 6000 m. The TV system consists of the onboard and underwater units. The onboard part comprises the control desk with video amplifier. The power for the underwater system is supplied through a special cable. The underwater equipment comprises the frame-bearer with light unit, the high-pressure housing containing a "Canon M1" digital camera and the power supply unit.

The TV system is directly controlled from onboard by the winch operator controlling visually the distance from the camera to the seafloor. There is a rope with a weight



*Underwater photo and television system*

attached to the frame which is usually towed on the seafloor and used to control the camera-seafloor distance. The rope is 1.5 m long. On/off switching of lights and video camera is done by the operator in the laboratory. The non-stop underwater record on the digital camera lasts for 2 hours in the "LP" mode. Onboard video-TV keeps a continuous record during the whole survey, which allows for up to 6 hours recording.

#### *Sampling Tools*

##### Gravity corer

Coring was performed using a 6 m long c. 1500 kg gravity corer with an internal diameter of 14.7 cm.

One half of the opened core was described on deck paying particular attention to changes in lithology, colour and sedimentary structures. All colours relate to Munsell Colour Charts. The other half was measured for changes in magnetic susceptibility using a Bartington Instruments Magnetic Susceptibility meter with a MS2E1 probe. Magnetic susceptibility reflects the ease with which a material can be magnetised. This property is most strongly influenced by grain-size, heavy mineral content and is inversely related to carbonate content and diagenetic ferric mineral reduction.

Samples were also taken for coccolith and micropalaeontological assays from smear slides. This was done to generate a preliminary chronostratigraphy for the cores.

### Box Corer

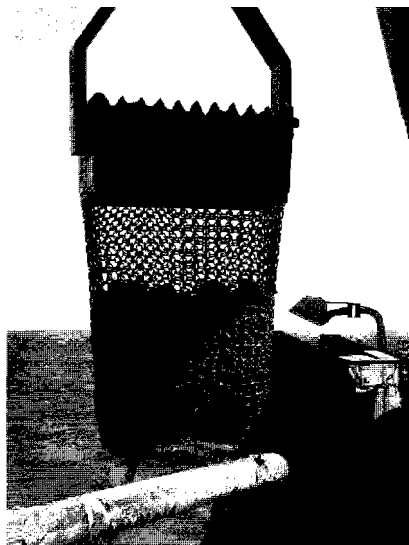
Box cores were taken using a Reineck box-corer with a 50 x 50 x 50 cm box capable of retrieving 185 kg of undisturbed seabed surface sample. Lowering and retrieving operations are conducted using a hydraulic A-shaped frame with a lifting capacity of 2 ton.



*Box corer*

### Dredge

The dredge comprises a 1 m<sup>2</sup>, circular steel gate with chain mesh bag trailing behind and a 0.5 ton weight 3 m in front of the gate. The mesh bag also has a rope bag

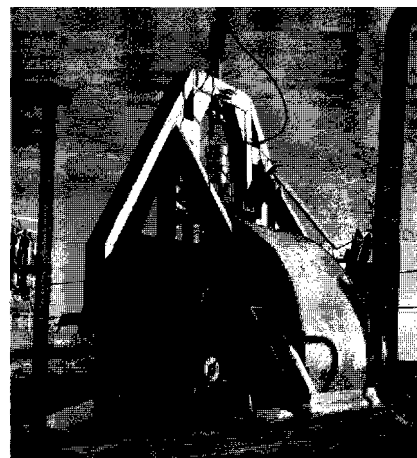


*Dredge*

inside and the mesh size is ~5 cm. The dredge was deployed ~250 m in front of the identified target site and the ship moved at 0.5 kts between 500 and 1500 m ensuring the dredge was pulled up-slope. On some sites, the bottom was monitored with a 3.5 kHz hull-mounted single-beam echosounder. At all times, the ship's velocity and position were monitored using GPS. Tension on the trawl-wire was monitored in the winch cab by both ink-line paper roll and with a tension meter. "Bites" of up to 10 tonnes on the trawl wire were recorded in this way.

### TV-guided grab

DG-1 grab system was used during the TTR-12 cruise. The 1500 kg system is able to sample dense clayey and sandy sediments as well as deep water basalts and sulphide ores. DG-1 can be used at depths up to 6000 m and closes by the difference in hydrostatic pressure. The maximum sample volume for soft sediment is 0.4 m<sup>3</sup>. The triggering mechanism is set off when the seabed is touched. The grab is positioned with the short base SIGMA 1000 underwater navigation system. The grab is equipped with a build-in camcorder which uses 90 min cassettes and records in Hi-Fi Video8 format. Video signal is also transmitted on board to enable control for the grab operation as well as back-up recording. The lights are powered by a rechargeable battery, enabling 1 hour of continuous operation. A second battery kept on board was used to perform consecutive dives.



*TV-guided grab*

# 1. EASTERN FAEROE MARGIN AND ROCKALL TROUGH (LEG 1)

## 1.1. Eastern Faeroe margin

### 1.1.1. Introduction and background

T. NIELSEN AND M. IVANOV

Over the last ten years increasing exploration for oil and gas has taken place within the Faroese economic zone. This has resulted in a greater need for mapping and understanding the processes that are shaping the seabed around the Faeroe Islands. Since 1997, TTR have contributed to these studies (TTR-7, TTR-8 and TTR-9) by detailed investigations of slope instability and bottom current activity. This has to a great extent been sponsored by GEM, a consortium of oil companies active in the region. Also this year the

successor of GEM, FOIB, has contributed to seabed studies in the Faeroe area (Fig. 1).

One of the objectives of this year's study was to investigate some mound features located at the eastern flank of the Fugloy Ridge at the northern entrance of the Faeroe-Shetland Channel. These have previously been reported as possible coral mounds based on conventional 2D seismics. Newly shot high-resolution seismics acquired by BGS and NIOZ have, however, revealed that the mounds are more likely mud-diapirs, an interpretation supported by TOBI sidescan recently acquired by SOC. The aim was to provide further information on these mud diapirs to better understand their formation.

The second objective was to investigate a minor slide, termed the GEM Raft, located at the central Faroese slope of the Faeroe-Shetland Channel. This raft was first observed on a TOBI sidescan record a few years ago, but has never been confirmed by any other type of investigation. The aim was

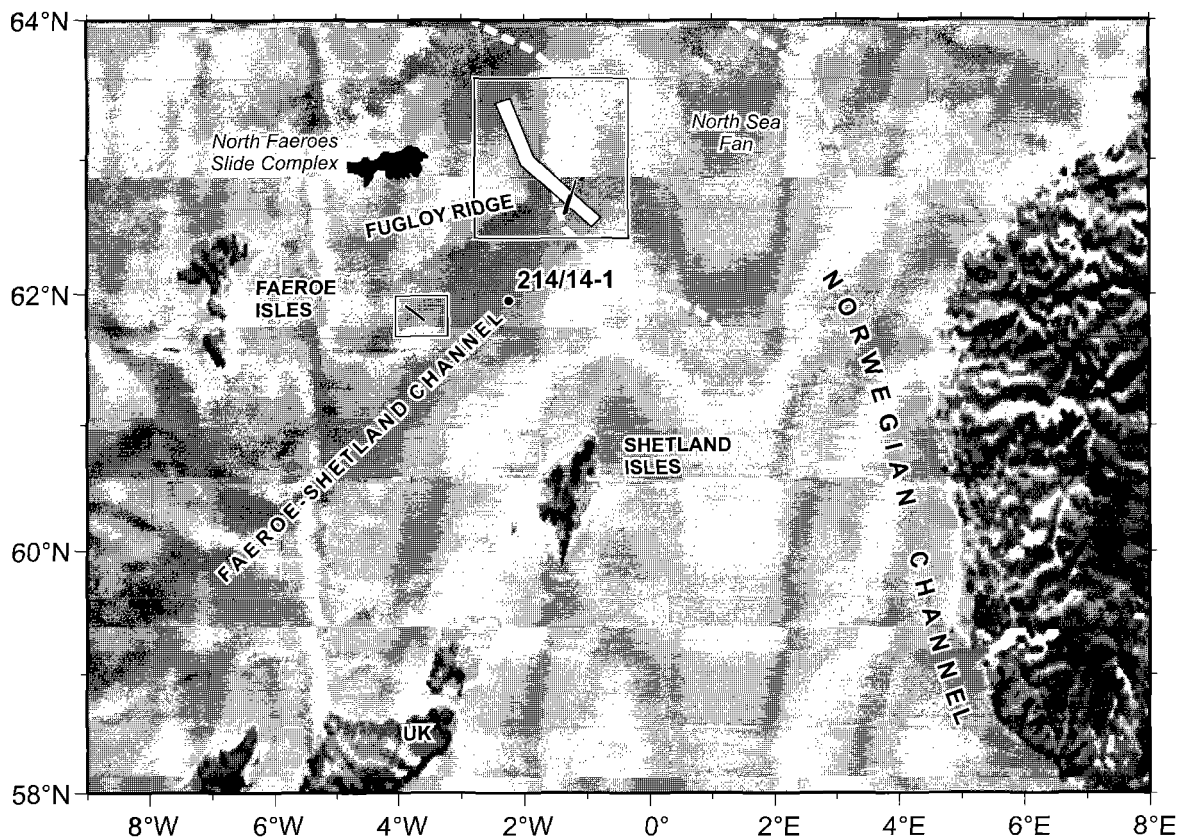


Figure. 1. Overview map of the Faeroe-Shetland Channel region showing the areas studied during Leg 1. Outlines of the North Sea Fan and location of well 214/14-1 are also shown.

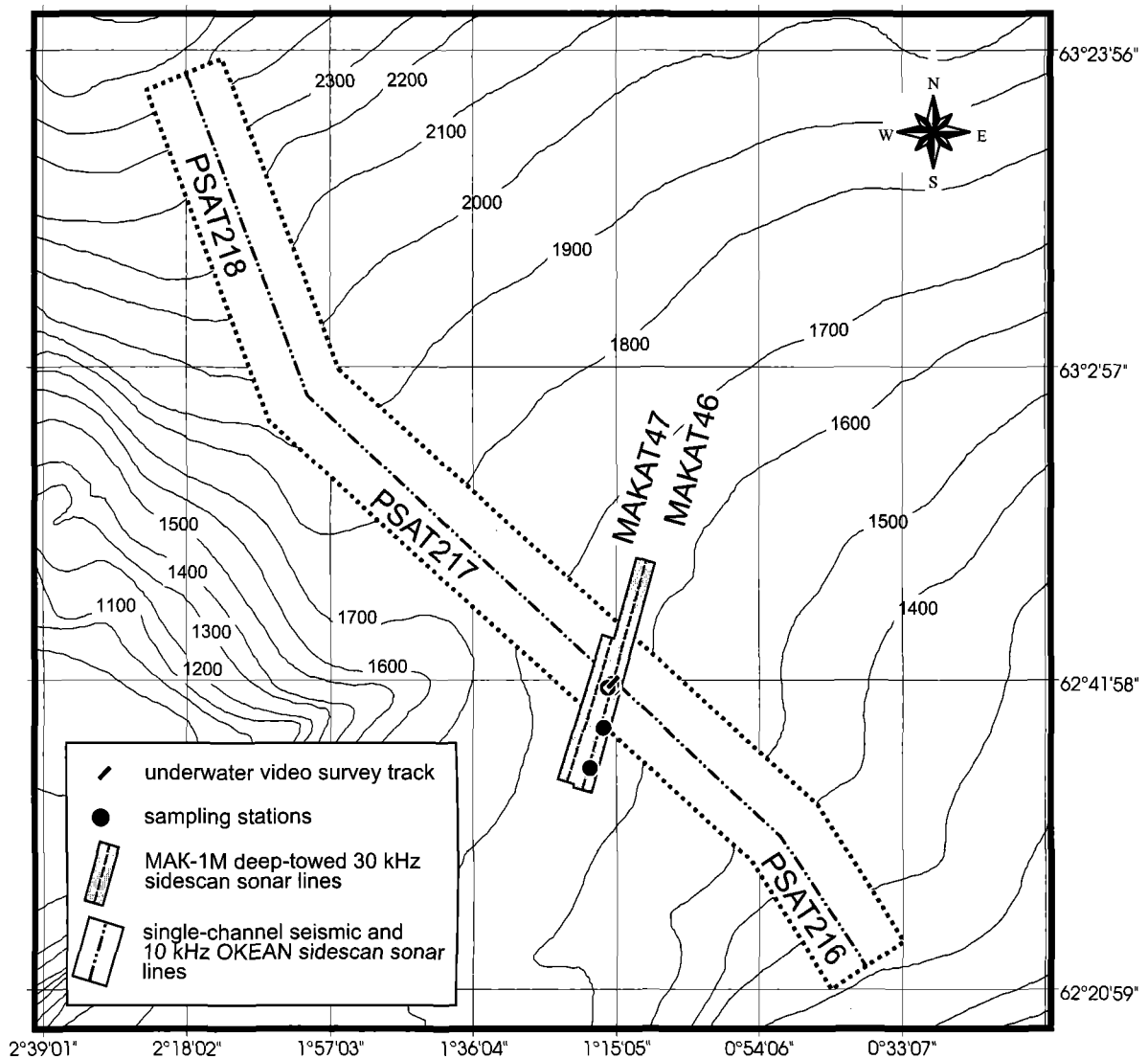


Figure 2. Location map of the eastern margin of the Faeroe platform and of the Faeroe Shetland Channel (Area 1). Depth in m.

thus to confirm the existent of the GEM Raft and to provide information on the last episode of instability.

To meet the objectives a range of acoustic and sampling techniques were used, i.e. seismic, OKEAN long-range sidescan sonar, MAK deep-towed sidescan sonar, gravity core, box core and video inspection.

### 1.1.2. Seabed mound field to the northeast of Fugloy Ridge

#### 1.1.2.1. Interpretation of seismic

M. KRUSE, T. NIELSEN AND A. VOLKONSKAYA

The purpose of the seismic study was to

get subbottom information of Study Area 1, where a cluster of mounds had been observed on the sea floor.

A seismic profile was conducted from southeast to northwest beginning in the Faeroe-Shetland Channel at the base of the Shetland slope, passing the rim of the Fugloy Ridge and continuing to the Norwegian Sea. The profile consisted of three seismic lines; PSAT-216, PSAT-217 and PSAT-218, starting from the southeast (Fig. 2).

The seismic profile is divided into six seismic units named Unit A to F from below (Fig. 3).

Unit A represents the acoustic basement, which is composed of Paleocene basalt (Andersen et al., 2000). The top of the unit is



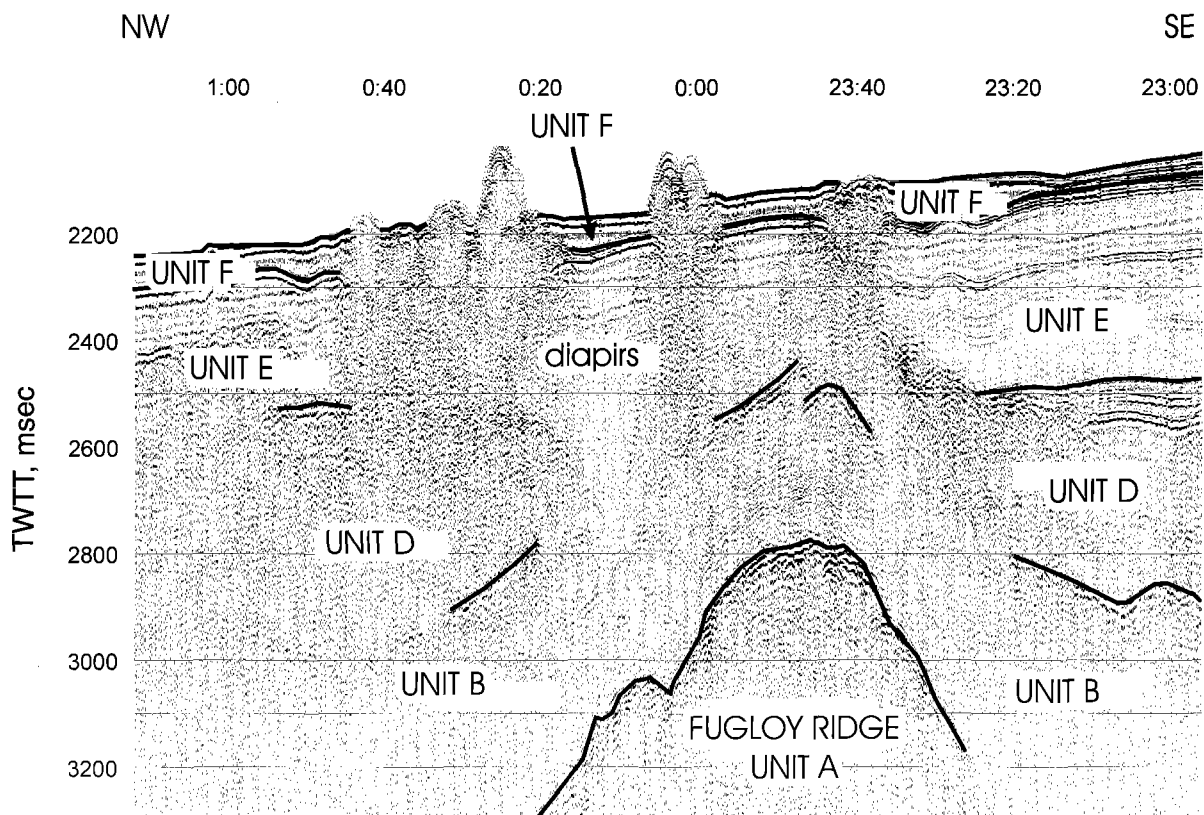


Figure 3. Seismic profile PSAT 217 showing main seismic units. Unit A: basalt, Unit B: Eocene/Oligocene sediments, Unit D: Miocene biosiliceous ooze, Unit E: North Sea Fan, Unit F: North Sea Fan.

marked by a strong reflector with a varied continuity. At the Shetland slope the basaltic unit is absent, otherwise it is found throughout the profile. Furthest to the north (PSAT-218) the top of the basalt is hummocky. This hummocky pattern indicates rapid cooling of the basalt under water and is known to represent the oceanic crust of the Norwegian Sea. At the Fugloy Ridge the basalt forms an anticline (Fig. 3). This anticline and the Shetland margin (PSAT 216) mark the boundary of the Faeroe-Shetland Channel. Further to the north the acoustic basement forms another anticline, which is characterised by a strong, continuous reflector and seaward dipping internal reflectors. Seaward dipping reflectors are known to mark the transition zone between the continental and the oceanic crust of the Faeroe Platform (Boldreel et al., 1993; Nielsen et al., 1998). Therefore the anticline is interpreted to be a transition zone. The Fugloy Ridge was formed by three post-basalt compressional phases starting in Late Paleocene, continuing

into Miocene (Boldreel et al., 1998).

Unit B can be seen along the entire profile. The top reflector is of medium intensity towards the south and gets hummocky and weak towards the north. Toplaps can be seen on the top reflector. Besides them there are hardly any internal reflections and the unit is mostly acoustically transparent. The unit follows the topography of the basalt and is proposed to be of Paleocene-Eocene age (Andersen, et al., 2000). Recent studies further south in the Faeroe-Shetland Channel have come to the conclusion that sediments of this age originate from the Shetland margin, while in the north they originate from the erosion of the uplifted Fugloy Ridge (Andersen, et al., 2000). The toplaps indicate that the top reflector of unit B represents an erosional surface. The hummocky nature of the top reflector to the north is possibly a result of the first or the second compressional phase, i.e. mid Eocene or latest Oligocene (Boldreel et al., 1998).

Unit C is only present in the north of the

profile, on line PSAT-218. The unit is characterised by weak parallel reflectors. An erosional surface can be seen on top of the unit. The age of the unit is proposed to be Oligocene (Nielsen et al., 1998). Onlaps onto the base reflector of the unit suggest a continuous subsidence of the Norwegian Sea due to thermal cooling of the oceanic crust throughout the deposition of Unit C. The erosion at the top of the unit is possibly the result of the second or third compressional phase, i.e. latest Oligocene or mid Miocene (Boldreel et al., 1998).

Unit D is characterised by disturbed internal reflectors and a disrupted top reflector in the Faeroe-Shetland Channel. On the Fugloy Ridge there are hardly any bottom and top reflectors and the internal reflectors have a chaotic pattern. The maximum thickness of the unit, found in the Faeroe-Shetland Channel, is about 550 ms. The unit forms a wedge, which thins out towards the northwest indicating that the material derives from an easterly direction. Due to the resolution of the seismic it is not clear whether the unit pinches out or continues as a thin veneer towards the northwest into the Norwegian Sea. The weak and partly missing reflectors on the Fugloy Ridge are interpreted to be caused by upward movement of lighter material, which is also causing the chaotic pattern of the unit in this area (Fig. 3). The proposed age of Unit D is Miocene and it is considered to be a biosiliceous ooze (Davies et al., 2001).

Unit E is characterised by transparent internal reflectors. It can be divided into several subunits, which gradually pinch out towards the north. The unit is most probably the southwesterly extension of the North Sea Fan (Nielsen et al., 2002) (Fig. 3). The fan has been built up by many flows of glacial deposits (King et al., 1998). The top reflector of the unit is strong and continuous except in the Fugloy Ridge area. Here the upward migrating material of unit D propagates into Unit E and locally breaks through the seabed forming diapirs (Fig. 3). In the area with the most extensive diapirism, the top of unit E is seen to form smaller lows and depressions, most likely as a result of mobilisation of the

underlying sediments. The topography of the basaltic basement of the Fugloy Ridge seems to be the controlling factor of the position of the diapirs. Towards the north, in the Norwegian Sea, the upper sediments are disturbed by small vertical faults. Similar fault patterns are observed in different places in the North Atlantic and they are interpreted as dewatering faults (Andersen et al., 2000). The vertical dewatering faults seen on the profile begin to appear where the North Sea Fan pinches out. The water originates from the Paleocene to Oligocene sediments of Unit B and C.

Unit F constitutes the surface unit in most of the study area but pinches out towards the Norwegian Sea. It is conformable to unit E but continues further upslope on the Shetland margin. The unit is interpreted as the youngest flow of the North Sea Fan. The internal structures are strong and parallel in the Faeroe-Shetland Channel, with the exception of an area at the base of the Shetland slope where a lens with weak and chaotic reflectors is found. This lens is interpreted as a mass flow deposit that most likely originates from instability of the Shetland slope. Basinward of the mass flow deposit, the internal reflectors top lap northward and are truncated at the seafloor. This indicates that the seafloor is locally erosional.

In the Fugloy Ridge area, sediments of unit F infill the smaller lows and depressions found at the top of the underlying Unit E. This is evidenced by onlaps and demonstrates that the lows pre-date the deposition of unit F. This suggests the diapirism to have been most intensive in an earlier phase. However the present day seabed topography shows an up-doming in connection with the diapirs and it must therefore be concluded that the process is still active.

1.1.2.2. Interpretation of OKEAN sidescan sonar and hull-mounted subbottom profiler

N. TUOMIKOSKI, J. LEVANDER,  
A. AKHMETZHANOV, M. IVANOV, P. SHASHKIN  
AND S. AGIBALOV

The 10 kHz OKEAN sidescan sonar, with a 6 km range to each side, and a 5 kHz hull-mounted subbottom profiler were deployed together with seismic profiling. Thus the OKEAN sonograph and the subbottom profile are both labeled PSAT-216 to -218. Due to the frequency of the OKEAN some penetration occurs. Therefore the sonograph not only shows the seabed but also some sub-seabed features.

The southeast part of line PSAT-217 and the entire PSAT-216 appear featureless and have a medium backscatter. However, a lens of chaotic and semi-transparent deposits beneath the seafloor on the subbottom profile indicates mass flow deposits in this area. The lens is covered by a surface layer, so the mass flow is only seen as diffuse, east-west striking, darker features on the sonograph. Further northwest an elongated area, with

generally high but varying backscatter, appears. Several highs recognised by higher backscatter and shadows are observed within the area. From the seismic and the subbottom profile this area is recognized as the region of mud diapirs (Fig. 4). Due to the penetration of the OKEAN it is not only the mud diapirs piercing the seabed but also the near seabed upward migrating material that are visible on the sonograph. The diapiric region on the sonograph strikes southeast-northwest and extends beyond the survey area in a southwesterly direction. East of the diapiric area and continuing towards the north narrow elongated features with strong backscatter occur (Fig. 4). They are mainly orientated parallel to the track. No obvious shadows are observed and the features seem to be isolated. On the subbottom profile the area with the narrow elongated features is characterised by a strong subbottom reflector, 10-15 m below seabed. This represents the top of seismic unit E. Neither the seismic nor the subbottom profiler have crossed any of the elongated features but a possible interpretation could be that they are caused by subcropping of seismic unit E. Continuing

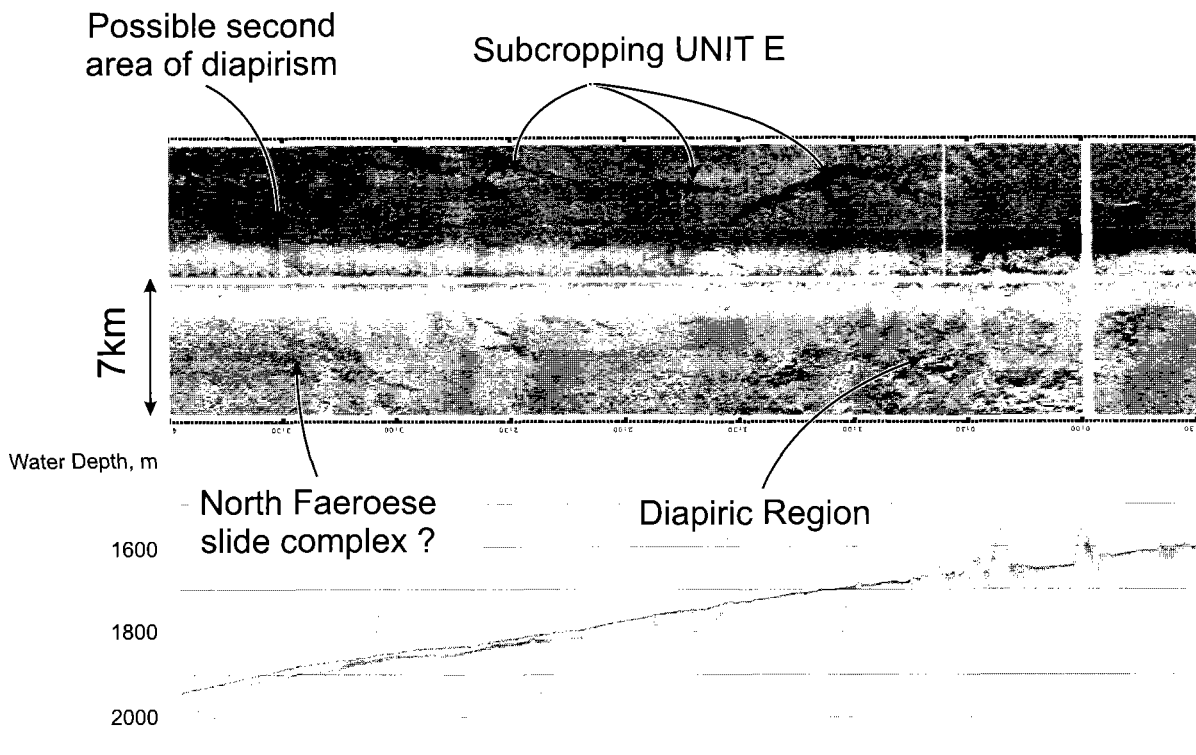


Figure 4. OKEAN PSAT-217 sonograph and subbottom profile record.

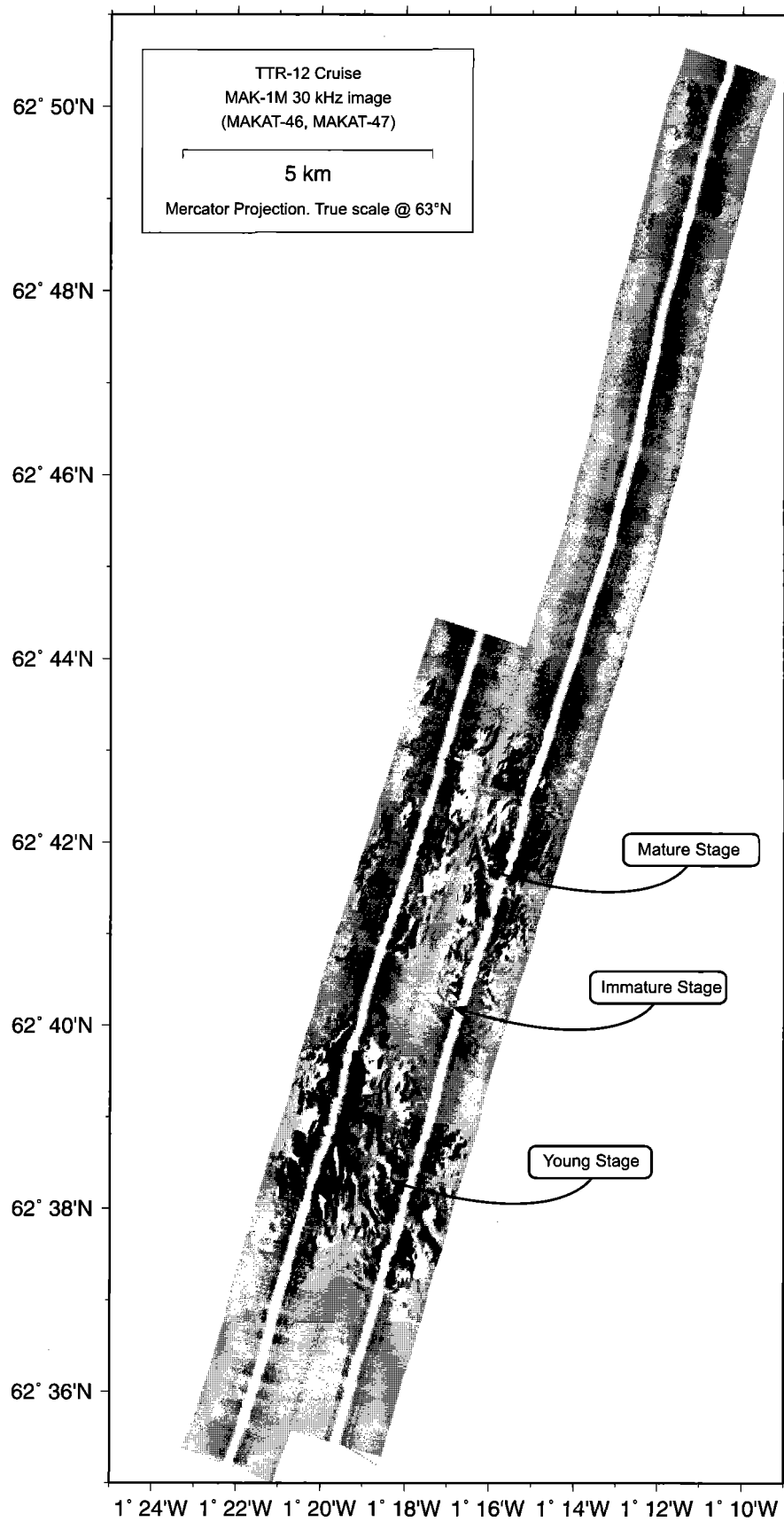


Figure 5. Mosaic of MAKAT-46 and MAKAT-47 sonographs (see Fig. 2 for positioning).

towards the northwest, a lobe shaped area of medium and uniform backscatter is seen entering the area from southwest (Fig. 4). A comparison with the subbottom profile indicates that the lobe shaped area corresponds to a region covered by a 15-20 m thick lens shaped, transparent surface layer. The layer is not visible on the seismic due to the lower resolution. Based on the shape and direction of the lobe we speculate that this surface layer originates from the northeastern Faeroe slope. At the northern rim of the lobe the subbottom profile shows a depression that is seen on the sonograph as a darker shaded area striking east-west. North of the lobe, continuing into the Norwegian Sea, a series of smaller lobe shaped features reach into the sonograph from the southwest. The lobes have a medium backscatter with narrow strings of higher backscatter giving the impression of overlapping deposits. Like the big lobe these smaller lobe shaped features are considered to originate from the north-eastern Faeroe slope. Since this slope is known as an area prone to instability, e.g. the North Faeroes Slide Complex (van Weering et al., 1998), we suggest that the lobes represent mass flow deposits from this slide.

At the eastern edge of the big lobe there is an area of varying darker backscatter. This resembles the backscatter pattern of the diapiric area and might represent a second area of diapirism. The seismic profile, showing upward migrating material close to the seabed immediately south of this second area, supports this interpretation. The seafloor on the subbottom profile PSAT-218 appears as an irregular surface. This is interpreted to be caused by the dewatering mentioned above.

#### 1.1.2.3. Interpretation of MAK sidescan and MAK subbottom profiler

N. TUOMIKOSKI, J. LEVANDER, A. AKHMETZHANOV,  
M. IVANOV AND P. SHASHKIN

Based on the seismic and the OKEAN data the high-resolution MAK system was used to get more details from the area with the diapirs. The MAK survey was operated

with a frequency of 30 kHz and a range of 1 km to each side, and it was kept at 100 m above the seafloor. Simultaneously with the MAK the hull-mounted 5 kHz subbottom profiler was recorded.

Two sonographs, MAKAT-46 and MAKAT-47, were recorded from north to south across seismic profile PSAT-217 (Fig. 2) and finally formed into a mosaic (Fig. 5). On the sonographs the diapirs occur as two separate regions with medium to strong backscatter (Fig. 5). The region to the south appears sub-circular while the region to the north is more elongated. Both regions possibly reach beyond the mapped area. The southern region is dominated by strong backscatter and appears blocky while the northern one is dominated by medium backscatter and appears smoother. Based on the subbottom profile and the sonograph we can divide the diapiric processes into three different stages of development:

- An immature stage: Diapirs that have not yet pierced the seabed. On the subbottom profile they are covered by sediment with dark horizontal reflectors (Fig. 6). These are suggested to be lithified layers forming a "cap-rock". On the sonograph this stage is seen as low to medium backscatter with a cauliflower pattern (Fig. 5).
- A young stage: Diapirs that have pierced the seabed. They are 25-50 m high and have a sharp and spiky appearance. On the subbottom profile they are often topped by broken and cracked "cap-rock" (Fig. 6). Small faults are seen in the broken "cap-rock", some of them filled with sediments. On the sonograph this stage has a medium to high backscatter and display a blocky pattern (Fig. 5).
- A mature stage: Well-developed diapirs that are 50-100 m high. On the subbottom profile they have a smooth and rounded appearance, with no visible remnants of "cap-rock" on the top (Fig. 6). On the sonograph these diapirs appear almost circular and display a medium to high backscatter (Fig. 5).

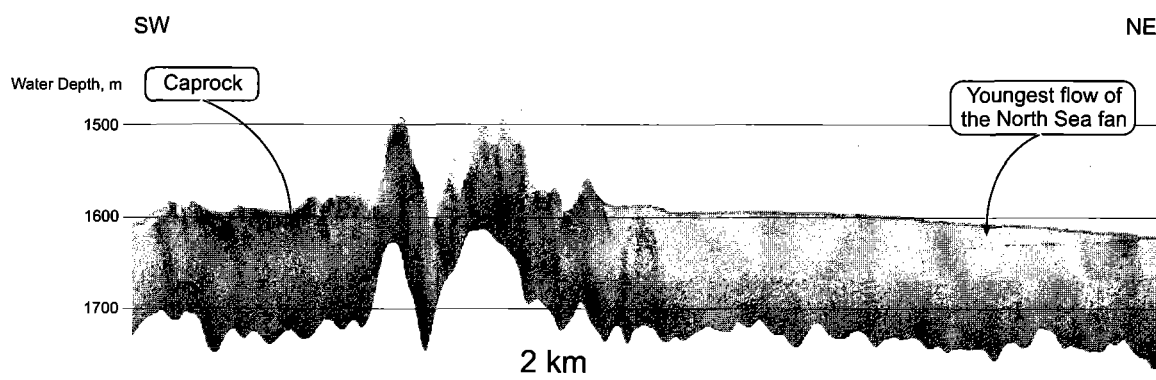


Figure 6. Subbottom profile of MAKAT-46 illustrating diapirs with "cap-rock" and youngest wedge of the North Sea Fan.

The sediments surrounding the diapiric regions are known from the seismic profile to originate from the North Sea Fan (see section on seismic interpretation). The subbottom profiles show two individual North Sea Fan flows pinching out towards the north. When not pierced by the diapirs, a 2-3 m thick layer covers the seabed in the entire study area. This surface layer gives a low backscatter on the sonograph. Where the youngest flow of the North Sea Fan pinches out, a curving shadow of higher backscatter appears. Otherwise the sonograph is featureless outside the diapiric region.

#### 1.1.2.4. Bottom sampling

I. MARDANIAN, A. MAZZINI, G. AKHMANOV,  
A. AKHMETZHANOV, E. KOZLOVA, H. MOELLER,  
V. TORLOV, A. SAMOILOV, E. SARANTSEV,  
A. SADEKOV, E. POLUDETkina, O. BARVALINA,  
E. BILEVA, AND V. BLINOVA

The main targets of sampling were diapiric structures, studied by geophysical methods, and the nature of the regional sedimentation. Three gravity core stations were occupied and one dredge station (Table 1). Core logs can be found in Annex I.

#### Core TTR12-AT358G.

The core was taken from the area of regional sedimentation outside the diapir fields (Fig. 7). The 504 cm of sedimentary succession contains two main intervals.

The upper 289 cm are clays, varying in colour from light olive brown to dark grey and dark greyish brown with few foraminifera. There is little coarse terrigenous material, except two intervals. Layers of sandy clay are found at 115-130 cm and at 140 cm. The 15 cm thick layer is formed of very dark greyish brown sandy clay. A 1.5 cm-thick, inclined layer of sandy clay is found 10 cm below. The layers are embedded in dark grey structureless clay. The uppermost 9 cm of the core is composed of light olive brown clay. Very dark grey clay at 174-194 cm contains patches of dark greyish brown clay. The 194-279 cm and 279-289 cm intervals, with a gradational boundary in between, are made up of dark greyish brown clay with foraminifera. The lower interval is more water-saturated. Bioturbation is found in the middle part of the core (174-289 cm).

The lower part of the core, more than 2 m thick, consists of structureless dark grey silty clay with sandy admixture and with gravel-sized rock fragments scattered through the interval. The structure of the sediment and the magnetic susceptibility curve indicate that this thick layer was formed as a debris flow.

The upper part of the sedimentary sequence probably resulted from hemipelagic deposition and could be the characteristic background sedimentation of the area. The sand-enriched layers could reflect bottom current activity. Debris flow deposits in the lower part of the core could be part of the

Table 1. Sampling sites on the Faeroe margin.

CORE No	DATE	TIME GMT	LATITUDE	LONGITUDE	DEPTH, m	RECOVERY, cm
AT-358G	20.06.02	14:37	62° 36,002N	1° 19,016W	1640	504
AT-359G	20.06.02	17:05	62° 38,712	1° 17,145	1558	166
AT-360G	20.06.02	20:27	62° 41,409	1° 15,835	1548	385
AT-361D	21.06.02	8:31 9:16	62° 41,676 62° 41,431	1° 15,944 1° 16,489	1607 1602	10 cm <sup>3</sup>
AT-362G	22.06.02	6:42	61° 47,044	3° 28,153	1441	428
AT-363G	22.06.02	9:16	61° 48,774	3° 35,346	1236	500.5
AT-364G	22.06.02	11:30	61° 48,871	3° 35,647	1223	418
AT-365G	22.06.02	13:36	61° 50,430	3° 40,123	998	154
AT-366G	22.06.02	16:08	61° 49,775	3° 38,232	1054	424
AT-367B	22.06.02	17:28	61° 49,777	3° 38,230	1049	29

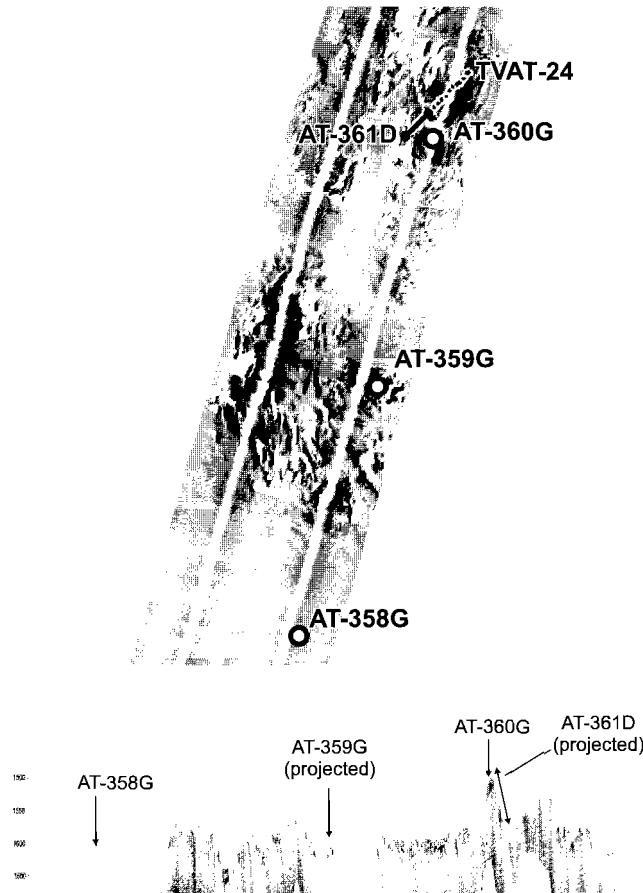


Figure 7. Sampling of the outcropping diapiric structures.

North Sea Fan glacial accumulation (King et al., 1998) or from other downslope movements.

#### Core TTR12-AT359

The high-backscatter area from the southern diapir field seen on the MAK sidescan sonograph was sampled (Fig. 7). Total length of the core is 166 cm.

The upper 105 cm is dark greyish brown marl with abundant sand and foraminifera. The 38-45 cm interval has enrichment of coarse sandy and gravel particles, probably IRD. Dropstones are found in the lower part of the interval and subhorizontal lenses of more lithified darker sediment in the middle part of the interval

Dark grey sandy silty clay with a few foraminifera comprises the middle part of the core. The interval is mainly homogeneous with some patches of brownish mud.

Lithified greenish brown diatomaceous ooze with sandy glauconite grains forms the lower 20 cm of the core.

Hemipelagic sediments of the upper part of the core settled in different sedimentological conditions and reflect changes of environments in the Late Pleistocene. The lithified diatomaceous ooze in the base of the core undoubtedly forms part of the diapir structure. Davies and Cartwright (2002) described large-scale diatomaceous accumulations in the area in the Miocene, so we can propose that the diatomaceous sediments form diapirs and were deposited in the Miocene.

#### Core TTR12-AT360G

The location of the core was assumed to be on top of a diapiric structure from the northern diapir field (Fig. 7).

The upper 40 cm layer in the core is olive and olive brown marl with foraminifera. Coarse silty/sandy admixture and foraminifera content increase down the interval. A few 1 cm nodules of green diatomaceous ooze are reported in the layer.

The lower 385 cm has silty clay, varying in colour from olive grey and brownish grey

to dark grey, with different amount of coarse fraction.

The 50-130 cm interval is formed by alternating olive grey and dark olive grey silty clays with varying coarse admixture. Small fragments of green diatomaceous ooze are observed in the base of the interval, which has an irregular inclined lower boundary.

Silty clay layers, varying in colour and with undulating boundaries, comprise the 130-185 cm interval. Accumulations include irregular fragments of more consolidated mud, which differs from the matrix by its coarse fraction content.

Relatively large fragments of green and light olive brown diatomaceous ooze appear in the 185-228 cm interval. In the lower part a fragment of consolidated black clay and a 3 cm nodule of light olive brown diatomaceous ooze are found.

The 231-298 cm interval contains fragments of green and light olive brown diatomaceous ooze up to 10 cm in size. The green colour is caused by glauconite admixture. The interval is overlain by a 3 cm layer of dark olive brown silty clay.

The lower part of the core (298-380 cm) is formed of nodules of diatomaceous ooze and clay and common rock clasts of gravel size surrounded by a silty clayey matrix. The boundary with the lowermost layer of consolidated clay is marked by a microfault.

The core is mostly composed of redeposited sediment with slump structures, inclined and undulating boundaries, microfaults and nodules of more consolidated matter. Due to abundance of the diatomaceous ooze fragments scattered in the sediment we assume that the core was probably obtained from the upper part of the diapir's slope. Thick accumulations on the slope caused by mass-wasting could reflect active growth of the diapiric structure.

#### Dredge TTR12-AT351D

The abrupt slope of the diapir from the northwestern part of the area was sampled by dredge to obtain extruded material (Fig. 7). A fragment of lithified light olive brown diatomaceous ooze, 20x15x15 cm in size, was



recovered. Smaller fragments of the same ooze were reported in the core TTR12-AT360G.

The bottom deposits within the area located on the continuation of Fugloy Ridge, northeastern entrance of the Faeroe-Shetland Channel, display diapir structures on the seafloor resulting from extrusion of accumulations probably of Miocene age. Extruded sediments are represented by two types of diatomaceous ooze, green and light olive brown in colour. Green ooze usually contains abundant glauconite grains up to coarse sand size. One of the cores has Late Pleistocene/Holocene accumulations formed by marl and silty clay overlaying diatomaceous ooze. Slopes of diapirs are built up either of lithified Miocene diatomaceous ooze or of redeposited late Pleistocene/Holocene sediments containing fragments of ooze. The background sedimentation in the area is also affected by processes of downslope mass-movement. Ice-rafting activity in the region is marked by the admixture of coarse grains in some layers (IRD) and by dropstones in the sediment.

#### 1.1.2.5. Conclusions

The combination of acoustics and sediment samples has revealed important information that allows us to conclude:

- The mound features can be classified as 'mud-diapirs'. The diapirs seen on the seabed are the visible parts of a larger complex.
- The diapirism is caused by subsurface sediment mobilisation. The extruded sediments have a very high content of diatoms and low magnetic susceptibility values, and can be classified as biosiliceous ooze. The age of the ooze is most likely Miocene.
- The diapiric process shows three stages of development: 1) An immature stage where the diapirs have not yet pierced the seabed and seem to form a "cap-rock"; 2) A

young stage where the diapirs have broken the "cap-rock", pierced the seabed and reached a high of 25-50 m; 3) A mature stage where the diapirs are up to 100 m high and have a smoother appearance.

- The compressional Fugloy Ridge seems to be a controlling factor for the formation of diapirs. However, it cannot be ruled out that diapirs are formed outside the ridge area, e.g. in the Norwegian Sea.

### 1.1.3. GEM Raft area on the central Faeroese slope of the Faeroe-Shetland Channel

#### 1.1.3.1. Interpretation of MAK sidescan sonar and subbottom profiler

N. TUOMIKOSKI, J. LEVANDER, A. AKHMETZHANOV, M. IVANOV AND P. SHASHKIN

The GEM Raft on the eastern Faeroe slope was investigated using MAK deep-towed sidescan sonar with 30 kHz frequency and 5 kHz subbottom profiler. It was towed at 100 m above the seafloor. One line, MAKAT-49 was run perpendicular to the Faeroe margin and downslope towards the Faeroe-Shetland Channel (Fig. 8). A hull-mounted subbottom profiler with a frequency of 5.1 kHz was also used, but in the interpretation only the deep-towed profiler is considered due to its better resolution.

The line is about 20 km long and is described from upslope to downslope and reaches from 680 to 1240 m water depth. The upslope is homogeneous and has a low backscatter. The uppermost layer, which will be referred to as layer A, covers the entire profile but changes character. The layer is characterised by continuous and parallel bedded reflectors which are locally cut off. They rest upon an irregular surface. Where the gradient is steeper, northeast-southwest trending ploughmarks can be seen. They are between 1.5-7.5 m deep and up to 100 m wide and they appear in water depths of 700-850 m. On the sonograph they seem to be swept by currents and covered by a thin layer of recent sediments although this is not

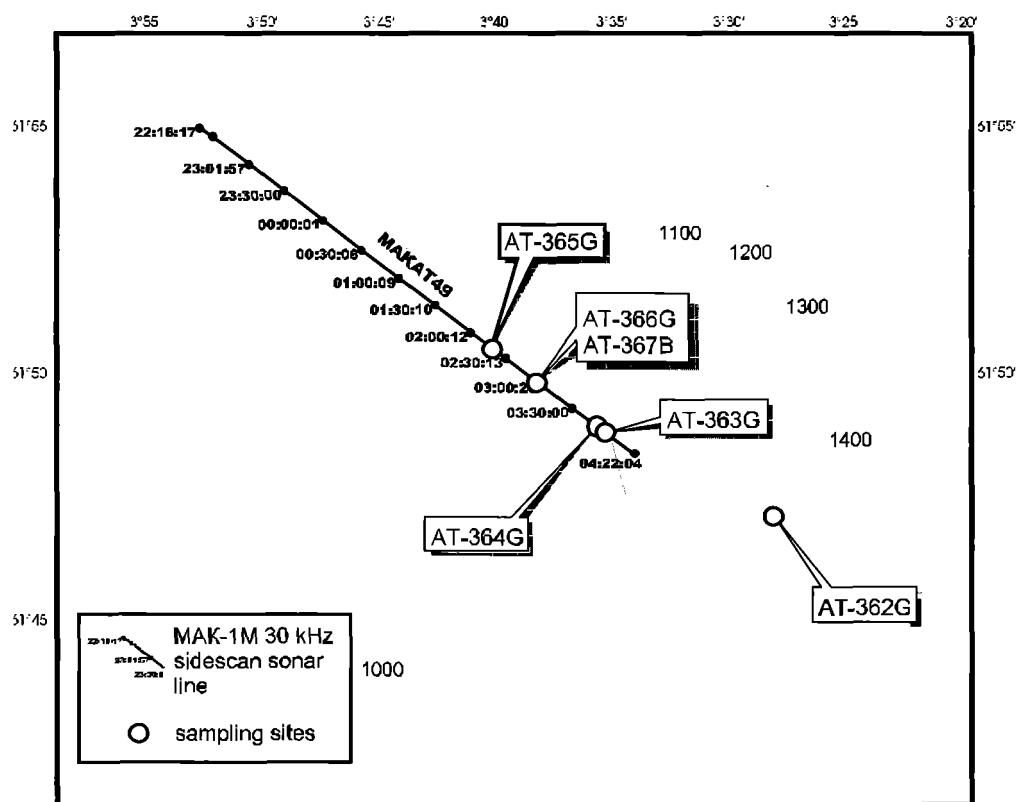


Figure 8. Location map of Area 2.

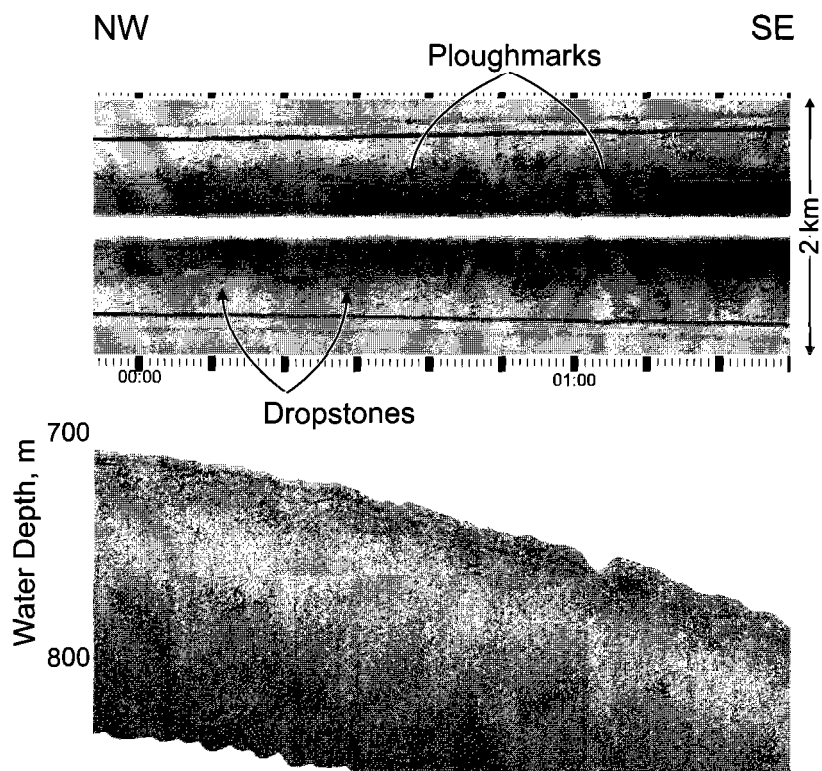


Figure 9. Section of the MAKAT-49 showing ploughmarks and dropstones on the upper part of the slope.

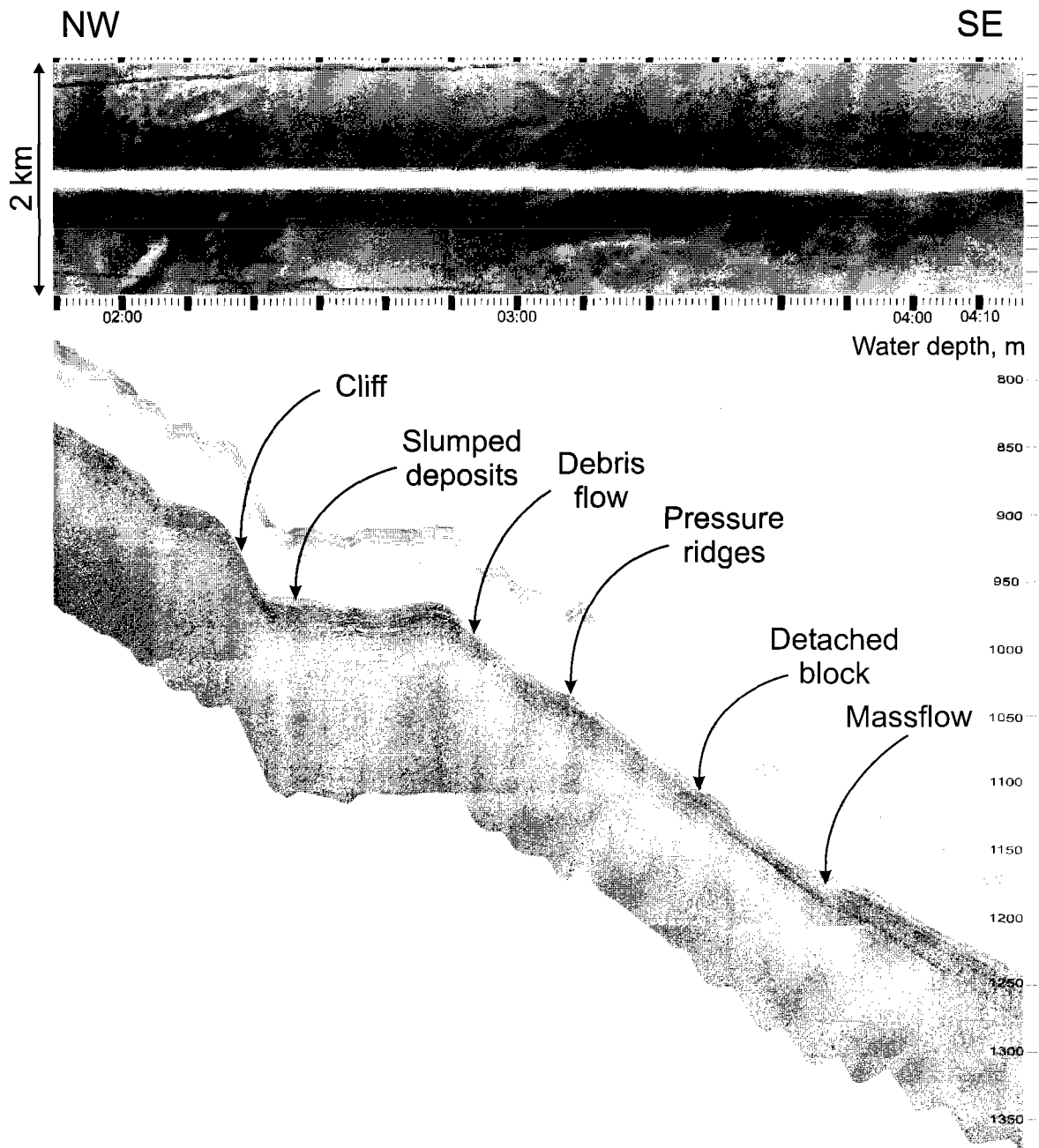


Figure 10. A sequence of the MAKAT-49 showing the complexity of downslope processes.

documented from the subbottom profile. Two of the ploughmarks are more distinct and have circular marks at their end (Fig. 9). Most probably the icebergs were in a stagnant stage while forming these marks. The ploughmarks are also seen as deeps on the subbottom profile. The ice has turbated the sediments so that the reflectors appear less parallel. The profile at around 700 m water depth shows not only iceberg turbation, but also the effects of forces from below. Southeast of the ploughmarks sliding and

slumping processes are observed. The amount of black specks increases downslope as far as the slumping area where they begin to decrease. They are interpreted as dropstones. Below the ploughmarks there is a dramatic increase in the slope gradient, forming an up to 50 m high cliff. The edge of the cliff has a higher backscatter and horse-shoe shaped incisions. Downslope of this cliff the seafloor levels out and forms a c. 1.5 km wide plateau in a water depth of 970 m. On the plateau a few slump deposits are seen

and these represent different slumping events. The material appears to come from the cliff above the plateau (Fig. 10) but could originate from a smaller scar further up slope. The slump deposit on the plateau shows no sign of recent sediment coverage, indicating a rather young age for the slump event. Layer A is thick and has strong parallel reflectors on the plateau and they are seen to be cut by the slump material. On the edge of the plateau this layer forms a threshold for the slumping material to continue downslope.

Downslope from the plateau a complex of downslope processes results in slumps, slides, pressure ridges, debris flows and detached blocks (Fig. 10). On the sonograph the slide complex is recognised by medium to strong backscatter. The appearance is hazy. The debris flow has a bottleneck shaped feeder channel. A detached block is shown as a dark homogeneous backscatter area and the mass flow is shown as an indistinct area of slightly lower backscatter with a diffused wavy pattern (Fig. 10). There is no obvious sign that the complex is still active, e.g. no sign of pressure ridges in front of the detached block and it is covered by a thin surface layer. This layer could explain the hazy appearance on the sonograph.

As both the lower and the upper slump complexes are seen to extend beyond the range of the study area the extension of the GEM Raft is not fully mapped on the line.

#### 1.1.3.2. Bottom sampling

I. MARDANIAN, A. MAZZINI, G. AKHMANOV,  
A. AKHMETZHANOV, E. KOZLOVA, H. MOELLER,  
V. TORLOV, A. SAMOILOV, E. SARANTSEV,  
A. SADEKOV, E. POLUDETkina, O. BARVALINA,  
E. BILEVA AND V. BLINOVA,

Five stations sampled with a gravity corer and one station sampled with a box-corer were used to study down-slope processes on the Faeroe slope in the central part of the Faeroe-Shetland Channel (Table 1). The small slide known as GEM Raft was the main target of investigation (Fig. 11).

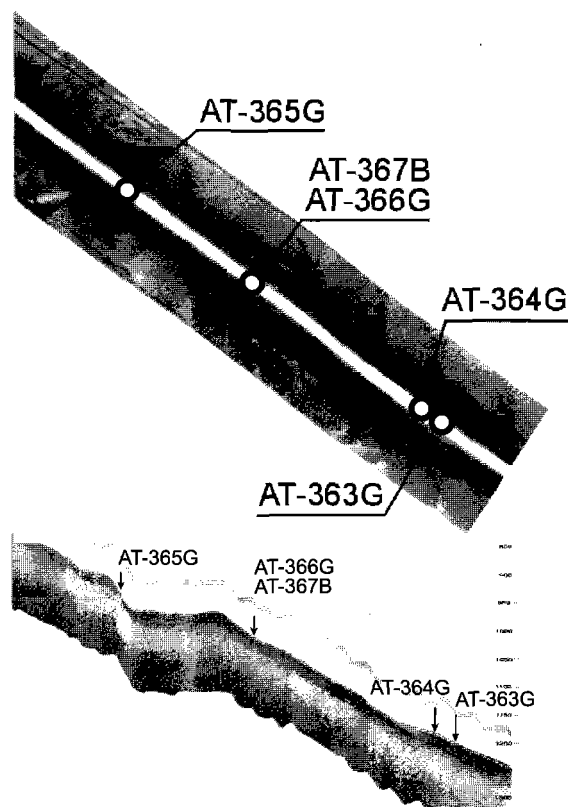


Figure 11. Sampling of slump structures.

#### Core TTR12-AT362G.

A 48 cm long core was taken from undisturbed sediments outside the GEM Raft to characterise background sedimentation in the area. The recovered succession consists of alternations of silty/sandy clays with clays without coarse terrigenous admixture. The near surface layer of olive brown silty clay with sand is 3 cm thick. Beneath are alternating grey clays and dark grey silty clays. At least nine cycles are seen in the core. As a rule, grey and dark grey intervals have gradational or bioturbated boundaries. The maximum thickness of dark grey layers is 30 cm. Lighter coloured layers sometimes exceed 50 cm. Such alternation of colour is probably caused by different carbonate content and reflects changes in depositional environments resulting from Late Quaternary climatic fluctuations.

#### Core TTR12-AT363G.

According to the geophysical survey the core was taken within the slide area (Fig.

11). Nevertheless the 5 m core contains alternating hemipelagic sediments, similar to those taken at the previous station. The sedimentary succession is similar to core TTR12-AT362G.

#### Core TTR12-AT364G.

The sampling site was located close to the previous station (Fig. 11). The corer recovered a 428 cm thick sequence similar to cores TTR12-AT362G and TTR12-AT363G.

#### Core TTR12-AT365G.

The steep slope with slump deposits was sampled. The 158 cm long core is mainly olive grey, olive brown, dark grey and dark grey brown clays with silty/sandy

admixture. Inclined and irregular boundaries are common. A few intervals consist of numerous fragments of stiff or water-saturated mud varying in shape, colour and in composition and often surrounded by silty clayey matrix. Deposits are characterised by slump and debris-flow structures. The core contains four layers of waterlogged silty clays, three of them are olive grey (48-49, 81-83 and 140-146 cm intervals) and one is dark grey brown (96-119 cm). Possibly such water-saturated layers were slide faces. An interval composed of stiff black silty clay, sharply differing from other sediments by its low magnetic susceptibility values, is seen in the base of the core, just above the lowermost sliding-surface (Fig. 12). The heterogeneity of deposits, the structures and the slide faces unambiguously characterise recently active downslope processes.

#### Core TTR12-AT366.

The core was taken below a small plateau with redeposited accumulations recognised on the MAK-1M sidescan record (Fig. 11). The core is 424 cm long. Brown, olive brown, grey brown and brown grey silty clays dominate the upper part of the core. The lower part is mostly dark, light and olive grey clays, which contain silty/sandy admixture in some cases. As well as layers with homogeneous structure some intervals contain fragments of clays differing from the matrix by colour, water content and coarse grain admixture. Such inclusions are more abundant at 61-96, 110-150 and 250-295 cm. Fragments up to 10 cm in size are found. These accumulations probably formed due to mixing of sediment deposited earlier by downslope transport. A layer of very dark silty clay with bioturbated upper and planar, sharp lower boundaries is noted in the lower part of the core. The interval has low magnetic susceptibility in contrast to other sediments recovered at the station.

#### Core TTR12-AT367B.

This box-core sample consists of grey brown and light grey brown silty clay with

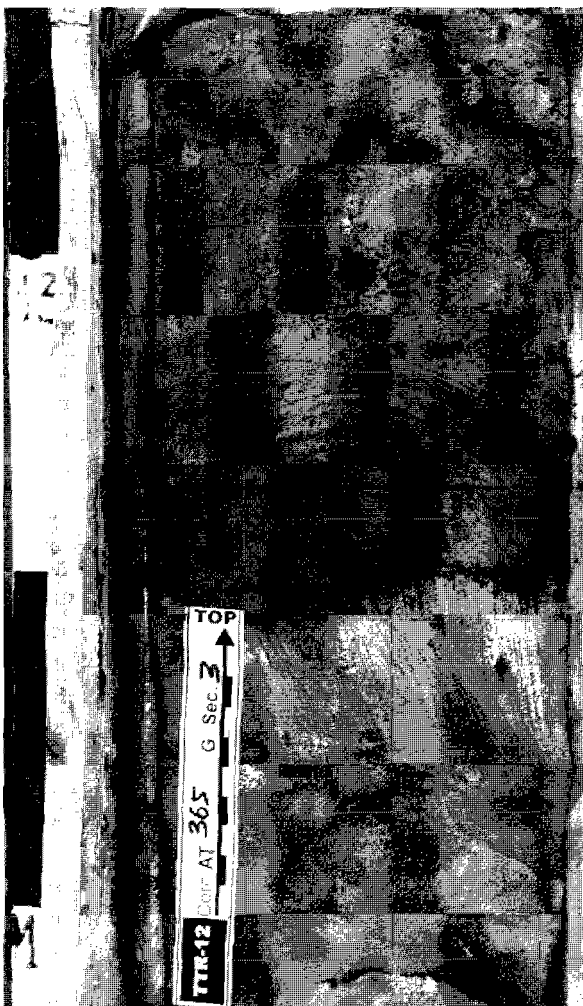


Figure 12. Sharp contact between slump deposits and underlying hemipelagic sediments (AT6365G).

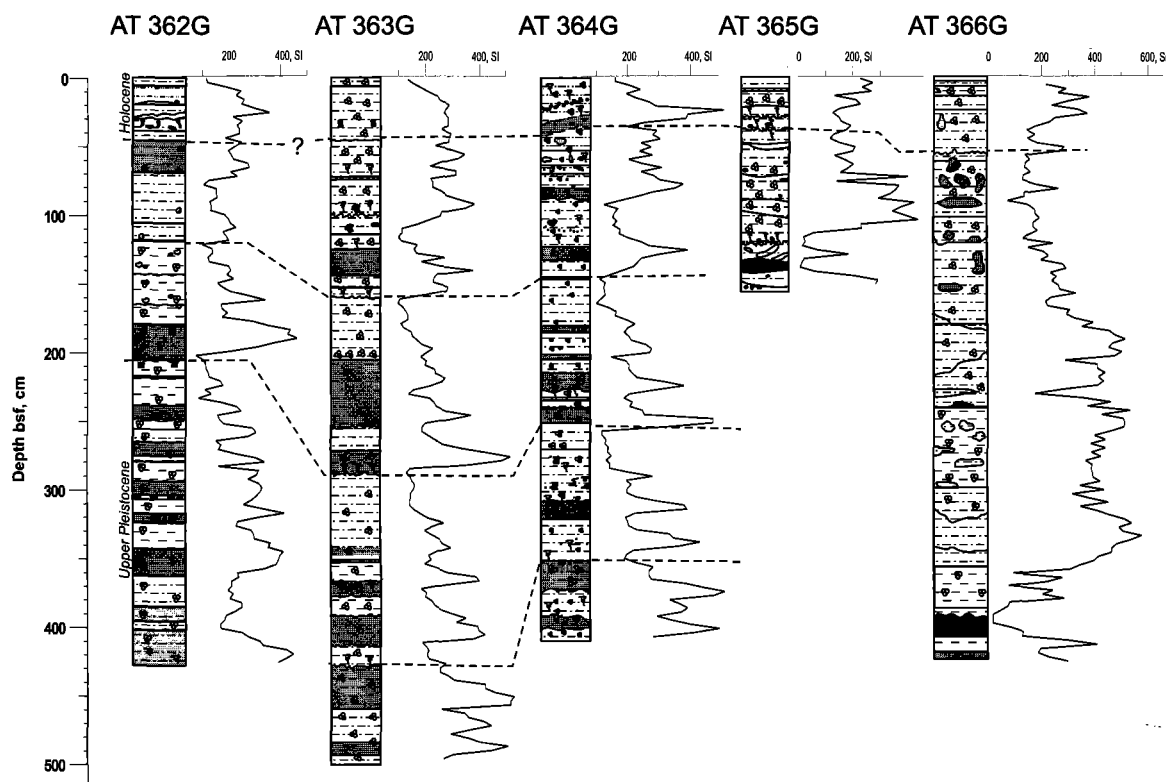


Figure 13. Correlation of sediment cores recovered on the northeastern slope of the Faeroe-Shetland Channel based on observed lithologies and magnetic susceptibility measurements.

foraminifera. Dark grey clayey fragments are present in the subsurface layer and at 22 cm depth. Total recovery was 29 cm.

The cores from the western slope of the Faeroe - Shetland Channel contained the following sedimentary successions:

- Undisturbed hemipelagic sediments both outside (TTR12-AT362G) and within (TTR12-AT363G, TTR12-AT364G) the slide area;
- Entirely from mass-wasting processes (TTR12-AT365G);
- Partly from by periodic downslope sediment transport and partly by hemipelagic sedimentation.

All studied deposits contain scattered dropstones.

The bottom deposits were correlated on the basis of lithology and magnetic susceptibility (Fig. 13).

The alternation of colours in hemipelagic sediments reflect climate fluctuations in the Late Quaternary: during warm periods lighter sediments with higher car-

bonate content were deposited, whereas glacial periods are characterised by dark sediments with higher terrigenous content.

Sediments from the Faeroe slope are characterised by relatively high magnetic susceptibility values.

It was confirmed that the GEM Raft formation was caused mainly by large-scale catastrophic failure. Later, most of the slope was covered by thick hemipelagic deposits, so cores taken below the plateau do not have redeposited sediments. Nevertheless, cliffs above and below a plateau collapsed after the main event and are possibly still active.

### 1.1.3.3. Conclusions

Some general conclusions can be drawn from the limited amount of data:

- The existence of the GEM Raft is confirmed. However, the actual size and direction of the raft cannot be determined based on the present study.

- The GEM Raft seems to consist of an upper and a lower part separated by a c. 15 km wide plateau.

- The upper part of the raft is the smallest and possibly the youngest. There is no sign that sediments cover the latest slump deposits. This is confirmed by the sediment samples. Buried slump deposits witness that this upper part has previously been prone to instability.

- The lower part of the raft shows a variety of down-slope processes, e.g. detached blocks, pressure ridges, slumps and debris flows. This lower part seems covered by a more recent sediment layer, and there is no clear indication that the processes are still active. This has been confirmed by sediment samples.

## 1.2. Rockall Trough seabed sampling

T. FUREY AND THE SHIPBOARD SCIENTIFIC PARTY OF THE TTR-12 CRUISE

During the second part of Leg 1 a seabed sampling programme was undertaken in the Rockall Trough on behalf of the Irish Geological Survey. Shallow cores were collected from both slopes and from the central part of the Trough in order to calibrate acoustic multibeam echosounder data recently acquired by the Geological Survey as well as for environmental and geotechnical studies.

A box corer was used at 17 stations with one sample retrieved by Kasten corer and 2 samples by the TV-guided grab sampler (Table 2, Fig. 14).

Samples recovered by boxcorer were subsampled for a number of analyses: macro- and microbiological, geochemical and geotechnical.

Most of the cores had a similar appear-

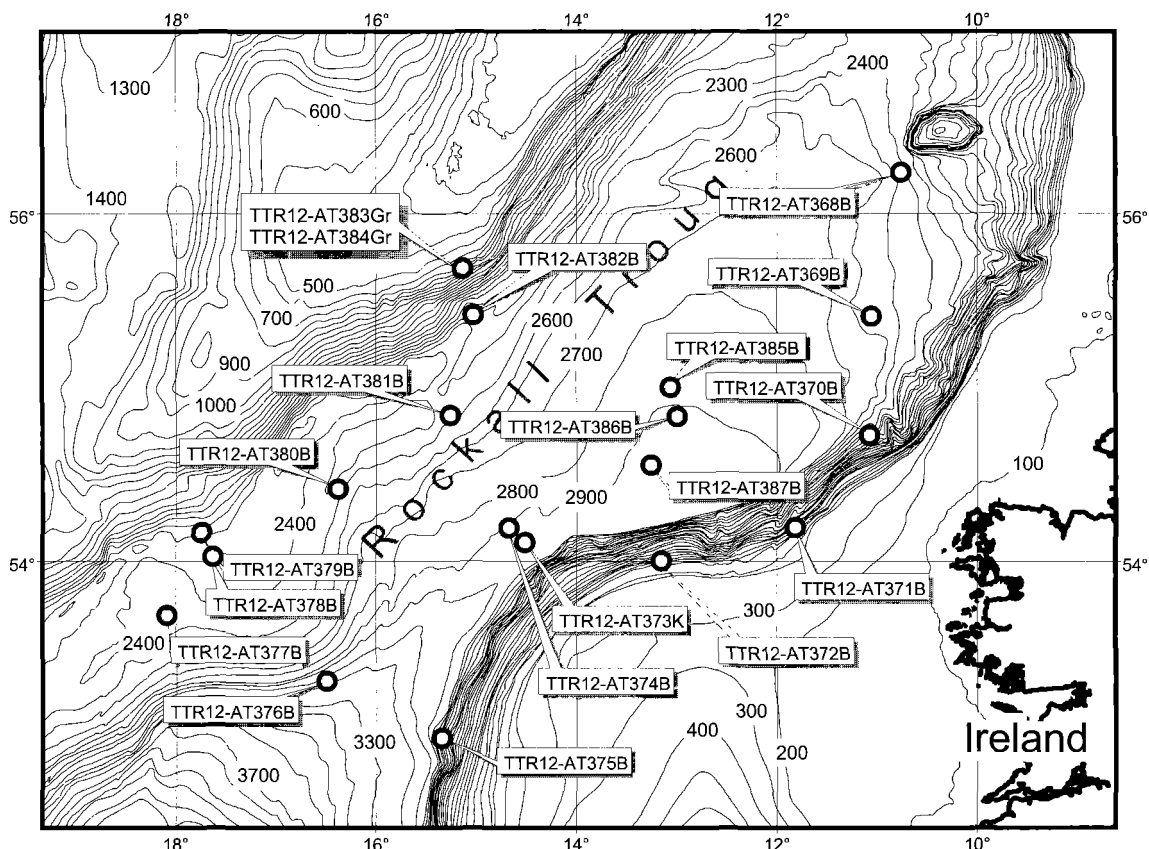


Figure 14. Location map of the sampling stations in the Rockall Trough.

Table 2. Sampling sites in the Rockall Trough.

CORE No	DATE	TIME, GMT	LATITUDE	LONGITUDE	Depth, m
AT-368B	24.06	16:37	56°13,737	10°46.106	2350
AT-369B	25.06	00:05	55°25,099	11°03.788	2540
AT-370B	25.06	11:53	54°44,097	11°05.355	2266
AT-371B	25.06	18:27	54°11,863	11°49.732	1299
AT-372B	26.06	02:46	54°00,048	13°09.411	922
AT-373K	26.06	15:55	54°06,543	14°31.151	2929
AT-374B	26.06	19:52	54°11,672	14°41.074	2781
AT-375B	27.06	05:45	52°56,429	15°21.120	2664
AT-376B	27.06	12:59	53°16,980	16°29.997	3187
AT-377B	27.06	21:33	53°40,671	18°05.582	2397
AT-378B	28.06	02:05	54°01,491	17°37.996	2440
AT-379B	28.06	04:57	54°09,975	17°44.994	2382
AT-380B	28.06	12:09	54°25,335	16°23.190	2327
AT-381B	28.06	18:50	54°50,904	15°16.014	2358
AT-382B	29.06	00:43	55°25,487	15°02.020	2250
AT-383G	29.06	13:07	55°41,263	15°08.617	703
AT-384G	29.06	15:56	55°41,278	15°08.580	693
AT-385B	30.06	06:41	55°00,730	13°03.816	2902
AT-386B	30.06	11:06	54°50,533	13°00.084	2919
AT-387B	30.06	15:40	54°33,811	13°15.831	2935

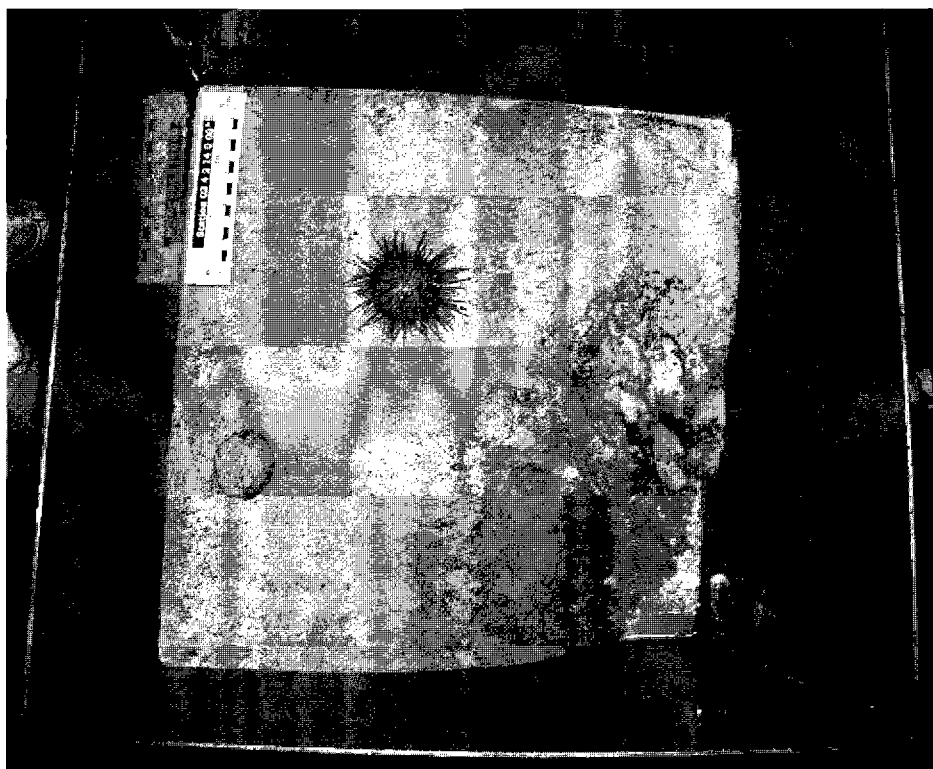


Figure 15. Sandy seafloor sampled at the station TTR12-AT372B (Water depth 922 m).



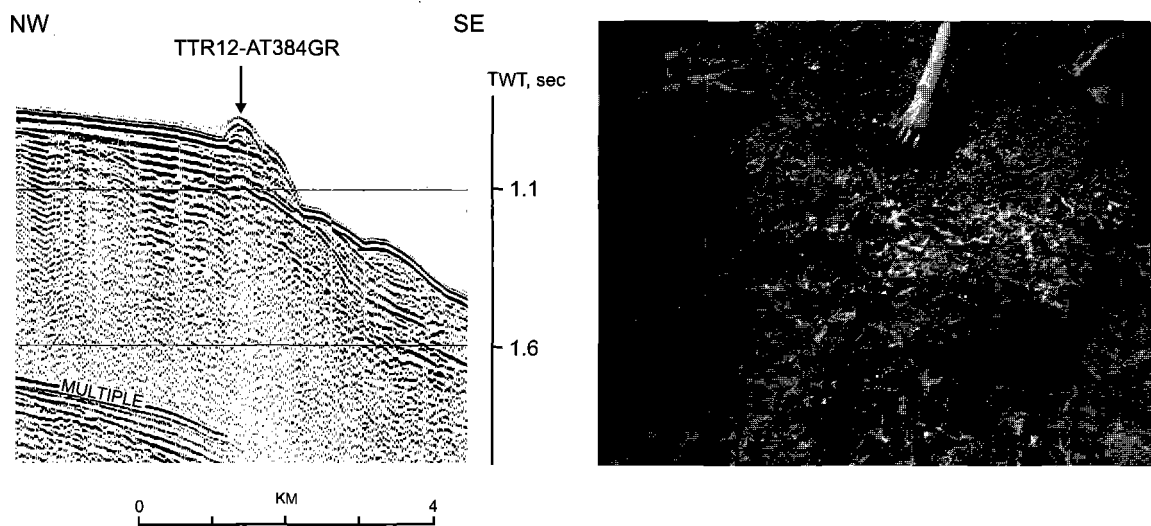


Figure 16. A fragment of the seismic line PSAT-21 (TTR-7 cruise, Kenyon et al., 1998) showing the carbonate mound sampled at the station TTR12-AT383Gr and TTR12-AT384Gr.

ance. Cores taken from the basin plain contained brownish grey marl with abundant foraminifera and some silt admixture. The upper 10-15 cm of the sequence were usually oxidized with a dark, manganese-rich layer underneath.

Two cores collected from the upper slope of the eastern flank of the Trough, at depths of 1299 and 922 m, recovered sequences of pale yellow medium to coarse sand with dropstones (Fig. 15).

Two TV grab sampling stations (TTR12-AT383Gr and TTR12-AT384Gr) were located on a presumed carbonate mound developing at the edge of an escarpment running along the upper slope of the western flank of the Rockall Trough (Kenyon et al., 1998) (Fig. 16). A large amount of coral debris was recovered with typical representatives of cold water fauna like Bivalvia, Gastropoda, Cidaroidea, shrimps, and others.

## 2. GULF OF CADIZ (LEG 2)

### 2.1. Introduction and objectives of the Leg 2

During TTR-9 (1999) a large mud volcano field was discovered in the Spanish and Moroccan sectors of the Gulf of Cadiz (Gardner, 1999; Kenyon et al., 2000; Gardner, 2001), based on a sidescan mosaic collected in the area in 1992 (courtesy of Joan Gardner,

Naval Research Laboratory (NRL), Washington D.C.). Five mud volcanoes were then identified: (1) TTR, Kidd and Adamastor, in the Eastern Moroccan Field, and (2) Yuma and Ginsburg, in the Middle Moroccan Field. Gas hydrates were recovered from the Ginsburg mud volcano. Since then, this area has been extensively investigated during the TTR-10 and the Anastasya cruises, in 2000 (Kenyon et al., 2001; Somoza et al., 2001), the TTR-11 cruise, in 2001 (Kenyon et al., 2002), and the Belgian

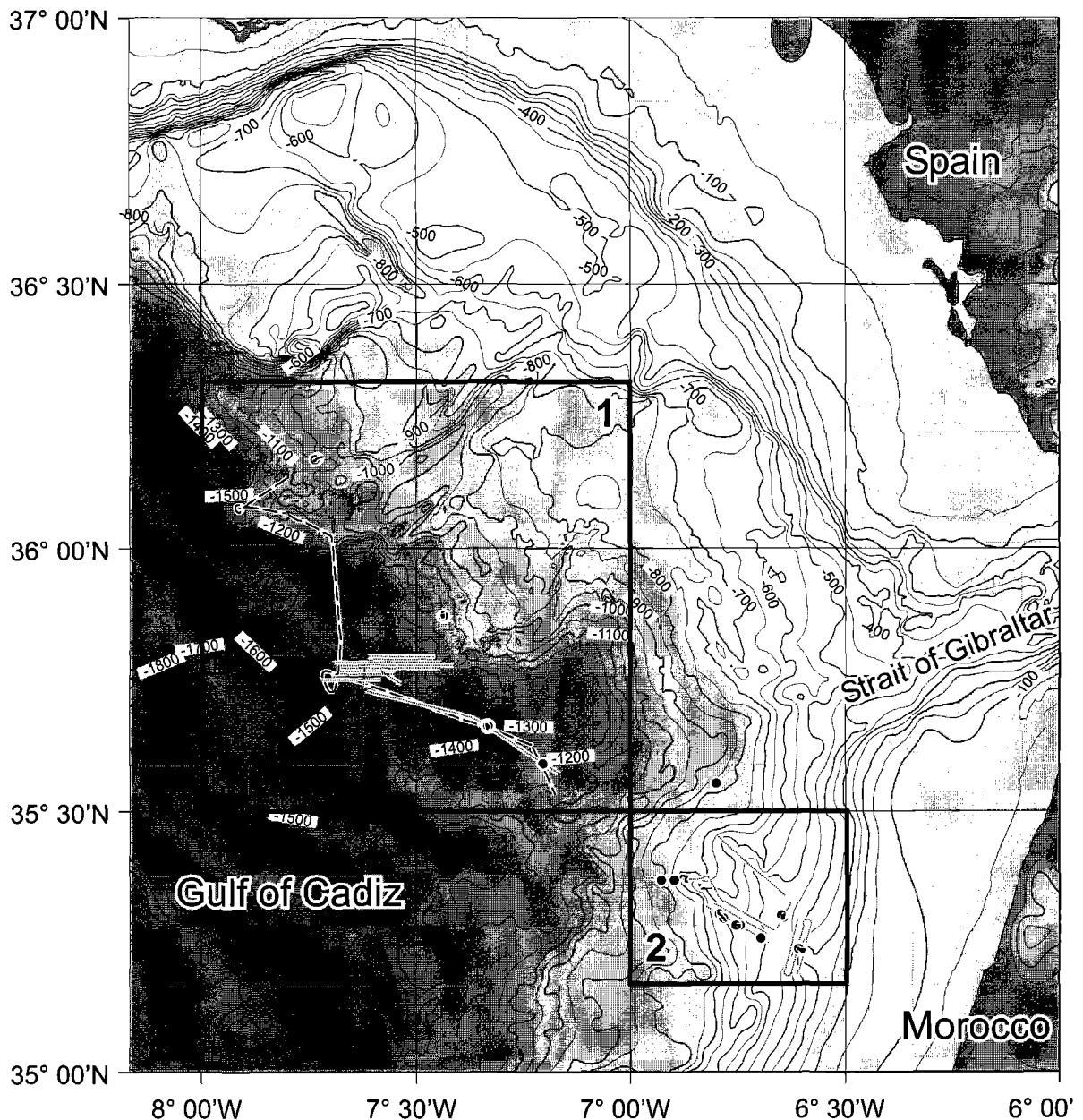


Figure 17. General location map of the Gulf of Cadiz showing study areas of the Leg 2. 1- South Portuguese Mud Volcano Field; 2 - El Araiche Mud Volcano Field.

Cadipor Cruise, in 2002. Over 20 new mud volcanoes have been discovered, as well as mud diapirs (Lolita, Iberico), often forming elongated diapiric ridges (e.g. Guadalquivir, Cadiz, Formosa, Vernadsky and Renard). Sampling has shown that some of the diapiric structures from the northern part of the Gulf of Cadiz, characterized by a strong-backscatter signature on the sidescan sonar mosaics, are covered with carbonate crusts and chimneys (e.g. Guadalquivir, Formosa and Cadiz). Gas hydrates have also been recovered from the Bonjardim mud volcano (Kenyon et al., 2001).

TTR-12 Leg 2 concentrated in three areas of the Gulf of Cadiz, each one with specific scientific objectives (Fig. 17). Area 1 is located between the Formosa Diapiric Ridge and the Jesus Baraza mud volcano; Area 2 is a sand lobe located southwest of the Aveiro mud volcano; Area 3 is the Al Araiche Mud Volcano Field, discovered in the Eastern Moroccan area, in May 2002, during a survey with the R/V Belgica. The main scientific objectives for Area 1 were: (1) to investigate an area of strong backscatter south of the Formosa Diapiric Ridge, thought to be covered by carbonate chimneys and crusts; (2) to investigate a few new features observed in the NRL sidescan sonar mosaic, some of which could represent mud volcanoes; (3) to revisit the Jesus Baraza and the Aveiro mud volcanoes to do more sampling and run underwater TV profiles. The main objective for Area 2 was to map in detail a sand lobe observed on the NRL sidescan mosaic, using very high resolution deep-towed MAK-1 sidescan sonar, to characterize the patterns of sand deposition. The main objectives for Area 3 were: (1) to image the sea floor in the El Araiche Mud Volcano Field and complement the swath bathymetry and high-resolution seismic data acquired during the Cadipor cruise; (2) to sample mud volcanoes and active fluid vents and document geosphere-biosphere interactions in this area. Integration with the existing data sets will allow reconstruction of the 3D geometry of the mud volcanoes, document the formation mechanisms, study their present activity and explore the biology associated with the mud

vents and fluid seeps.

## 2.2. Geological setting

L. PINHEIRO

The Gulf of Cadiz, located at the front of the Betic-Rifian Arc, has had a very complex geological history and undergone several episodes of rifting, compression and strike-slip motion, since the Triassic (Wilson et al., 1989; Dewey et al., 1989; Maldonado et al., 1999). The westward migration of the Gibraltar arc during the Late Tortonian caused the Gulf of Cadiz to form as a forearc basin (Bonnin et al., 1975, Auzende et al., 1981; Maldonado and Comas, 1992; Maldonado et al., 1999). After the emplacement of the thrusting units, gravitational sliding of the mobile shale and salt stocks formed a giant mass-wasting deposit, the Gibraltar Olistostrome, that migrated west towards the Horseshoe and Seine abyssal plains. The olistostrome body consists of a chaotic mixture of Triassic, Cretaceous, Paleogene and Neogene sedimentary units, overlying a Palaeozoic basement, and it is characterized on seismic reflection profiles by chaotic, high-amplitude reflectors with diffractions and hyperbolic reflections (Riaza and Martinez del Olmo, 1996). These chaotic units involve a huge volume of mud and salt diapirism of Triassic salt units and under-compacted Early-Middle Miocene plastic marls (Maldonado et al., 1999).

Throughout this area, pockmarks, extensive mud volcanism, carbonate mounds and chimney structures related to hydrocarbon rich fluid venting and mud diapirism are observed (Baraza and Ercilla, 1996; Kenyon et al., 2000). In the northeastern sector of the Gulf of Cadiz, authigenic carbonate chimneys and crusts have been collected from the Iberico mud diapir, discovered in 2000 (Diaz del Rio et al., 2001). To the east of this structure a large NE-SW diapiric ridge, the Guadalquivir Diapiric Ridge (GDR) is observed, from the shelf break to 1200 m. This ridge controls the orientation of the main channel of the Mediterranean Outflow Water (MOW) undercurrent and it is com-

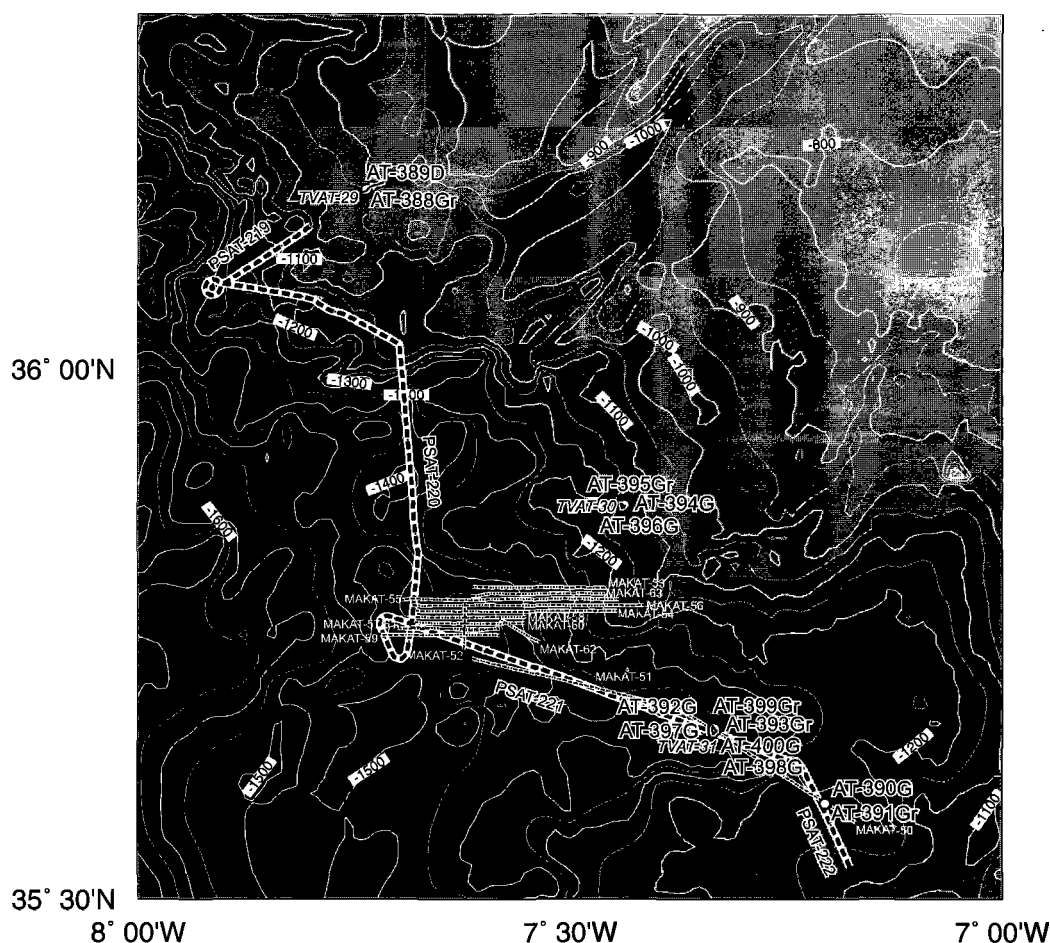


Figure 18. Location map of the South Portuguese Mud Volcano Field.

posed of a series of wide, sub-circular conical mounds surrounded by ring-shaped seafloor depressions. Most of these depressions are filled by contourite deposits of the MOW. Some of them, mainly on the right side of the main MOW channel, are formed down-current of the mounds and the depressions have a step-like profile, often symmetric with benches along the slopes.

### 2.3. South Portuguese mud volcano field

#### 2.3.1. Seismic data

L. PINHEIRO, R. PERALTA, A. VOLKONSKAYA,  
I. KUVAEV AND S. AGIBALOV

During the first part of Leg 2, four contiguous single channel seismic lines (PSAT-219, PSAT-220, PSAT-221 and PSAT-

222), with a total length of about 112 km, were acquired in the Portuguese sector of the Gulf of Cadiz, in an area of mud volcanoes, micro-basins and diapiric ridges (Fig.18). The seismic lines are located at the base of the continental slope, in water depths of 1000 m to 1400 m, more or less parallel to the slope. The maximum penetration is over 1 sec TWT, with an optimal theoretical vertical resolution of about 4 m. The lines cross several approximately circular features, visible on the NRL sidescan mosaic, between the southern end of the Formosa Diapiric Ridge (Line PSAT-219) and the Jesus Baraza mud volcano (PSAT-222).

The tectonic deformation increases to the NW, from Line PSAT-222, over the Jesus Baraza mud volcano, to Line 219, close to the southern end of the Formosa Diapiric Ridge. It changes from long-wavelength asymmetric folds (Lines PSAT-222 and PSAT-221), to

shorter wavelength and larger amplitude asymmetric folds (Line PSAT-221) and to a more pure-strike-slip regime with positive flower structures in the vicinity of Formosa Diapiric Ridge (Line PSAT-219).

Six main seismic units separated by major unconformities were identified on the seismic lines and tentatively correlated with the seismic stratigraphy defined by Maldonado et al. (1999). From base to top, these are: (1) Olistostrome/accretionary

complex unit, characterized by chaotic, high amplitude reflectors with diffractions and hyperbolic reflections; (2) Messinian units, characterized by low-amplitude seismic facies with continuous, almost parallel reflections and intense folding and faulting (M2-M3); the upper boundary of this unit is a prominent unconformity that laterally changes into a correlated conformity; (3 and 4) Pliocene units (P1 and P2), separated by a well defined unconformity: P1 is character-

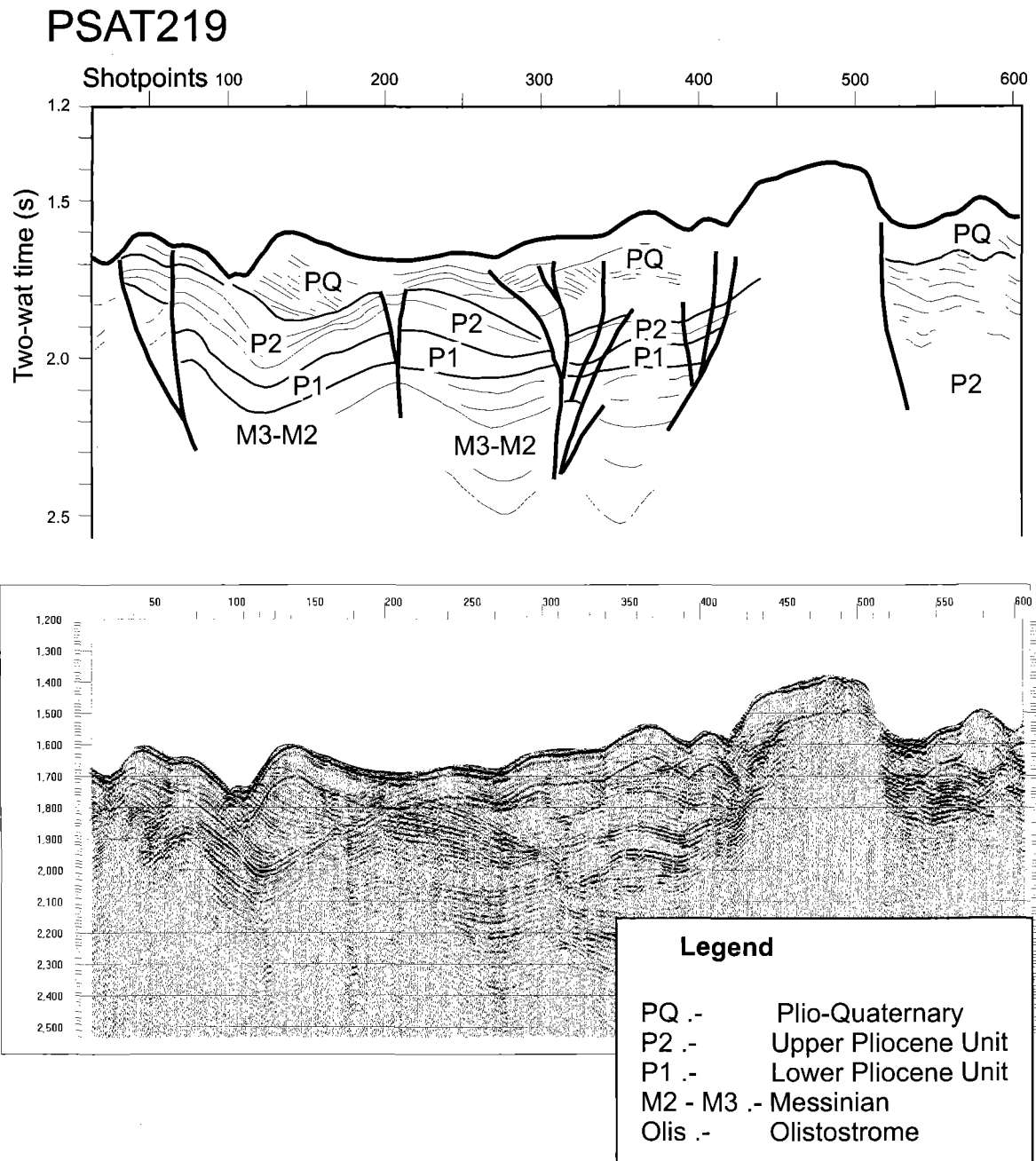


Figure 19. Interpretation of seismic line PSAT-219 across Formosa Diapiric Ridge.

ized by a generally continuous sequence of transparent and low to medium amplitude internal parallel reflections with high amplitude at the top; P2 is a well stratified unit with high amplitude, continuous reflections with lateral facies variations; (5) Late Pliocene-Quaternary sequence (PQ). It is a transparent unit with parallel and oblique reflections, showing only minor deformation. Its lower boundary is a major continuous erosional unconformity. The internal reflection pattern displays a significant northwestwards increase in its thickness with lateral facies variations. The facies changes in this unit are probably caused by the development of contourites and erosional surfaces in the northwest part of the Gulf of Cadiz, well evident on Line PSAT-219, due to the circulation of the Mediterranean Outflow Water.

Diapirs and mud volcanoes vertically disrupt the stratification. They are characterized by a dome-shaped elevation at the sea floor and a reflection-free seismic facies flanked by high-amplitude upturned reflections that interfinger with Units 2, 3 and 5 (Pliocene and Plio-Quaternary units, respectively).

#### Line PSAT-219 (Fig. 19)

This WNW-ESE line (SP1-SP623; Fig. 19) is about 21 km long. It is located close to the Guadalquivir Channel and Guadalquivir Diapiric Ridge. Two deformed domains are separated by a vertical no-event zone, probably a diapiric ridge, between SP430-SP500.

Northwards of this diapiric ridge, the Units 2, 3 and 4 are deformed, and a flower structure is identified. These units are folded and cut by normal and inverse faults, related to uplift of the ridge. Southeast of this feature, the Units P1, P2 and PQ, attributed to Pliocene and Plio-Quaternary, respectively (Maldonado et al., 1999), have a more simple structure.

The seismic unit PQ is characterized by complex seismic facies and changes laterally from a transparent acoustic response to low amplitude sequences. These facies variations are related to overbank deposits of the

Guadalquivir Channel or to contourite sediments. This unit covers a major erosive discontinuity that is well seen on this profile.

#### Line PSAT-220 (Fig. 20)

Line PSAT-220 (SP 623-1594) is about 33 km long and runs almost in a N-S direction, cutting Tasyo Field (Somoza et al., 2000). The mean depth penetration is about 500 ms TWT. All the topographic highs have a gentler southern slope.

Between SP1050 and SP1580 the top of the accretionary complex/olistostrome is visible as a semi-continuous reflector of high-amplitude, low frequency chaotic reflections at 400-450 ms TWT of depth

Tachuela mound (SP1210) disrupts stratification and only a few and small high-amplitude reflections occur at its southern flank. A possible inverse fault or thrust can be related to this mound and divides the profile into two sectors with different degrees of deformation. The deformation increases northwards (SP650-SP1200), and it is shown by the development of folds with increasing minor wave-length and faults affecting P1 and P2. Pliocene units are thicker at the north side of Tachuela mound (450-500 ms TWT) than at the south side (about 200 ms TWT).

In the southern sector (SP1200-SP1550), the deformation is represented by thrust-faults dipping southeast, which cut all the seismic units. Some of these faults seems to offset the sea-floor. Normal faults are also more common on the south side than on the north side, where they are seen only at the top of some antiforms.

#### Lines PSAT-221 and PSAT-222 (Fig. 21)

The main morpho-structural features identified in seismic lines PSAT-221 (trending WNW-ESE) and PSAT-222 (trending NNW-SSE) are, from NW to SE: a double dome-shaped feature, probably related to diapiric intrusion (SP2350-SP2500); the Captain Arutyunov mud volcano (SP2300-SP2500); a scarp associated with a thrust fault (SP3100); and the Jesus Baraza mud volcano (SP3300-SP3500). The sea-floor between

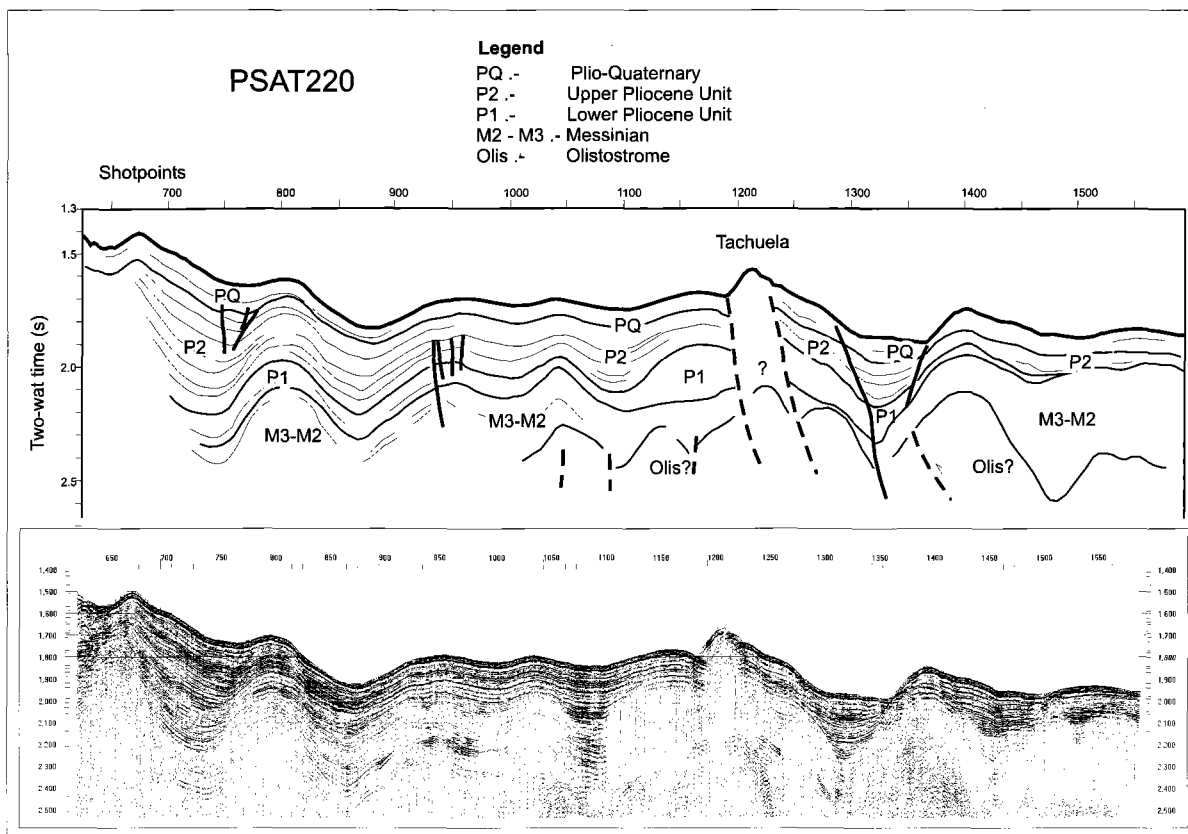


Figure 20. Interpretation of seismic line PSAT-220.

these features shows a smooth, sub-horizontal topography.

The top of the accretionary complex/olistostrome is best recognized in the line PSAT-222 (SP3150-SP3500), but it could also be identified in line PSAT-221 (SP1850-SP2050). It is cut by several southeast-dipping thrust-faults.

Above this structural complex there is possibly the Messinian seismic unit (M2 and M3). This is a transparent unit with some high amplitude discontinuous reflectors. Its upper boundary is a major erosional unconformity. This surface corresponds to the Miocene - Pliocene-Quaternary boundary according to Maldonado et al. (1999).

The Pliocene units P1 and P2 rest above the unconformity. The former is a transparent unit with some high amplitudes near its top. The P2 unit consists of a succession of alternating transparent sub-units and sub-units with continuously stratified parallel reflectors. The thickness of unit P1 decreases towards the north, from about 200 ms in line PSAT-222 (SP3050) until it disappears in the line PSAT-221 (SP2050).

The PQ onlaps a basal erosional unconformity. This unit is either a transparent unit (PSAT-221, SP2500-SP3100; and PSAT-222), or a unit with a succession of continuous and parallel reflectors, especially near its base.

The main structures recognized in these two seismic lines reveal northwestwards increasing deformation, shown by the presence of southeast-dipping thrust-faults, affecting all the seismic units, even the most recent one. Some of these faults seem to disrupt the sea-floor, and may be active. In the line PSAT-221 (SP1900) a north-dipping fault is identified, which appears to have normal movement, or at least, had been a normal fault in the past, and which did not suffer a strong inversion. The deformation is also shown by the presence of long-wavelength asymmetric folds, which affected especially the seismic units M2 and M1. The seismic units above them do not show this kind of folding.

On the single channel seismic data, the Captain Arutyunov mud volcano is characterized by several stacked outflow lenses

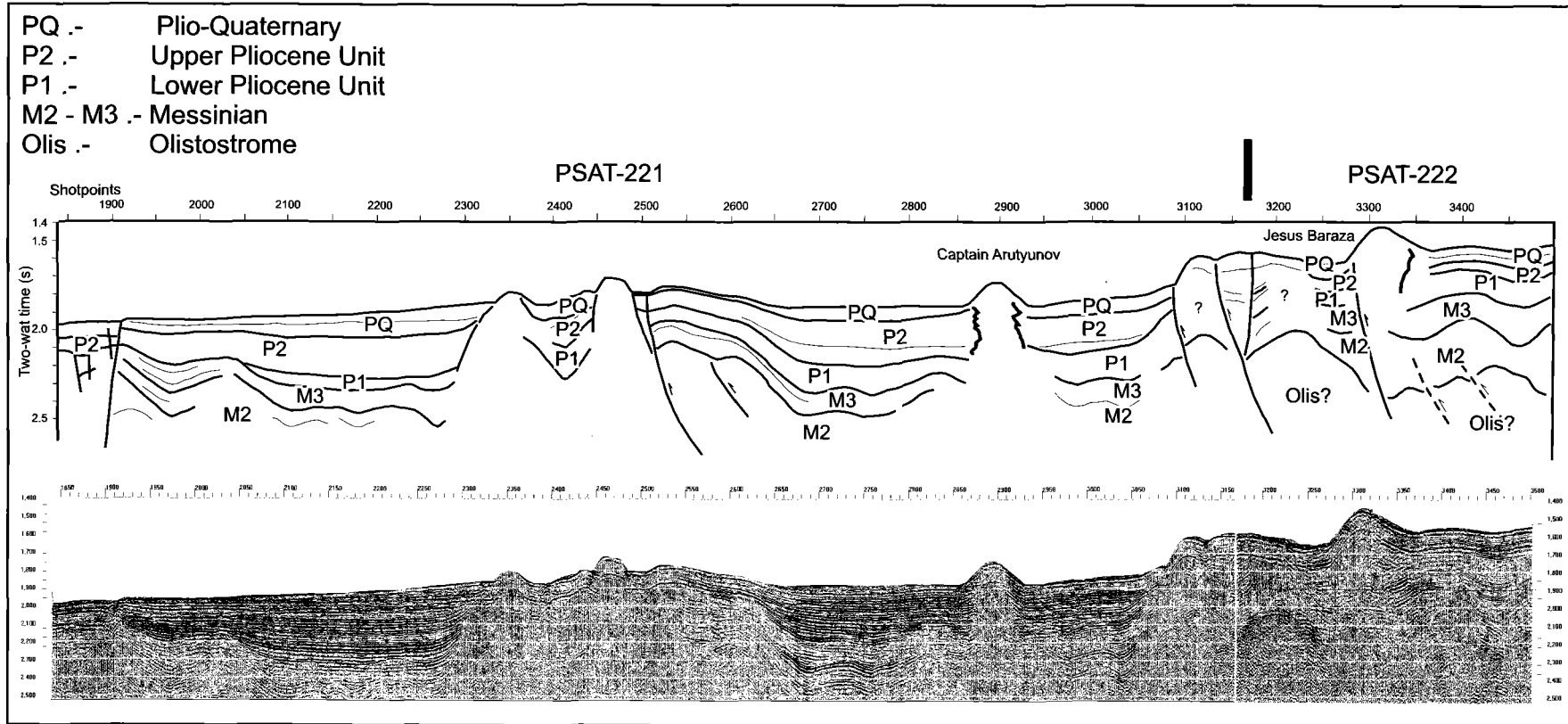


Figure 21. Interpretation of seismic lines PSAT-221 and PSAT-222.



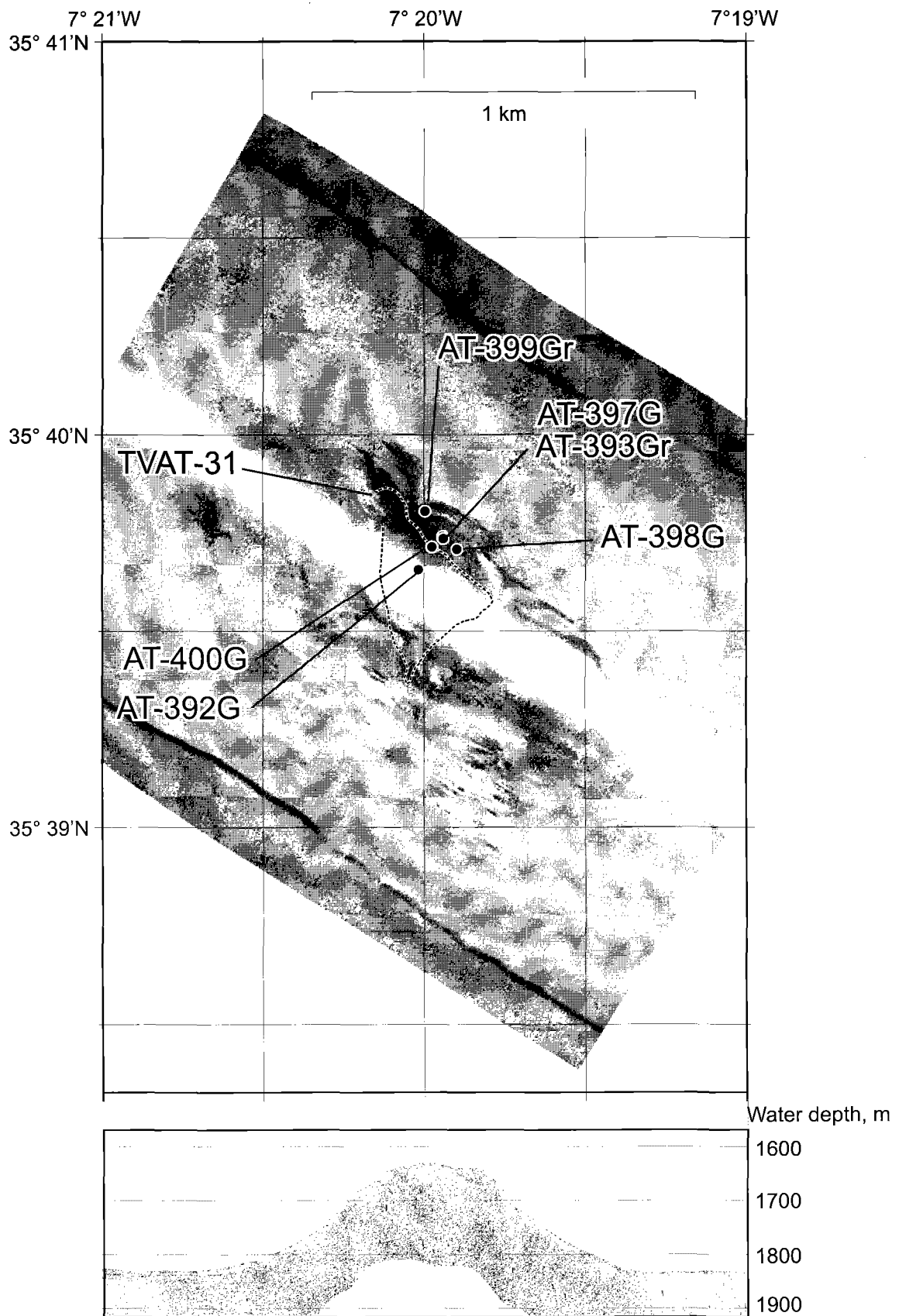


Figure 22. Fragment of sonograph and subbottom profiler records along the line MAKAT-50 showing the Captain Arutyunov mud volcano.

around a conical hill. The lowest level of outflow occurs about halfway through the Late Pliocene-Pleistocene sequence. The feeder system and the root of the mud volcano are not imaged.

The Jesus Baraza mud volcano has an asymmetrical shape with a steep, probably fault-bounded, northern flank and a smoother southern flank with several stacked outflow lobes.

### 2.3.2. Sidescan sonar data

N. R. PERALTA, L. PINHEIRO, M. IVANOV AND  
A. AKHMETZHANOV

Two survey lines (MAKAT-50 and MAKAT-51) were run using the MAK-1M deep-towed system with frequency of 30 kHz. MAKAT-50 crossed two structures which were thought to be mud volcanoes.

#### *Captain Arutyunov mud volcano*

A new mud volcano, named Captain Arutyunov after the late captain of the R/V *Profesor Logachev*, was discovered during the seismic survey. The Captain Arutyunov is an individual cone-shaped mud volcano on a flat basin floor (Fig. 22). It is about 100 m high, 2 km in diameter and has a 300 m wide circular crater at the top. The crater's structure is represented by a series of concentric rims. Several high backscattering mud flows are seen running down the flanks. Their flame-like shape suggests a low viscosity for the flows. At the base of the southern slope of the volcano there is an area with a blocky texture, which probably represents debris resulting from slope failure.

#### *Jesus Baraza mud volcano*

Whereas the Captain Arutyunov is not directly affected by faults, the morphology of the Jesus Baraza is partly controlled by its setting on top of a large diapiric uplift crossed by seismic line PSAT-222. The Jesus Baraza mud volcano is an asymmetrical hill with an ellipsoidal top (Fig. 23). It is about 150 m high, the crater is 1.6 km long and

about 600 m wide and has a concentric structure, similar to that of the Captain Arutyunov. It appears that the asymmetry of the crater area results from the presence of another, younger, crater developing about 300 m to the south of the older one. The sonograph shows evidence of a failure of the southern flank of the mud volcano resulting in displacement of a sediment block with dimensions of about 200x500 m. There is an area of high backscatter associated with the failure which is interpreted as a mud flow field.

Line MAKAT-51 was run during a transit to the next study area and crossed another diapiric ridge, well seen on seismic line PSAT-221. The sonograph did not show the presence of fluid escape structures. However the seabed topography was clearly affected by the diapiric uplift processes which resulted in elevated blocks and horst-like structures. Shallow slides and thinning of the sediment drape on the tops of the elevations indicate recent activity of the ridge (Fig. 24).

### 2.3.3. Bottom sampling

A. MAZZINI, G. AKHMANOV, M. CUNHA,  
A. AKHMETZHANOV, E. KOZLOVA, V. TORLOV,  
A. SAMOILOV, E. SARANTSEV, A. SADEKOV,  
E. POLUDETkina, O. BARVALINA, E. BILEVA,  
V. BLINOVA, N. USUPASHVILI, C. VASCONCELOS AND  
M. RACHIDI

During the first and the second parts of Leg 2 bottom sampling was focused on the northwestern and central areas of the Gulf of Cadiz (Table 3, Annex I). The Formosa Diapiric Ridge was investigated in the northwestern area and several mud volcanoes in the central area.

#### *Northwestern area, Formosa Diapiric Ridge*

The first subject for bottom sampling was a structure characterized by strong backscattering and well expressed on the 10 kHz SeaMap mosaic provided by the Naval Research Laboratory of USA. Two sites (TTR12-AT388GR and TTR12-AT389D) were

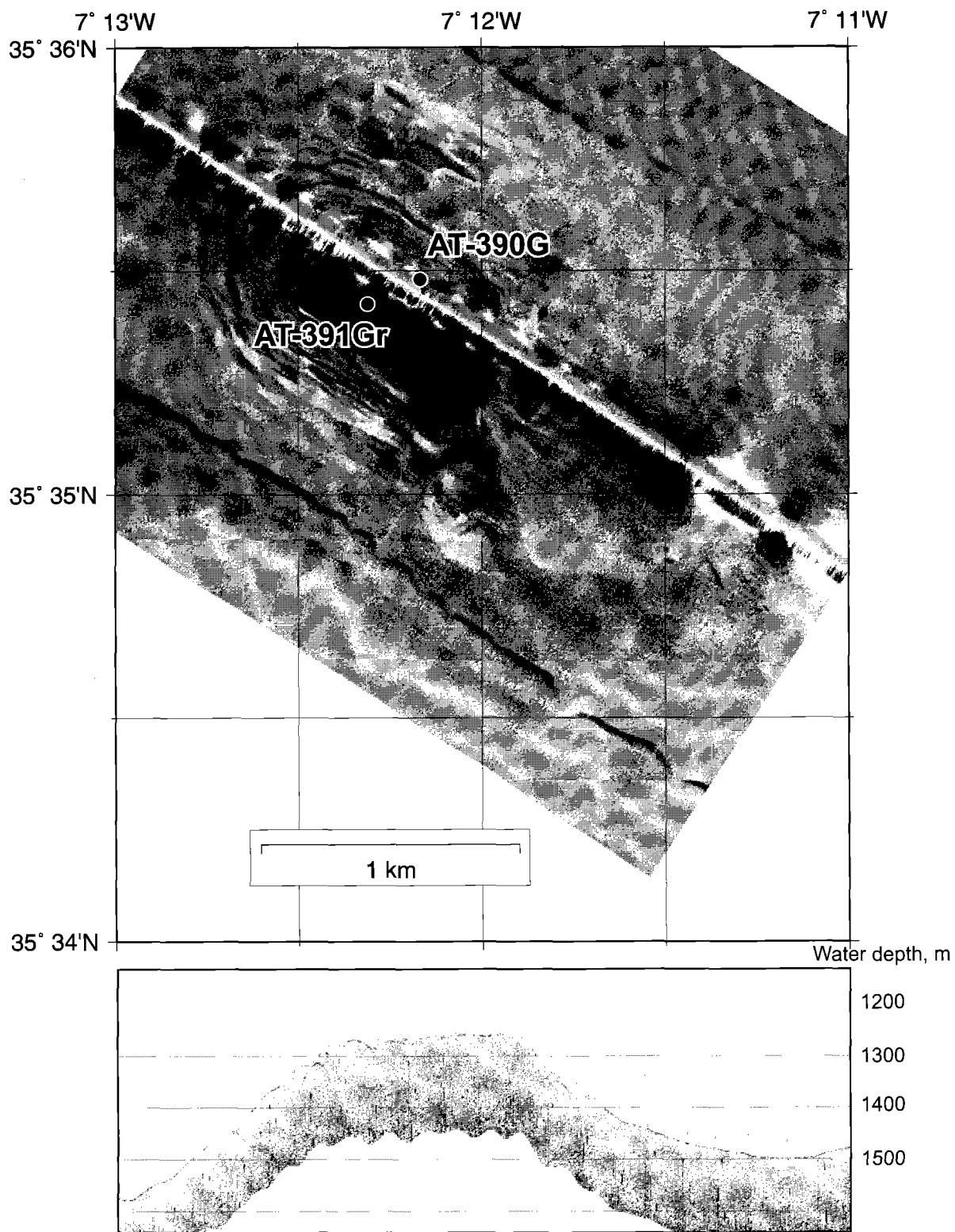


Figure 23: Fragment of sonograph and subbottom profiler records along the line MAKAT-50 showing the Jesus Baraza mud volcano.

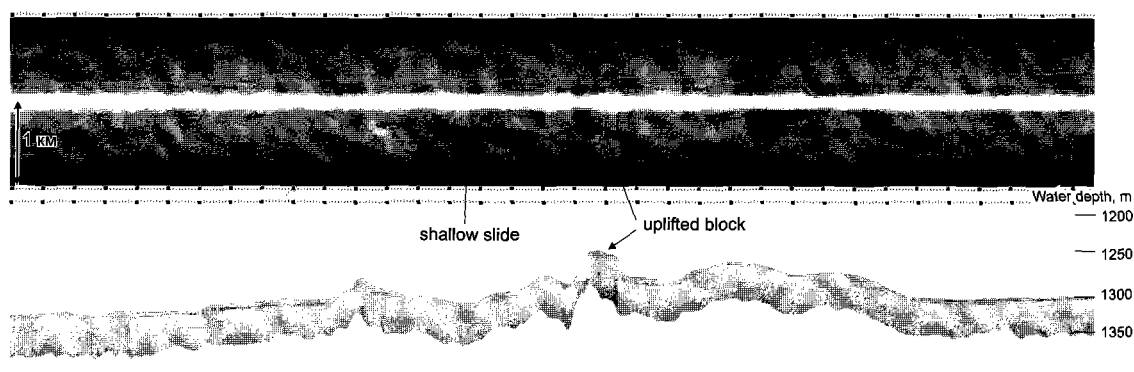


Figure 24. Fragment of sonograph and subbottom profiler records along the line MAKAT-50 showing seabed topography affected by the underlying diapiric ridge.

sampled in order to collect carbonate crusts which were expected to cover the diapiric ridge.

The TV grab recovery consisted of carbonate chimneys up to 2 cm in diameter and 25 cm in length, with a large proportion of these joined together as doublets or even triplets. The cement was aragonite. There were many cemented bivalve fragments (cf. Fam. Arcidae and other species) in the chimneys. Specimens of sponge (Porifera), serpulidae tubes (Polychaeta) and Bryozoa colonies were collected from the chimneys' surface.

Large samples of authigenic carbonate rocks were sampled by dredging. They were represented by slabs (20x50x5 cm) and isometric blocks (up to 25 cm in diameter) with large numbers of cemented bivalve (cf. Fam. Arcidae and other species) and coral fragments. All samples from both stations were oxidized.

#### Central area.

#### Jesus Baraza mud volcano

##### Station TTR12-AT390G

The upper 10 cm of the sequence is light greyish-brown marl with foraminifera, with a sandy admixture and large numbers of Pogonophora (Fam. Siboglinidae). The remaining section of the core consisted of grey, poorly sorted mud breccia with a clay matrix, a sandy-silty admixture, and angular and poorly rounded clasts of various sedi-

mentary rocks up to pebble size. This interval is gas saturated, with a smell of H<sub>2</sub>S and gas escape structures.

The core indicates that the mud volcano is active.

##### Station TTR12-391Gr

The upper 10 cm of the recovered section is water-saturated light-brownish carbonate clay with silty and sandy admixture and large numbers of Pogonophora (Fam. Siboglinidae), one large carnivorous gastropod and five Solemyidae specimens (4-8 cm in length). The interval contained several grey and brown, tabular (up to 3 cm thick) and very porous (pores are up to 7 mm in diameter) carbonate crusts.

The lower part of the sequence is light greyish dense mud breccia, consisting of clay matrix with claystone, sandstone and marlstone clasts of gravel and pebble size. Mud volcano sediments are intensively gas saturated (with a strong smell of H<sub>2</sub>S).

#### Captain Arutyunov mud volcano

##### Station TTR12-AT392G

Mud volcano sediments are grey, very poorly sorted mud breccia with a clay matrix and sandy-silty admixture, with angular and semi-rounded rock clasts (gravel to pebble in size). Clasts are mostly claystone, marlstone and sandstone fragments. The mud breccia was strongly gas saturated

(with smell of H<sub>2</sub>S and with gas escape structures). The mud breccia is covered by a thin veneer of brownish-grey pelagic marl.

Large numbers of Pogonophora (Fam. Siboglinidae), Polychaete and Scyphozoan tubes, and a Solemyidae shell fragment were found in the sediments, suggesting recent eruptive activity of the mud volcano.

#### Station TTR12-AT393Gr

Similar to the previous station. Mud breccia with a large number of rock fragments. Clasts (mainly claystones, marlstones, siltstones and sandstones) were separated and grouped into 30 lithologies.

#### Station TTR12-AT397G

The sample was collected from the mud volcano crater. The core consists of mud breccia, covered by 3 cm of marl, rich in foraminifera and with a sharp base. Mud breccia is grey, with clayey matrix, with randomly scattered fragments of lithified rocks (pebble size). The mud breccia had a strong smell of H<sub>2</sub>S. The uppermost layer contains a large number of Pogonophora (Fam. Siboglinidae).

#### Station TTR12-AT398G

Also from the mud volcano crater. Sediments consist mainly of grey porous mud breccia with randomly distributed fragments of semi-lithified rocks in a clayey matrix. The upper 3 cm are oxidized. Pogonophora are found in the uppermost part of the recovered section.

#### Station TTR12-AT399Gr

The TV grab collected a representative sample of mud breccia from the outermost part of the mud volcano crater.

A large quantity of grey mud breccia with randomly scattered rock fragments (gravel size) was recovered. The uppermost interval (upper 3 cm) is oxidized.

Fauna included: Pogonophora (Fam.

Siboglinidae), Polychaete worms, a few average sized Crustacea (isopods and amphipods), some unspecified Echinoderma, bivalve shell fragments (probably Fam. Thyasiridae) and fragments of Pteropoda.

#### Station TTR12-AT400G

The central part of the mud volcano crater was sampled. Recovery consisted of grey mud breccia with lithified and semi-lithified rock fragments. The mud breccia has very high gas-saturation and gas hydrate occurrence (millimetric crystals). Absence of coarse grained admixture is another distinctive feature of the recovered sediments.

Specimens of Pogonophora (Fam. Siboglinidae) are very common in the recovered sediments. A few Polychaete and Scyphozoan tubes are also found.

### Aveiro mud volcano

#### Station TTR12-AT394G

The sedimentary sequence is subdivided into three intervals. The upper one (0-4 cm) is brown marl with foraminifera. The middle interval (4-91 cm) is light grey homogeneous, bioturbated marl with foraminifera. The lower interval is mud breccia with a clayey matrix and a large number of sedimentary rock fragments (up to 0.5-1 cm diameter).

#### Station TTR12-AT395Gr

Light brownish grey marl with foraminifera and rock fragments (up to 0.5 cm in diameter) was recovered.

#### Station TTR12-AT396G

The upper 23 cm consist of brownish-grey marl with foraminifera. The lower part of the sequence (~96 cm) is dark grey mud breccia with clayey matrix, and silty admixture, with angular and semi-rounded rock fragments (gravel and pebble in size), represented mainly by claystones, sandstones and

Table 3. Sampling sites in the Gulf of Cadiz.

CORE No	DATE	TIME. GMT	LATITUDE	LONGITUDE	POSITION	DEPTH. m
AT-388Gr	08.07.02	15:53	36°10.263N	7°43.819W	OKEAN	1079
AT-389D	08.07.02	17:26 18:14	36°10.271N 36°10.123N	7°43.772W 7°44.121W	OKEAN	1080 1068
AT-390G	09.07.02	10:25	35°35.481N	7°12.168W	Jesus Baraza mud volcano	1102
AT-391Gr	09.07.02	12:03 13:20	35°35.426N 35°35.439N	7°12.311W 7°12.264W	Jesus Baraza mud volcano	1104 1105
AT-392G	09.07.02	16:02	35°39.656N	7°20.018W	Captain Arutyunov mud volcano	1320
AT-393Gr	09.07.02	17:16 17:55	35°39.544N 35°39.740N	7°20.044W 7°19.942W	Captain Arutyunov mud volcano	1336 1327
AT-394G	11.07.02	02:17	35°52.225N	7°26.243W	Crater of Aveiro mud volcano	1098
AT-395Gr	11.07.02	03:20 04:22	35°52.216N 35°52.226N	7°26.197W 7°26.282W	Aveiro mud volcano mud volcano	1098 1094
AT-396G	11.07.02	06:08	35°52.318N	7°26.206W	Aveiro mud volcano mud volcano	1090
AT-397G	13.07.02	15:13	35°39.735N	7°19.940W	Captain Arutyunov mud volcano	1326
AT-398G	13.07.02	21:19	35°39.709N	7°19.898W	Captain Arutyunov mud volcano	1322
AT-399G	13.07.02	22:43 23:49	35°39.728N 35°39.805N	7°19.816W 7°19.997W	Captain Arutyunov mud volcano	1332 1339
AT-400G	14.07.02	01:32	35°39.714N	7°19.976W	Captain Arutyunov mud volcano	1324
AT-401G	14.07.02	06:00	35°33.154N	6°48.036W	Tanger mud volcano	794
AT-402G	14.07.02	06:52	35°33.168N	6°48.105W	Tanger mud volcano	773
AT-403G	15.07.02	02:03	35°15.360N	6°41.890W	Fuiza mud volcano	385
AT-404G	15.07.02	03:22	35°16.865N	6°44.764W	Gemini mud volcano. Larger crater	433
AT-405G	15.07.02	04:14	35°16.853N	6°45.330W	Gemini mud volcano. Smaler crater	432
AT-406GR	15.07.02	13:09 13:13	35°18.142N 35°18.148N	6°47.667W 6°47.666W	Coral Bank escarpment	555 550
AT-407GR	15.07.02	16:12 16:26	35°17.672N 35°17.695N	6°47.060W 6°47.082W	Coral Bank escarpment	562 560
AT-408G	16.07.02	14:34	35°17.756N	6°38.685W	Mercator mud volcano	368
AT-409D	16.07.02	15:14 15:39	35°17.688N 35°17.929N	6°38.603W 6°38.903W	Mercator mud volcano	397 375
AT-410D	16.07.02	17:17 17:43	35°17.796N 35°18.014N	6°38.716W 6°38.986W	Mercator mud volcano	366 392
AT-411G	16.07.02	23:42	35°14.029N	6°36.207W	Al Idrisi mud volcano	210
AT-412D	17.07.02	00:17	35°14.252N 35°14.193N	6°36.725W 6°36.609W	Al Idrisi mud volcano	235 230
AT-413G	17.07.02	12:40	35°22.048N	6°55.759W	TTR mud volcano	695
AT-414G	17.07.02	13:38	35°22.043N	6°53.985W	Small elevation on MAKAT-75	709

marlstones. There is no smell of  $H_2S$  or gas escape structures.

### Tanger mud volcano

Line PSAT121 (TTR-9) crossed a dome shaped structure, characterized by a strong backscatter on the acoustic seabed image. Bottom sampling confirmed that this is a mud volcano. The volcano was named after one of the cities of Morocco.

#### Station TTR12 -AT401G

The recovery consists of grey mud breccia with randomly distributed fragments of lithified and semi-lithified rocks. The upper 4 cm are oxidized. Breccia is bioturbated with burrows, filled with greyish-brown sediments (similar to the upper 4 cm) in the interval 22-53 cm.

#### Station TTR12-AT402G

Sediments, recovered by the gravity corer are mainly mud breccia, covered with a clay layer (23 cm). The boundary between these layers is sharp. The mud breccia was grey in colour and contains fragments of lithified and semi-lithified rocks (up to 2 cm in size). The interval is gas-saturated which suggested recent activity of the Tanger mud volcano.

## 2.4. Sand lobe mapping

N. H. KENYON, A. AKHMETZHANOV, M. IVANOV,  
P. SHASHKIN AND I. KUVAEV

### *Introduction*

Part of Leg 2 was devoted to a high-resolution study of a sand lobe. The lobe is one of the three very similar lobes identified on the 10 kHz SeaMap imagery obtained by the NRL of USA (Gardner et al., 2002; Habgood et al., 2003) as prominent low backscattering features.

The lobe selected for the TTR study is located beyond the termination of the Gil Eanes contourite channel (Kenyon et al.,

2000; Habgood et al., 2003). The channel is formed by the Mediterranean Outflow Water, descending downslope from a depth of about 500 m to about 1200 m. The outflow transports a large amount of coarse-grained sediment along the channel. At a depth of 1200 m the bottom current lifts off the seafloor and becomes an intermediate water mass and does not influence the seabed any further. It is believed that the sandy sediments, which accumulate at this depths at high sedimentation rates, become prone to failure and a gravity flow system develops beyond this point forming a sand lobe at the bottom of the basin.

A piston core, taken from the lobe by Southampton Oceanography Centre (Habgood et al., 2003), recovered a sequence of massive sand with some mud clasts. During the TTR-11 cruise (Kenyon, 2002) a single high-resolution line with MAK-1M deep-towed sidescan sonar system in 100 kHz mode was run across the lobe revealing that the lobe actually represents a complex system of erosional and aggradational channels (Kenyon et al., 2002; Akhmetzhanov et al., 2002; Habgood et al., 2003).

The aim of the TTR-12 study of the lobe system was to obtain a high-resolution mosaic of the whole gravity flow system, from source to sink, using the sidescan system in the 100 kHz mode.

### *Results*

The survey consists of 11 closely spaced lines, each 700 m wide and from 9 to 13 km long. The lines were spaced at 600 m, thus providing sufficient overlap to achieve a complete coverage of the seabed. Deep towed 5 kHz subbottom profiles with a meter-scale resolution will be used to produce detailed bathymetric and isopach maps of the sand lobe system.

Three principal areas are identified: source area, transit area and depositional area (Fig. 25).

The source area is near the termination of the Gil Eanes channel and is above a water depth of 1150 m. The seafloor has an irregular topography dominated by south-

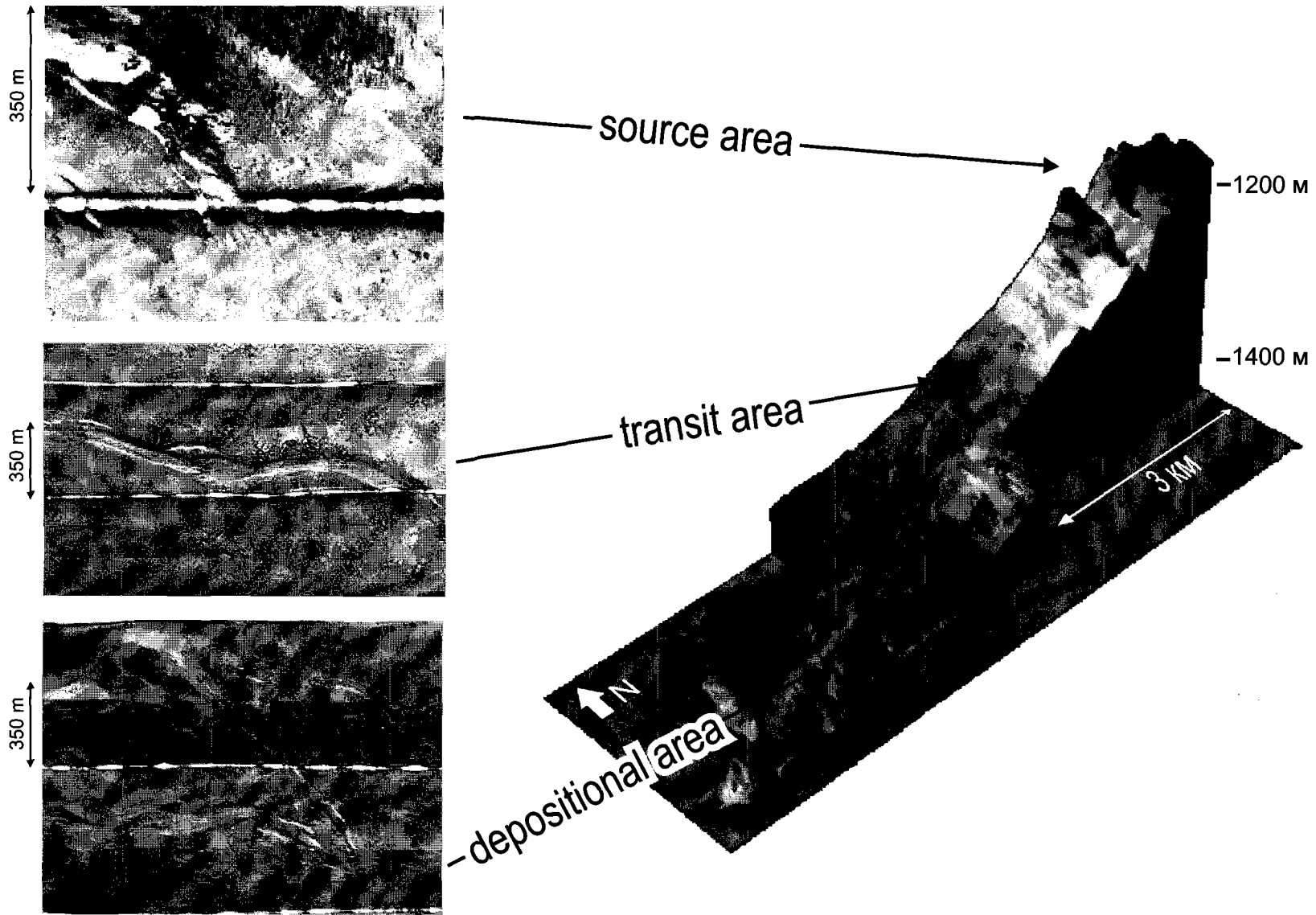


Figure 25. Block-diagram, showing seabed relief and details of the sand lobe system.



north trending ridges and troughs due to the presence of mud waves and escarpments. Local slopes are up to  $10^\circ$ . The 100 kHz sonograph shows a complex backscatter pattern, mainly due to the topography but also reveals low backscattering fields of mobile sand waves. The westernmost ridge has an opening beyond which there is a 250 m wide and 50 m deep sinuous channel running downslope through the transit area.

The transit area represents a gently dipping, generally smooth seafloor with a gradient of about  $1^\circ$  extending to a depth of about 1450 m, beyond which there is a reduction in slope gradient. Soon after leaving the opening in the ridge the channel becomes braided with a series of shallow, only few meters deep, distributaries developing to the north of the main slightly sinuous channel. The width of the channel remains about 250 m but its depth decreases to 2-5 m at the base of the slope suggesting a change from erosional to aggradational mode. The erosional, downstream facing grooves feathering the channel and distributaries, which were observed during the previous short survey (Kenyon et al., 2002), are very abundant along the system. Near the base of the slope the main channels develop levees, which, from the absence of penetration on the sub-bottom profiler record, are built up primarily of sand.

Beyond the break of the slope at 1450 m depth the seafloor flattens and the sonograph reveals a complex pattern of bifurcating channels. Sometimes channels cross each other, suggesting the presence of several systems of different age. The most recent system is located at the southern part of the lobe and is fed by the main channel. The position of this channel system fits well with the area of the lowest backscatter on the 10 kHz SeaMap image, interpreted as the youngest portion of the lobe (Habgood et al., 2003). The channels are from 10 to 50 m wide and often have well defined narrow levees. Subbottom profiler records show that the channels have an aggradational nature and the levees are a few metres high elongate elevations on the seafloor. The subbottom profiler records also indicate that the sand lobe seen on the son-

ographs corresponds to the uppermost acoustically chaotic package with sharp flat base and irregular upper surface. The thickness of this package is up to 8 m in places and it is thicker underneath the channel-levee complexes. The package overlies an acoustically well-stratified sequence. There are indications that the sequence may contain several other chaotic packages similar to the uppermost one.

The main results of the survey are:

- Complete coverage of the sand lobe was obtained;
- Presence of mobile sand feeding the system was established;
- Evolution of the channel system in a downslope direction from erosional to aggradational was observed;
- Importance of channelised features in the depositional area was recognised;
- High-resolution subbottom profiler data were collected, enabling a reconstruction of a detailed bathymetry and a map of the thickness of the sand body.

## 2.5. El Araiche mud volcano field

P. VAN RENSBERGEN, D. DEPREITER, M. IVANOV  
AND SHIPBOARD SCIENTIFIC PARTY OF THE TTR-12  
CRUISE

### 2.5.1. Introduction

The El Araiche mud volcano field consists of several mud volcanoes crowning two diapiric ridges (Fig. 26). The diapiric ridges are about 20 km long, they rise up from water depths of about 700 m and stretch to the shelf edge. The northernmost ridge, the Vernadsky ridge, has a NW-SE trend. About 10 km to the south, the Renard ridge has a WNW-ESE orientation and consists of a series of mud volcanoes (from W to E: Lazarillo de Tormes, Gemini, Don Quichot and Fiuza) and has steep fault bounded flank to the South (the Pen Duick escarpment). Between these two ridges three isolated mud volcanoes occur; (from W to E): Adamastor (see Kenyon et al., 2000), Mercator, and the

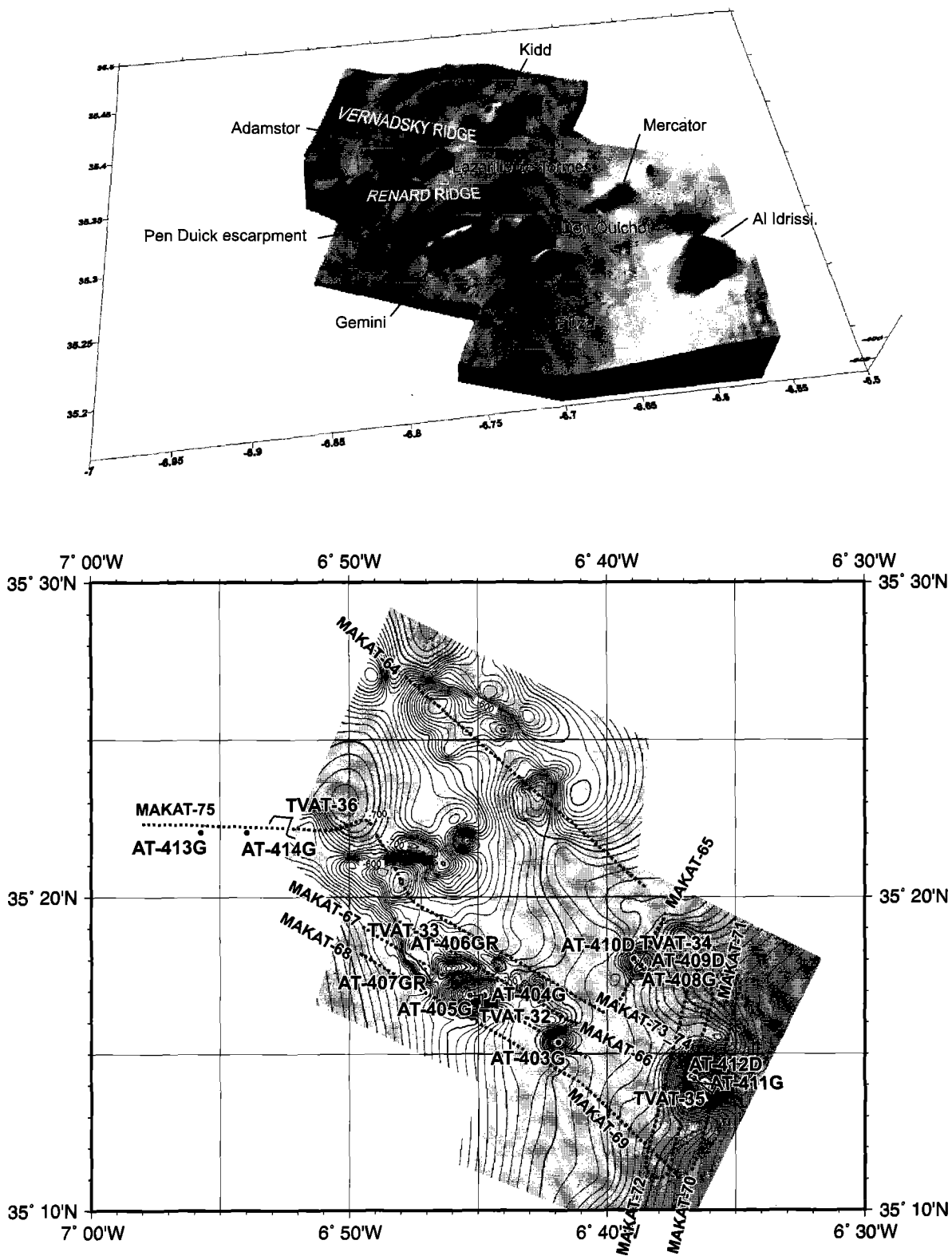


Figure 26. Location map of the El Araiche mud volcano field study area.

largest mud volcano in the field, Al Idrissi.

MAK1 sidescan sonar lines with a total length of about 160 km were acquired over the Vernadsky ridge (MAKAT-64) and over the Mercator mud volcano (MAKAT-65), and mosaics of sidescan sonar lines over the Renard ridge area (MAKAT- 66, 67, 68, and 72) and over the large Al Idrissi mud volcano (MAKAT-69, 70,71) were produced. TV lines and sample stations were selected on the basis of the sidescan sonar profiles (Fig 26).

### 2.5.2. Sidescan sonar data

#### *Vernadsky ridge area*

The Vernadsky ridge was surveyed by a single MAK1 sidescan sonar line but no samples or other detailed studies were made. Two distinct structures are identified on the line. There is a circular mud volcano associated with a diapiric uplift at the western tip of the ridge. The volcano is about 300 m in diameter and has several medium to high backscattering flows on its flanks. The seabed to the west and south of the mud volcano is covered with abundant compressional ridges. Considering the presence of a mud volcano this may indicate active uplifting of the ridge. The other structure is seen further to the southeast and represents a flat-topped elevation with a relatively steep slope, well seen on the sonograph as patchy, high backscattering areas. The Kidd mud volcano discovered during TTR-9 cruise (Kenyon et al., 2000) represents a part of this elevation and indicates its diapiric nature.

#### *Renard ridge area*

The Renard ridge is a NW-SE trending ridge apparently bounded by sub-parallel faults. Along the southern flank of the ridge several structures were identified:

#### *Fiuza mud volcano*

Fiuza is a conical shaped mud volcano, about 2.24 km wide at the base and 0.5 km at the top. The mud volcano is about 125

m high, the water depth at the top of the mud volcano is 400 m. It is characterized by a series of concentric rims with high-backscatter mud flows extending down the flanks, and up to 1.3 km from the crater.

#### *Gemini mud volcano*

Gemini is a large mud volcano with two separate circular craters (Fig. 27). The base of the mud volcano is about 4.9 km long and 2.5 km wide. The largest, eastern crater has a diameter of about 0.9 km, the western crater has a diameter of about 0.6 km. Both craters seem to be separated by an almost N-S trending fault. The twin mud volcano is 200 m high, and the water depth at the top is about 400 m. The mud volcano is also characterized by typical concentric rims and mud flows. Mud flows are especially large at the western side where they extend about 1.8 km down the slope. The craters were sampled by gravity cores AT 405G (eastern crater) and AT 404G (western crater). The craters and the sharp contact between the craters were seen on the TV line TVAT32.

#### *Pen Duick escarpment*

The Pen Duick escarpment is a fault scarp of about 4.5 km long, west of Gemini. The escarpment is about 100 m high, the waterdepth at the top is 525 m (Fig. 27). The escarpment changes from a NW-SE direction to an almost N-S strike. At the top of the escarpment, a platform with irregular backscatter pattern occurs. The eastern part of the platform is characterized by a hummocky topography. To the west the pattern changes to parallel elongated ridges. Gullies occur at the base of the escarpment.

The top of the platform was imaged along TV line TVAT33. On the basis of the TV images, TV guided grab samples were taken from dead coral banks (AT407GR) and a fault zone with carbonate slabs (AT406GR). The coral bank consists of a dead coral framework with terrigenous mud matrix with few living corals at the top. It is indicative of a more favourable coral habitat in the past, possibly related to strong currents in

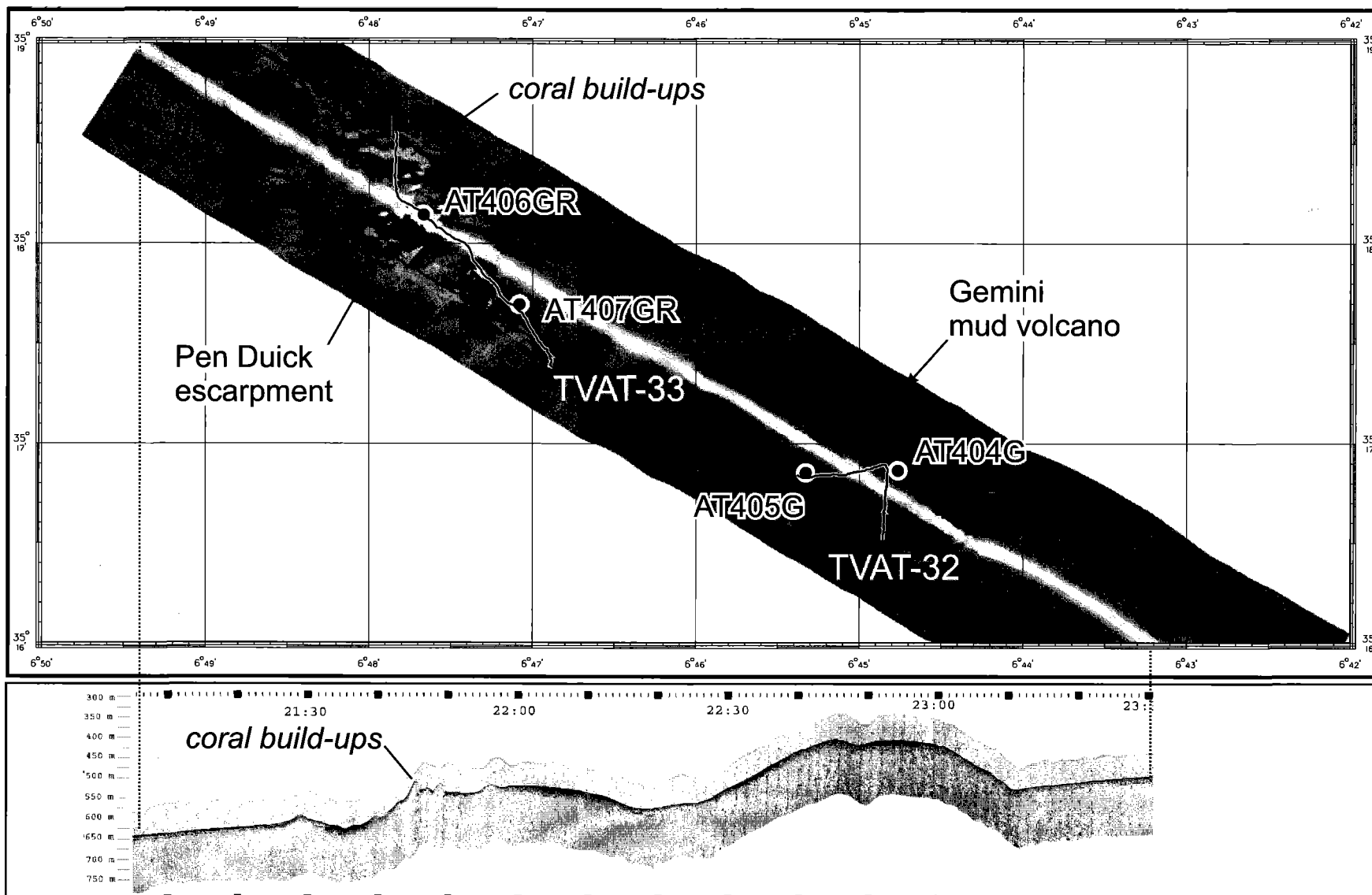


Figure 27. Fragment of line MAKAT-68 showing the Pen Duick escarpment and Gemini mud volcano.

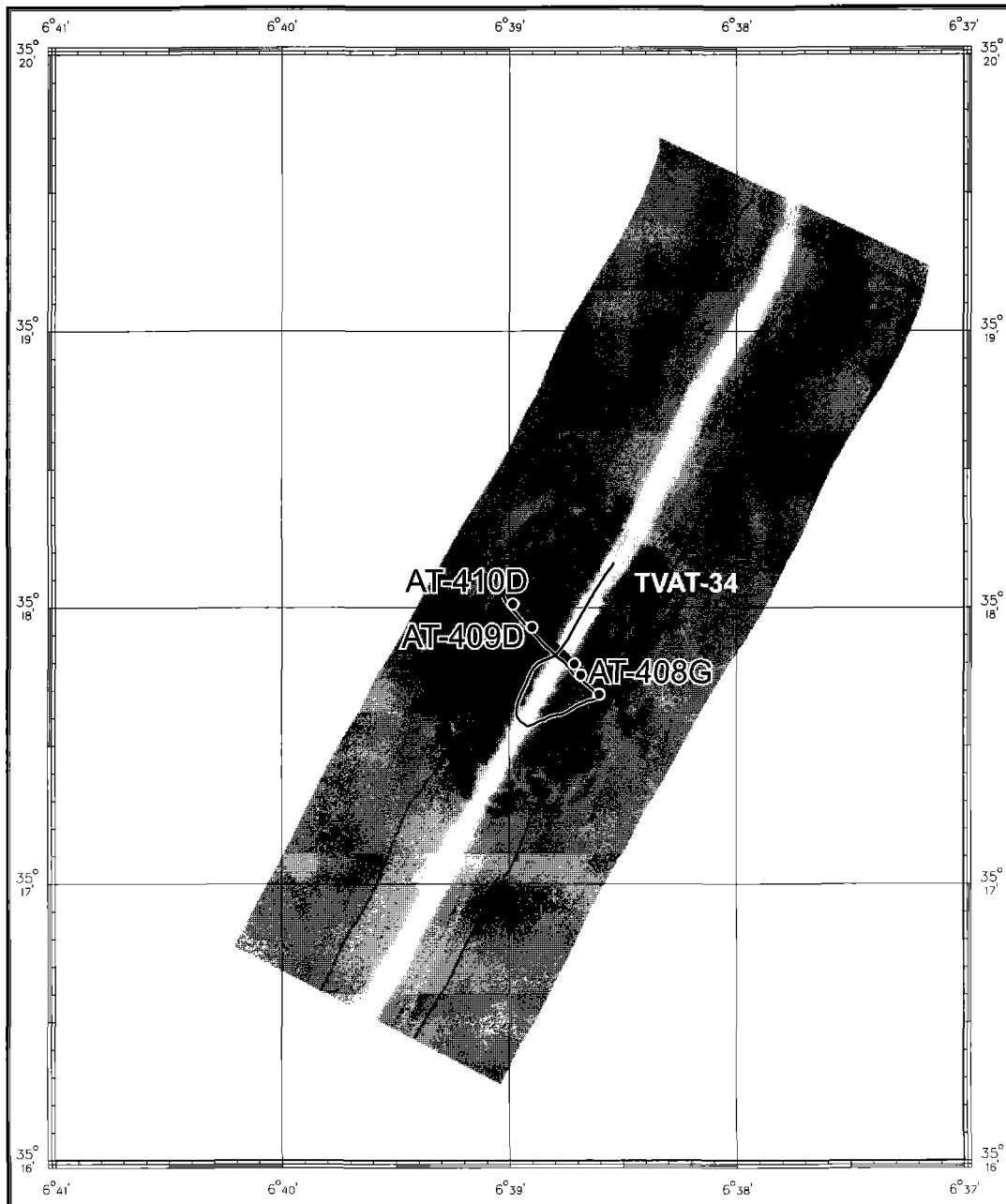


Figure 28. Fragment of line MAKAT-65 showing the Mercator mud volcano.

this area. The carbonate slabs consist of carbonate cement with shells, corals and other debris and may indicate present or past expulsion of hydrocarbon gases, probably along a fault zone.

Along the northern bounding fault a series of small mud volcanoes occur. They are Don Quichot, Lazarillo de Tormes, and two smaller, unnamed features. They have small craters with outflow lenses of especially high-backscatter.

#### *Isolated mud volcanoes*

#### Mercator mud volcano

Mercator is a conical shaped mud volcano, about 1.84 km wide at the base and 0.5 km at the top. The mud volcano is about 125 m high. The water depth at the top of the mud volcano is 350 m. It has a series of semi-concentric rims (rose petal pattern) with high-backscatter mud flows extending down the flanks (Fig. 28).

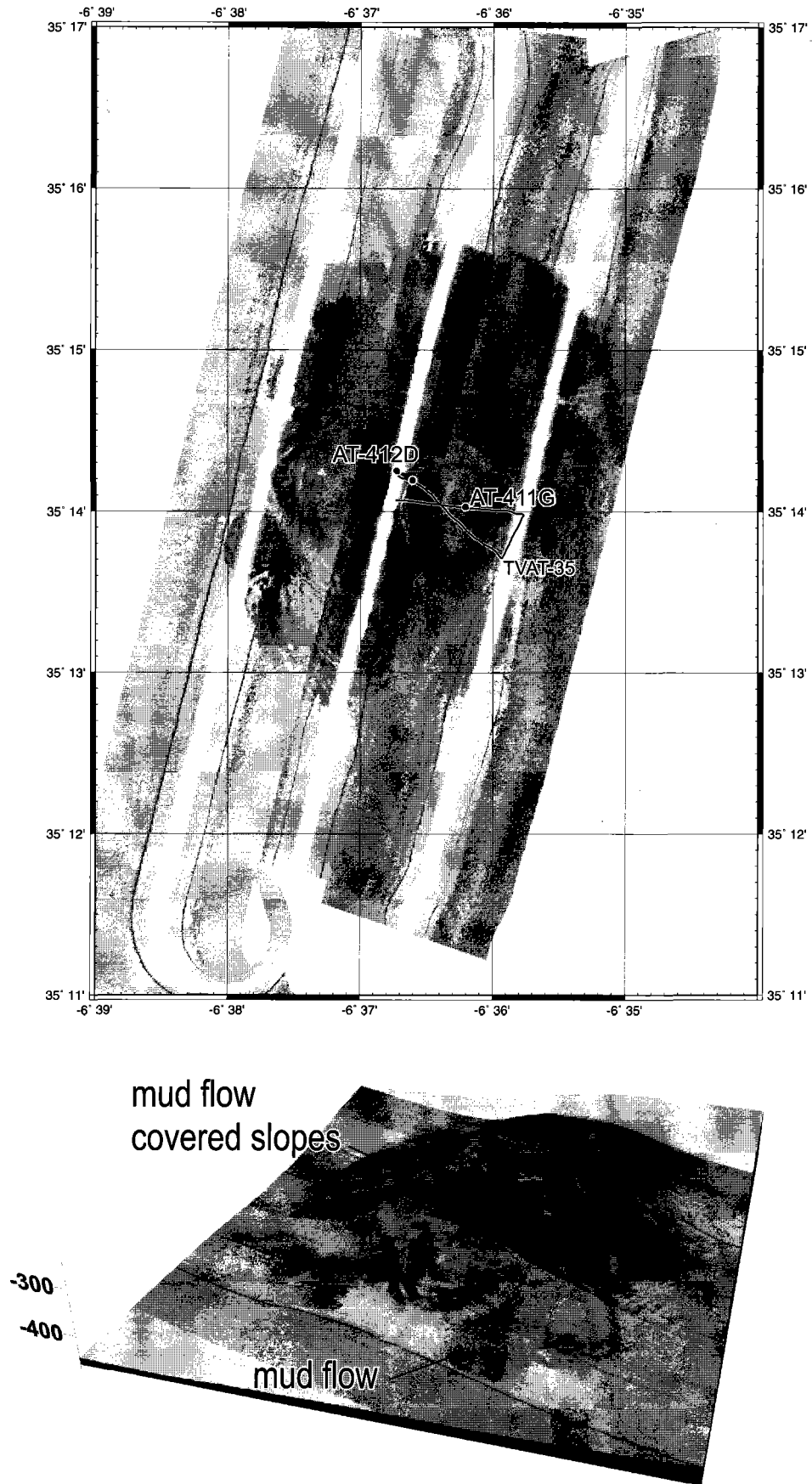


Figure 29. 30 kHz sonograph and perspective image of the Al Idrissi mud volcano based on multibeam bathymetry and MAK-1M acoustic data.

### Al Idrissi mud volcano

Al Idrissi is the largest mud volcano of the El Araiche mud volcano field. It is also a conical-shaped mud volcano, about 5.3 km wide at the base and 1.4 km at the top. The mud volcano is about 225 m high. The water depth at the top of the mud volcano is about 225 m. The Al Idrissi mud volcano is located on the very edge of the Moroccan shelf, forming a rounded promontory. The rims of the crater seem less developed than at other mud volcanoes but the mud flows are very large, especially at the western side, where they form over 2.5 km long mud flow lobes (Fig. 29).

#### 2.5.3. Bottom sampling

A. MAZZINI, G. AKHMANOV, A. AKHMETZHANOV,  
E. KOZLOVA, V. TORLOV, A. SAMOILOV,  
E. SARANTSEV, A. SADEKOV, E. POLUDETkina,  
O. BARVALINA, E. BILEVA, V. BLINOVA,  
N. USUPASHVILI AND M. RACHIDI

Location of core sites are listed in Table 3. Core logs can be found in Annex I

### Fuiza mud volcano

#### Station TTR12-AT403G.

A sequence of grey mud breccia overlain by a thin (12 cm) marl layer with foraminifera and pogonophora was recovered. The mud breccia has a clayey matrix, very gas-saturated and contains fragments of lithified and semi-lithified rocks. The boundary between marl and mud breccia layers is sharp.

Sampling data suggest that the Fuiza mud volcano is active at the present time.

### Gemini mud volcano, larger crater

#### Station TTR12-AT404G.

The recovered sequence contains two mud flows: 1) from 12 to 32 cm, below a pelagic upper layer from 0 to 12 cm; and 2)

from 32 to 160 cm with a pelagic upper section in the interval from 32 to 36 cm. The pelagic intervals are greyish-brown bioturbated marl with coarse-grained admixture.

Within the lower flow there are two intervals, at 60-83 and 118-126 cm, of granulated mud breccia. This may indicate a complex sedimentation pattern involving redeposition of mud breccia by a strong bottom current.

### Gemini mud volcano, smaller crater

#### Station TTR12-AT405G.

There is a sequence of grey mud breccia with clayey matrix, large numbers of rock fragments (up to 3.5 cm in diameter), with a strong smell of H<sub>2</sub>S and with gas escape structures. The upper 11 cm are oxidized.

### Coral bank escarpment

#### Stations TTR12-AT406Gr and TTR12-AT407Gr.

A coral bank found on the TVAT-33 profile was sampled using the TV-grab. The recovery consists of a large amount of corals mixed with light-brownish, very water-saturated marl with foraminifera in the upper part and with grey marl in the lower. Samples of corals, bivalve shells and authigenic carbonate crusts were taken for biological and geochemical investigations.

### Mercator mud volcano

#### Station TTR12-AT408G.

Sediments, recovered from the volcano crater, consist of grey mud breccia covered with light brown pelagic marl. The absence of H<sub>2</sub>S smell suggests that the volcano is not active in the sampled area at the present time.

Stations TTR12-AT409D and  
TTR12-AT410D.

Two dredges were collected after analysis of video records along the line TVAT-34. A large quantity of sandstones, siltstones, claystones and calcite vein fragments were recovered.

Al Idrissi mud volcano

Station TTR12-AT411G.

The sequence consists of mud breccia with a weak smell of H<sub>2</sub>S. The upper 5 cm of the sequence are lag deposits consisting of winnowed clasts up to pebble size. The presence of this layer indicates that the area is affected by a strong bottom current.

Station TTR12-AT412D.

Rock fragments, recovered by dredge consist of rusty-yellowish sandstones and siltstones with a characteristic honeycomb pattern, the result of chemical weathering. Large numbers of Hydrozoa colonies were also found.

TTR mud volcano

Station TTR12-AT413G.

The upper 98 cm of the sequence, recovered from the TTR mud volcano, is grey marl with a large quantity of coral fragments. The lower part is grey mud breccia with clayey matrix, sedimentary rock fragments, and coral debris in the upper 20 cm.

Such sediments could be formed by mixing of mud breccia and coral debris.

Station TTR12-AT414G.

A small elevation, seen on the MAK-1M sidescan sonar mosaic, was sampled at this station. The core recovered an almost 3 m long sequence of interbedded brownish grey and grey clay. The sediment is bioturbated, with foraminifera and a large quantity of coral fragments. Colour changes in the

clay are due to variations in carbonate content.

Station TTR12-AT415D.

The dredge recovered fragments of well-cemented fine-grained sandstones mixed with sediments, consisting of carbonate clay with foraminifera, bivalve and gastropod fragments.

Station TTR12-AT416Gr.

The recovery consisted of coral debris and light brownish, very water-saturated marl and grey dense carbonate clay. Samples of corals, carbonate crusts and bivalve shells were taken for biological investigations.

#### 2.5.4. Main results

An extensive data set was collected in the El Araiche mud volcano field. All major structures were covered with sidescan sonar surveys. Visual observations of some of the features recognised on sonographs were carried out with the underwater video system. Sampling indicated that some of the studied mud volcanoes are active at the present time. A detailed study of Pen Duick escarpment revealed that cold water corals can colonise fields of mud breccia and form large build-ups associated with mud volcanoes.



### 3. ALBORAN BASIN (LEG 3)

#### 3.1. Introduction and objectives of Leg 3

M.C. COMAS AND M. IVANOV

The Alboran Basin originated during the early Neogene from crustal thinning at the site of a former (Cretaceous to Paleogene) collisional orogen. The basin has a complex tectonic history that involved superimposed extension and compression or contraction stages occurring from the early Miocene (Aquitanian? -Burdigalian) to the present day. ODP drilling in the Alboran Basin and commercial wells on its margins have provided substantial information on the metamorphic nature of the Alboran basement, and on the sedimentary sequences filling the basin. Different studies on the extensive network of commercial and academic seismic reflection profiles existing in the region have constrained the structures and timing of tectonic processes occurring in the basin, as well as the internal architecture of the early Miocene to Recent thick (up to 7 km) sedimentary cover (see Comas et al, 1999 for related references).

As far as the objectives of TTR-12 Leg 3 are concerned, it is important to note that the mud-diapir province recognized in seismic profiling in the West Alboran Basin is thought to be formed by over-pressured olistostromes and shales of the early Miocene (Aquitanian? -Burdigalian) age, which form the basal sedimentary unit in the basin. The mud diapirism is related to middle Miocene extensional processes, but intensive diapirism resumes by post-Messinian times and continues until the Holocene (e.g. Comas et al., 1992; Watts et al., 1993; Chalouan et al., 1997; Perez-Berzuz et al., 1997; Comas et al, 1999). The potential presence of mud volcanoes within the mud diapir province has been suggested from seismic reflection data, but it was only by TTR-9 Leg 2 (1999) results that the existence of mud volcanoes was proved by both geophysical data and sam-

pling (Talukder et al., in press; Sautkin et al., 2003).

The nature and ages of the Pliocene to Pleistocene sedimentary record in the basin is well constrained by results from three ODP Leg 161 drill-sites (Comas, Zhan, Klaus et al., 1996). The reflector that marks the basal limit of the Plio-Quaternary sequence, known elsewhere in the Mediterranean as the "M reflector", corresponds to a strong erosional and locally angular unconformity overlying various older sedimentary sequences, or marking the top of the metamorphic basement or volcanic edifices (Comas et al, 1992).

The Pliocene to present-day sedimentation pattern on the Alboran margins and shelves includes carbonate, mixed carbonate and terrigenous deposits. Turbidite systems are related to source-to-sink processes through incised submarine channels of various magnitude that erode the margin from the shelf areas to the basin plain. Canyon pathways have been frequently controlled by fault development. Major contourite drifts in the Alboran Sea are related to contour currents around the Gibraltar Strait sill.

The Almeria Turbidite System, in the East Alboran Basin, was initiated during the Upper Pliocene and developed until the upper Quaternary (Alonso and Maldonado, 1992). The depositional lobes associated with the Almeria channel shifted to the east, leaving the sedimentary system almost inactive in the latest Upper Quaternary (Estrada, 1994; Estrada et al., 1997). The recent tectonics that affected the Almeria canyon has produced a rejuvenation of specific parts of the canyon, leading to a reactivation of the ancestral Almeria channel (Estrada, 1994; Cronin et al., 1995).

Carbonate and mixed carbonate-siliclastic sediments accumulated in areas located higher up the margin and sheltered from direct terrigenous input. Organisms living on the platform and their derived skeletal particles are the typical components of bryomol and rhodalgal facies that characterize temperate carbonates (Braga and Comas, 1999).

The morphology of the Alboran mar-

gins is characterized by the presence of narrow shelves and steep talus, submarine channels that connect with south Iberian rivers, and deep sea fan lobes on the lower continental slope and adjacent basin plain. Slope instability processes result in extensive developments of scars and slump masses. Furthermore, structural highs (formed of metamorphic basement rocks, volcanic edifices, or of former sedimentary rocks) result in numerous seamounts on the margins.

One of the more conspicuous characters of the Alboran basin's tectonics is the recent to present-day activity that results in frequent earthquakes affecting both offshore and onshore regions. This active tectonics results from the latest contractive structural evolution of the region (from late Miocene to Present). The post-Messinian structural pattern mainly involves faulting (normal to reverse, or strike-slip faults) related to complex wrench fault zones developed from the latest Miocene. Faults and related structures shaping the Alboran margins continue onshore within late-Miocene to recent fault-zones, and have conditioned the present day shoreline (Comas et al., 1999).

#### *Aims and Objectives*

TTR-12 Leg 3 aimed to contribute to a better understanding of the late Cenozoic to present-day tectonic, sedimentary and climatic history of the SE Iberian margins and adjacent basins with a process-oriented, multidisciplinary, integrated geological and geophysical approach. It addressed questions in the field of mud volcanism, sedimentary systems, basin stratigraphy, paleoceanography and tectonics.

Three areas were selected for multi-equipment surveys. Two areas are in the mud diapir province of the West Alboran Margin and the third area is on the Almeria continental margin (Fig. 30).

Main scientific objectives in these areas were to investigate:

1. Sea floor expression, extruded materials and shallow structures of mud volcanoes in the West Alboran Basin: The TTR-12 survey in the West Alboran Basin (WAB)

was planned as a continuation of the TTR-9 survey of the area (Kenyon et al., 2000), during which two mud volcanoes (Granada and Marrakesh mud volcanoes) were discovered indicating the presence of a mud diapir province in the southern WAB (Comas et al., 2000; Talukder et al., 2000; Talukder et al., in press, Sautkin et al., 2003). We planned to revisit the mud volcano field in this area to complete the TTR-9 results by imaging known and possible mud volcano structures with high resolution sidescan sonars, and by sampling the extruded material from the top of the Granada mud volcano. Furthermore, the survey aimed to prove and characterize possible mud volcanoes in the northern WAB (Perez Berluz et al. 1997). Sampling and dating mud-volcano extruded materials will allow us to understand the relationships between mud diapirs and volcanoes, to understand the evolution of the diapirism, and to better know the lithologic composition of olistostromes that form the mud diapir province from the basal Unit VI of the Alboran sedimentary cover (Jurado and Comas, 1992; Comas et al., 1992, 1999). Sidescan sonar surveys and seismic profiling across volcanoes and diapirs will reveal the nature of mud volcanism and fluid flow in the Alboran Basin, as well as constraining the tectonic setting during the development of such mud diapirs and volcanoes.

2. The Almeria turbidite system and the Almeria canyon: The Almeria turbidite system represents an exceptional scenario for establishing a detailed architectural and morphological study, and quantification, of the margin-basin depositional behaviour. The Almeria canyon was first imaged during TTR-2, and also well understood from extensive high-resolution swath bathymetry and sidescan sonar records from the HITS cruise (BIO HESPERIDES, 2001). The TTR-12 survey concentrates in the lower and distal parts of the turbidite system. By combining previous data and TTR-12 results we aimed to define the morphological features (meanders, levees, lobes, etc.) of submarine valleys (canyon and turbidite channels) transporting sediments from the platform to the basin, as well as the bed forms and facies pattern of

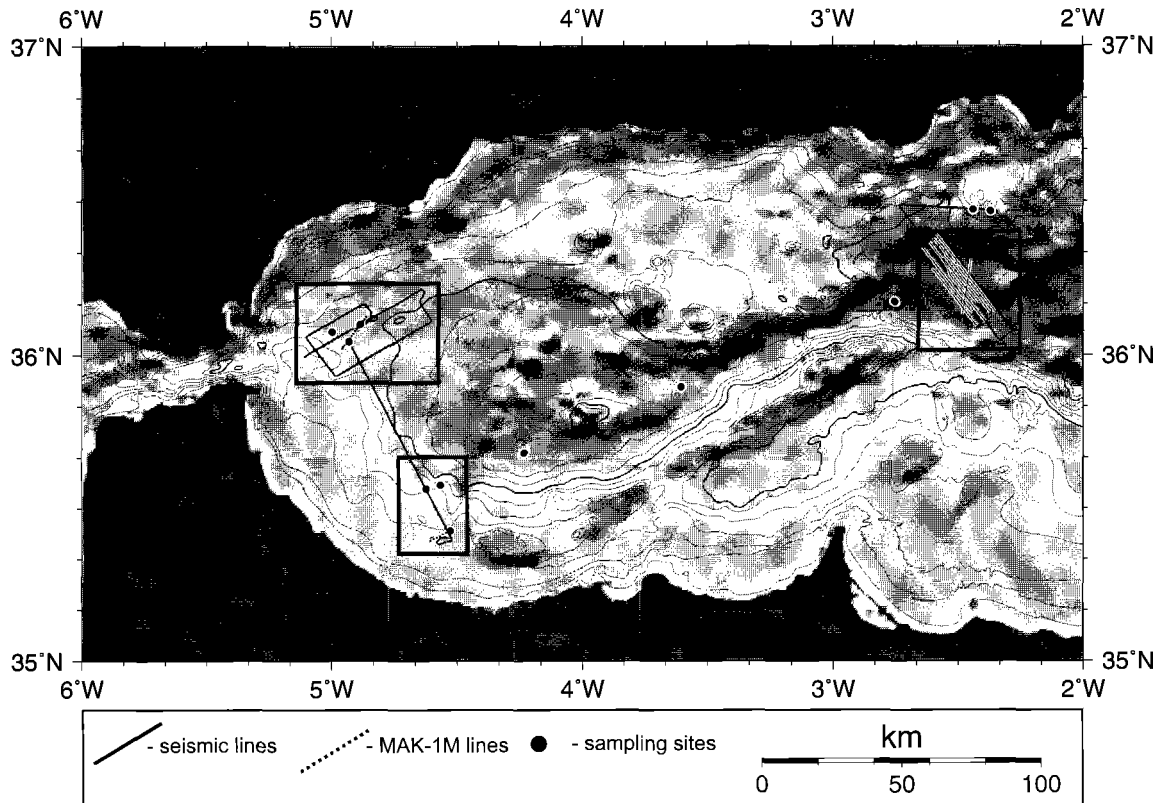


Figure 30. Location map of areas surveyed in the Alboran Sea during TTR-12 Leg 3.

sediment accumulation from the channeled area to the base of the slope. The survey also aims to define the morphologic characteristics of a sediment wave field developed on the right levee of the Almeria channel (Estrada, 1994; Cronin et al., 1995) in order to establish the flow characteristics and determine if these sedimentary structures are linked to the Almeria channel or related to deep bottom currents. Further research will allow modeling of the turbidite system by defining its architecture and dimensions, turbidite facies associations, external and internal source area, and sedimentary activity.

3. Shallow structures and seafloor expression of the Carboneras-fault system, and structural highs, in the Almeria Margin:

The Carboneras-fault system encompasses sites of seismogenic fault development (active tectonics) related to recent episodes of strike-slip, extensional or compressional faulting, occurring up to the Holocene. Some of these faults are located above shallow earthquake epicenters. High-resolution swath bathymetry and sidescan sonar/ back-scattering records (SIMRAD mosaic and

TOBI images) taken during the HITS cruise (BIO HESPERIDES, 2001) show that these faults deform the sea floor to some extent. TTR-12 survey aimed to extend the HITS structural dataset by obtaining high-resolution seismic profiles across these faults, and to image a possible expression of seafloor faulting on high resolution sonographs from the Almeria lower margin. Integrated studies of the acquired high-resolution seismic reflection profiles and previous geological and geophysical data will be used to map the 3D geometry and offset of structures (transfer, en echelon, branching and splay faults), and to determine fault kinematics and tectonic control on the seafloor morphology. We also planned to study structural highs of the Almeria margin, known from previous seismic profiles and sidescan and multibeam images. From geological data onshore in the eastern Betic Cordillera it is known that these highs can be formed by volcanic and metamorphic rocks or by carbonate deposits. TTR-12 aimed to study the seamounts by TV runs, hard-rock dredging or grabbing in order to understand the nature and the age

of these highs.

**4. Paleoclimate reconstruction in the western Mediterranean during the last 20,000 years:** Coring of Holocene pelagic sediments during TTR-12 is for high-resolution analysis (bio- and chrono-stratigraphy, geochemical and isotopic studies) to characterize the climate changes during the last 20,000 years. Paleoclimatic reconstruction will be for the last glacial, the Younger Dryas and the period of the deposition of the most recent sapropel (S1). These changes encompass ocean circulation, atmosphere input (eolian fluxes), and sedimentary response, as well as the fluctuations of biological productivity. High sedimentation rates in the Alboran Sea basin should provide excellent resolution for the interpretation of regional and global climate changes.

Expected results from Leg 3 would have implications for oil exploration, high-resolution mapping, slope instabilities, seismic risk, and coast line fluctuations. Furthermore, we aim to provide field and analytical data to fulfil strategic purposes,

and to support future drilling proposals in the westernmost Mediterranean basins to the "Integrated Ocean Drilling Program" (IODP).

### 3.2. Mud volcanoes in the Alboran Basin: main results

Seismic data profiling (single channel), sidescan sonographs (both OKEAN and the deep-towed MAK-1M), and sampling (gravity coring and grab sampling) were carried out in the WAB to study structures and material of mud diapirs and mud volcanoes. Two areas, one in the northern WAB and another in the southern WAB, were selected on the basis of previous data from the whole region (Fig. 30).

Seven seismic reflection and accompanying OKEAN lines were obtained in the northern WAB, trending both ENE and NNW. MAK-1 deep-tow images were obtained along two perpendicular profiles (trending NE and NW) through two newly discovered mud volcanoes. A NNW-SSE seismic line (line PS-201MS) connecting the

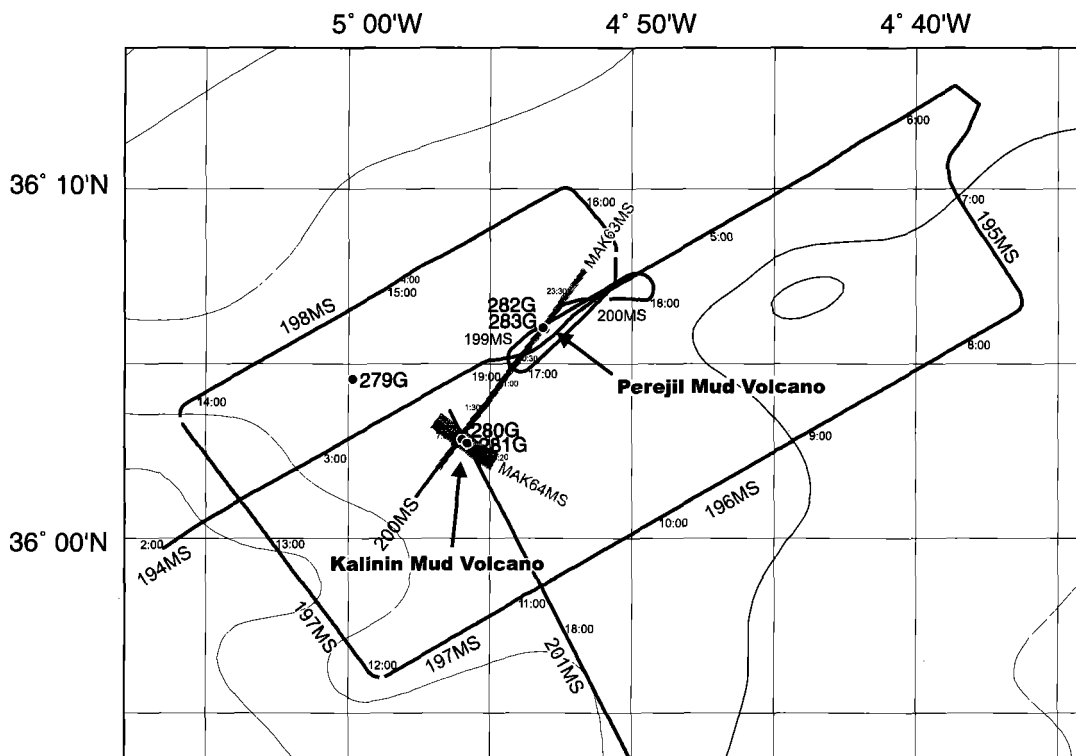


Figure 31. The northern sector of the West Alboran Basin showing the seismic profiles, sidescan images, gravity and dredge samples obtained during Leg 3. Location of Perejil and Kalinin mud volcanoes are shown.

northern and southern mud-volcano areas, was obtained for the purpose of seismic correlations in the WAB. In the southern WAB three seismic lines were acquired through a previously known mud volcano and a newly discovered structure. Two MAK-1 lines crossed three of the mud volcanoes.

The survey in the northern WAB revealed the presence of two well-developed mud volcanoes named Kalinin and Perejil (Fig. 31). In the southern WAB two new mud volcanoes were encountered and named Mulhacen and Dhaka, in addition to the Granada and Marrakesh mud volcanoes discovered during the TTR-9 cruise.

The structure and morphology of these mud volcanoes in the two areas have been imaged both in high-resolution seismic reflection profiles and MAK sonographs.

Gravity cores and TV guided grab samples were taken on the tops and flanks of the mud volcanoes.

### 3.2.1. Mud volcanoes in the northern West Alboran Basin

#### 3.2.1.1. Airgun seismic and hull mounted profiles.

J.I. SOTO, A. TALUKDER, G. MARRO, F. FERNANDEZ, M. COMAS, M.J. JURADO, A. VOLKONSKAYA, I. KUVAEV AND S. AGIBALOV

A total of seven profiles were collected in the northern WAB.

#### Seismic units

Seismic profiles show three seismic units containing fairly constant seismic facies (Fig. 32). We present here the general characteristics of these units, and more detail is described for each individual profile. We have selected key discontinuities to separate the uppermost two seismic units, but it should be noted that these units display also internal discontinuities that are difficult to correlate between the different single-channel profiles when they are not crossing each other.

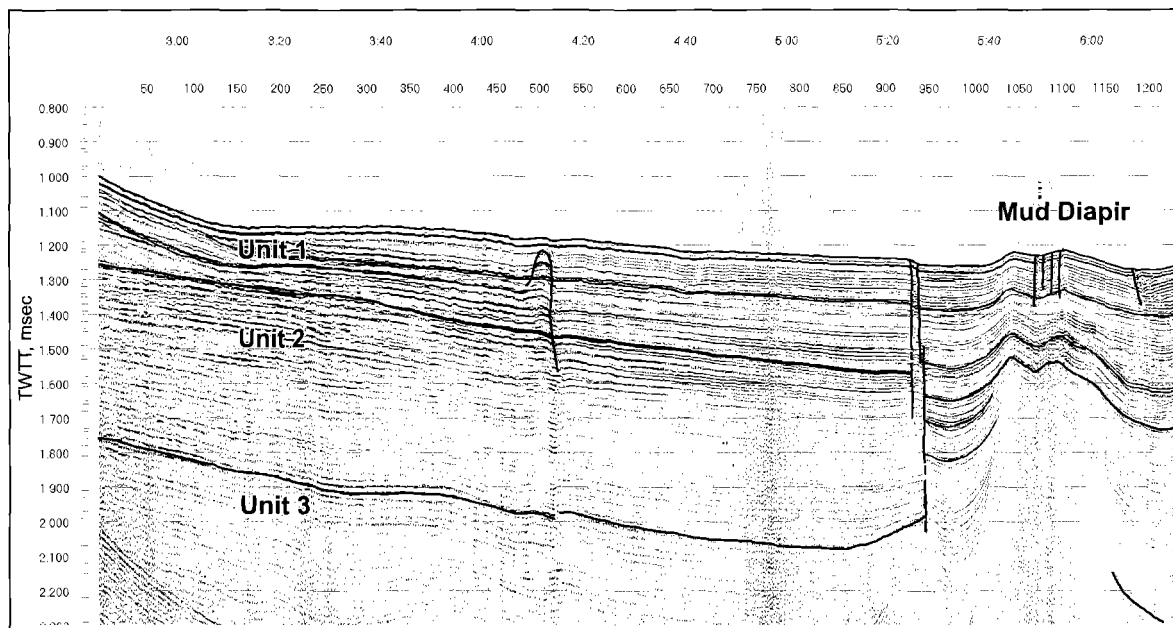


Figure 32. PS-194MS line and simplified interpretation showing the main seismic units (Units 1 to 3) distinguished in the northern West Alboran Basin, and some of the main structures, namely high-angle normal faults, diapiric highs, and mud volcanoes. Note the occurrence of the M-reflector (top of Unit 3), deduced by seismic correlation with crossing multi-channel lines.

The uppermost unit, Unit 1, Quaternary and possible late-Pliocene in age, has a highly-reflectivity basal unconformity with an onlap geometry toward the basin margins, changing laterally to a paraconformity in the center of the basin. The thickness ranges from a maximum of 400-500 ms, achieved in mud-diapir marginal troughs, to a minimum of 200 ms. The basal unconformity probably dips toward the NE and, based on seismic correlation between these single-channel profiles, we suggest that it changes in seismic character toward the south, becoming a paraconformity with a reduced reflectivity. Unit 1 has an overall transparent acoustic character and displays two sub-units: a low-reflective upper portion with thin continuous reflectors, and a lower portion with thick, high-amplitude reflectors.

The intermediate unit, Unit 2, of probable Pliocene age, has two well-depicted sub-units. The upper sub-unit, with a fairly constant thickness of 100-150 ms, shows high-amplitude continuous reflectors. In places an internal unconformity separates this upper sub-unit from the lower one, with its generally transparent seismic character. The lower sub-unit displays significant changes in thickness, ranging from more than 900 ms to 500 ms. Unit 2 may increase in thickness toward the south. The lower boundary of Unit 2 has been distinguished in some of the lines by seismic correlation with commercial multi-channel seismic profiles, tied with borehole data. It corresponds to the M-reflector (the Messinian unconformity), and is seen on seismic records as a high-amplitude double reflector.

Unit 3 (of late Miocene age) is occasionally seen as a semi-transparent seismic unit with scarce high-amplitude reflectors beneath the M-reflector.

#### Seismic Line PS-194 MS

This line runs for 21.2 nm with an ENE-WSW trend and shows the M-reflector clearly (i.e. the base of Unit 2). A mud volcano, deforming Units 1 to 3, is also observed at the northeast end (Fig. 32). High-angle

normal faults affecting Unit 1 and reaching the sea-floor are also seen in its summit, and can be interpreted as collapse structures. A narrow pop-up of the overall reflectors forming units 1 to 3 is also seen in the center of the profile, affecting up to the sea-floor. This structure is interpreted as a by-pass section of a mud-diapir (with associated Perejil mud volcano) clearly seen in the simultaneous OKEAN profile. At the southwestern end of the profile, and coinciding with an increase in the seafloor slope, Unit 1 has a downlap geometry, coalescing the uppermost reflectors in a subhorizontal internal unconformity. This section of the profile corresponds to the northern end of the Ceuta drift, and shows the internal structure of this contourite body.

#### Seismic Lines PS-195MS and PS-196MS

Line PS-195MS runs for 3.6 nm with a NNW-ESE trend and shows a gentle dip of the reflectors toward the south. The M-reflector is seen discontinuously at 2.3 and 2.7 sec.

Line PS-196MS runs for 20.8 nm with an ENE-WSW trend and the base of Unit 2 is not clearly seen. The most conspicuous structures are two mud diapirs seen at the centre of the profile. Both diapirs have high-angle normal faults, representing collapse structures that affect up to Unit 1 and locally reaching the sea-floor. Unit 1 achieved a maximum thickness of 300 ms beneath the marginal troughs of the two mud diapirs. At the southwestern end of the profile, several angular unconformities are seen inside Unit 2, together with a semi-transparent seismic facies. The seafloor here has an irregular and undulating geometry that may be due to the presence of gullies.

#### Seismic Lines PS-197MS and PS-198MS

Line PS-197MS runs for 8.8 nm with a NNW-SSE trend. Seismic units on this line (Unit 1 and Unit 2) are subhorizontal.

Line PS-198MS runs for 12.3 nm with a ENE-WSW trend. It is the closest to the WAB northern margin and has a shallow and nearly flat M-unconformity at 1.6-1.75 sec.

Both seismic units, Unit 1 and Unit 2, show a slight increase in thickness to the northeast (from 2.0 to 2.5 sec and 3.0 to 4.0 sec, respectively). In the central portion of the profile there is a narrow (less than 1.8 km in diameter) cylindrical structure, with subvertical walls and transparent seismic facies, that deforms the basal unconformity of Unit 1. This structure probably corresponds to a piercing, non-outcropping mud-diapir.

#### Seismic Line PS-199MS

This line consists of two segments (about 3 and 2.5 nm long) which runs with a NE-SW trend across the Perejil mud volcano. The volcano is seen as a positive structure of 1300-1400 m in diameter and 100 ms elevation (75-80 m high) with vertical walls clearly seen up to 3 s depth. Toward the mud volcano walls the shallower reflectors (< 1.3 s depth) are deformed, whereas the deeper reflectors are usually undeformed (> 1.3 s). The relationships between the mud volcano feeder channel and the nearby sedimentary sequences, indicates a punctuated history of mud ascent during the deposition of Units 1 and 2.

#### Seismic Line PS-200 MS

This line runs for 6.5 nm with a NE-SW trend, across the two mud diapirs recognized in the northern WAB. The northern mud volcano in the profile corresponds to Perejil mud volcano (already described in the Line PS-199MS), whereas the southern feature, seen as a depression (1000x700 m and 20 m depth, according to MAK-1 profiling data) and with a southern subvertical slope, corresponds to the Kalinin mud volcano. The reflectors toward the feeder-channel of this volcano show different terminations, with geometries ranging from upwarped to flat-lying attitudes (Fig. 33). The abundant hyperbolic diffractions in the feeder channel, together with the diffuse feeder-channel walls, suggest that this line probably bypasses the centre of the mud volcano.

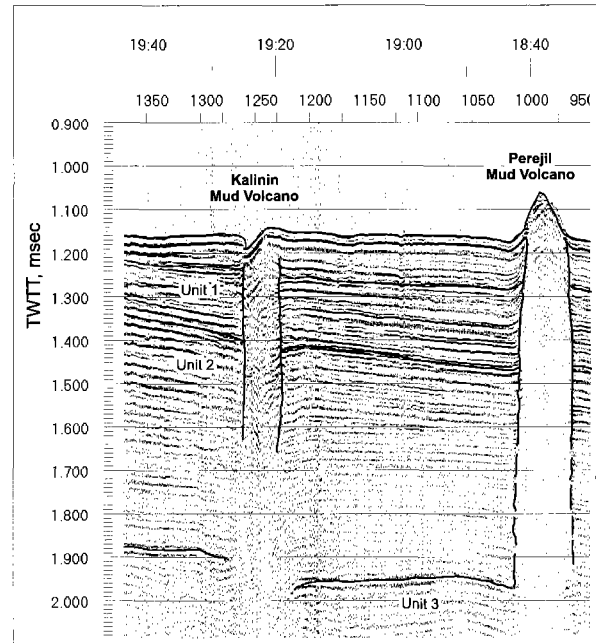


Figure 33. PS-200MS line across the Kalinin and Perejil mud volcanoes showing main features of mud volcano structures in the West Alboran Basin.

#### Seismic Line PS-201 MS

This line runs for 35 nm with a NNW-SSE trend, and connects the northern and the southern sectors of the WAB. The line was selected to cross the strike of the major depocenter of the WAB, and to pass through the northern (Kalinin) and the southern Granada and Dhaka mud volcanoes. Line PS-201MS crosses several diapiric highs and mud volcanoes. In its northern part it shows a sub-outcropping diapiric high (13 km SSW of the Kalinin mud volcano), draped by a thin sedimentary layer (30-50 ms). In its southern part, two tapered mud diapirs occur at different depths (below a sedimentary sequence >1 s and 200 ms thick), and two mud volcanoes are also seen. These two mud volcanoes correlate with the Granada (northern) and Dhaka (southern) mud volcanoes, already seen in the OKEAN mosaic obtained on the TTR-9. The Dhaka mud volcano is also imaged in the multichannel seismic line CONRAD 828 (Talukder et al., in press).

Mud diapiric highs along the line make it difficult to correlate lower seismic units between the northern and the southern

WAB, whereas Unit 1 and Unit 2 are more easily correlated through marginal troughs. This, together with the increase in thickness revealed by Unit 2 toward the south, makes it impossible to recognize the M-unconformity (the basal boundary of Unit 2) in the deepest portion of the WAB and also in the southern WAB.

A mud diapir in the southern sector of the profile has a chaotic seismic facies with strong, discontinuous reflections. In contrast, the seismic facies of the deeper mud diapir is not clearly distinguished in the profile, and it is seen deforming and uplifting the probable M-unconformity (below 2 s).

Unit 1 has a basal unconformity well depicted throughout the profile, and seen as a high reflective band. This unconformity is deformed by the diapiric highs and is cut by the feeder channel of the mud volcanoes. It shows a general increase in thickness toward the south (from 200 ms to 400 ms). Two sub-units with the same seismic facies correspond to those already described in the northern WAB (profile PS-194MS). The lower sub-unit shows onlap geometries toward the diapiric highs, whereas the upper one usually draped these structures. This observation suggests an important episode of diapiric ascent (both in the northern and the southern WAB) during the deposition of Unit 1 (i.e. Quaternary).

Unit 2 shows an important increase in thickness toward the south and it is also deformed by the diapiric highs, where it has its minimum thicknesses (800 ms). This unit is clearly formed by two sub-units with contrasting seismic facies, the upper sub-unit shows a parallel stratified facies (maximum thickness of 500 ms) and the lower sub-unit has a transparent seismic facies (minimum thickness of 450 ms). The upper sub-unit 2 pinches out toward the diapiric highs, whereas the lower sub-unit 2 seems to be deformed by these structures. If this is the case, it could suggest another diapir ascent episode during the deposition of Unit 2 (i.e. during the Pliocene).

## Hull mounted profiles

Nine hull mounted 5.1 kHz profiles, accompanying seven single-channel and OKEAN profiles (PS-194MS to PS-200MS) and two MAK lines (MAK-63MS and MAK-64MS), were obtained in the northern sector of the WAB. The basin plain in the study area has continuous, parallel bedded reflectors with a reflectivity that diminishes toward the mud volcanoes. Pockmarks seen as small sea floor depressions are also observed around the mud volcanoes. The sediments in the higher slopes of the profiles (e.g. western slope of the PS-196MS profile) are believed to be part of the northern end of the Ceuta contourite drift.

### 3.2.1.2. Sidescan sonar data

M. MOLINOS, A. TALUKDER, F. ESTRADA,  
A. AKHMETZHANOV, P. SHASHKIN, I. UVAROV AND  
E. SPUNGINA

Seven lines were run using the OKEAN long range sidescan sonar and two with the deep towed MAK-1 system concurrently with the 5.1 kHz hull mounted profiler. MAK lines were run in order to image precisely the mud volcanoes in the northern WAB.

#### Line MAK-63MS

This line is 6.5 nm long and runs roughly parallel to the PS-200MS seismic profile (trending NE-SW). A range of 700 m and a frequency of 100 kHz were used. The northeastern part of the line generally has a featureless, medium-low reflectivity seabed apart from circular depressions, interpreted as pockmarks, which are spread throughout the record. Pockmarks have dimensions of about 30 m diameter and are about 5-6 m deep. The main feature on the sonar record is a circular mud volcano named Perejil (Fig. 34), recognizable in the middle of the sonar track line with a summit of about 230 m and a circular base at 1160 m depth, having dimensions of about 300 m in diameter and a maximum elevation about 90 m. Small chan-



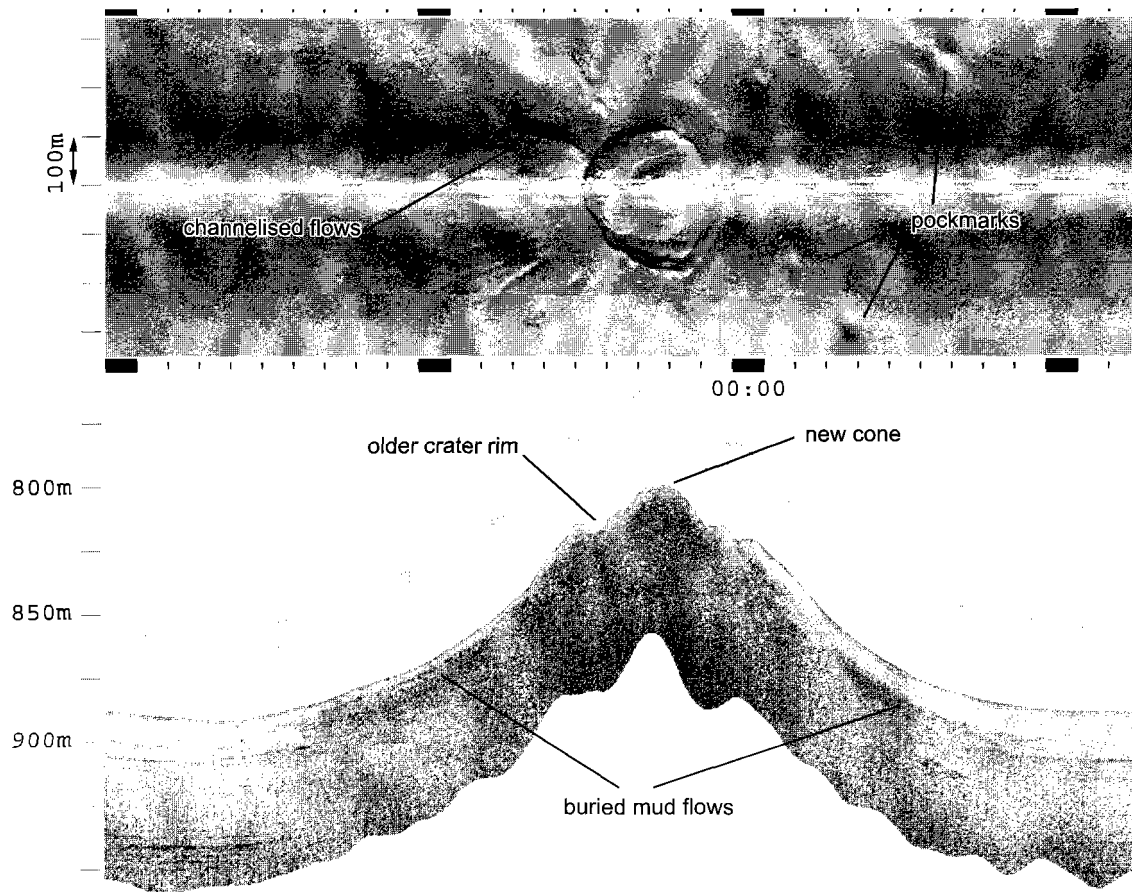


Figure 34. Part of MAK-63MS sidescan image (100 kHz) and sea-bottom profile (5 kHz) across the Perejil mud volcano in the northern West Alboran Basin.

nel-like structures emanate from the mud volcano structure and are specially evident at the western flank. Inside the Perejil mud volcano there is a small crater (95 m in diameter and 20 m elevation), suggesting the existence of several phases of growth.

The southwestern part of the line shows a medium-low reflectivity seabed with several randomly scattered circular pockmarks up to 5 m deep. The main feature is the circular Kalinin mud volcano, which is almost fully imaged by the sidescan and has a negative relief (Fig. 35). The mud volcano has a diameter of approximately 700 m and a strongly asymmetric crater with a steeper southern wall (24° gradient), a gentle northern wall (4° gradient) and a maximum depth of 25 m. Small groups of depressions (probably pockmarks) are found around the southern crater flank. Individual depressions are less than 3 m deep.

#### Line MAK-64MS

This line is 2 nm long and runs NE-SW, roughly perpendicular to the MAK-63MS line, crossing the centre of the Kalinin mud volcano. The Kalinin mud volcano is asymmetrical in plan view (1000 x 700 m) and is characterized by two depressions (19 and 21 m deep) bounding a central high within the volcano crater.

### **3.2.2. Mud volcanoes in the southern West Alboran Basin**

#### *3.2.2.1. Airgun seismic and hull mounted profiles*

J.I. SOTO, A. TALUKDER, G. MARRO, F. FERNANDEZ,  
M.C. COMAS, A. VOLKONSKAYA, I. KUYAEV AND  
S. AGIBALOV

Three short seismic lines were acquired through two of the mud volcanoes

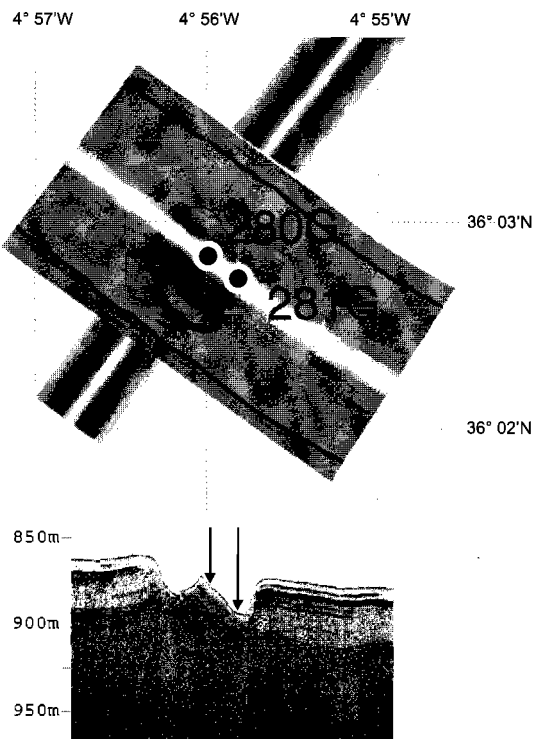


Figure 35. Fragments of MAK-63MS and MAK-64MS sonographs and subbottom profiler record across the Kalinin mud volcano.

of the southern WAB together with the regional profile (PS-201MS) connecting the northern and southern mud volcanoes areas (described above) (Fig. 36).

#### Seismic Line PS-202MS

This line runs for 3.3 nm with a E-W trend, by-passing the centre of the newly discovered Mulhacen mud volcano. The two upper seismic units (Unit 1 and Unit 2) recognized in the northern WAB are also identified in this profile. The bottom of Unit 2 (the M-unconformity) probably corresponds to a high amplitude reflector seen at 1.7 s. Nevertheless, we cannot confirm this interpretation because in the regional line PS-201MS this reflector disappears southward (mainly because Unit 2 increases in thickness congruently). The width of the feeder channel of the Mulhacen mud volcano increases with depth (from 640 m wide at 600 ms to 1470 m wide at 900 ms), showing a conical geometry that continues downward as a cylindrical pipe (below 900 ms ). The lower

section of Unit 1 (150 ms thick) dips toward the volcano walls as does the basal unconformity of this unit. The upper section of Unit 1 (200 ms thick) shows an offset at both sides of the mud volcano, being uplifted and sub-horizontal on the western side and dipping gently toward the channel on the eastern side. Unit 2 is semi-transparent, and the scarce reflectors seen in the profile dip toward the mud-volcano feeder channel.

#### Seismic Line PS-203MS

This line runs for 3 nm with E-W trend (parallel to Line PS-202MS) through the centre of the Mulhacen mud volcano (Fig. 37). The seismic facies and geometrical relationships between the seismic units and the mud volcano, are similar to those already described in Line PS-202MS. The mud-volcano feeder-channel is wider than on the parallel line (2.3 km at 700 ms and 3.2 km at 1.0 ms ). It also has a conical culmination that passes gradually downward (1 s) into a cylindrical shape.

#### Seismic Line PS-204 MS

This line runs for 3.7 nm with a NE-SW trend, crosses all the seismic lines in the southern WAB, and passes through the Mulhacen mud volcano. This volcano is seen as a wide cylindrical tube (2.5 km wide below 800 ms) narrowing upward to a broad conical summit (1.9 km wide at 600 ms ), and is covered by a thin layer of recent sediments (<50 ms ). The seismic facies and geometrical relationships between the seismic units and the mud-volcano feeder pipe are similar to those described previously. The more remarkable feature seen on this line is another mud diapiric high, close to the Mulhacen mud volcano. This mud diapir is seen as a narrow structure (probably <1000 m in diameter) that deforms the basal unconformity of Unit 1. The lower portion of this unit appears as a package of continuous, high-amplitude reflectors that dip towards the diapir. It is interpreted as a collapse structure, suggesting that the diapirism stopped at the base of Unit 1 (i.e., during the lower Quaternary). A

## 3.2.2.2. Sidescan sonar data

M. MOLINOS, A. TALUKDER, J.I. SOTO, F. ESTRADA,  
G. MARRO, F. FERNANDEZ, A. AKHMETZHANOV,  
P. SHASHKIN, I. UVAROV, M. OSIPENKO AND  
A. KOSTINENKOVA

Four lines were run using the OKEAN long range sidescan sonar: PS-201MS (transit from the northern to southern WAB), PS-202MS, PS-203MS, and PS-204MS, with a total length of 10 nm (excluding PS-201MS). Two lines, MAK-65 and MAK-66, were also run with the deep-towed MAK-1 hydroacoustic system (30 kHz and 2000 m sonar range and 5 kHz subbottom profiler).

Line MAK-65

This line is 5.25 nm long and trends SW-NE, running perpendicular to line PS-201MS. The seabed is generally characterized by medium to low reflectivity. The main features seen are two highs, recognizable at the NE end and in the middle of the line, which correspond to the Mulhacen and Dhaka mud volcanoes, respectively. The Mulhacen has a maximum elevation of 50 m and Dhaka is slightly higher, reaching 63 m high. Both mud volcanoes are about 700 m in diameter. Locally, small areas of medium to high reflectivity can be observed around the volcano summit and could be associated to small topographic highs and depressions. Mulhacen mud volcano has a steep cone (35 m high and 500 m wide) on a wide platform (12-15 m high), suggesting multiple mud-flow episodes.

Line MAK-66MS

This is a short line about 1.3 nm long running SW-NE perpendicular to line PS-201MS that crosses the Granada mud volcano. This mud volcano has a conical morphology having an estimated diameter of 1200 m and height of 100 m. Small elongated depressions and narrow channels are observed running down the mud volcano flank towards the north

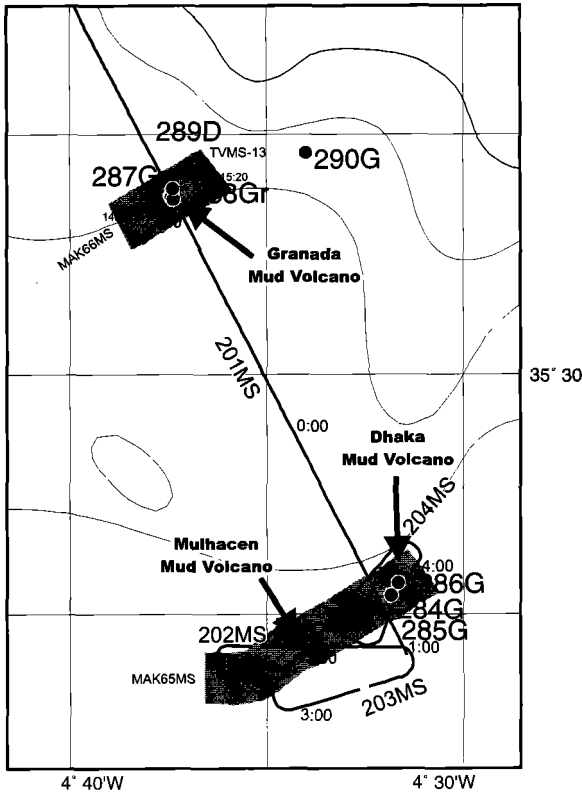


Figure 36. The southern sector of the West Alboran Basin showing seismic and sidescan survey lines and sampling stations carried out during Leg 3. Location of the Granada, Dhaka, and Mulhacen mud volcanoes are also shown.

synclinal fold is also seen on the northern flank of the Mulhacen mud volcano and represents a marginal trough which tightens with depth.

Hull mounted profiles

Five 5.1 kHz profiles, accompanying the air-gun seismic and OKEAN profiles (PS-202MS to PS-204MS) and the two MAK lines (MAK-65MS and MAK-66MS), were obtained in the southern sector of the WAB, representing a total 16.5 nm of profiling. These bottom-sediment profiles show continuous, parallel-bedded reflectors with a high reflectivity around the surveyed mud volcanoes.

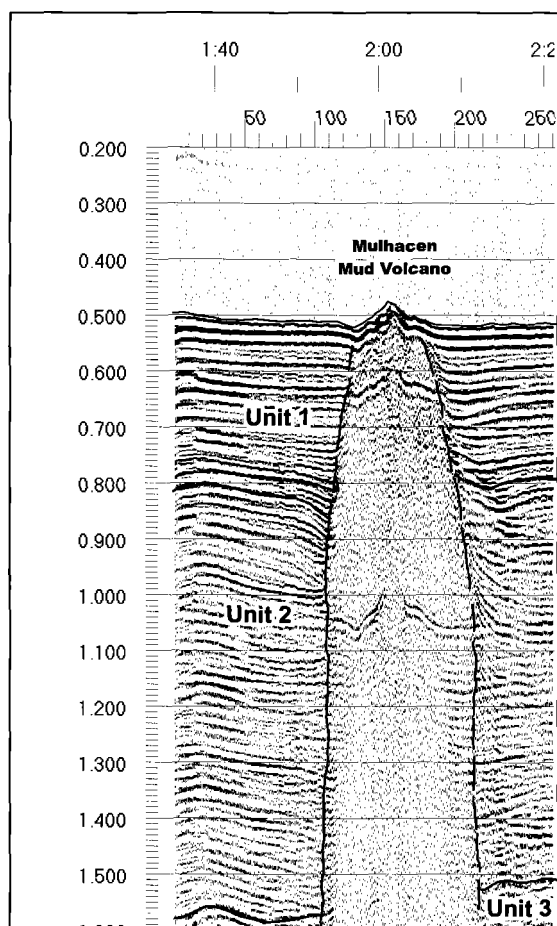


Figure 37. PS-203MS line across the Mulhacen mud volcano in the southern West Alboran Basin showing the main seismic features present in the area around the mud volcano structure.

### 3.3. The Almeria margin: main results

The survey in this area was conducted to complete and enlarge structural, morphological and sedimentary data acquired by the HITS cruise in the summer of 2001, carried out onboard the BIO HESPERIDES on the Almeria margin. The acquired data are expected to contribute to tectonic and sedimentary research targets in the Almeria margin. Airgun seismic profiles and sidescan sonographs (MAK-1 and OKEAN) were carried out in order to study the distal morphologic expression of the Almeria channel and the Andarax turbidite system, but also to constrain the shallow structure and seafloor expression of the Carboneras wrench-fault zone and the active tectonic signatures in the region (Fig. 38). Additional video recording

and dredging on hard-rock seamounts were conducted on the Sabinal Bank.

#### 3.3.1. Seismic profiling and interpretation

F. ESTRADA, J.I. SOTO, M.C. COMAS, M.J. JURADO,  
G. MARRO, A. VOLKONSKAYA, I. KUVAEV AND  
S. AGIBALOV

Three seismic and OKEAN lines were obtained in the Almeria margin in one area comprised between 36°00'N and 36°30'N and 2°44'W and 2°16'W. Lines PS-205MS and PS-206MS are NNW-SSE oriented and PS-207MS is oriented WNW-ESE. The ship's course change at the beginning of line PS205MS at shot point 132 should be noted. Line PS-206MS was run in two parts: a NW section (line PS-206aMS) and a SW section (line PS-206MS).

The seismic profiles obtained on the Almeria margin show the four main seismic units, from Miocene to Quaternary in age (Fig. 39), determined by ODP Leg 161 drilling (Comas et al., 1996). In the surveyed area of the Almeria margin these units overlie an irregular and fractured acoustic basement that reaches its maximum depth in the East Alboran Basin, at the eastern end of the Alboran trough. The seismic lines run over the lower continental slope and across the deep basin where the sedimentary depocenter of the East Alboran Basin develops. The Plio-Quaternary units depict a sedimentary wedge that is thicker towards the distal reaches of the basin. Structural features from recent tectonics are observed as faults affecting sediments and conditioning sharp, near vertical boundaries of acoustic basement highs (Chella and Sabinal seamounts)

The uppermost seismostratigraphic unit (Unit 1), of Quaternary age, is characterised by parallel stratified facies although in places it has discontinuous stratified facies (Fig. 39). The lower boundary of Unit 1 is characterised by a high-amplitude continuous reflector over which several downlap reflector terminations are seen. Internally, Unit 1 has several discontinuities that evolve to paraconformity towards the basin. Unit 1 also shows lens-shaped reflector packages

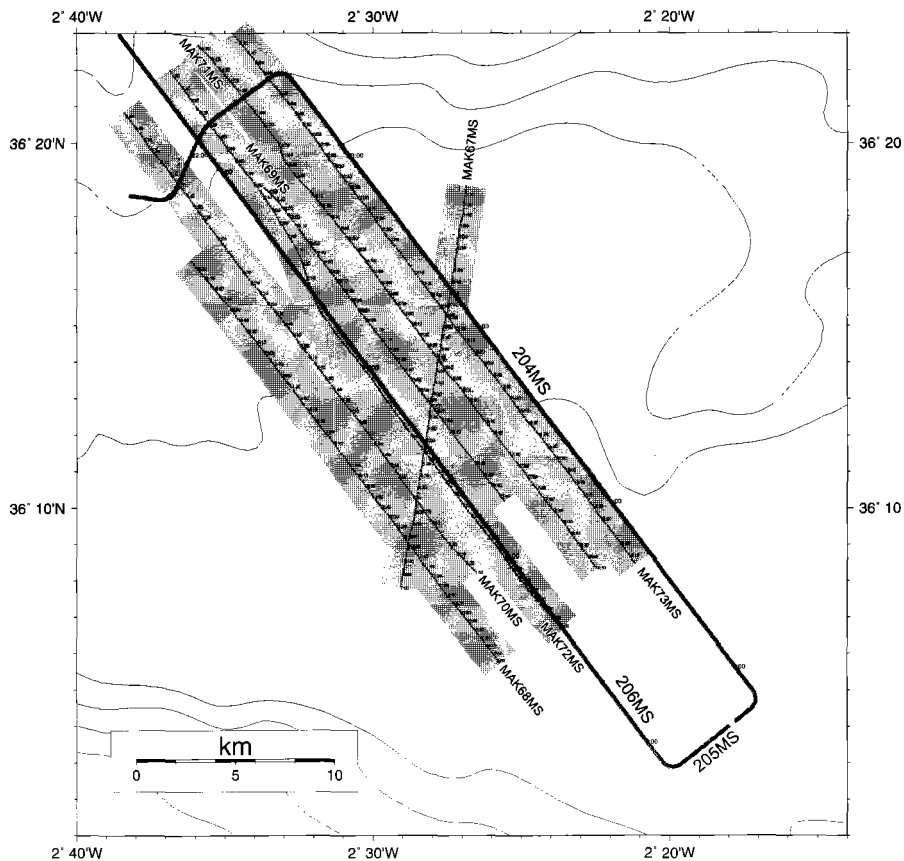


Figure 38. The northern sector of the EAB showing the seismic profiling and sidescan imaging carried out during Leg 3.

that are interpreted as related to the Andarax turbidite system. The part of this Unit far from the influence of the Almeria canyon is characterized by sheet drape seismic facies. Locally, and close to the external levee of the Almeria channel, undulating reflectors are observed, probably related to the development of a sediment wave field (Fig. 39). In the East Alboran and Alboran trough depocenters, Quaternary reflectors have a planar geometry with a fairly constant thickness, which decreases upslope.

Unit 2, late Pliocene in age, has a variable thickness and is divided in two sub-units. The upper Subunit 1 is characterized by parallel-stratified and discontinuous-stratified seismic facies, both with high reflectivity (Fig. 39). These facies are interpreted as related to the early development of the Almeria Turbidite System (Estrada et al., 1997). The lower Subunit 2 has parallel-stratified facies of lower reflectivity, being in

some cases acoustically semitransparent. The boundary between Subunit 1 and 2 is marked by a high amplitude reflector against which downlapping reflector terminations are observed. Subunit 2 onlaps and covers acoustic basement highs, smoothing the irregular early Pliocene surface.

Unit 3, early Pliocene, has rather homogeneous, stratified, semitransparent seismic facies, and reflectors onlap against the walls of the structural highs (Figs. 39 and 40). The thickness of Unit 3 is highly variable as it fills an irregular and tectonised surface of the acoustic basement. This results in the development of several small ponded basins. The base of Unit 3 corresponds to the M-reflector, an erosional unconformity in the whole Alboran Basin, which is seen as a high amplitude reflector except when Unit 3 overlies structural highs.

Unit 4 is tentatively assigned to the late Miocene and shows a highly reflective

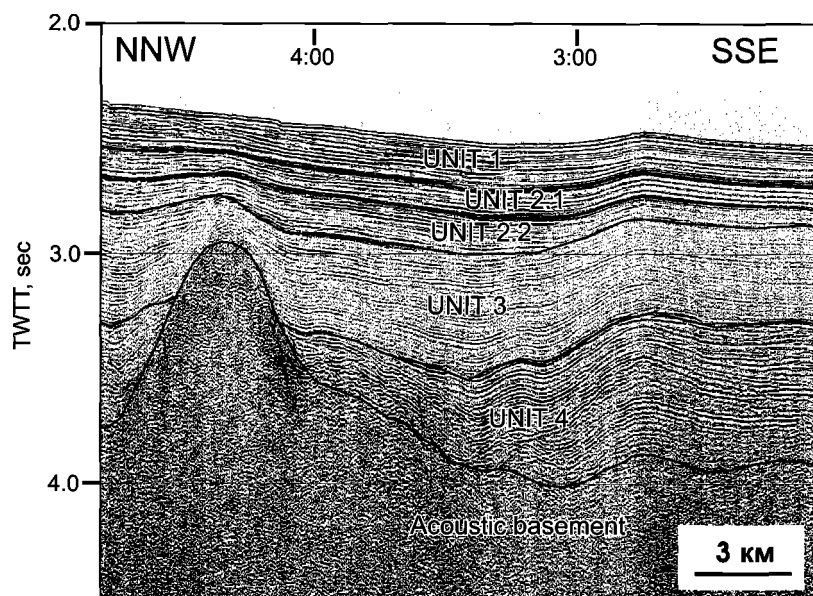


Figure 39. PS-206MS line and simplified interpretation showing the main seismic units (Units 1 to 4) distinguished in the EAB, and some of the main structures seen in this region.

seismic response, with stratified-to-chaotic facies. Unit 4 is tilted and strongly faulted in the seismic profiles (Fig. 39). The thickness of Unit 4 is very variable and the unit is almost absent on the continental slope (Fig.40).

#### Seismic Line PS-205 MS

This profile runs for 31 nm with a NW-SE trend across the transition from the lower portion of the northeastern margin of the EAB to the Alboran Trough (at 1900 m depth). Unit 1 has an average thickness of 250-300 ms which decreases to the north to 100-120 ms, and is bounded by a continuous, high amplitude reflector. This reflector decreases in amplitude towards two basement highs. Unit 2 and Unit 3, on the contrary, have different seismic facies, showing stratified (200-120 ms thick) to semi-transparent facies (150-500 ms thick) with high amplitude reflectors. The boundary between these two units is not well seen along the profile, and could correspond to a discontinuous, high-amplitude reflector seen at 3.0-3.1 s. Unit 2 and Unit 3 together achieve a maximum thickness at the marginal troughs between basement highs (700-800 ms), thinning gradually toward the highs (minimum values of 150 ms). The basal unconformity of

Unit 3 (the M-reflector) is only seen locally and is faulted, with discontinuous and disrupted high amplitude reflectors, that appear at different depths (3.2, 2.7, and 2.9 s). Beneath the M-reflector, a stratified unit with moderate amplitude reflectors is locally seen (Unit 4, upper-Miocene in age), with a minimum thickness of 400 ms. The top of the acoustic basement appears in places as a boundary with a high dip, that corresponds to high-angle faults, whereas at the top of the highs it diminishes in reflectivity and appears as a thick package of discontinuous, high-amplitude reflectors.

#### Seismic Line PS-206MS

This profile runs for 32 nm with a NNW-SSE trend. In addition to the seismic facies and the thicknesses of the units described above, several other structures are seen clearly in this profile. It cuts the initial reaches of the Almeria channel and further upslope, near to the Chella Bank, the Palomares fault zone is seen. The basement appears clearly faulted with fractures that commonly dip southward. These faults produce abrupt changes in elevation of the top of the basement, beneath the sedimentary infill. In the Palomares fault zone there is a

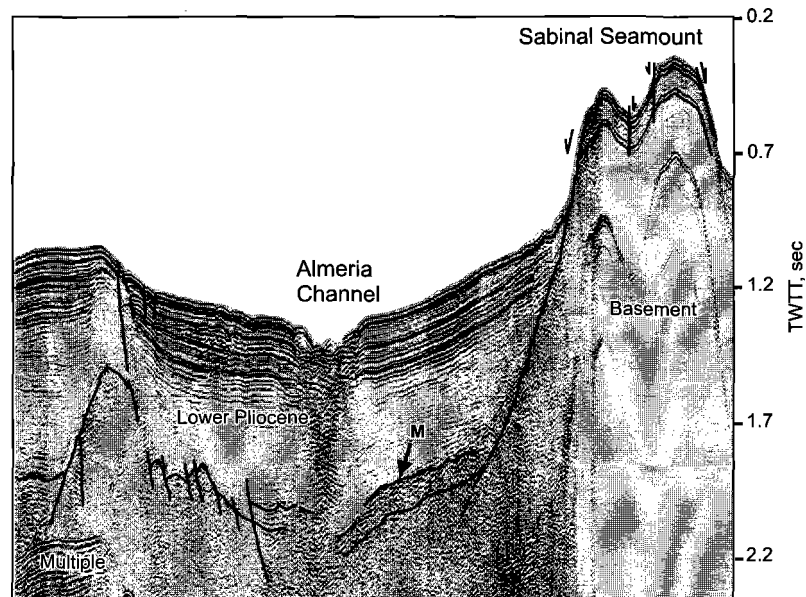


Figure 40. PS-207MS line across the continental slope showing the Almeria channel and the Carboneras fault.

high-angle fault that bounds a basement high and continues upwards, affecting the more recent sediments and the sea-floor. At the seafloor it is seen as a degraded fault escarpment. Fold structures are also recognised along the profile affecting the lower sedimentary sequences. These folds deform the M-unconformity and are congruent with the reflectors of Unit 4.

#### Seismic Line PS-207 MS

The line is 19 nm long and runs W-E from the Chella to the Sabinal banks, crossing the Almeria canyon at right angle. The Palomares fault zone is seen at the western end of the profile (near the Chella Bank) as a high-angle fault, dipping eastward, and affecting the sea-floor. It continues downward, affecting the basement which appears as a horst structure, with the M-unconformity placed at different depths (1.8 and 1.9-to-2.1 s) on both sides of this high. The western slope of the Sabinal Bank is bounded by a master, westward-dipping high-angle fault. Other high-angle normal faults, affecting the Unit 1 and the sea-floor, merge toward this fault. The steep walled Almeria canyon is seen at the centre of the profile. The seismic facies representing the canyon deposits are characterized by high-amplitude, discontin-

uous reflectors with abundant diffractions. The present-day position of the Almeria canyon coincides with the places where the M-unconformity lies deeper on the profile (at 2.1-2.2 s).

#### **3.3.2. Sidescan sonar data**

F. ESTRADA

Seven MAK-1 lines (MAK-67MS, MAK-68MS, MAK-69MS, MAK-70MS, MAK-71MS, and MAK-72MS) were run on the Almeria margin using the MAK-1M deep-towed system, with the sidescan at 30 kHz and 2 km range (apart from MAK-72A in where the swath was 3 km) together with a 5 kHz subbottom profiler. These lines make a mosaic of the distal part of the Almeria turbidite channel, in order to image the trace of the channel as well as the associated morphological features (small channels, meanders, lobe deposits, etc).

#### Line MAK-67MS

The line is 8.5 nm long and runs NNE-SSW. The seabed is has medium to low reflectivity and is mainly featureless. Narrow and shallow channel-like structures run parallel-oblique to the centre line, crossing it at

two points, in the northern and central parts of the line. The more significant channels crossing the center line range between 150-200 m wide and are probably up to 8 m deep.

#### Line MAK-68MS

The line is 10 nm long running NW-SE. The seabed is also characterised by low-medium reflectivity and is generally featureless. Faint evidence of a meandering channel is seen in the central area although it seems to have poor bathymetric expression and may be partly buried.

#### Line MAK-69MS

The line is 7.8 nm long and runs NW-SE. A highly meandering channel is seen throughout the whole area covered by the sidescan sonar. The channel has a general NW-SE trend presenting frequent changes of direction towards the SE (downslope). It has two prominent loops in the northern area and becomes less sinuous downslope, crossing the center line at least three times along its course. Another channel is seen, apparently disconnected from the main one, that meanders and loses its expression. The Almeria channel narrows progressively and loses its bathymetrical expression southward, from about 230 m wide and 10-11 m deep in the northern area to 110 m wide and less than 5 m deep towards the SE. The seabed has a generally low-medium reflectivity with highly reflective patches, locally associated with the channel walls and floor in the northern area.

#### Line MAK-70MS

The line is 10.8 nm long and NW-SE trending. The line shows a flat, medium-low reflective seabed and it is generally featureless. At the northern end there is an area of small, scattered, high reflective elongated pockets. These could correspond to coarser sediment or boulders.

#### Line MAK-71MS

This line shows the morphology of the Almeria channel system more clearly than the others. It is 12 nm long and NW-SE trending. At the northwestern end, where the seafloor is steepest, there is a highly meandering channel system composed of several cross-cutting channels (Fig. 41). These structures vary downslope from highly meandering channels of about 400 m wide and more than 30 m deep, to straight, shallow and narrower channels (150-75 m wide and less than 15 m). Towards the basin plain, characterised by a sub-horizontal seafloor, the channel system seems to vanish, losing its bathymetric expression.

#### Line MAK-72MS

The line is 7 nm long and trends NW-SE. This line generally has a medium-low reflectivity, although some isolated meandering channels are seen scattered throughout. The absence of any marked contrast of reflectivity between these meandering structures and the rest of the seafloor suggests that they could either have been covered by homogeneous sedimentation or that they are not deeply-incised.

#### Line MAK-72aMS

The line is 4.8 nm long and trends NW-SE. This line was run with a longer range in order to obtain full coverage of the Almeria channel between other lines. It shows a highly meandering channel that goes downslope from 300 m wide and 25-30 m deep to about 100 m wide and 10 m deep.

Preliminary results of the sidescan survey indicate that the distal reaches of the Almeria channel system are mainly characterized by a medium to low backscatter level. The 5.5 kHz profiles suggest that the surveyed area is covered by a few meters thick sedimentary drape, probably responsible for the overall medium to low backscatter. However, the acoustic response of the channels displays high to low backscatter (Fig.



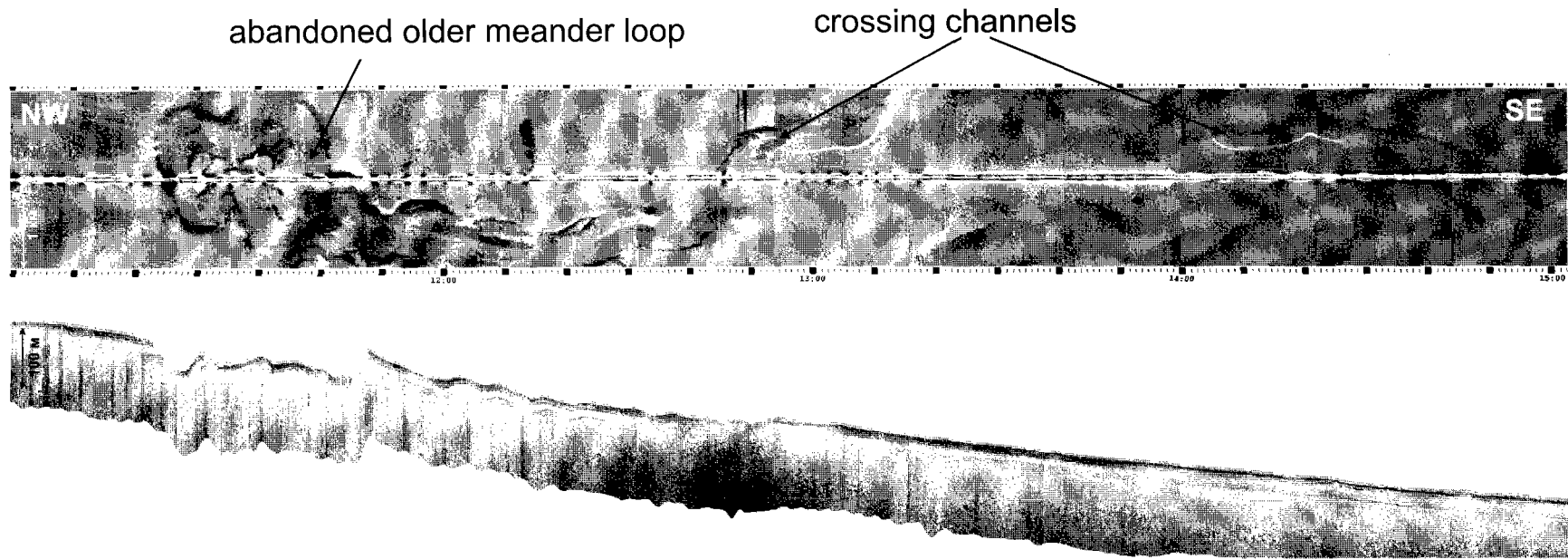


Figure 41. MAK-71MS sidescan image (30 kHz) showing an abandoned meander with a breached levee from where small channels evolve and an ephemeral small channel crossing an older abandoned one.

41). This different acoustic response seems to be related with the relative age of the channels and the distal or proximal position with respect to the main feeder channel.

Several small channels have been identified with an overall NW-SE direction and different ages, as suggest by the fact that some of them cut earlier ones (Fig. 41). These channels display a sinuous to straight course and some closed meander loops. The preliminary results suggest that many of these small channels, initiating from the main Almeria feeder channel, are ephemeral conduits probably related to periods of canyon reactivation or episodic increases in sediment supply. Such active periods can be related to earthquake events, common in the Almeria upper slope. In addition, subbottom profiler records display buried V-shaped incisions that probably are older than abandoned channels.

The sediment wave field, developed close to the right levee of the channel does not have enough topographic expression to be detected by the MAK-1 sidescan sonar as a thin sedimentary cover probably smoothes the relief. In spite of this, the subbottom profiles have undulating high amplitude reflectors. These sediment waves prograde upslope and future measures of their morphology will provide more information about their origin.

### 3.4. Bottom sampling

A. MAZZINI, F. MARTINEZ-RUIZ, F. RODRIGUEZ-TOVAR, G. AKHMANOV, A. AKHMETZHANOV, E. KOZLOVA, V. TORLOV, A. SAMOILOV, E. SARANTSEV, A. SADEKOV, E. POLUDETkina, O. BARVALINA, E. BILEVA, V. BLINOVA, F. J. JIMENEZ ESPEJO

#### 3.4.1. Introduction

Three main locations and a coring profile were chosen for bottom sampling during the Leg 3 (Fig. 30). The sites were selected on the basis of the OKEAN and MAK sidescan sonar images, seismic lines and bathymetry data. Sampling stations are grouped and described according to the

study locations:

- Location 1 includes the northern part of the West Alboran Sea basin within a mud volcano province.
- Location 2 includes the southern part of the West Alboran Sea basin within the mud volcano province, discovered and studied for the first time during the TTR-9 cruise.
- Location 3 is on an elongated topographic high that follows the NW-SE orientation of the fault system.

A set of pelagic cores for paleoceanographical reconstruction of the westernmost Mediterranean was collected during the transit legs. Pelagic cores will be described in a separate section.

A total of sixteen sampling stations were completed for a total of thirteen gravity cores (total recovery 37.9 m), two dredge samples and one TV grab sample (Table 4, Annex I).

#### 3.4.2. Location 1

Four gravity cores were taken in Location 1. The gravity cores sampled two newly-mapped dome-like structures. The sampling confirmed their mud volcanic nature and the structures were named Kalinin and Perejil mud volcanoes.

##### *Kalinin mud volcano*

Cores 280G and 281G were respectively from the top of the crater and lowermost part of the moat of Kalinin mud volcano. Core 280 had a top few centimetres of soupy marl containing shell fragments and occasional Pogonophora followed by one metre of bioturbated hemipelagic clay. Structureless and stiff mud breccia completed the lower part of the core down to 334 cm. The 305 cm of core 281G showed similar recovery but with a thicker unit (154 cm) of hemipelagic cover. Despite the thick hemipelagic cover, the presence of Pogonophora suggests seepage of hydrocarbon gases.

Table 4. Sampling sites in the Alboran Sea.

STATION NO	DATE	TIME GMT	LATITUDE	LONGITUDE	POSITION	DEPTH, M	RECOVERY, CM
279G	21.07.02	08:55	36°04.563N	4°59.844W	Pelagic core	877	289
280G	21.07.02	10:26	36°02.828N	4°55.973W	Kalinin mud volcano	908	334
281G	21.07.02	11:07	36°02.715N	4°55.803W	Kalinin mud volcano	924	305
282G	21.07.02	12:37	36°05.981N	4°53.091W	Top of the Perejil mud volcano	845	293
283G	21.07.02	13:16	36°06.018N	4°53.158W	Top of the Perejil mud volcano	841	233
284G	22.07.02	10:27	35°25.400N	4°31.854W	Top of the Dhaka mud volcano	360	262
285G	22.07.02	11:08	35°25.398N	4°31.853W	Top of the Dhaka mud volcano	360	244
286G	22.07.02	12:02	35°25.646N	4°31.668W	Dark patch on the slope of the Dhaka mud volcano	420	194
287G	22.07.02	23:28	35°33.708N	4°37.424W	Granada mud volcano	615	246
288Gr	23.07.02	00:05 01:10	35°33.715N 35°33.692N	4°37.434W 4°37.410W	Granada mud volcano	615 620	Full grab volume
289D	23.07.02	02:24 03:01	35°33.657N 35°33.874N	4°37.362W 4°37.384W	Granada mud volcano	634 617	Few clasts
290G	23.07.02	05:18	35°34.612N	4°34.004W	Pelagic core	854	284
291G	23.07.02	08:40	35°40.952N	4°13.970W	Pelagic core	1520	331
292G	23.07.02	13:31	35°53.850N	3°36.330W	Pelagic core	1536	371
293G	23.07.02	19:17	36°10.414N	2°45.280W	Pelagic core	1840	402
294D	24.07.02	21:39 22:25	36°28.302N 36°28.295N	2°26.071W 2°26.821W	Mound	560 500	Single fragment of basalt

#### *Perejil mud volcano*

Two cores (282G and 283G) were retrieved from the top of Perejil mud volcano. Core 282G had on upper 2 m of silty marl, soft and bioturbated, mixed with mud breccia matrix and occasional clasts. Mud breccia became dominant towards the bottom of this unit and characterised the remaining 293 cm of the core. Core 283G consisted of structureless mud breccia except for the first centimetre of brown soupy marl.

The recovery might indicate that core 282G is from an area within the crater where mud flow could mix with hemipelagic sedi-

ment due to limited supply of mud volcanic material. Core 283G has very little hemipelagic capping and was characterised by smell of H<sub>2</sub>S suggesting that the station was situated close to the more active part of the volcano. Results show that the mud volcano is currently active.

#### 3.4.3. Location 2

Six gravity cores were retrieved from the Location 2. Three stations are from a newly mapped mud volcano Dhaka and three from the Granada mud volcano, previously studied during the TTR-9.

*Dhaka mud volcano*

Cores 284G and 285G sampled the top part of the Dhaka mud volcano. Core 284G retrieved 65 cm of sediment. The top 8 cm were water saturated marl, rich in siliciclastic grains interpreted as soupy mud breccia mixed with hemipelagic deposition, beneath a 12 cm thick layer extremely rich in forams, shell fragments and siliciclastic grains, indicating shell debris mixed with mud breccia sediment. From 20 to 45 cm a coral rich layer suggests coral debris mixed with mud breccia matrix. A sharp boundary separated the stiff lowermost ordinary mud breccia unit.

As in core 284G, 244 cm of core 285G showed the top 6 cm of siliciclastic rich water saturated marl, followed by a unit (down to 75 cm) containing coral-shell fragments and coarse mud breccia matrix. Again a sharp boundary divided the underlying mud breccia.

Core 286G was sampled from a high backscatter area on the flank of the Dhaka mud volcano. The total recovery consisted of 194 cm with the usual top 10 cm of water saturated marl, followed by more consolidated marl mixed with mud breccia matrix. A sandy clay unit of mixed pelagic and mud volcanic material, enriched in large shell fragments, defined the boundary (at 55 cm) with the stiff mud breccia.

The recovery from the three stations indicates a relation between mud volcanic activity and coral colonies choosing a hard substratum to develop.

*Granada mud volcano*

Three stations were selected for the Granada mud volcano. A gravity core (287G) was taken from the top of the structure. Almost the entire recovery (246 cm) consisted of structureless mud breccia topped by 10 cm of soupy and oxidised mud breccia. The volcano was sampled again with the TV grab (288Gr) in order to obtain a representative collection of mud breccia clasts. A few hydrozoa and coral branches were found in the top oxidised layer. Numerous clasts of

differing size (from centimetric up to 30x30x15cm) and lithology were collected for further laboratory studies. A last attempt to retrieve large blocks and inferred carbonate crusts, observed during the TV profile was done with a dredge (289D). Several clasts and one big block (30x30x15cm in size) were found in the soupy matrix.

The recent activity of the Granada mud volcano was confirmed.

**3.4.4. Location 3**

A residual topographic high oriented with the NW-SE fault system, revealed high backscatter on the OKEAN sidescan sonar image. A single dredge station (294D) was carried out along the flank of this feature. The sediment retrieved consisted of grey soupy marl rich in foraminifera, containing wormtubes, echinoid needles, coral fragments (*Lophelia* sp.), one gastropod and one brachiopod fragment. A small clast (3x1x1 cm in size) of probable basaltic basement rock was also retrieved.

**3.4.5. Pelagic cores**

A total of five pelagic sediment cores were recovered in the Alboran Sea basin for paleoceanographical studies. High sedimentation rates in the Alboran Sea basin supply an excellent record of climate change. Selected sites are expected to provide a high resolution analysis of paleoenvironmental conditions during the last 20,000 years, as well as a millennial to decadal resolution of the regional/global climate variations during this time period.

Core 279G

Core 279G was taken in the north-western part of the western Alboran Sea basin and is at the westernmost site of an East-West transect within the Alboran Sea basin. This site is also a key area for the analysis of water mass exchange between the Atlantic and the Mediterranean, and for the establishment of circulation patterns. The first 60 cm of the sediment recovered were

lost during recovery, the remaining 289 cm of the core consisted of grey structureless hemipelagic clay, bioturbated throughout and with occasional shell fragments.

Cores 290G and 291G were taken in the southern part of the West Alboran Sea basin.

#### Core 290G

The total recovery of core 291G was 284 cm. The first 12 cm consisted of the usual brownish, soupy foraminifera rich marl. The rest of the core consisted of greyish hemipelagic clay, diffusely bioturbated with sparse shell fragments.

#### Core 291G

The corer recovered 351 cm of sediment. The first 2 cm were brown water saturated marl. The rest of the core consisted of greyish brown marly clay, diffusely bioturbated, rich in foraminifera becoming greyish clay towards the bottom. This unit was interrupted at 70 cm by a 2 cm thick layer of fine to medium sand, extremely rich in forams, showing inverse grading. At 306 cm a succession (inverse graded) of clayey-silty-sandy intervals with foraminifera admixture again interrupted the main hemipelagic unit.

#### Core 292G

Core 292G was recovered between the East and the West Alboran basin and was selected on the basis of the present circulation patterns in the Alboran Sea. The analysis of this site is specially aimed to reconstruct changes in circulation and its influence on marine palaeoproductivity.

The recovery consisted of 371 cm thick hemipelagic succession with occasional burrows and highly bioturbated intervals. The top 5 cm showed brownish oxidised soupy marl with forams.

#### Core 293G

Station 293G is located in the East

Alboran Sea basin and provided an excellent record of 402 cm of hemipelagic sedimentation. The top 10 cm show soupy marl with foraminifera. The marly layer is interrupted at 2 cm by a thin black layer, most likely representing the uncoupling of Mn and Fe during diagenetic processes. The rest of the core included a hemipelagic succession with locally stronger bioturbation (note at 180 cm a 25 cm long burrow). At 383 cm a thin dark layer of silty clay divided the hemipelagic sequence.

## 4. TYRRHENIAN SEA (LEG 4)

M. MARANI, F. GAMBERI, M. IVANOV AND  
SHIPBOARD SCIENTIFIC PARTY OF TTR-12, LEG 4

### *Introduction*

The Tyrrhenian Sea is a young back-arc basin composed of two distinct sub-basins, Vavilov (6-4 Ma) and Marsili (<2 Ma), floored by oceanic crust. A unique feature of these basins is the presence of large volcanic seamounts located in their axial region. Moreover another large submarine volcanic complex is formed on the continental margin along the northern boundary of the Marsili basin (Fig. 42). These three seamounts, with differing scientific targets, were the focus of research during the TTR-12 cruise.

The principal aims of the 4th Leg of

the TTR-12 cruise were to investigate the make-up of the Marsili and Vavilov Seamounts by means of seismics, deep-towed sidescan sonar, deep-towed video imagery and sampling. The Palinuro Seamount hydrothermal system was studied through deep-towed sidescan sonar and video imagery and sampling.

Previously acquired multibeam bathymetry of the Tyrrhenian region represented the baseline data for the above investigations.

### 4.1. Marsili Seamount

#### 4.1.1. Introduction and geological setting

Marsili seamount is positioned in the most recent ocean floored portion of the back-arc, the Marsili basin, that developed in

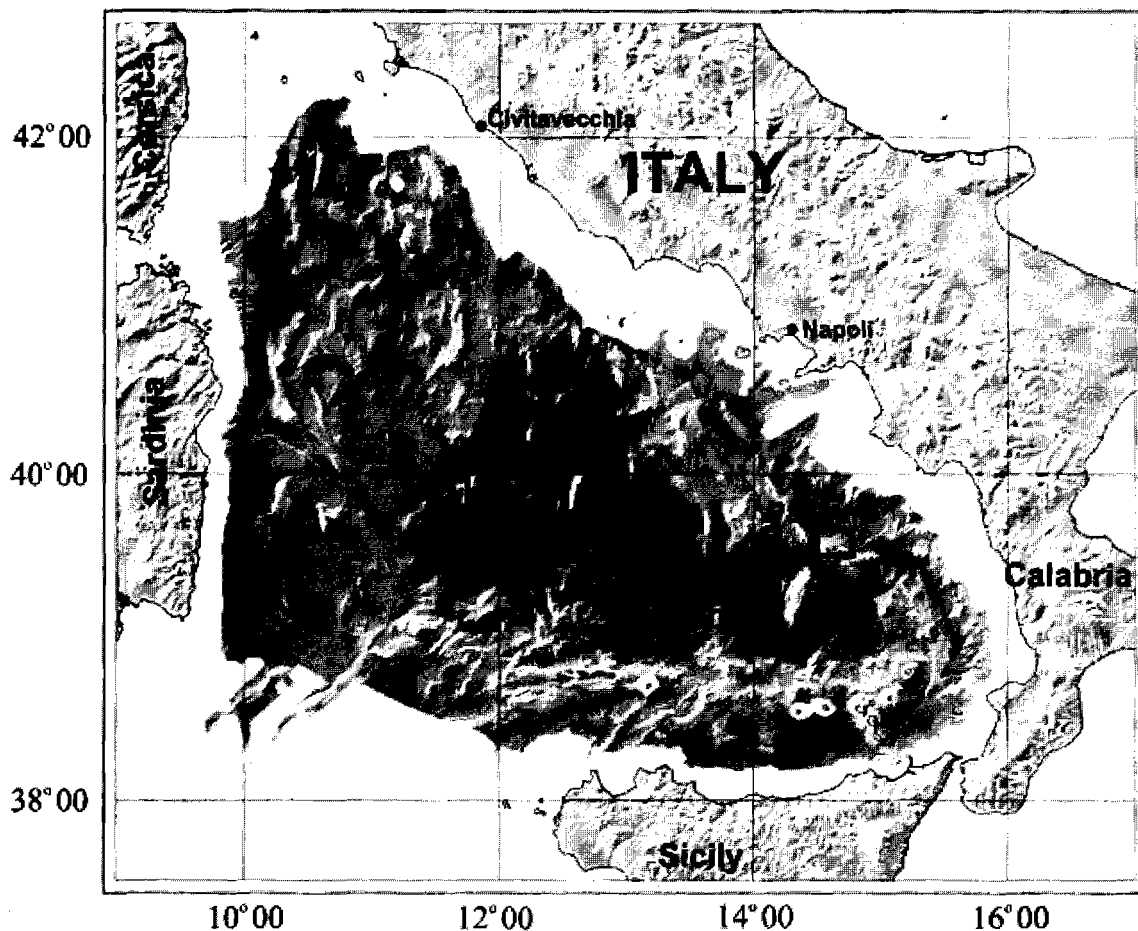


Figure 42. Location map of the investigated areas in the Tyrrhenian Sea during Leg 4 of the TTR-12 cruise. Investigations were focused on the three largest seamounts: the Palinuro, Marsili and Vavilov volcanoes. Multibeam bathymetry by IGM of CNR..

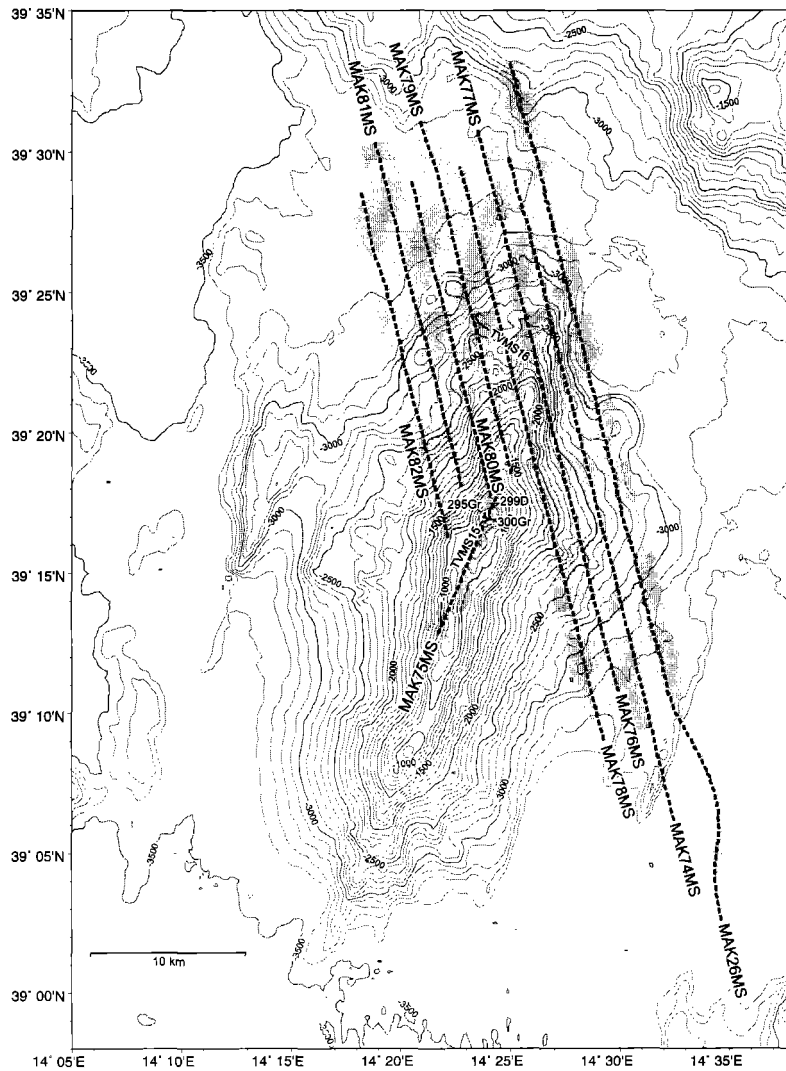


Figure 43. Location map of the deep-towed MAK sidescan sonar profiles, the two TV runs and the three sampling stations on the Marsili Volcano. The volcano is characterized by a linear summit region, a seamount field in the north-western portion and smooth flanks to the south.

last 2 Myr above the seismically active and steeply dipping, north-westerly subducting Ionian slab (Kastens et al., 1987).

The seamount occupies the centre of the flat-lying, 3500 m deep Marsili basin. It rises from the basin-floor to a minimum depth of 489 m, and is elongated in a NNE-SSW direction. It has a roughly elliptical shape, with a length in the order of 60 km and a maximum width of 30 km (Fig. 43).

Distinctive morphological features of the volcano summit axis region, portions of its flanks and the immediate surrounding basin floor were the targets for investigation.

#### Summit Axis

The roughly linear summit region of the Marsili seamount stretches 25 km NNE-SSW along the main axis of the volcano, approximately bounded by the 1000 m isobath. Linearity of the generally very narrow (0.5-1 km) summit axis is formed by the alignment of contiguous elongated volcanic cones. An isolated circular volcanic cone, 200 m high, is the most elevated portion of the seamount, and represents the northern termination of the summit axis region.

### *Flanks*

Large, isolated volcanic cones and terraces characterise the north flanks of the Marsili volcano, mostly lying at depths between 2300 m and 3000 m. The cones possess generally circular bases with diameters ranging from 800 to 1500 m. Most are flat-topped, several have central craters and some present horseshoe-shaped summits. The cones are not aligned although they occur in flank regions affected by scarps. In particular, numerous 150 m high scarps upon which some of the cones and terraces are located, cut across the lower flanks of the volcano. In contrast, the southern flank of the volcano shows no significant areas of constructional volcanism, and presents a smoother topographic profile.

### *Surrounding basin floor*

This area is in general flat-lying, however, horst and graben structures are evident both in the south-eastern and north-western portions, flanking Marsili volcano symmetrically. The basin is the site of mainly turbiditic sedimentation, fed by the Stromboli Canyon, the major pathway for sediment transport in the area (Gamberi and Marani, 1999).

#### **4.1.2. Sidescan sonar (MAK 1M)**

##### *Objectives*

The aim of the studies was to utilise the deep-towed sidescan sonar system (MAK 1M) to obtain high-resolution sonar imagery of the major morphological zones of the volcano (Fig. 43).

In general, the targets were to identify the most volcanically and tectonically active portions of the volcano in order to understand the mechanisms that have governed the growth of such a large edifice (volume in the order of 1500 km<sup>3</sup>). A direct implication of this study was the recognition of the areas more prone to instability and the recognition of the subsequent mass transfer processes.

Particular study was devoted to

understanding the "sonar texture" and its correlation to the eruptive characteristics of the lavas that fed the construction of the numerous small seamounts on the volcano flanks, and the possible differences between the flat-topped and conical edifices. Special attention was also paid to detail the relationship between tectonics and volcanism at the scale of a single flank seamount.

### *Results*

#### General Summary -Mosaic (Fig. 44)

The composite mosaic, made from all the MAK sidescan sonar lines, gives an exceptional picture of the geological processes acting on the Marsili volcano. Firstly, the contrast between the high backscattering northern region and the lower backscatter characterising the southern portions of the volcano is striking. These characteristics are due to asymmetrical activity, both in terms of volcanism and tectonics (or volcano-tectonics). The northern area has lava terraces and small seamounts and associated scarps, while the southern area is characterised by volcanoclastic sediment mobility in the form of flows and landslides. In the following sections, a more detailed description of the various morphological zones of the volcano is given, bearing in mind that the relationships between the zones are only to be appreciated from the mosaic.

#### Summit

The summit axis of the volcano was mapped from the summit cone and across two of the elongated cone ridges. Given the relatively shallow water depth (500-600 metres) and the very rough topography of the mapped area, the results can be considered satisfactory. The summit cone has two peaks that seem to be separated by N-S trending linear scarps, likely due to faulting. Southwards, a generally flat area develops, interrupted by large elongated linear cones. This flat region is the site of smaller sized volcanic constructions.

An example of one of the elongated



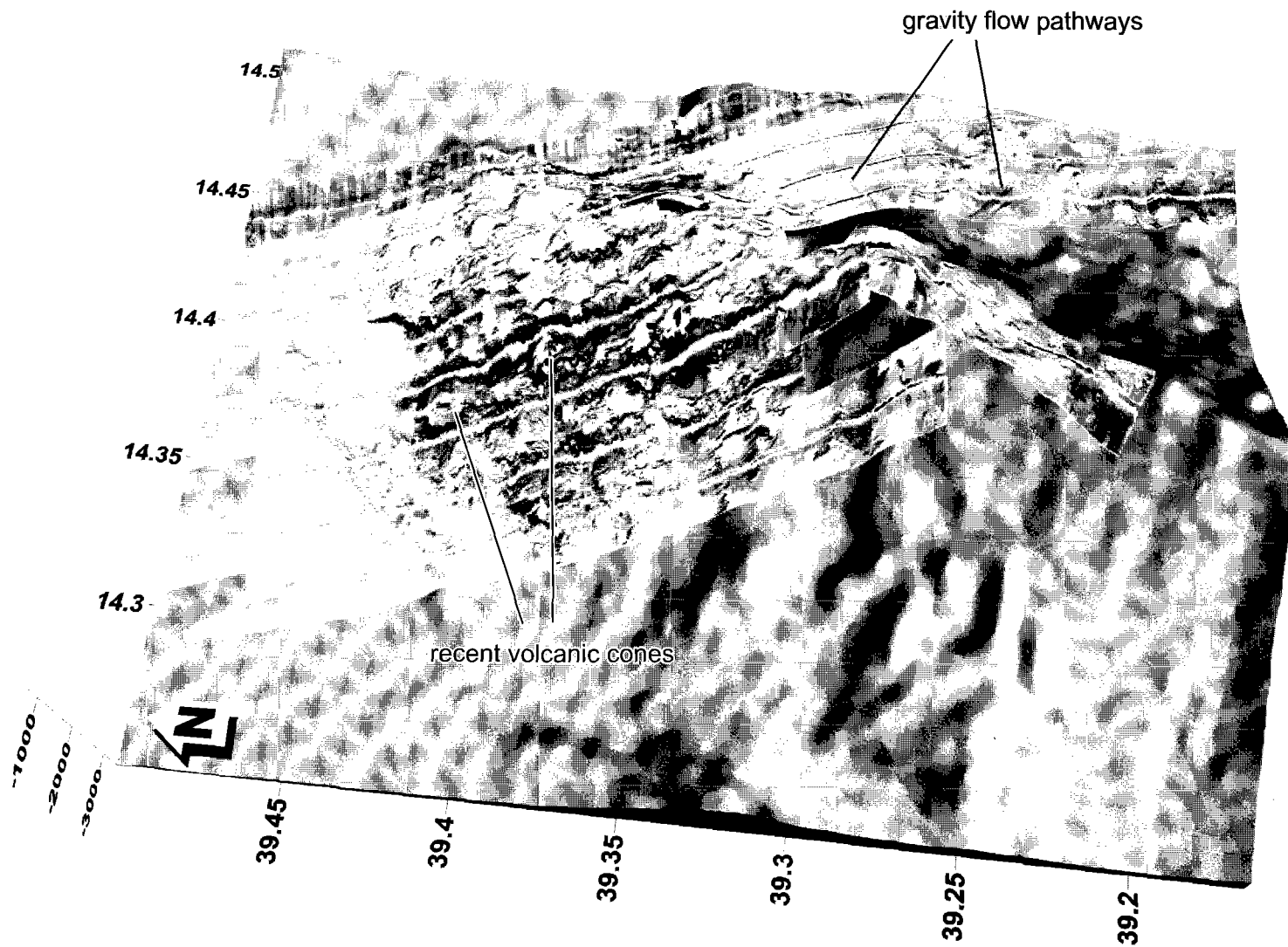


Figure 44. Perspective view of the Marsili seamount, showing MAK sidescan sonar coverage draped on bathymetry by IGM of CNR. The prevalence of recent volcanism in its northern portion and sediment gravity flows and slides in the southern part are clearly seen.

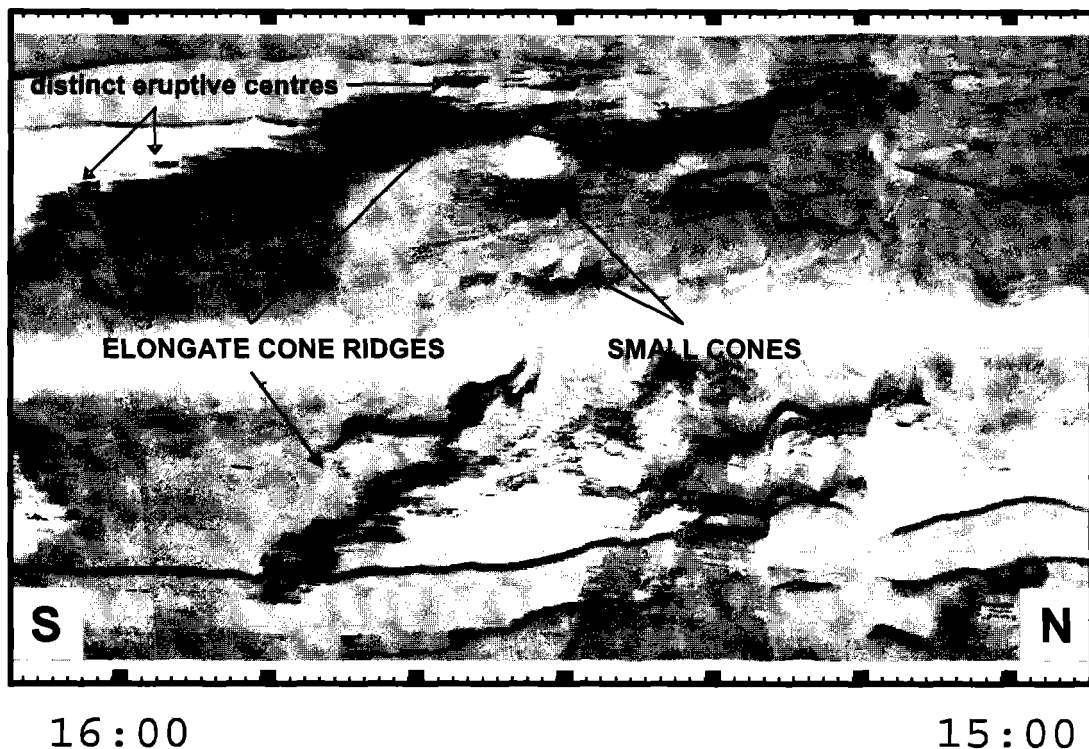


Figure 45. Portion of MAK line 75 in the summit region.

cones (Fig. 45) is shown on the line MAK-75 (15:00-16:20). On the western side of this line, coalescing elongated cones are characterised by medium backscatter slopes casting large shadows which also show evidence of gravity flow activity. The tops of the cones show that there probably are several distinct eruptive centres. On the opposite side, the flank of another elongated cone is outlined by high backscatter, superposition of linear scarps and a shadow.

### Flanks

The south-eastern flank of the volcano presents in general a low backscatter pattern in keeping with the presence of a sedimentary cover of variable thickness, as shown by the hull-mounted and MAK sub-bottom profilers. In this part of the volcano, line MAK-78 (16:00-17:00) shows down-slope running bands of higher backscatter which are likely to be pathways of coarse-grained sediment gravity flows (Fig. 46). Instability and sediment removal is also widespread over large portions of the investigated area.

Slide and slump scars and related depositional bodies are characterised by blocky texture on the sidescan sonar and irregular reflections on the sub-bottom profiler, typical of debris flow and debris avalanche deposits.

The southernmost portion of this area presents a high backscatter pattern related to circular volcanic edifices. Four of the seamounts are shown on the line MAK-78 (13:300-15:30) (Fig. 47). Two of them show up as elevated features on the sub-bottom profiler records. To the west, the largest one, centred at 14:25 presents a summit crater in contrast to the adjacent seamount at 14:10 that is topped by a dome. The other two seamounts are located to the north, where a conical seamount develops with a low backscatter sedimented flat top, and to the south where another flat-topped seamount is present, capped by a circular dome. The steep flanks of the seamounts are mainly made up of high backscattering rocky outcrops with hummocky type texture. At the base of the seamounts, accumulation of mass wasting material is evidenced by a medium blocky backscatter texture on the sidescan

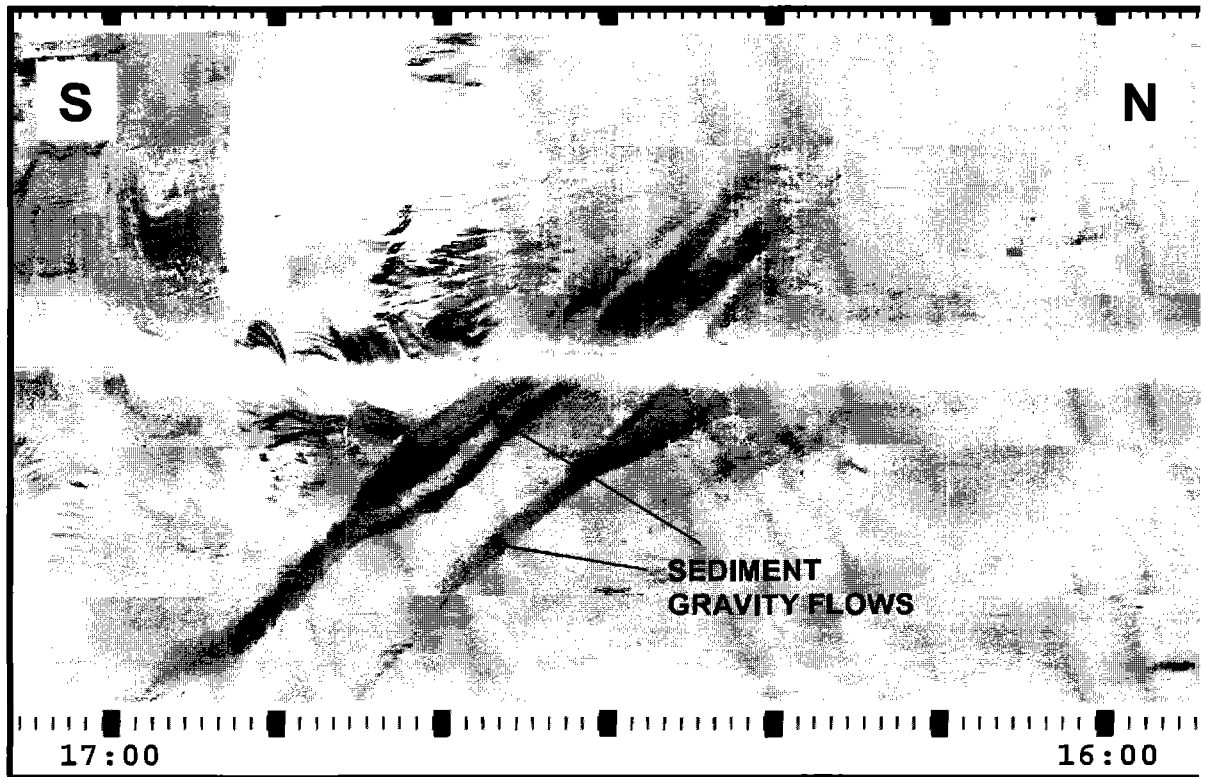


Figure 46. Portion of MAK line 78 located in the south-east region of the volcano.

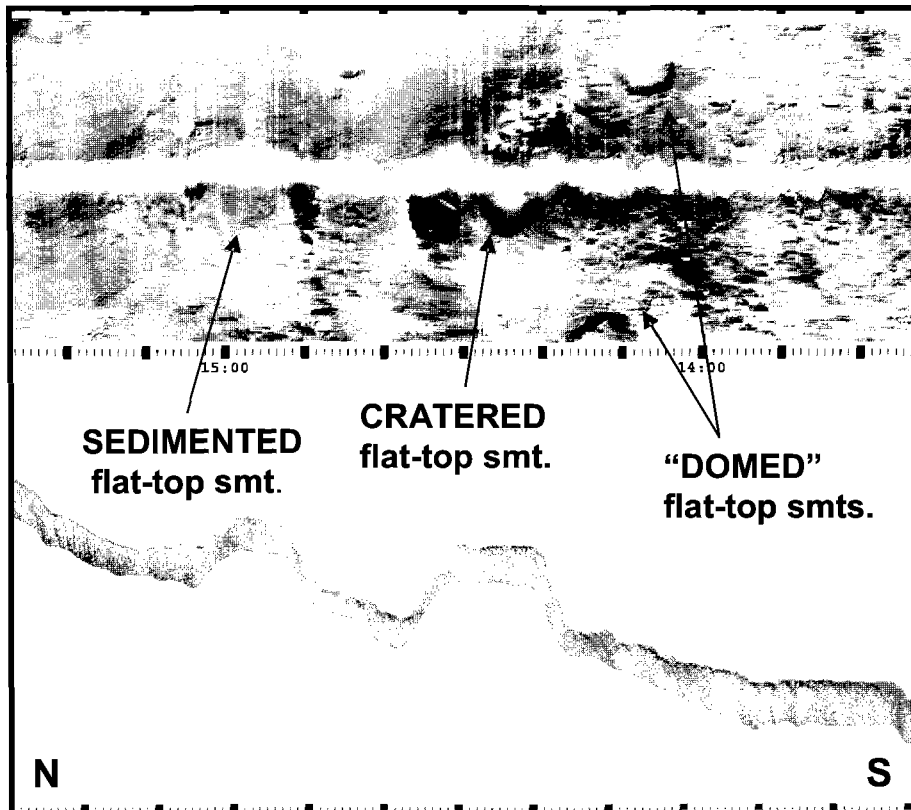


Figure 47. Portion of MAK line 78 in the southern cone field.

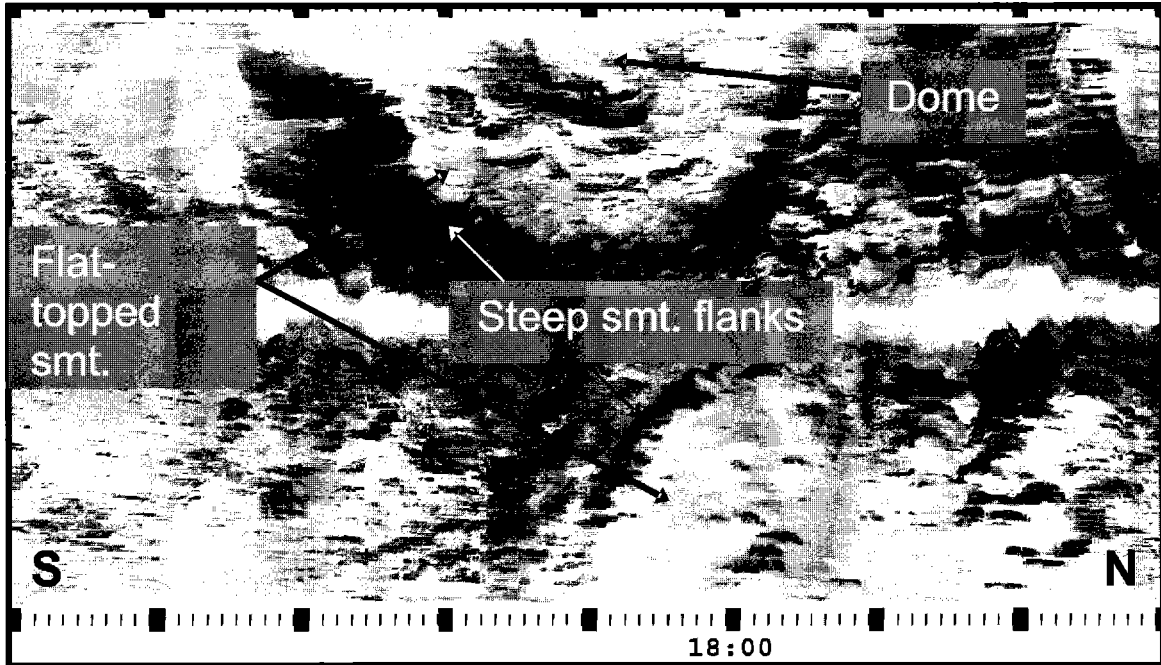


Figure 48. Portion of MAK line 80 showing flat-topped seamounts from the NW seamount field.

sonographs and irregular seafloor on the sub-bottom profiler records.

Line MAK-80 (17:30-18:40) (Fig. 48) illustrates two volcanic seamounts from the north-western flank of the volcano with high backscattering, steep flanks and lower backscattering flat summits upon which circular elevated domes develop, outlined by their higher backscattering slopes. These flat-topped seamounts are widespread over all the north-western flank of the volcano, thus contributing in a major way to the construction of this portion of the Marsili seamount. The eastern part of this same line, from 13:50-15:30 (Fig. 49) also shows one of the scarps oriented in a NNE-SSW direction which dissects the slope of the edifice. The scarp is a high backscattering feature and its height increases to the north. It has a very rugged upper portion and is in places affected by smaller scale elongated scarps. Hanging blocks and re-entrants are due to mass wasting processes that result in the accumulation of smooth medium backscattering coarse grained aprons at the scarp base, which diverge downslope (western part of the line).

Basin floor

The boundary between the basin floor and the volcanic edifice is in places abrupt, being marked by high-standing scarps. In other places, on the contrary, the flank/basin boundary is continuous, with flank dip gradually passing to the basin floor. In the vicinity of the volcano, the basin floor is affected by mass wasting events that originate from the seamount, interrupting the otherwise very low backscattering and well layered seabed.

The eastern part of the line MAK-78, (23:30-02:00) shows a high backscatter scarp (Fig. 50), that distinctly marks the boundary between the basin floor and the Marsili volcano. It is composed of two separate segments that are likely to be the walls of faults, overlapping for 200 m across a breached relay ramp. In the adjacent abyssal plain several small channels show up, on the sub-bottom profiler records, as erosional areas that cut through the acoustically well layered turbiditic sequence of the basin. On the sidescan sonar image, the channels correspond to discontinuous, narrow areas of high backscatter, well distinguished from the low backscatter of the basin turbidites.

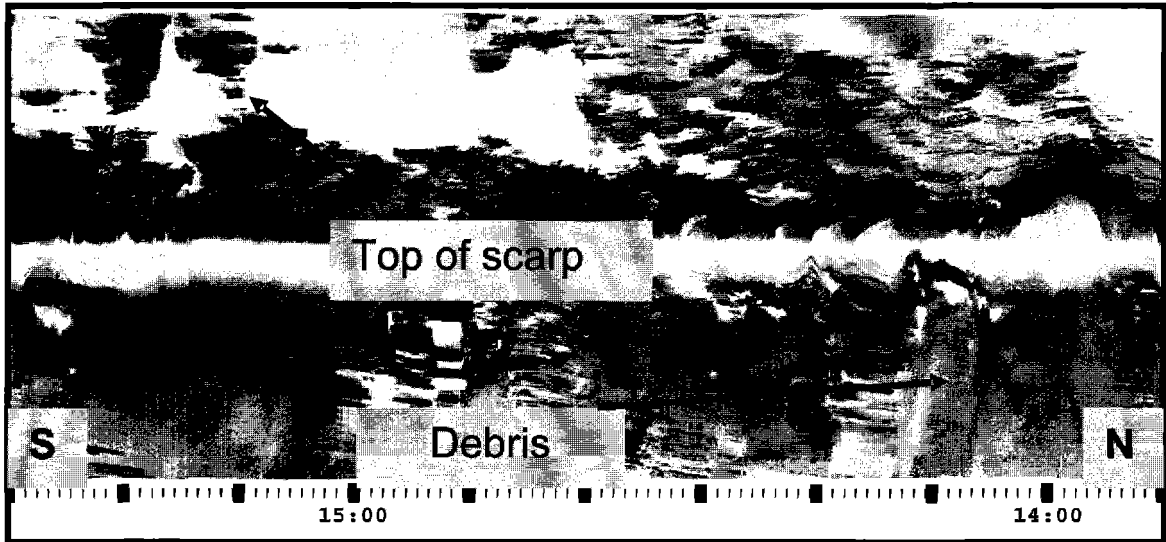


Figure 49. Portion of MAK line 80.

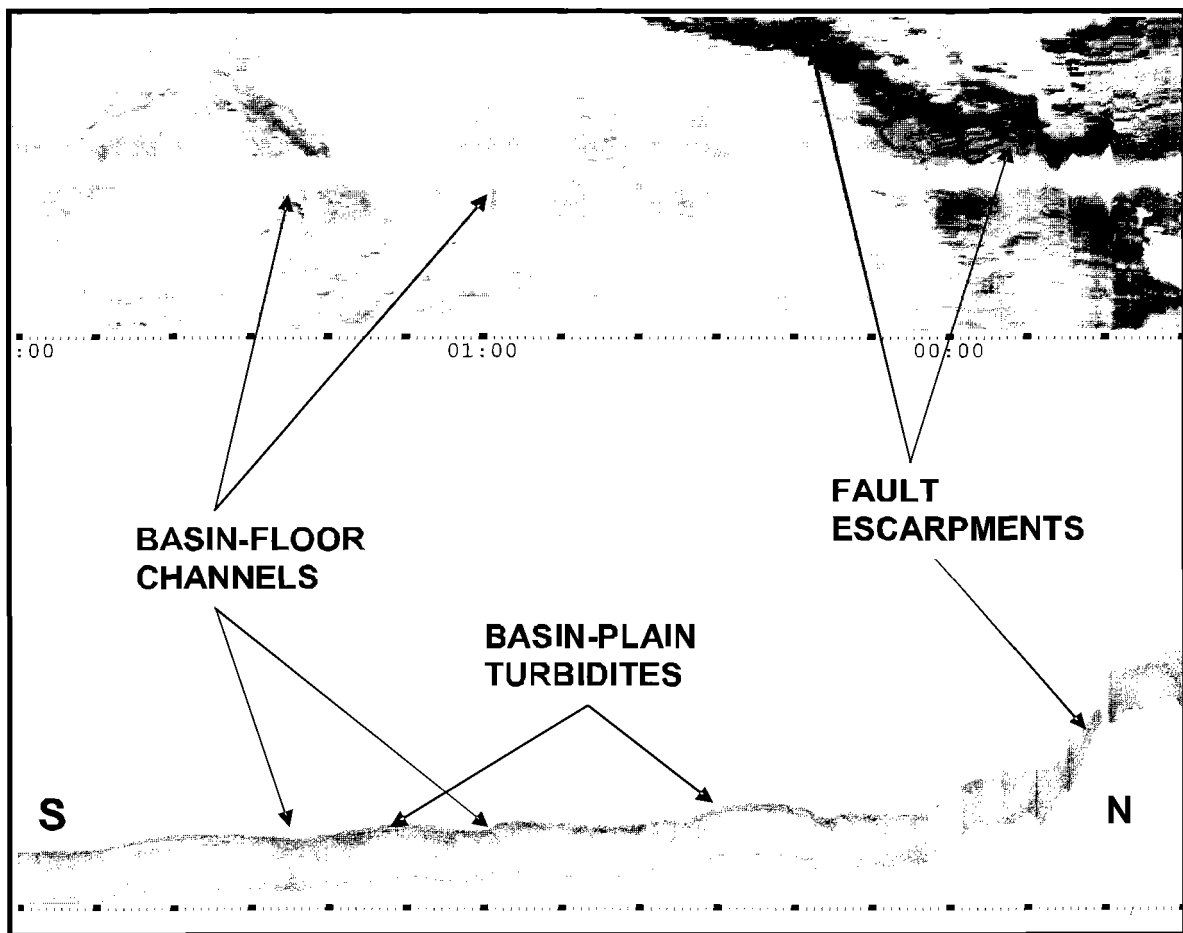


Figure 50. Portion of MAK line 78, with associated deep-towed profiler record showing the volcano base and basin characters.

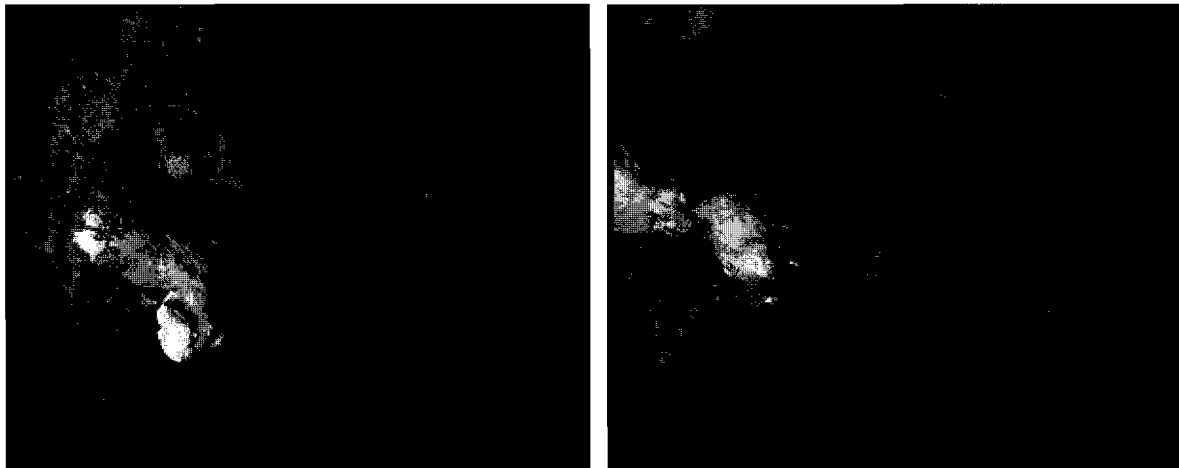


Figure 51. Examples of the chimney structures in the summit area of the Marsili volcano. The brighter portions are the sites of active deposition of Fe oxyhydroxides.

#### 4.1.3. TV seabed inspection

##### *Objectives*

Due to its intrinsic value of direct observation but necessarily limited spatial coverage, deep-towed TV imagery was used to investigate the processes that govern the growth of the small seamounts that are constructed on Marsili. In particular, the summit cone of the volcano at depths between 500-600 m (TVMS-15) and two flat-topped seamounts on the NW flank, at a depth in the order of 2500 m (TVMS-16), were targeted on the basis of the swath bathymetry and sidescan sonar data.

##### *Results*

##### TVMS-15

The most important result of this camera run was the discovery of a field of hydrothermal chimneys, located above a steep scarp that exposed the lavas making up the base of the summit cone. Most of the lava types seen in the run were pillow lavas, and associated debris aprons. The chimney field is made up of max. ~ 1 m high chimneys (Fig. 51), generally grey in colour except where their tips or part of them are red/orange. The seabed in the chimney field has a platy appearance, perhaps also due to hydrothermal deposition. No active venting was

observed. However, the bright colours due to Fe oxyhydroxides and the very soft nature of some of the chimneys show that low temperature hydrothermal deposition takes place. It is reasonable to assume that the higher temperature stage of sulphide production is now extinct in the observed area. This latter activity has been proven by the sampling of a sulfide fragment during a previous cruise (Marani et al., 1999).

##### TVMS-16

The run traversed the flank of one of the small seamounts that are common on the north-western flank of the Marsili volcano. It passes from the sedimented floor to the seamount, through the extensive pillow lava debris apron that covers its flanks, up to well developed, in situ, pillow lavas in its topmost part. The observations make an important contribution to the interpretation of sidescan sonar data of the numerous other seamounts of the area.

#### 4.1.4. Bottom sampling

In order to characterise the chimney area, two TV-controlled grab and dredge samples were collected from the summit area of the Marsili volcano (Table 5).

Table 5. Sampling sites in the Tyrrhenian Sea.

CORE No	DATE	TIME GMT	LATITUDE	LONGITUDE	POSITION	DEPTH, m
295Gr	3.08.02	01:16 01:40	39°17.031N 39°17.007N	14°23.848W 14°23.831W	Marsili volcano	535 525
296Gr	8.08.02	07:23 07:40	39°32.522N 39°32.543N	14°42.657W 14°42.660W	Palinuro volcano	580 588
297K	8.08.02	08:38	39°32.490N	14°42.539W	Palinuro volcano	601
298Gr	8.08.02	10:53 12:02	39°32.517N 39°32.545N	14°42.674W 14°42.664W	Palinuro volcano	585 579
299D	8.08.02	15:42 15:59	39°16.993 N 39°17.089N	14°23.834W 14°23.841W	Marsili volcano	524 526
300Gr	8.08.02	19:07 20:02	39°17.027 N 39°17.014N	14°23.823W 14°23.826W	Marsili volcano	507 506

## Results

### TV-controlled grab

#### TTR12-295GR

An area of Fe oxyhydroxide deposition was sampled, made up of red clay and numerous soft oxyhydroxide crust fragments, probably portions of chimney (Fig. 52).

#### TTR12-300GR

The grab recovered large fragments of lava that form the substrate on which the chimney field is located (Fig. 52).

### Dredge

#### TTR12-299D

This sample also recovered numerous lava fragments, some showing the characteristic outer layer of pillow lavas (Fig. 52).

## 4.2. Palinuro Seamount

### 4.2.1. Introduction and geological setting

The Palinuro seamount is composed of 5 coalescing volcanic edifices that represent the E-W trending northern boundary of the Marsili Seamount. The highest peak of the Palinuro volcano tops at 70 m and is a flat

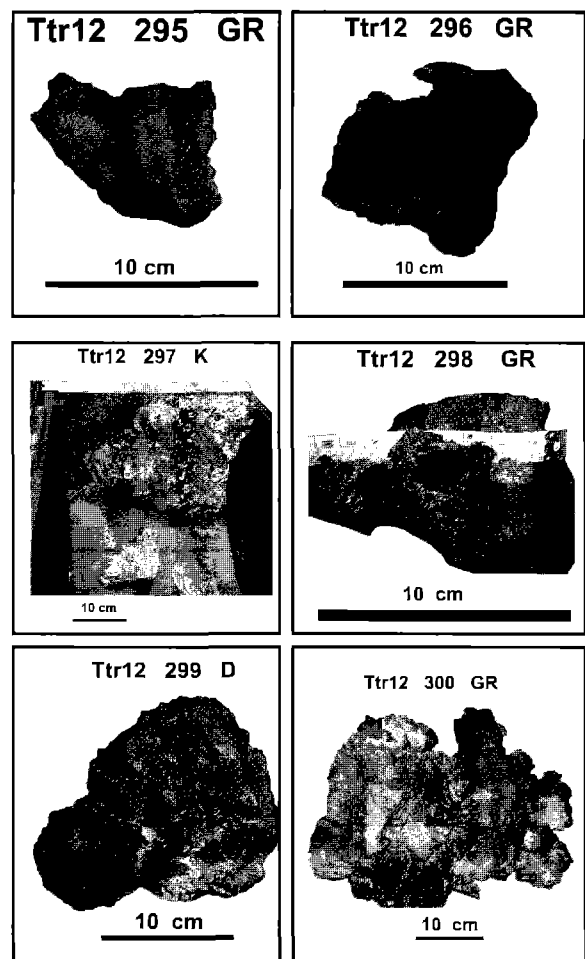


Figure 52. Examples of the samples recovered during Leg 4. Samples 296, 297 and 298 are from the Palinuro volcano, the rest are from the Marsili volcano.

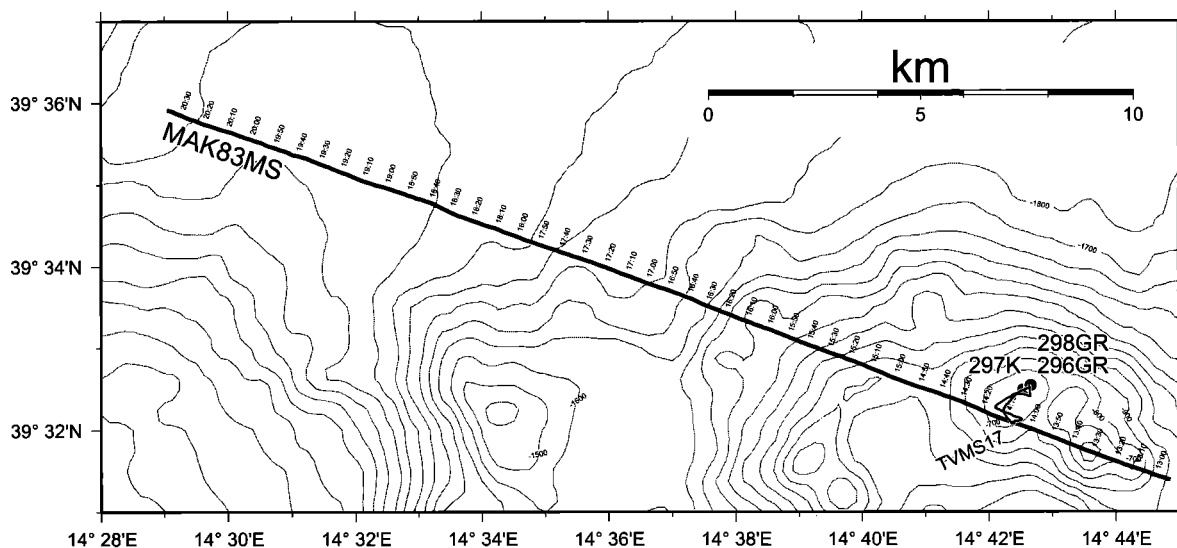


Figure 53. Location map of MAK line 83, TV run 17 and sampling sites on the Palinuro volcano.

area that was probably emergent during the last low-stand of the sea level. Numerous records of hydrothermal activity, mainly of low-temperature Fe-Mn crusts, have been reported from various portions of the volcanic complex (Eckhardt et al., 1997). In addition, sulphide deposits, both as stringer-like veins and fragments of extinct chimneys covered by Mn crusts have been collected on the westernmost peak of the volcano (Minniti and Bonavia, 1984; Marani et al., 1999).

#### 4.2.2. MAK sidescan sonar data

##### *Objectives*

One MAK profile, line MAK-83, was acquired (Fig. 53) with the aim of selecting the most promising route for a subsequent TV seafloor observation run and sampling, focussed at evaluating the seafloor style of hydrothermal circulation and related mineralisation. The line crosses the westernmost volcanic edifices of the Palinuro complex and its western slope.

##### *Results*

Line MAK-83 shows several volcanic cones composing the edifice. The cone intended for the subsequent investigations with deep tow video and sampling is seen

between 13:50-14:40 (Fig. 54). It has a twin peaked summit characterised by medium acoustic backscatter, within which several small scarps stand out as patches of higher backscatter. The upper flank of the edifice is steeper, and has high backscatter and arcuate scarps corresponding to outcropping volcanic rocks. The lower portions of the flank are mainly covered by a thin layer of sediments that thickens away from the cone. Two high backscattering ridges radiating westwards from the cone are also seen on the sonograph.

#### 4.2.3. TV seabed inspection

##### *Objectives*

The TV seafloor inspection run was devoted to determine the spatial extent of the hydrothermal mineralisation, the presence of various types of deposits and host rock alteration, and possibly to recognise active vent sites and related fauna.

##### *Results*

Numerous sites of hydrothermal deposition were observed on TVMS-17. Also in this area, chimneys were up to 1 m high (Fig. 55) and are commonly topped by red Fe oxyhydroxide precipitation. In places, small,



#### 4.2.4. Bottom sampling

Two TV-controlled grab samples and a Kasten core were collected from the summit area of the Palinuro seamount (Table 5).

##### *Results*

##### TV-controlled grab

##### TTR12-296GR

The grab collected large and small fragments of black manganese crust. The larger fragment (Fig. 52), shows large vacuoles on one side (inner part of chimney) and a smoother outer chimney surface. The sample demonstrates that manganese crusts also build chimneys, in addition to Fe oxyhydroxides.

##### TTR12-298GR

In this case, one of the Fe oxyhydroxide chimneys was sampled. Figure 52 shows an example of the crusts making up the chimney, clearly deposited around a main fluid flow orifice.

##### Kasten corer

##### TTR12-297K

The core was located in one of the

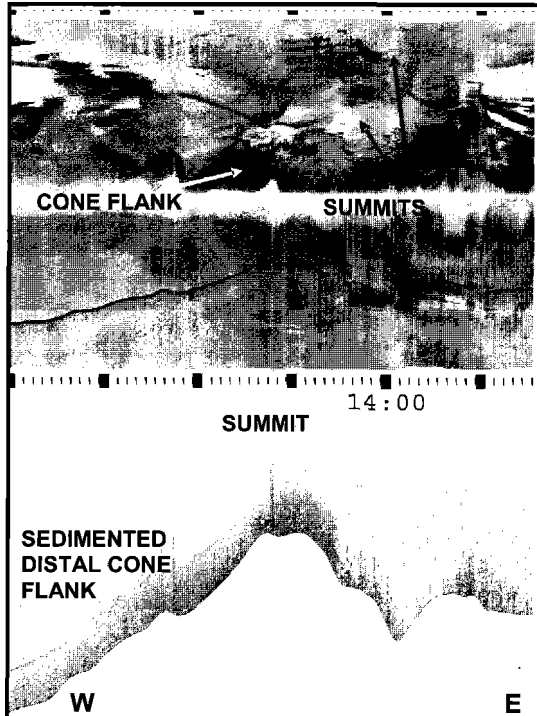


Figure 54. Portion of MAK line 83 showing the area of the investigated cone.

up to 0.5 m scarps, were seen to control the location of the chimneys with the latter growing along the scarps. Large patches of very intense activity of burrowing organisms were observed. The presence of these patches is believed to be due to the scattered character of hydrothermal fluid flow.

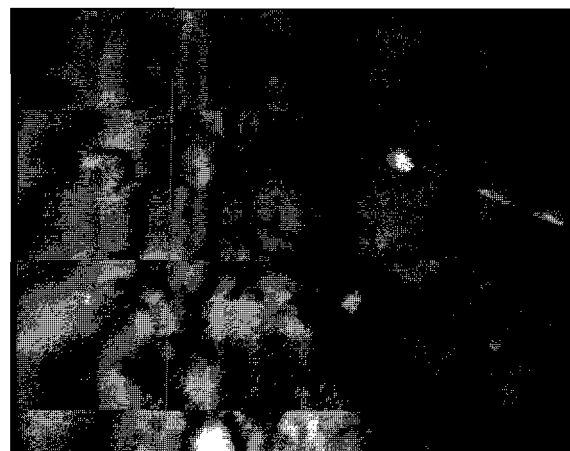
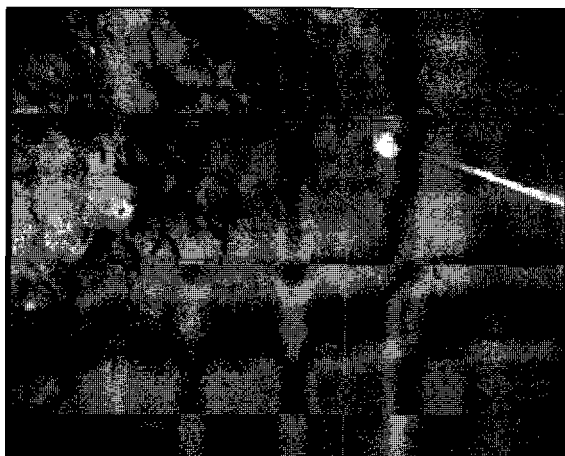


Figure 55. Examples of chimney structures found on the Palinuro volcano. Note the fallen chimney in the right image.

patches of concentrated burrowing. It shows that beneath a thin veneer of sediment, the sea floor in the area is made up of white, moderately consolidated kaolinite (Fig. 52) which passes at depth to a grey clay, very similar to that observed in other hydrothermal settings (Marani et al., 1997) where argillitic alteration of volcanic rocks is very advanced.

### 4.3. Vavilov Seamount

#### 4.3.1. Introduction and geological setting

The Vavilov basin is the oldest oceanic basin formed above the Ionian subducting plate in a back arc position, with its formation being ascribed to the interval between 6 and 4 Ma. In the central portion of the basin the Vavilov seamount rises from the flat basin floor (3500 m deep) to depth of 700 m. The seamount is 40 km long, elongated in a NNE-SSW direction and shows a prominent asymmetry. The western flank is steeper and smoother than the eastern one which, in contrast, shows a rugged topography due to the presence of small seamounts (Fig. 56).

The Vavilov seamount separates the Vavilov basin into a western and an eastern basin. A tilted continental block, the De Marchi seamount, represents the western boundary of the oceanic crust of the Vavilov Basin. The basin itself is not, however, flat and is interrupted by several structural highs. In particular the N-S Gortani ridge is present to the north of the Vavilov seamount while the arcuate D'Ancona ridge crosses the whole basin with an E-W direction before turning north behind the De Marchi Seamount. This complex structural setting causes the western Vavilov basin to be almost isolated from the adjacent basins: to the west the Sardinia Valley basin and to the east the eastern Vavilov basin. To investigate the area, four seismic lines were shot, crossing the whole eastern Vavilov basin and part of the western one. Together with the seismics, long-range OKEAN sidescan data were also acquired. Finally, a deep-towed MAK-1M sidescan sonar line was acquired along the western base of the volcano.

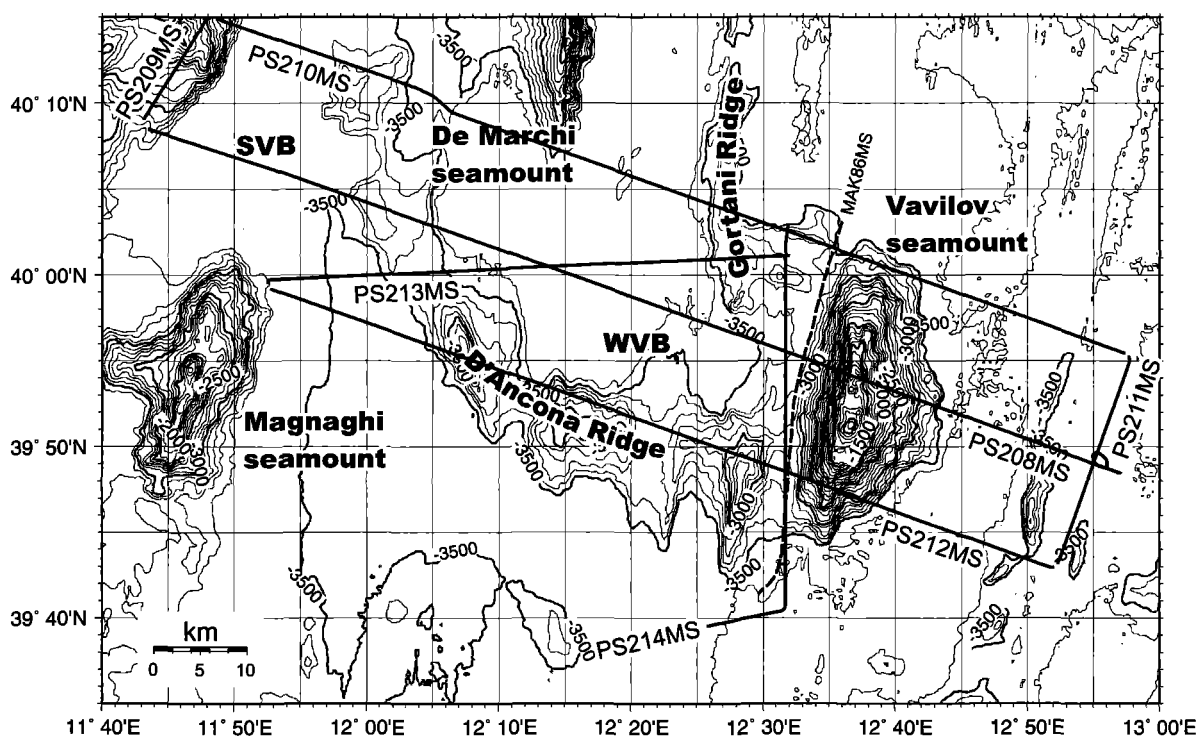


Figure 56. Location map of seismic lines and MAK sidescan sonar line in the Vavilov volcano region.

### 4.3.2. Seismic data

#### *Objectives*

The structural setting of the eastern portion of the Vavilov basin was the target of this study, with emphasis on the relationships between the different structures and their position within or outside the supposed area floored by oceanic-like crust. Another objective was to determine the nature of the western flank of the Vavilov seamount, in order to understand whether its formation is due to flank collapse or other causes.

#### *Results*

##### Line PS208MS (Fig. 57)

The line starts to the east of the Vavilov seamount, in the eastern Vavilov basin, and images a high covered by poorly reflecting hemipelagic sediments (07:00-07:20) and the basin floor showing continuous reflections that make up its turbiditic infill (07:20-08:00). The basement of the basin at 5.1 sec. is marked by a set of high amplitude reflectors. The Vavilov seamount flank borders the basin to the west (08:00-08:40) and presents hyperbolic reflections probably resulting from its rugged topography. On the contrary, the western flank (08:40-09:20) shows a very sharp and continuous reflection. Immediately at the western base of the volcano (09:20-10:00), at around 4.7 sec., high amplitude reflections are visible, covered by only 100 msec of sediments showing discontinuous reflections. The basement of the western Vavilov basin, which reaches the maximum depth of approximately 5.7 sec. in its central part, presents two culminations (at 10:40 and 12:00) where the basement is located at a depth of 4.8 sec. The overlaying sedimentary package presents a very well developed seismic layering reflecting its general turbiditic nature. However, in two areas (10:00 and 10:30) the above-basement seismic reflections become faint along narrow and sharp regions which extend to the seafloor and displace it. The basement high at 12:00 bounds to the west an area where the base-

ment is at a depth of 5.2 secs. The D'Ancona ridge is imaged between 12:40 and 14:00 and is a faulted structural high covered by a sedimentary unit with a thickness of 300 msec. Seismic line 208 crosses the Sardinia Valley basin (14:00-15:20). It has a relatively flat, highly reflective basement at 5.4 secs, and a sedimentary infill which is almost 1 sec. thick. The upper part of the sedimentary infill is discontinuous reflections with lenticular geometry, probably the result of erosion due to distal reaches of the Sardinia Valley channel observable on the seafloor at 14:00.

##### Line PS212MS (Fig. 57)

Running south of line PS208MS, the line crosses the southern extreme of Vavilov seamount between 03:40 and 04:20. From 04:20 to 05:20 the western Vavilov basin is imaged with a basement at a depth of 5.6 secs and the sedimentary infill represented by continuous reflections, similar to those of PS208. The southern, E-W trending, portion of the D'Ancona ridge occupies most of the profile from 05:20 to 09:40. It is represented by several structural highs, with a variable thickness of sedimentary cover. Small hanging basins are developed between the highs. The Sardinia Valley basin is crossed between 09:40 and 11:00. Here the extensive erosion at the seafloor results in truncations of the uppermost reflections. The fault-tilted basement gently dips toward the south-east from 4.6 to 5.1 sec, being overlapped by the sediment fill.

##### Line PS210MS (Fig. 58)

The northernmost line was shot from west to east. It crosses a series of structural highs. Between 17:00 and 18:00 the Sardinia Valley basin is developed with the basement at 5.1 sec, and a basin infill of 600 msec. The D'Ancona Ridge, crossed from 17:40 to 19:20, is sedimented and faults result in narrow depressions where the basement depth is 5.4 sec. Between 19:20 and 20:00 the eastern Vavilov basin is crossed, presenting a structural and sedimentary setting similar to that of line PS208MS. Basement highs separate

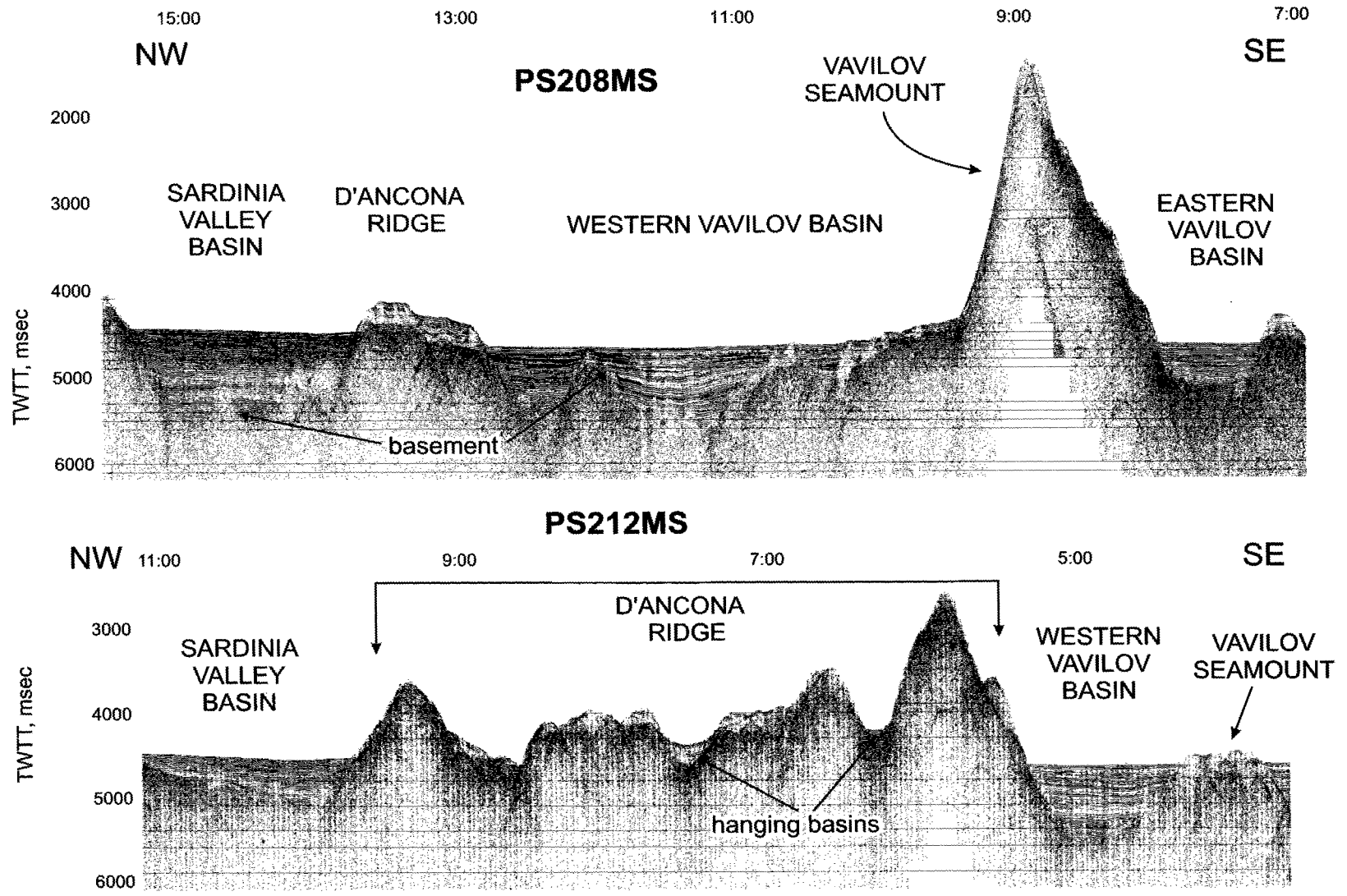


Figure 57. Seismic lines 208 and 212 in the Vavilov volcano region.

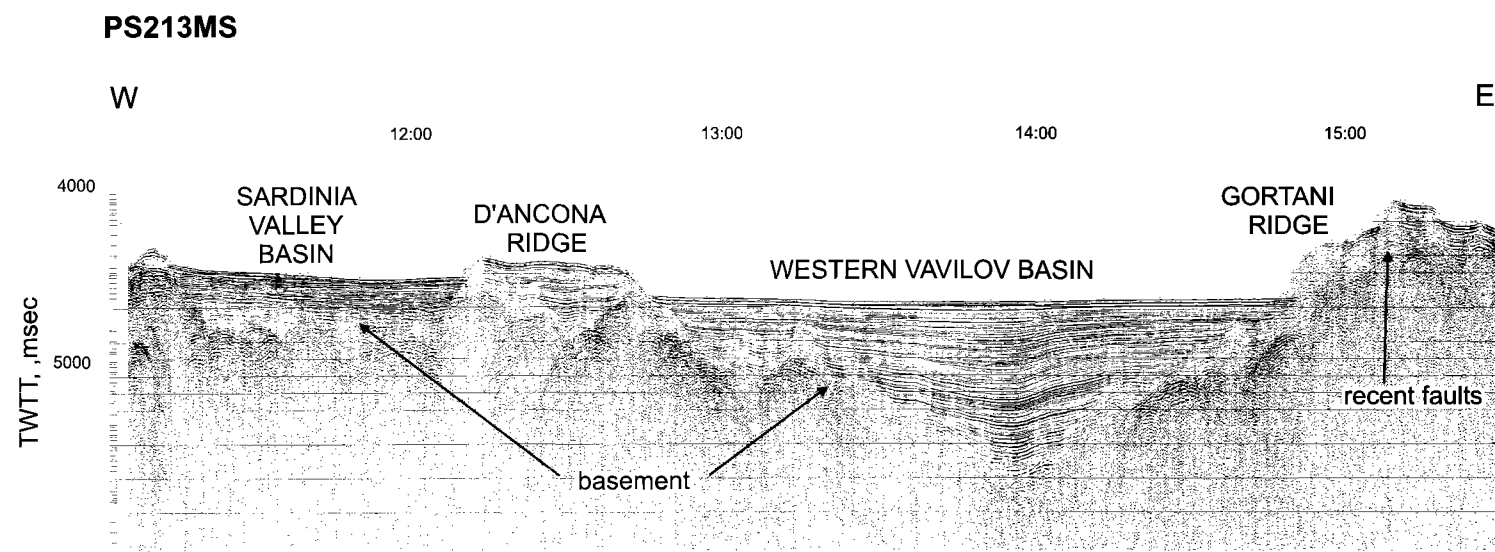
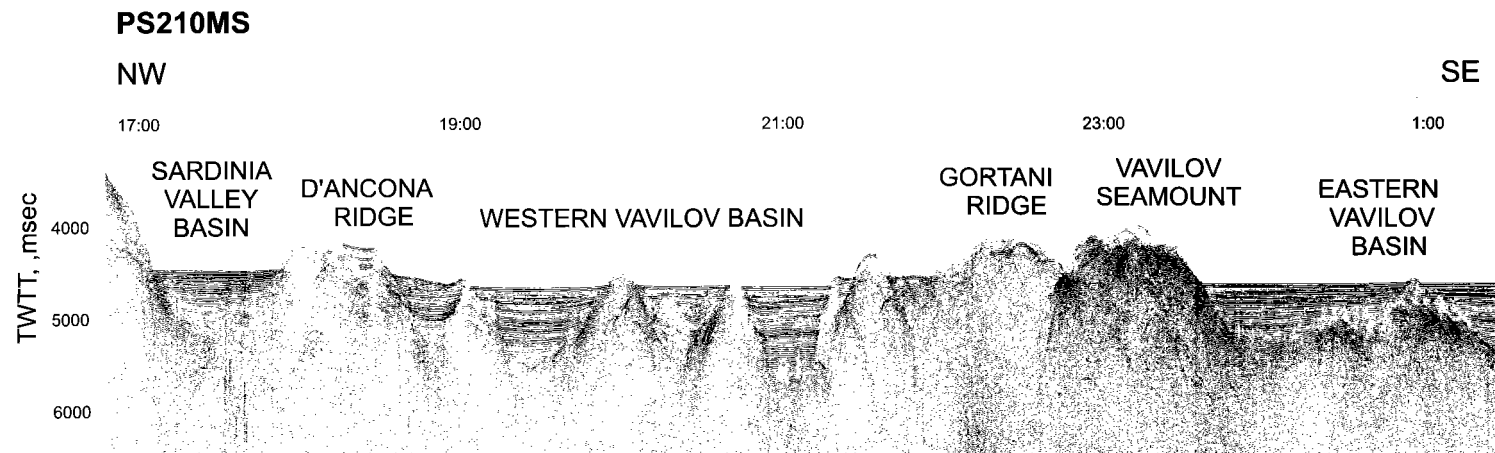


Figure 58. Seismic lines 210 and 213 in the Vavilov volcano region.

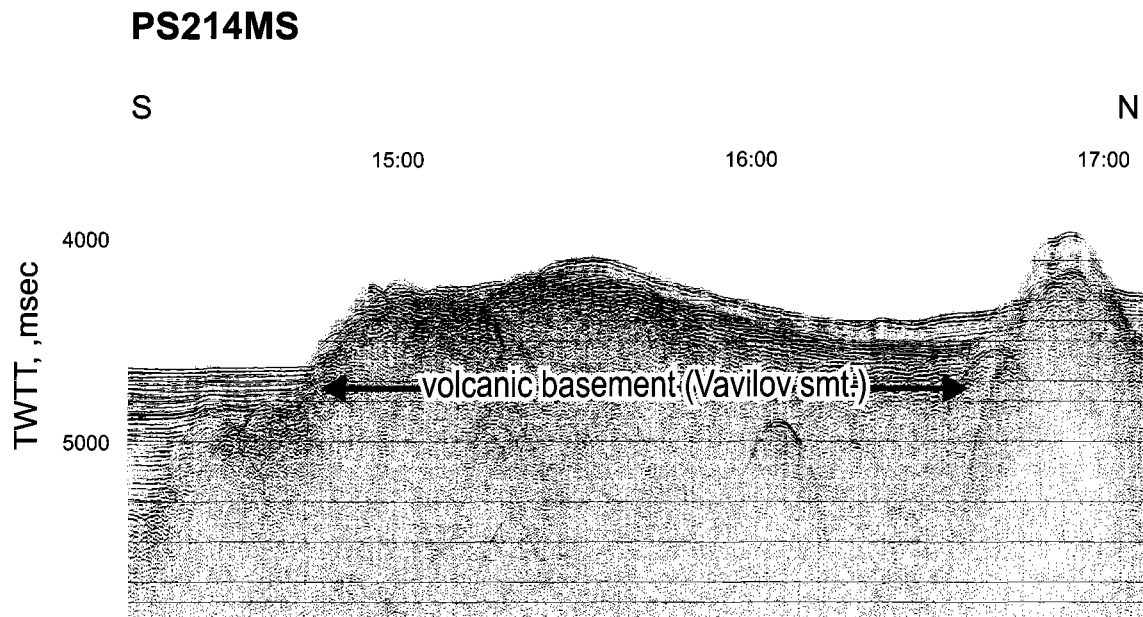


Figure 59. Seismic line 214 along the western base of the Vavilov volcano.

distinct basins with variable basement depth and thickness of the sedimentary infill. The fill is at times (20:00-20:40) deformed and with uplifted reflectors. From 22:10 to 22:40 the Gortani ridge is crossed and merges with the Vavilov seamount, crossed between 22:40 and 23:50. The line then enters the eastern Vavilov Basin subdivided by the northern continuation of the structure described in line PS208MS. Basement depth is in the order of 5.4 secs.

#### Line PS213MS (Fig. 58)

Running in a W-E direction, it was planned to cross the three NW-SE striking lines. To the west, from 00:00 to 04:00, it shows the Sardinia Valley basin with a package of highly discontinuous reflectors up to 500 msec thick. The package is probably composed of numerous isolated lenticular bodies, resulting from erosional and depositional processes guided by the Sardinia Valley channel. At present the Sardinia Valley channel results in an area of seafloor erosion, with reflections truncated at the seafloor, that is greater than on the previous lines. From 4:00 to 6:00 the D'Ancona ridge is seen as a faulted structural high, covered by a package of sediments 500 msec thick. From

6:00 to 13:00 the Vavilov basin is crossed. The basement lies at a depth of at least 5.8 sec, marking the deepest structural depression of the study area. The sedimentary infill consists of a well reflective sequence that sags in the central portion of the basin, probably as a result of differential compaction. The line ends over the southern termination of the Gortani ridge that has some steps in the basement. The steps result from faulting that also affects the overlying sedimentary package and can be traced up to the seafloor.

#### Line PS214MS (Fig. 59)

The line runs from south to north along the western base of the Vavilov volcano. After crossing the southern extension of the Sardinia Valley basin, the basement is seen to rise and change character. In fact, the strong discontinuous reflectors and numerous hyperbolae denote the volcanic basement of the Vavilov volcano. Sediment cover increases to the north (probably due to the line direction) whereas at the end of the line, the E-W trending southern portion of the Gortani ridge is crossed.

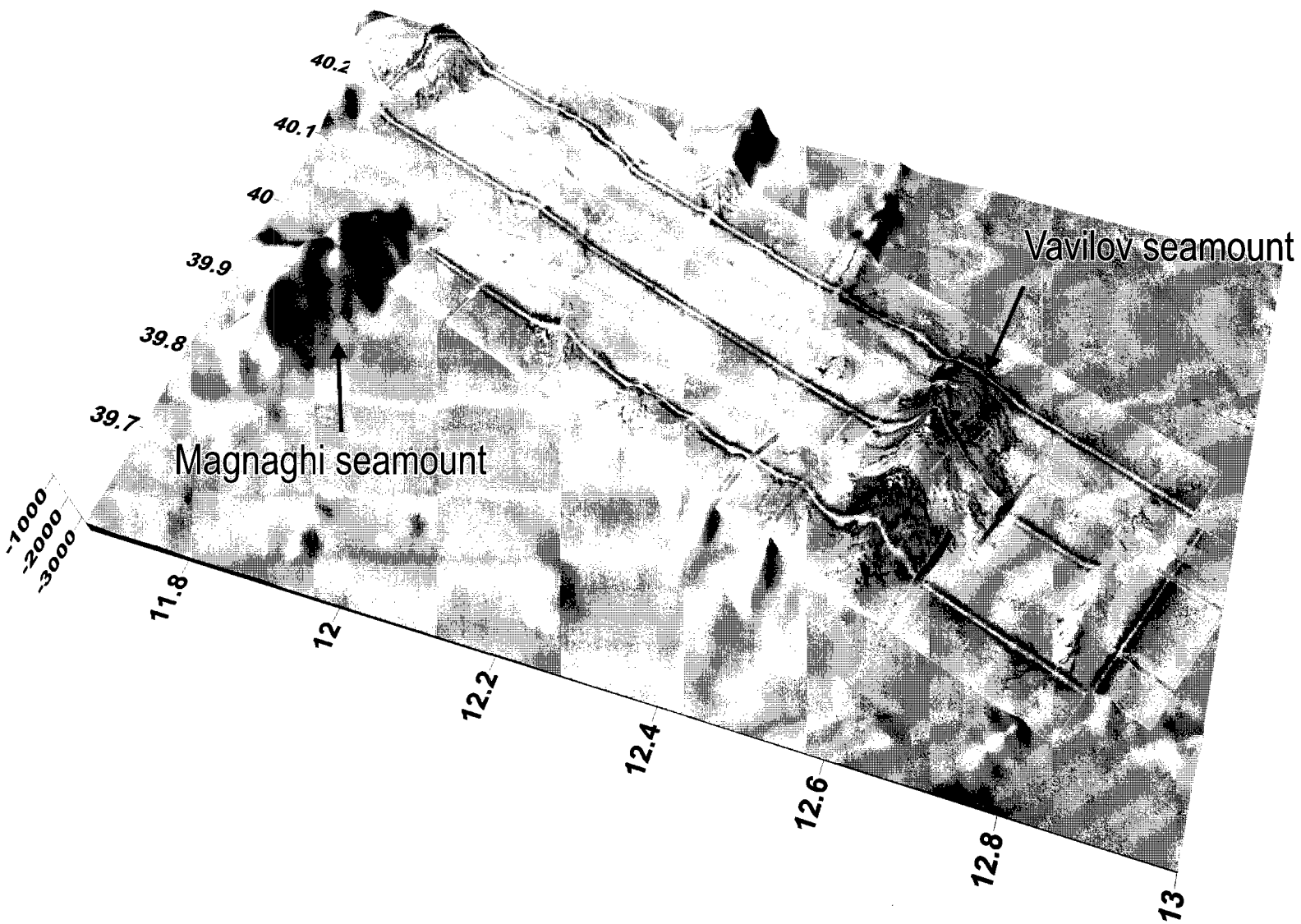


Figure 60. Perspective view of the Vavilov Basin seafloor showing OKEAN sidescan sonar coverage. Bathymetry by IGM of CNR.

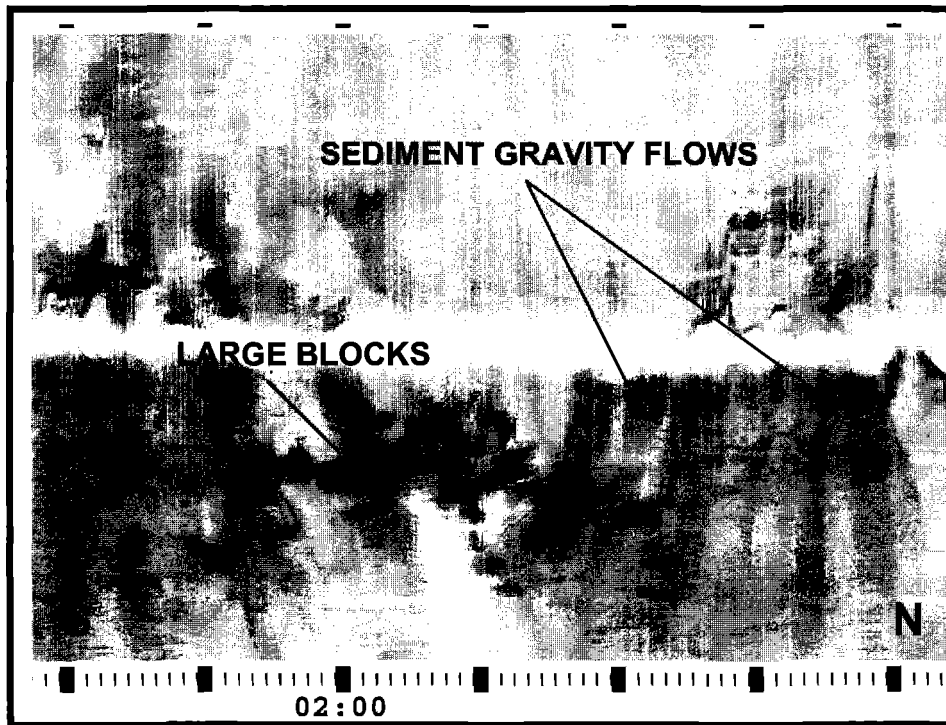


Figure 61. Portion of MAK line 84 along the western base of Vavilov volcano.

#### 4.3.3. OKEAN long range sidescan sonar mosaic

The regional OKEAN mosaic covers the entire Vavilov Basin and the seamount (Fig. 60). It confirms the results of the seismic survey indicating that the major structure of the D'Ancona Ridge is to great extent sediment covered. Along the southern part of the Sardinia Valley Basin, there is an indication of slides originating from the D'Ancona Ridge that collect in a faint channel running south of it. The western portion of the Vavilov volcano shows two nested landslide headwalls. This perhaps is an indication of repeated collapses of this part of the volcano.

#### 4.3.4. MAK sidescan sonar data

A MAK sidescan sonar line (MAK-84) was acquired along the western base of the Vavilov volcano, close to the track of seismic line PS214MS. The line begins in the southernmost extension of the Sardinia Valley Basin at 3600 m water depth. It follows the slope towards Vavilov volcano where the entire sonograph shows high backscattering

patches of large fallen lava blocks and striations due to sediment gravity flows (Fig. 61). The area without fallen blocks is sedimented, indicating that the debris avalanche, probably resulting from a sector collapse, is not a recent event.



## 5. AZORES MARGIN (LEG 5)

### *Lucky Strike segment*

#### 5.1. Aims and objectives

J. H. MONTEIRO, M. IVANOV, M. CUNHA, T. ALVES,  
P. FERREIRA, AND S. NAVE

Leg 5 used 10 days of the TTR-12 cruise on the Azores margin (Fig. 62). The first 5 days were spent investigating a sedimentary basin to the southwest of the Azores Archipelago and 5 days to continue the sampling and investigation of the Lucky Strike segment in continuation of the work done during TTR-10.

The aims of the first half of Leg 5 were to study the slope sedimentary apron south of the Azores Plateau in order to determine the morphology, thickness, and structure of the sediments using the 3.5 kHz profiler, OKEAN long range sidescan sonar, seismic reflection air gun profiler and MAK-1M deep-towed sidescan sonar. Sediment cores were collected to the north and the south of the Azores front in order to understand the paleoceanography and paleoproductivity of the area.

In the area of the Lucky Strike segment the aim was to study the geochemistry and petrology of the Lucky Strike central volcano and its relation with tectonics. TV and MAK-1M deep-towed sidescan sonar surveys were followed by TV grab sampling and dredging.

Another important objective of Leg 5 was to study faunal assemblages of the visited areas by means of seabed observations and bottom sampling.

#### *Abyssal apron*

Abyssal aprons are a major physiographic feature of the ocean floor south of the Azores Plateau and east of the Mid Atlantic Ridge. They can be considered as representatives of the archipelagic aprons described from the Pacific Ocean by Dietz and Menard (1953). The term "abyssal apron" was considered by Emery and Uchupi (1984) as more descriptive and less confusing than the previous term "outer rises".

It is well documented that the northern Mid-Atlantic ridge between 31°N and 41°N is the site of a long wavelength geochemical anomaly associated with the Azores hot spot. Since 1975 several expeditions have been made to collect samples from the different segments between these latitudes, and geochemical gradients were described based on element and isotope ratios. Unfortunately, these kinds of studies are, essentially, based on dispersed long scale sampling (4 or 5 samples for each rift segment) and little is known about element distribution on a more detailed scale.

The Lucky Strike segment of the slow-spreading Mid-Atlantic Ridge is characterised by an unusually large central volcanic complex with a history of explosive eruption and hydrothermal activity. This 65 km long, second order ridge segment is centered on 37°17.5' N and 32°16.5' W. At its deepest ends, the segment is 3200 m deep. Bathymetry and sidescan sonar imagery together reveal a slow-spreading ridge segment that has a large composite volcanic plateau at its centre. This central volcanic complex rises from a mean basal depth of 2200 m (Fig. 62).

The sidescan sonar imagery (TOBI data) and the bathymetry of the entire Lucky Strike segment, allows the establishment of different volcanic episodes and the spatial relations between them. All of these data make it possible to choose sampling targets, that represent diverse magmatic events that have occurred in the last million years. The rock sampling of the different well defined locations allows the geochemical characterization of the large central volcanic complex and the definition of a magmatic evolution history, which can be correlated with the tectonic and geophysical data already obtained.

Until now, data obtained was from small scale rock sampling during the TTR-10 cruise (Kenyon et al., 2000) in the segment of a topographic high. The high hosts the Lucky Strike Hydrothermal Field, which has large geochemical variations corresponding to the action of different degrees of differentiation

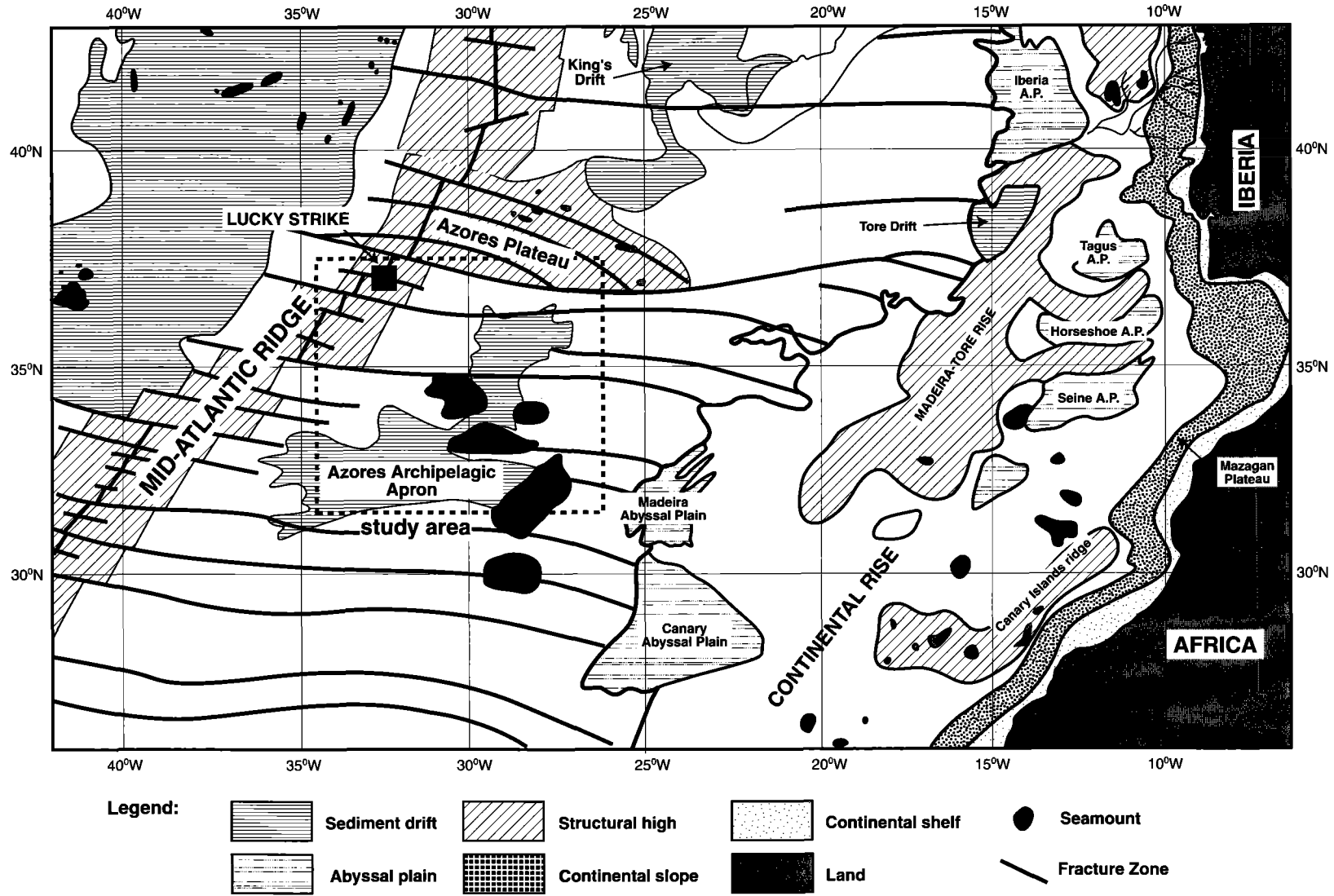


Figure 62. Physiography of the Atlantic margin southwest of Iberia showing the study area and the location of the Azores Archipelagic Apron. Modified from Emery & Uchupi (1984).

processes and, to some extent, to the existence of source heterogeneities. The latter can be better defined through the use of isotope data. Moreover, the fact that the samples collected during the TTR-10 cruise are located very close to the hydrothermal vents, may indicate that their original chemistry was affected by hydrothermal fluids.

Sampling on the large central volcanic complex will lead to understanding of variations of petrology in time (collecting samples positioned at some distance from the rift) and space, and of the geochemical gradients along the segment (and their relationship with depth). It will help to establish the chemical relations between MORB chemistry and hydrothermal activity. All of these data can be correlated with bathymetric and other geophysical data. This will make possible correlation between the physical and tectonic segmentation of the ridge and the magmatic regime of the ridge as manifested by changes in chemical composition.

## 5.2. Seismic data

T. ALVES, A. VOLKONSKAYA, S. BOURIAK,  
J. VICENTE, J. MONTEIRO AND M. IVANOV

### 5.2.1. Seismic data interpretation

In this section we describe the seismic stratigraphy of the margin south of the Azores using the seismic data from the TTR-12. The interpretation of lines PSAT 223 and PSAT 224 is based on the methodology of Mitchum et al. (1977) and Hubbard et al. (1985). Thus, genetically related stratal units are divided into seismic megasequences, sequences and facies following the seismic-stratigraphic frameworks described in Hubbard et al. (1985). In total, 3 megasequences, 5 sequences and 9 seismic facies are identified in the surveyed area south of the Azores Plateau (Figs. 62 and 63).

The basement in the surveyed area is of Paleogene age, volcanic in origin, being capped at the Azores Plateau by Oligocene nannooozes with a 50% carbonate content (Emery and Uchupi, 1984). This Paleogene basement is bounded to the west (~30°W

Seismic Megasequence	Seismic Sequence	Seismic Facies
<b>C</b>	<b>C10</b>	C10.c
		C10.b
		C10.a
<b>B</b>	<b>B10</b>	B10.d
		B10.c
		B10.b
		B10.a
<b>A</b>	<b>A30</b>	
	<b>A20</b>	
	<b>A10</b>	A10.b
		A10.a

Figure 63. Seismic stratigraphy of the study area.

north of the Atlantis Fracture Zone; ~35°W south of this same lineament) by Neogene to Quaternary crust (Fig. 64). To the east (~25°-30°W), Mesozoic crust has been identified.

The slow spreading of oceanic crust away from the Mid-Atlantic Ridge formed a diachronous volcanic basement, which is divided into distinct crustal segments by major E-W fracture zones (i.e. Azores-Gibraltar Fracture Zone, Atlantis Fracture Zone (Fig. 64) (Emery & Uchupi, 1984). From the Azores Islands (Chron 5-6) to the western part of the Plato Seamount (Chron 30), these crustal segments of gradually older basement are covered by a sediment veneer older than the Oligocene (Fig. 65 and Table 6).

Table 6. Main characteristics of seismic sequences recognized in the Azores margin study area.

Megasequence	Age of base	Sequence	TWTT thickness (ms)	Seismic facies	Internal character, geometry and terminations
C	Pliocene?	C10	0-200	C10.c	High to moderate amplitude, sub-parallel reflections.
				C10.b	Transparent.
				C10.a	High to moderate amplitude, sub-parallel reflections. Baselap.
B	Middle Miocene (Magnetic Anomaly 6)	B10	100-500	B10.d	Low amplitude to transparent, sub-parallel reflections. Low continuity.
				B10.c	Triplet of high amplitude, continuous reflections.
				B10.b	Low amplitude to transparent, sub-parallel reflections. Low continuity.
				B10.a	Sub-parallel and mounded reflections of moderate to high amplitude and low continuity. Baselap.
A	Paleocene (Magnetic Anomaly 30)	A30	100-200		Low to moderate amplitude, sub-parallel reflections. Wedge-shaped. Baselap on its contacts.
		A20	100-180		Moderate amplitude, sub-parallel reflections. Baselap on its contacts.
		A10	0-300	A10.b	High to moderate amplitude, sub-parallel reflections. Wedge-shaped in places.
				A10.a	Chaotic to diffractive reflections. Baselap on the upper and lower boundaries. Fills depressions on the basement. Wedge-shaped in places.

These pre-Oligocene sedimentary units are, in turn, covered by Oligocene-Neogene to Recent sediments, analogous to those identified on the Azores Plateau.

#### *Megasequence A*

The lowermost megasequence A comprises bowl- to wedge-shaped sequences that fill the irregular topography of the basement (Fig. 65). Locally, the megasequence shows moderate folding. The top of megasequence A is marked by baselap of the overlying reflections within megasequence B. Its base is also characterised by baselap onto a diffractive to chaotic substrate marking the top of the acoustic basement (Figs. 65 and 66). The acoustic basement is highly irregular and in places interrupted by mounded features.

Megasequence A consists of three seismic sequences and its thickness ranges from 0 ms to 450 ms TWTT (Table 6). The megasequence is thicker south of the Plato seamount (33°15'N) and within distinct half-grabens/grabens located between the Atlantis Seamount and the Azores Islands (Fig. 65). Its presence between Magnetic Anomalies 6 and 30 indicates a lower Miocene-Paleocene age for the unit (Fig. 64 and Table 6).

Sequence A10: This occurs at the base of the megasequence A and comprises chaotic to high amplitude internal reflections of poor to moderate continuity. Sequence A10 is not identified north of the Trident Ridge. Chaotic to diffractive reflections occur on its base (facies A10.a) while high to moderate amplitude, sub-parallel reflections (facies A10.b) are frequent at the top of the

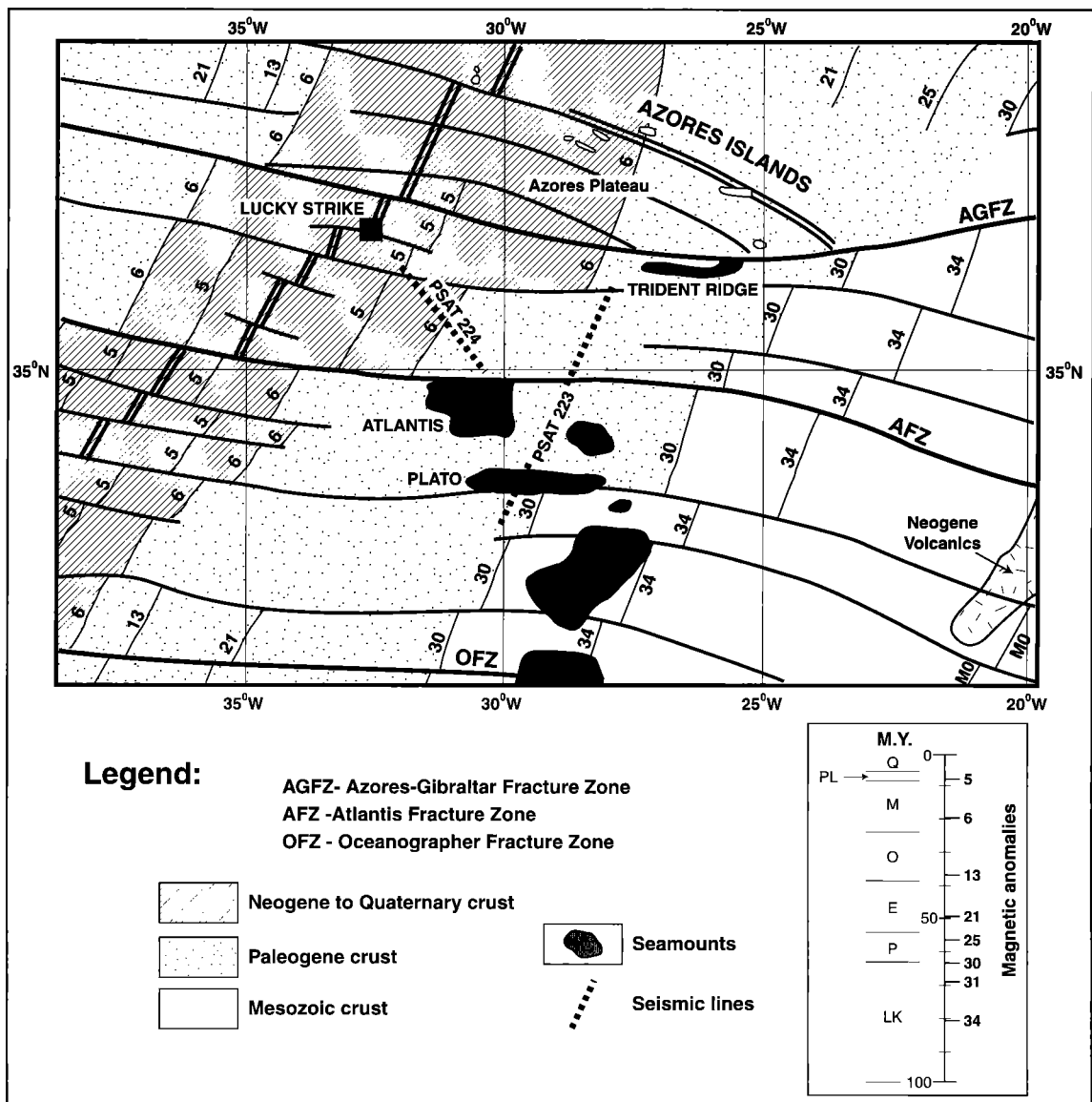


Figure 64. Location of the acquired seismic data in relation to the age of the underlying oceanic crust. Note the Mesozoic age of the eastern flank of the Plato Seamount, near the southern part of line PSAT 223. Modified from Emery & Uchupi (1984).

sequence. The top and base of sequence A10 show baselap of the adjacent reflections. However, sequence A10 is difficult to distinguish from the overlying sequences A20 and A30 in most of the studied area, except within the half-graben sub-basins located north of 36°15'N (Fig. 65). The thickness of A10 varies from 0 ms to 300 ms TWTT, being higher in the latter half-grabens where the sequence is wedge shaped.

**Sequence A20:** This is composed of moderate amplitude, sub-parallel internal reflections. The sequence covers the underly-

ing sequence A10 without showing a wedge-shaped geometry (Fig. 65). The upper and lower boundaries of A20 are marked by baselap of the adjacent reflections. Its thickness varies between 100 ms and 180 ms TWTT and, similarly to A10, does not occur north of the Trident Ridge.

**Sequence A30:** Internally, this sequence comprises sub-parallel, low to moderate amplitude internal reflections. Sequence A30 covers the underlying sequences A10 and A20 and/or the irregular acoustic basement throughout the study area

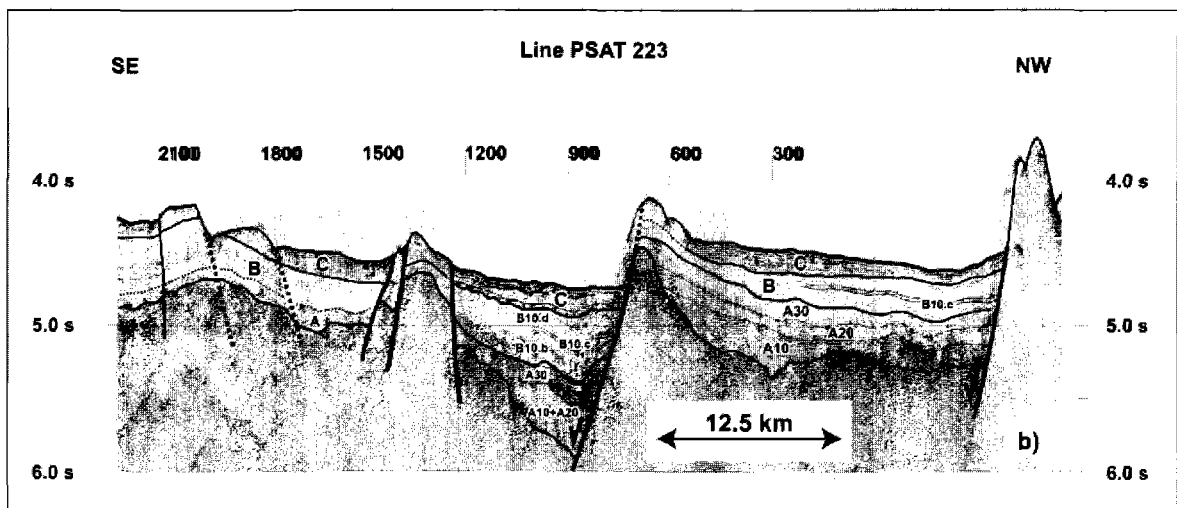
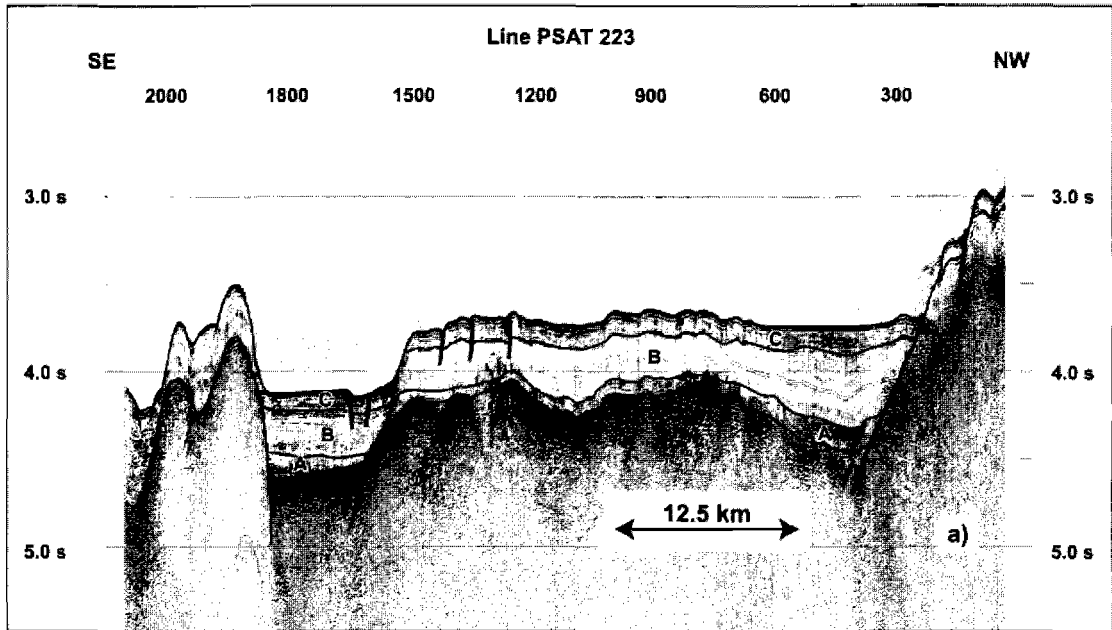


Figure 65. Interpretation of line PSAT 223, showing a) the southernmost flank of the Azores Plateau; b) the structure of the area ranging from the Trident Ridge to the Atlantis Seamount (see Figure 64 for location). The seismic stratigraphy of the post-basement sedimentary units is represented in detail in Fig. 63.

(Fig. 65). Wedge-shaped geometries are visible within half-graben sub-basins. The thickness of A30 varies from less than 100 ms to 200 ms TWTT.

#### Megasequence B

Megasequence B is formed by a single seismic sequence (sequence B10) from 100 ms to more than 500 ms TWTT in thickness. Sequence B10 shows high amplitude folding, covering the relatively smooth palaeo-topog-

raphy that was inherited from the deposition of megasequence A over the rugged acoustic basement. The upper boundary of megasequence B locally has erosional truncation and/or baselap. Its lower boundary is marked by baselap. Since megasequence B covers the acoustic basement west of the Magnetic Anomaly 6 (middle Miocene), its base can be dated as middle Miocene (Fig. 66 and Table 6).

**Sequence B10:** The sequence shows low amplitude, irregular internal reflections,

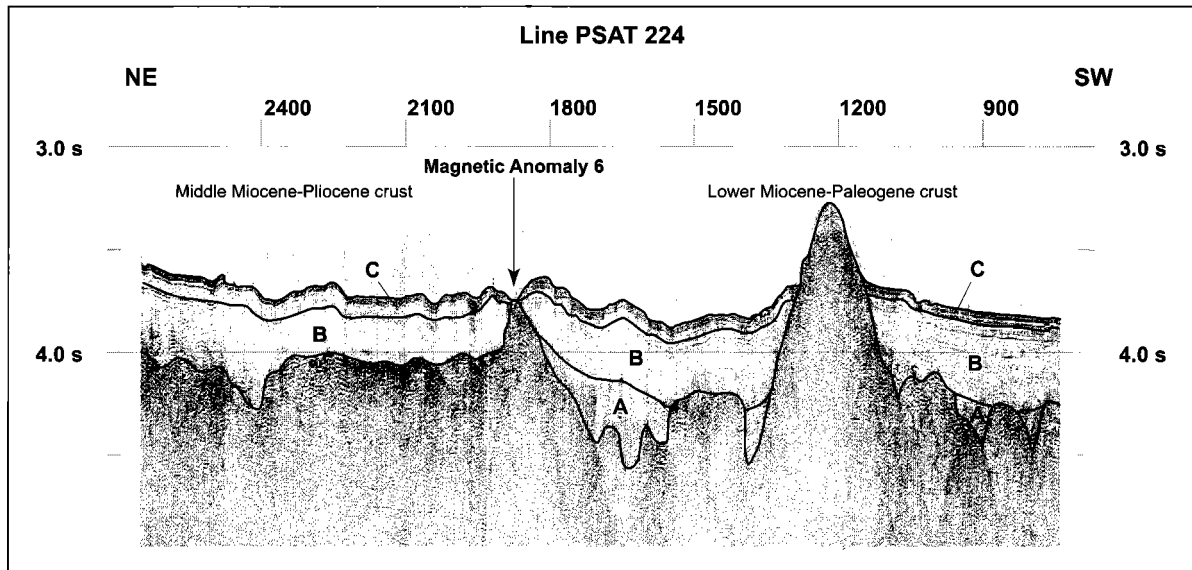


Figure 66. Interpretation of line PSAT 224. Note the irregular acoustic basement in the area, comprising multiple mounded features of probable volcanic origin.

occasionally interrupted by moderate to high amplitude reflections. This character allows the definition of four seismic facies in its interior (Table 6). The lowermost facies B10.a comprises sub-parallel to mounded internal reflections of moderate to high amplitude and low continuity. Its thickness varies from 20 ms to 300 ms TWTT. Facies B10.b and B10.d are composed of low amplitude, sub-parallel reflections. Their thicknesses vary from 50 ms to 150 ms TWTT. Separating both, Facies B10.c forms a triplet of moderate to high amplitude reflections, not identified south of 34°30'N.

#### *Megasequence C*

Megasequence C covers the moderately deformed megasequences B and A that fill the inherited basement topography and fault-bounded grabens/half-grabens (Fig. 65). The megasequence shows minor deformation and a single seismic sequence (C10; Table 6). Line PSAT 224 shows megasequence C covering the basement west of the area where Magnetic Anomaly 5 (intra-Pliocene) is recorded (Fig. 66). This suggests a Pliocene-Quaternary age for the unit (Table 6).

Sequence C10: This is mainly composed of sub-parallel, high to moderate

amplitude reflections (Fig. 65). The top of C10 is coincident with the sea floor. Locally, its base is marked by baselap of its internal reflections onto the top of the underlying seismic megasequence B. In half-graben sub-basins, erosional truncation of the underlying reflections in B10 is also visible. However, in most of the surveyed region, the boundary between the sequence C10 and the underlying units is marked at the base of the first high amplitude reflections covering the low amplitude, occasionally transparent, sequence B10. Sequence C10 is sub-divided in three seismic facies. The lowermost facies, C10.a, shows high to moderate amplitude, sub-parallel internal reflections, similar to those of the uppermost facies C10.c. The intermediate facies C10.b has a transparent character. In total, the thickness of sequence C10 varies from 0 ms to 200 ms, showing greater thickness north of 35°30'N.

#### 5.2.2. Structure of the study area

The proximity of the study area to the mid-Atlantic Ridge is reflected by the presence of two types of basement structures: 1) intra-basinal mounds of probable volcanic origin; 2) half-graben and graben blocks in which megasequence A shows lateral growth onto the main boundary faults. The base-

LINE PSAT 223 - Schematic Sections

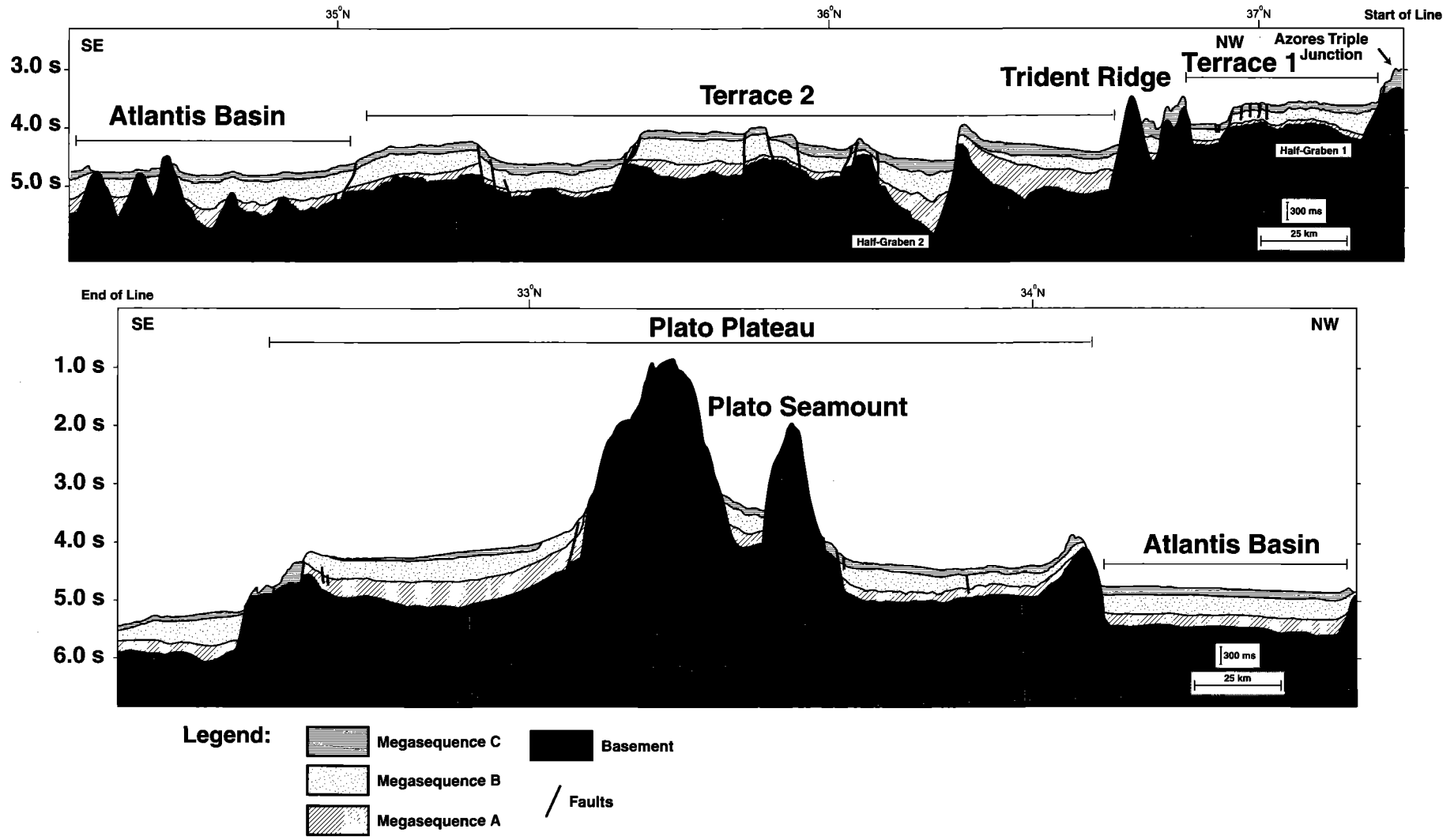


Figure 67. Schematic section of line PSAT 223 depicting the thickness of the sedimentary layers covering the oceanic crust in the study area.



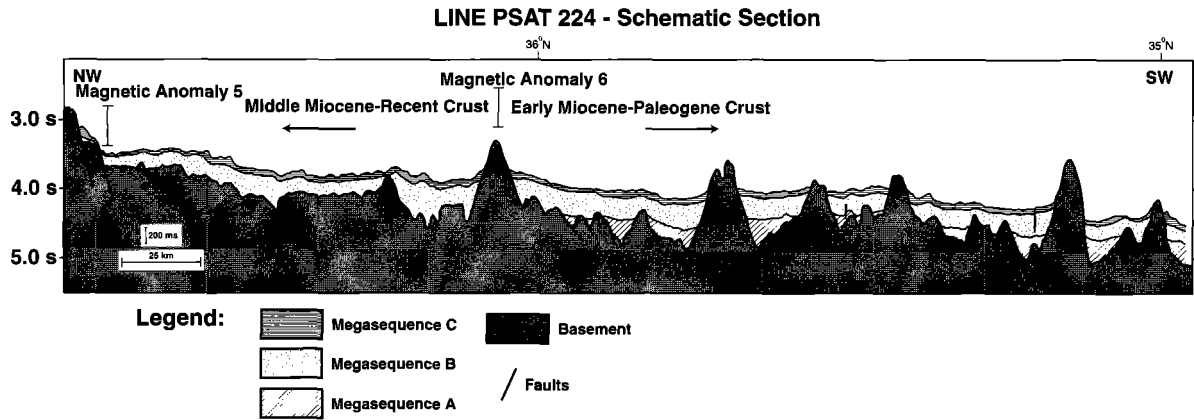


Figure 68. Schematic section of line PSAT 224 depicting the thickness of the sedimentary layers covering the oceanic crust in the study area.

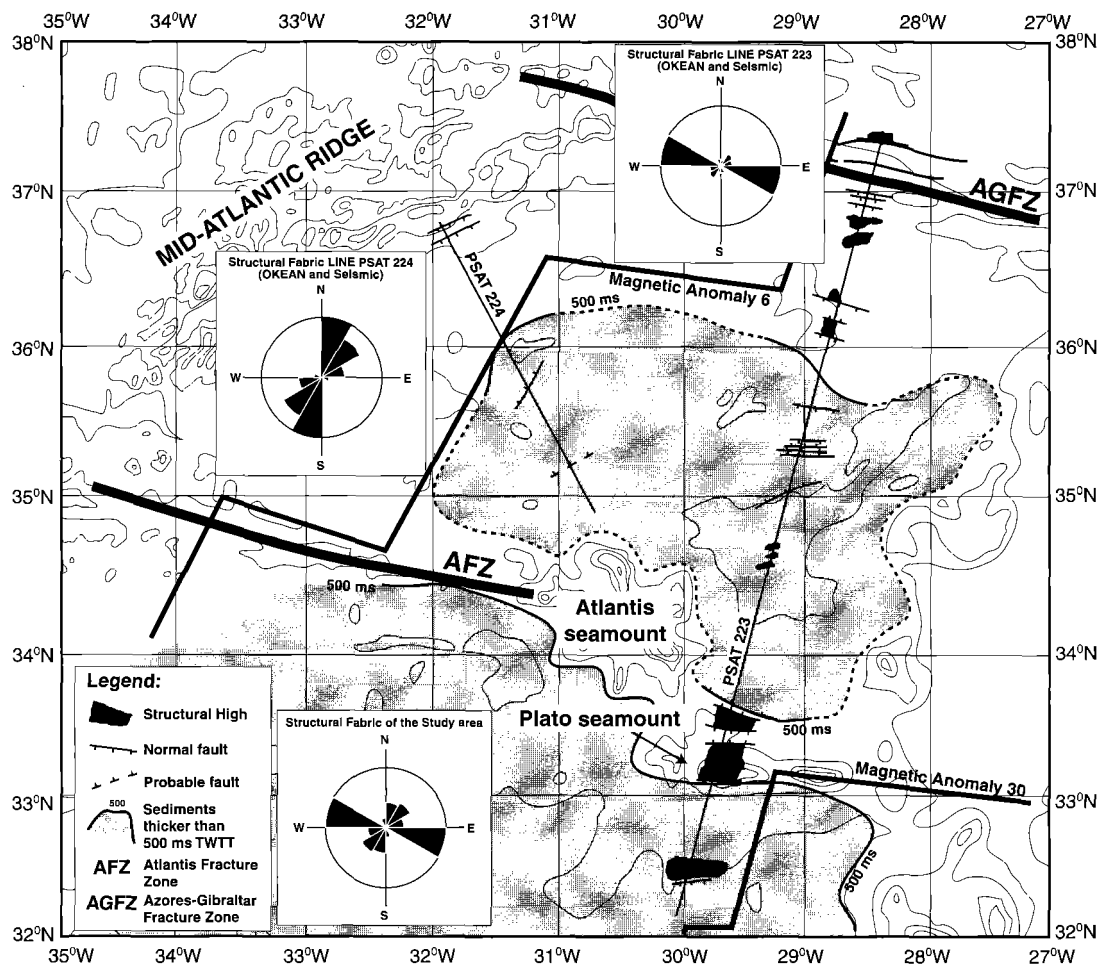


Figure 69. Main structural trends taken from OKEAN sonograph and sedimentary basins on the margin south of Azores.

ment is very irregular due to the development of the latter structures forming a multitude of fault and/or mound-bounded troughs filled with wedge to bowl-shaped sequences.

#### Line PSAT 223

Line PSAT 223, east of the Atlantis seamount, suggests the predominance of half-graben/graben blocks as the main structures of the crust (Figs. 65 and 67). The oceanic crust is here divided into tilted blocks separated by normal faults. The tilted blocks form two structural terraces (Terrace 1 and Terrace 2) north of the 35°N, marking the existence of an irregular, gently south-tilting continental slope (Fig. 67). Southward tilting faults are predominant from the Azores Plateau to 35°N and south of 33°N. From 35°N to the Plato Seamount, northward tilting faults are more common and delimit the deepest part of the surveyed region (Atlantis Basin).

The thickness of the sedimentary cover can reach 900 ms TWTT in the Atlantis Basin and south of the Plato Seamount. These latter zones are separated by a plateau (Plato Plateau) extending from 34° 15'N to 32° 30'N (Fig. 67).

#### Line PSAT 224

The northwest trending line PSAT 224 was acquired between the Atlantis Seamount and the Mid-Atlantic Ridge. Normal faults (southeast and northwest dipping) are less frequent in line PSAT 224 when compared to line PSAT 223 (Figs. 67 and 68). The acoustic basement shows here a series of mounds that have a predominant northeast trend on OKEAN data (Fig. 69).

As on line PSAT 223, the three seismic megasequences, A, B and C, show moderate folding and cover a highly irregular acoustic basement. For this reason, the sedimentary units in line PSAT 224 show an unequal distribution and major thickness variations (Fig. 66). Megasequence A pinches out and disappears towards the northeast, being absent north of the area where

Magnetic Anomaly 6 occurs.

#### *Structural fabric and sediment distribution*

In order to characterise the structure and sediment distribution of the margin south of the Azores, a combined structural-isochron map was produced using OKEAN and seismic reflection data (lines PSAT 223 and PSAT 224) (Fig. 69). The main structural trends change spatially in the study area, with line PSAT 223 showing dominant east-northeast lineaments that contrast with the primary north-northwest lineaments in line PSAT 224. Overall, the former structural fabric is dominant over the latter and imposes a general east-northeast trend in the study area. Structures with an east-northeast trend are parallel to the main transform faults (i.e. AGFZ, AFZ and OFZ) that occur in the area. They are responsible for the structuring of the margin northwest of the Atlantis seamount (line PSAT 223, Figs. 65 and 69). In contrast, the north-northwest trending features identified in PSAT 224 are related to the trend of the Mid-Atlantic Ridge located immediately to the west of the line (Fig. 69).

The sedimentary units that cover the volcanic basement south of the Azores are thicker (> 500 ms TWTT) in an area ranging from 36°N to the Atlantis and Plato seamount and south of this latter feature, roughly between 32°W and 28°W (Fig. 69). North of 36°N, only smaller half-graben sub-basins contain sediments with more than 500 ms TWTT in thickness (Fig. 66).

### **5.3. Coring of the archipelagic apron south of the Azores Plateau**

S. NAVE

#### *Introduction*

The sedimentation of the plankton south of the Azores Islands is significantly influenced by the hydrography of the Azores Front Current System, centered at 34°N. The impact of hydrographic fronts on the population dynamics and on the distribution of microorganisms is of special interest,

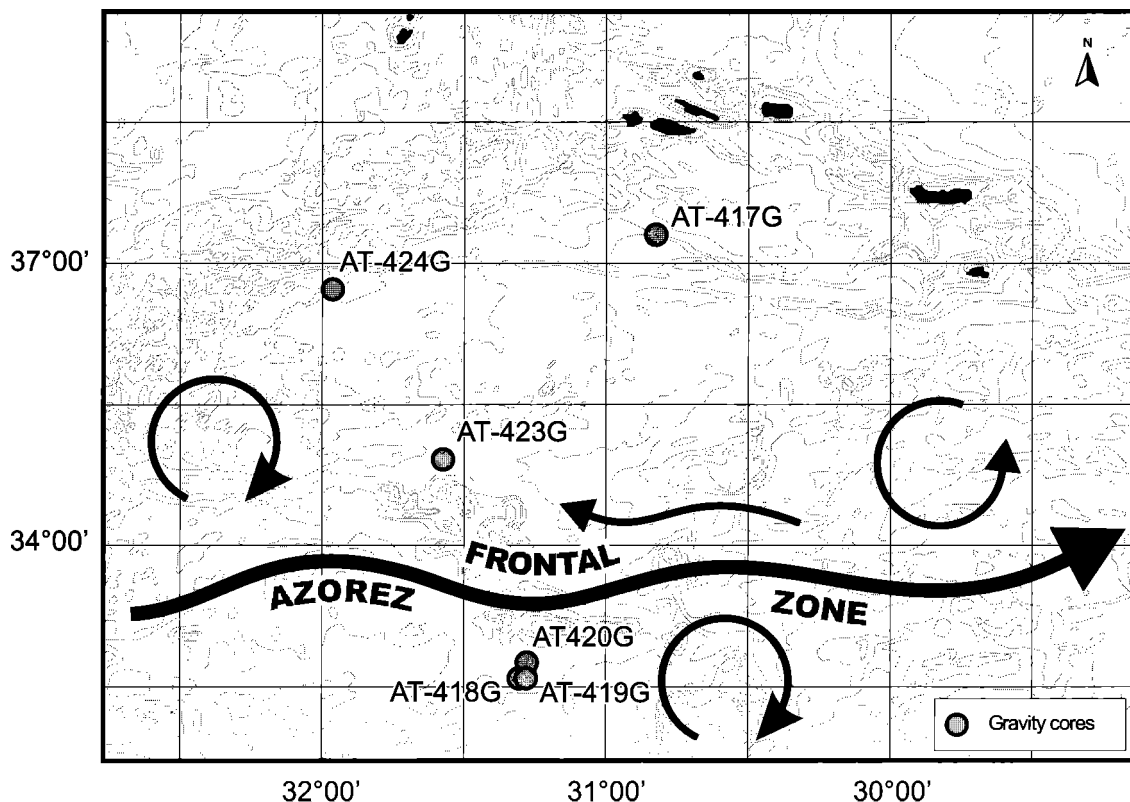


Figure 70. Bathymetry and location of the gravity cores crossing the Azores Frontal Zone. Adapted from Report and Preliminary Results of METEOR Cruise M 45/5, *Berichte, Fachbereich Geowissenschaften, Universitet Bremen, No. 163, 2000.*

because hydrographic fronts are potential areas of enhanced production of plankton.

The Azores Current is the southern branch of the Gulf Stream, and is present throughout the year, extending to water depths of at least 1000 m and is about 50 km wide (Kse and Siedler, 1982; Klein and Siedler, 1989; Gould, 1985). The current meanders and is accompanied by eddies to the north and cyclonic and anti-cyclonic recirculation to the south which leads to the occurrence of regional upwelling and downwelling (Kse and Siedler, 1982; Gould, 1985; McClain and Firestone, 1993; Alves and de Vendierre, 1999).

The Azores Front (AF) separates the 18°C Subtropical Mode Waters from the colder and fresher water masses of the transitional to subpolar zone.

The study of the impact of the Azores Current and associated AF on the sedimentation of plankton, through analysis of the cores recovered along a north-south profile crossing the recent position of the AF, will

help to map late Quaternary frontal dynamics.

#### *Objective*

The main aim is to study the sedimentary sequences, which reflect the effects of paleoceanography and paleoclimate south of the Azores Islands.

#### *Core location and sampling*

Five of the six attempts at recovery were successful, using the 6 m gravity corer. The location of the cores was selected from 3.5 kHz profiles (Fig. 70, Table 7).

Three cores were recovered north of the Azores Front, and the other two to the south of it. A total of 1328 cm of sediments were collected with lengths varying between 155 and 373 cm. The cores were collected in water depths between 2600 and 3470 m.

As soon as a gravity core was on deck, it was cleaned, cut in 1 m sections,

Table 7. Sampling sites in the Azores Front study area.

Core	Date	Latitude (N)	Longitude (W)	Water depth (m)	Recovery, cm
AT-417G	21.08.02	37°16.16	28°24.8	2834	155
AT-418G	23.08.02	32°33.78	29°53.38	3240	empty
AT-419G	23.08.02	32°34.43	29°53.19	3148	212.5
AT-420G	23.08.02	32°43.76	29°50.43	3224	293.5
AT-423G	25.08.02	34°54.80	30°41.65	3470	372.5
AT-424G	26.08.02	36°42.08	31°52.48	2606	294

closed at both ends of each section and finally labeled.

The sediment trapped in the core catcher was also collected into an identified bag for all gravity cores apart from AT-419G. The core catcher sediment was pelagic ooze varying from light gray silty clay (AT-417G) to very stiff pinkish brown sandy clay (AT-420G, AT-423G) and stiff pale brown sandy clay (AT-424G).

As the cores were not opened on board, no preliminary results from the gravity cores were available during the cruise.

#### 5.4. Deep-towed sidescan sonar and TV survey data

##### 5.4.1. Eastern part of Lucky Strike Segment

P. FERREIRA AND M. CUNHA

##### *Objectives*

Geological observations of the eastern off-axis summit in the central part of the segment was the main objective of this TV survey. The area surveyed was centered on: - 37°16.50'N, 32°10.50'W.

From the model linking volcanic and tectonic cyclicity to hydrothermal activity for the Lucky Strike field, it was expected that there would be related pyroclastic and hydrothermal deposits (sulphide rubble, old sulphide chimneys) in this central, off-axis volcanic complex.

Particular emphases was put on the geological setting of the area, the relation

between the lithologies and bathymetry, and the observations of volcanoclastic and sulphide deposits. Sampling the area, based on the images obtained, was the final objective of this operation.

##### *Geological Summary*

Prior to the TV survey on the eastern off-axis summit of the Lucky Strike segment, a MAK line (MAKAT-77) was run with a sidescan frequency of 100 kHz.

Start: 37°18.19'N / 32°09.36'W

End: 37°15.51'N / 32°10.70'W

The sonograph shows detailed variations in acoustic texture of this off axial floor. The highest point in the topography has two different textures: to the north of 37°17'N there are well marked linear reflectors, closely spaced, sub-parallel and with a general trend of 15° (Fig. 71). In the northernmost part, the intensity of these reflectors is lower, having more homogeneous backscattering, that could be due to the presence of sediments that cover the rock substrate. It is estimated that this sedimentary cover is thin in places where the linear reflectors are pronounced.

To the south of 37° 17' N, the western part of the line is very homogeneous and has a high backscatter level with a smooth acoustic texture. The sonograph also shows a narrow band of low backscatter cutting across the area. The eastern side of the line has the same type of linear reflectors as

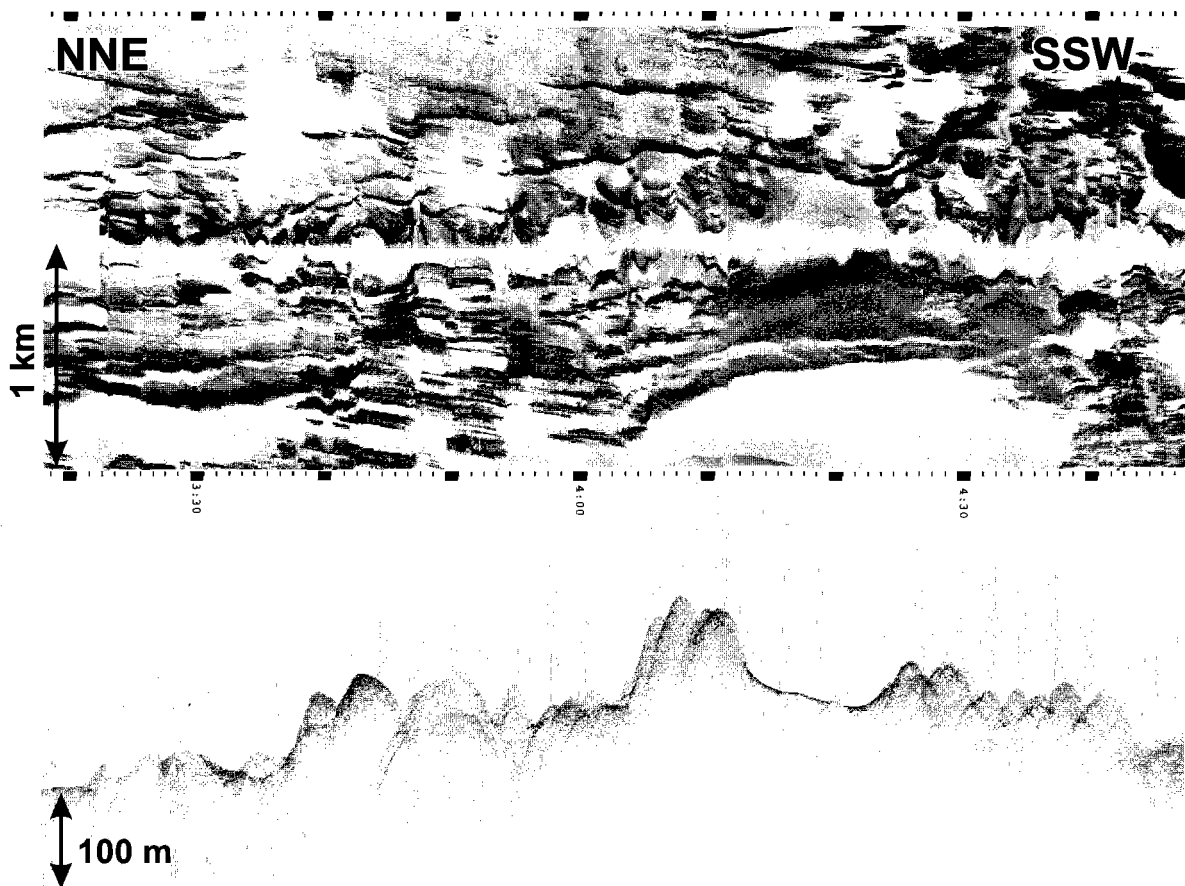


Figure 71. Fragment of MAKAT-77 line showing outcrops of volcanic rocks in the eastern part of the Lucky Strike segment.

described above, and some small dome-like structures.

The highest backscatter is most likely due to basaltic rock outcrops (or areas where this rock type dominates over the other types - sediment and carbonate crust). The lowest backscatter is produced by sedimented seafloor, and the intermediate backscatter level corresponds to carbonate crust with abundant coral.

According to the video record along the line TVAT-39, the distribution of lithologies seems to be very uniform over all of the surveyed area. In some basalt-dominated areas, the larger outcrops produce very irregular topography with well developed fault scarps. Other basalt-dominated areas show different dimensions of rock blocks, which are rounded in shape and are partially surrounded by sediments. Sometimes it is possible to see the basalt rocks below carbonate

crusts. Sediment is very homogeneous, with ripple marks and bioturbation in places. Carbonate crusts and sedimented areas are very abundant and show up on more than 80% of the video record. They appear in different proportions and usually are very rich in corals. The carbonate crusts must be very similar to ones collected in the rift scarp (sample AT-429D).

#### 5.4.2. Southern part of the Lucky Strike Segment. Menez Hom high

F. MARQUES AND P. FERREIRA

##### *Objectives*

The survey in the Menez Hom area aimed to identify geological structures/features that would indicate possible escape of methane-rich fluids through diffuse or

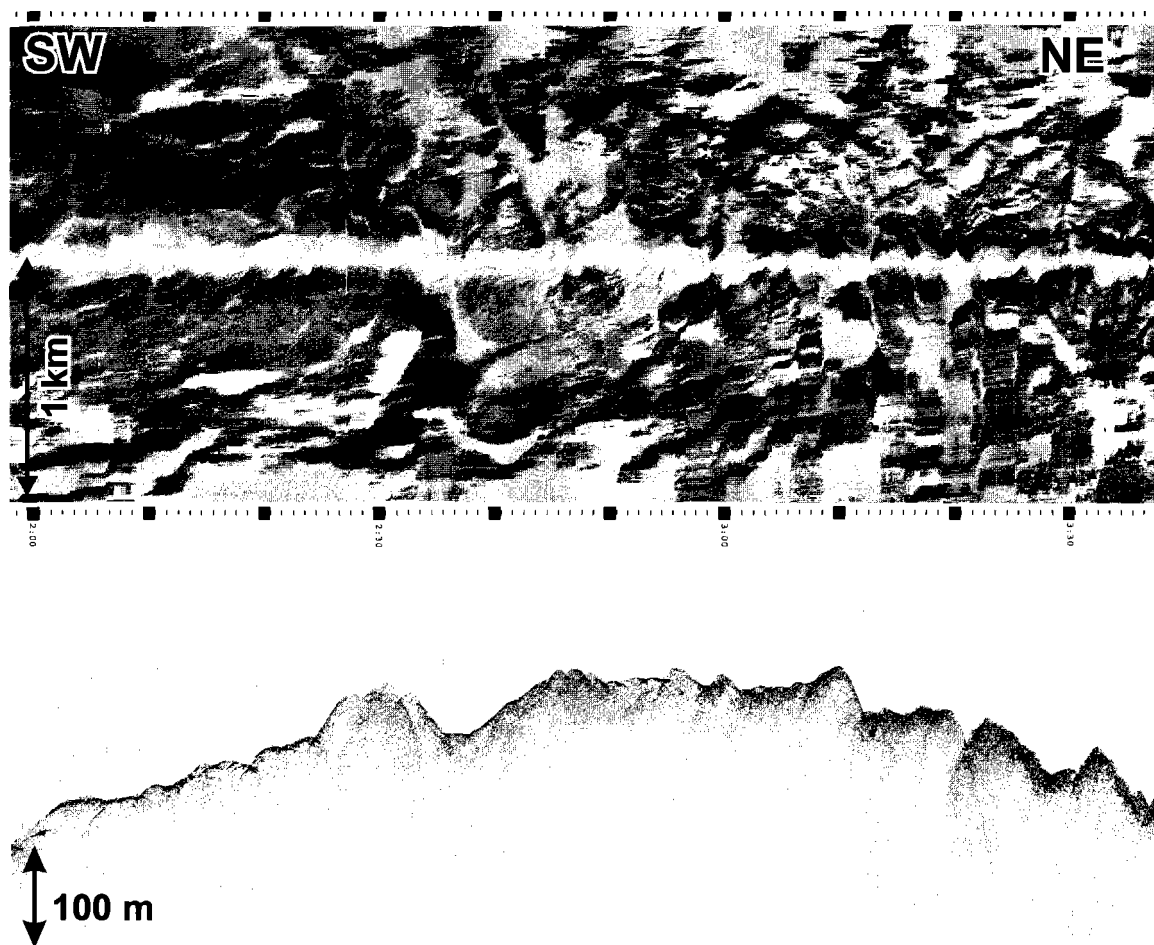


Figure 72. Fragment of MAKAT-78 line showing outcrops of serpentinites in the southern part of the Lucky Strike segment.

focused systems.

Start: 37°07.90'N / 37°08.25'N  
 End: 32°29.13'W / 32°25.77'W.

#### Geological Summary

Line MAKAT-78 was run across the Menez Hom bathymetric high in order to establish the bathymetric limits and to define the outcrop locations.

Start: 37°07.90'N / 32°29.13'W  
 End: 37°08.25'N / 32°25.77'W.

The shallowest point along the MAK line had a depth of about 1025 m and represented an area of high backscatter suggesting the presence of massive outcrops of serpentinites. This was later confirmed by a TV sur-

vey. The MAK data indicate that the Menez Hom area is mainly composed of numerous outcrops of massive rocks, identified as serpentinites (Fig. 72). The rocks are roughly oriented at 45°.

Sediments are not common and they appear mainly on flat areas between the serpentinite outcrops.

The Menez Hom is located at the southern end of the Lucky Strike segment and comprises a suite of completely serpentinitized ultramafic rocks. The outcrops that usually represent bathymetric highs and the video record along line TVAT-39 showed that they are composed of large blocks of extremely deformed serpentinites, with a brecciated or, more rarely, a foliated texture. Most of the serpentinite blocks are bounded by sharp scarps that represent shear planes and can be tens of meters high. These struc-

tures appear to have an en-echelon arrangement. One can see alternate steps of serpentinite outcrop (with sharp planes) and flat areas covered by sediments. The steps have scattered serpentinite debris at the base. The sediments have few specimens of pelagic fauna or evidence of bioturbation.

No areas of methane-rich fluid escape were detected.

## 5.5. Biology

M. CUNHA, M. JOSE AMARAL AND N. PERALTA

### *Methods*

#### Grab and dredge samples

Conspicuous animals were picked from the surface of the sediments and rocks. Specimens were also recovered from rock washings and sorted from sieved sediments. A column of sieves with 2, 1 and 0.5 mm mesh size was used. The fauna of the two coarser fractions was sorted on board and kept in 70% ethanol. The finer fraction (0.5 mm) of the sieved sediments was preserved in 10% neutralised formaline stained with Rose Bengal and will be sorted later under a stereoscopic microscope. A preliminary listing of the fauna collected is shown in Table 8.

#### Deep towed TV

Preliminary mapping and lists of the fauna (Table 9) were made from real time observations of video footage.

### *Results*

#### Atlantis Seamount

The sampling in this area included deep-towed TV (TVAT-37), dredging (AT-421 D) and grabbing (AT 422 GR).

TVAT-37: The footage was made at the top of the seamount in areas showing high backscattering in the MAK mosaic (MAKAT-76). Basalt blocks and crusts, covered by undetermined epifauna were observed in all areas but were more frequent

in the second area. Small unidentified crustaceans were frequently observed swimming at the surface of sediments. The megafauna was dominated by different species of large siliceous sponges, whip corals and other cnidarians that were especially abundant in the first and second areas (south). A few small crabs were seen hanging on whip corals. Different species of fish were also observed in all areas but were more abundant in the third and fourth areas (north).

AT-421D: Three large siliceous sponges were recovered from the dredge material. Smaller sponges, hydrozoans and small anemones were attached to the surface of the sponges and rocks. Polychaete worms associated with the large sponges were also collected.

AT-422GR: Colonies of living madreporarian coral, other corals and one gorgonian were collected in this operation. No sediments were recovered.

#### Lucky Strike Segment

The sampling in the Lucky Strike segment was carried out in five areas: i) north of the vent field; ii) inside the vent field; iii) east of the vent field, iv) south of the vent field; v) west of the vent field).

#### i) Northern area

The sampling in this area included two TV grabs (AT-425 GR and AT-426 GR).

AT-425 GR: A few specimens of polychaete worms, peracaridan crustaceans and gastropods (mostly empty shells) were retrieved mainly from sieved sediments. Biological debris included abundant pteropod shells and some foraminiferans.

AT-426 GR: Living organisms were not present in this sample.

#### ii) Vent field

The sampling in this area included three TV grabs (AT-427 GR, AT-428 GR and AT-436 GR).

AT-427 GR: A few specimens of chaetopterid worms (Polychaeta) and per-





acarid crustaceans were recovered from the blocks of volcanic glass sampled during this operation.

AT-428 GR and AT-436 GR: Brittle stars (Ophiuroidea), some chaetopterids and other polychaete worms (mostly empty tubes) were picked from the collected hydrothermal slabs. A few specimens (peracarid crustaceans and polychaete tubes) were also recovered from the washings of the rocks. Biological debris consisted mostly of bivalve shells (*Bathymodiolus*).

iii) Eastern area

The sampling in this area included deep towed TV (TVAT-38), dredging (AT-429 D and AT-431 D) and grabbing (AT-430 GR).

TVAT-37: The footage was recorded at the off-axis summit, east of the Lucky Strike, crossing three areas with different degrees of acoustic backscattering (see MAKAT-77, Fig. 71). The first area, corresponding to an intermediate backscattering, was characterized by the presence of abun-

dant dead coral branches and debris. This area had abundant megafauna dominated by different species of cnidarians (e.g. sea fans, solitary corals) and sponges. A few shrimps, echinoderms (asteroids, echinoids and ophiuroids) and fishes represented the mobile fauna. The second area, corresponding to low backscattering, was characterized by the presence of bare sediments with scarce fauna. Only a few ophiuroids and echinoids were observed in this area. The third area, corresponding to high backscattering, was characterized by the presence of basalt blocks. Sponges dominated the megafauna in this area. Gorgonians and other cnidarian species were also observed but with lower densities compared to the first area.

AT-429 D: A large amount of dead deep-water corals (blackened by a thin manganese layer) was recovered during this dredge operation. The corals had abundant epifauna that included different species of large and small sponges, several species of cnidarians including some living polyps of madreporarian corals, polychaete worms, ophiuroids and crinoids.

Table 9. Listing of the biological specimens identified during a real time observation of video footage.

Phylum		TVAT-37	TVAT-38	TVAT-39
Porifera	Sponges	spp	spp	spp
Cnidaria	Undetermined cnidarians	spp	spp	spp
	Sea anemones			+
	Gorgonians		+	
	Whip corals	+		
	Madreporarian corals		+	
Mollusca	Gastropods	+		
	Scaphopod			+
	Octopus	+		
Annelida	Polychaete worms	cf		
Arthropoda	Undetermined crustaceans	+		+
	Shrimp		+	+
	Crabs	+	+	+
Echinodermata	Sea stars		+	
	Brittle stars		+	+
	Sea urchins	+	+	+
Chordata	Fishes	+	+	+
Biogenic traces	Burrows	+		+
	Tracks		+	+
Biological Debris	Coral	+	+	

AT-431 D: Conspicuous living organisms were not present in this sample.

AT-430 GR: The sample consisted of one large pillow lava block from which a large gorgonian and a siliceous sponge were recovered.

#### iv) Southern area

The sampling in this area included dredging and grabbing operations (AT-432 D, AT-434 D, AT-435 D and AT-433 GR). The fauna recovered from the rocks collected was very scarce and included mainly different species of siliceous sponges, cnidarians (Hydrozoa, Anthozoa, Scyphozoa) and polychaete worms

#### Menez Hom

The benthic studies in this area included only deep-towed TV (TVAT-39). The footage crossed serpentinite scarps corresponding to high backscattering in the MAK mosaic (MAKAT-78, Fig. 72). The sessile fauna consisted mostly of different species of cnidarians and some sponges. The scarps were in some cases separated by areas of sediments with numerous burrows and other biogenic traces (resting, crawling and feeding traces).

## REFERENCES

- Akhmetzhanov A.M., Kenyon N.H., Habgood E.L., Gardner J., Ivanov M.K. and Shashkin, P., 2002. Sand lobes in the Gulf of Cadiz: towards better understanding of clastic reservoir high-resolution architecture. In: M. Cunha, L. Pinheiro and A. Suzyumov (Eds.), *Geosphere/Biosphere/Hydrosphere Coupling Processes, Fluid Escape Structures and Tectonics at Continental Margins and Ocean Ridges*. International Conference and Tenth Post-Cruise Meeting of the Training-Through-Research Programme, Aveiro, Portugal. IOC Workshop Reports, 183, UNESCO, 23.
- Alonso, B. and Maldonado, A., 1992. Pliocene-Quaternary margin growth patterns in a complex tectonic setting: North-Eastern Alboran Sea. In: A. Maldonado (Ed.), *The Alboran Sea*. *Geo-Mar. Lett.* 12 (2/3), 137-143.
- Alves, M. and de Vendierre, A. C., 1999. Instability dynamics of a subtropical jet and applications to the Azores Front Current System: Eddy-driven mean flow. *Journal of Physical Oceanography*, 29 (5), 837-864.
- Andersen, M.S., Nielsen, T., Sorensen, A.B., Boldreel, L.O. and Kuijpers, A., 2000. Cenozoic sediment distribution and tectonic movements in the Faeroe region. *Global and Planetary Change*, 24, 239-259.
- Auzende, J.M., Olivet, J.L. and Pastouret, L., 1981. Implication structurales et paleogeographiques de la presence de Messinien a l'ouest de Gibraltar. *Marine Geology*, 43, 9-18.
- Baraza, J. and Ercilla, G. 1996. Gas-charged sediments and large pockmark like features on the Gulf of Cadiz slope (SW Spain). *Marine and Petroleum Geology*, 13, 253-261.
- Boldreel, L O. and Andersen, M.S., 1993. Late Paleocene to Miocene compression in the Faeroe-Rockall area. *Petroleum Geology of Northwest Europe: Proceedings of the 4th conference*, The Geological Society, London, 1025-1034.
- Boldreel, L.O. and Andersen, M.S., 1998. Tertiary compressional structures on the Faeroe-Rockall Plateau and relation to northeast Atlantic ridge-push and Alpine foreland stresses. *Tectonophysics*, 300, 13-28.
- Bonnin, J., Olivet, J.L. and Auzende, J.M., 1975. Structure en nappe a l'ouest de Gibraltar. *C.R. Academy of Science*, 280(5), 559-562.
- Braga, J.C. and Comas, M.C., 1999. Environmental significance of an uppermost Pliocene carbonate debris flow at site 978. In: Zahn, R., Comas, M.C. and Klaus, A. (Eds.), *Proceedings Ocean Drilling Program, Scientific Results*, 161, 77-81.
- Chalouan, A., Saji, R., Michard, A. and Bally, A. W., 1997. Neogene tectonic evolution of the Southwestern Alboran Basin as inferred from seismic data off Morocco. *American Association of Petroleum Geologists Bulletin*, 81, 1161-1184.
- Comas, M. C., Platt J. P, Soto, J. I. and Watts, A. B., 1999. The origin and tectonic history of the Alboran basin: insights from Leg 161 results. In: Zahn, R., Comas, M. C. and Klaus, A. (Eds) *Proceeding Ocean Drilling Program, Scientific Results*, 161, 555-579.
- Comas, M. C., Soto, J. I. and BASACALB cruise (TTR-9 Leg 3) Scientific Party 2000. A tectonic overview of mud diapirs and related mud volcanoes in the Alboran Basin. In: Comas, M. C. and Akhmanov, G. G. (Eds.) *Geological Processes on European continental margins*, IOC Workshop Report, 168, UNESCO, 29-30.
- Comas, M., Platt, J.P., Soto, J.I. and Watts, A.B., 1999. The origin and tectonic history of the Alboran Basin; insights from Leg 161 results. *Proc. ODP, Sci. Results*, 161, College Station, 555-580.
- Comas, M.C, Garcia-Duenas, V. and Jurado, M.J., 1992. Tectonic evolution of the Alboran Sea Basin. *Geo-Marine Letters*, 12, 157-164.
- Comas, M.C., Zahn, R. and Klaus, A., 1996. Preliminary results of ODP Leg 161. *Proceeding Ocean Drilling Program, Preliminary Results*, 161, 1-1679.
- Cronin, B.T., Kenyon, N.H., Woodside, J., den Bezemer, T., van der Wal, A., Millington, J., Ivanov, M.K. and Limonov, A., 1995. The Almeria canyon: a meandering channel system on an active margin, Alboran Sea, Western Mediterranean. In: K.T. Pickering, R.N. Hiscott, N.H. Kenyon, F. Ricci Lucchi and R.D.A. Smith (Eds.). *Atlas of Deep Water Environments: Architectural Style in Turbidite Systems*. Chapman and Hall, London, 84-88.
- Davies, R., Cartwright, J., Pike, J. and Line, C., 2001. Early Oligocene initiation of north Atlantic deep water formation. *Nature*, 410, 917-920.

- Davies, R.J., and Cartwright, J., 2002. A fossilized opal A to opal C/T transformation on the north-east Atlantic margin: support for a significantly elevated palaeogeothermal gradient during the Neogene? *Basin Research*, 14, 467-486.
- Dewey, J.F., Helman, M.L., Turco, E., Hutton, D.H.W. and Knott, S.D., 1989. Kinematics of the western Mediterranean. In: Coward, M. (Ed.) *Alpine Tectonics*. Spec Publ. Geol. Soc. London, 45, 265-283.
- Diaz del Rio, V., Somoza L., Martinez-Frias J., Hernandez-Molina, F.J., Lunar, R., Fernandez-Puga, M.C., Maestro, A., Terrinha, P., Llave, E., Garcia A., Garcia, A. C. and Vazquez, J.T., 2001. Carbonate chimneys in the Gulf of Cadiz: Initial report of their petrography and geochemistry. In: Akhmanov, G. and Suzyumov, A. (Eds.), *Geological processes on deep-water European margins*. IOC-UNESCO Workshop Report 175, 53-54.
- Dietz, R. S. and Menard, H.W., 1953. Hawaiian Swell, Deep, and Arch, and subsidence of the Hawaiian Islands. *Journal of Geology*, 61, 99-113.
- Eckhardt, J.D., Glasby, G.P., Puchelt, H. and Berner, Z., 1997. Hydrothermal manganese crusts from Enarete and Palinuro seamounts in the Tyrrhenian Sea. *Marine Georesources and Geotechnology*, 15, 2, 175-208.
- Emery, K.O. and Uchupi, E., 1984. *The geology of the Atlantic Ocean*. Springer-Verlag, New York, 1050 pp.
- Estrada, F., 1994. La Conca nor-oriental de la Mar d'Alboran: evolucio durant el Pliocene i el Quaternary. Master's Thesis, Univ. Central de Barcelona, 195 pp.
- Estrada, F., Ercilla, G. and Alonso, B., 1997. Pliocene-Quaternary tectonic-sedimentary evolution of the NE Alboran Sea (SW Mediterranean Sea). *Tectonophysics*, 282, 423-442.
- Gamberi, F. and Marani, M., 1999. Architecture of the Sardinian margin siliciclastic depositional systems. Annual meeting; Italian Sedimentology Group, CNR. *Giornale di Geologia*, 61, Serie 3C, 224-225.
- Gardner, J.M., 1999. Mud volcanoes on the Moroccan Margin. *ESO Transactions*, 80(46), 483.
- Gardner, J.M., 2001. Mud volcanoes revealed and sampled on the Moroccan continental margin. *Geophysical Research Letters*, 28(2), 339-342.
- Gould, W. J., 1985. Physical oceanography of the Azores Front. *Progress in Oceanography*, 14, 167-190.
- Habgood E.L., Kenyon N.H., Akhmetzanov A., Weaver P.P.E., Masson D.G., Gardner J. and Mulder T., 2003. Deep-water sediment wave fields, contourite sand channels and channel mouth sand lobes in the Gulf of Cadiz, NE Atlantic. *Sedimentology*, 50, 483-510.
- Hubbard, R.J., Pape, J. and Roberts, D.G., 1985. Depositional sequence mapping to illustrate the evolution of a passive continental margin. In: O.R. Berg, D. Woolverton (Eds.); *AAPG Memoir* 39, 93-115.
- Jurado, M.J. and Comas, M.C., 1992. Well log interpretation and seismic character of the Cenozoic sequence in the Northern Alboran Sea. *Geo-Marine Letters*, 12, 129-136.
- Kastens, K.A., Mascle, J., Auroux, C., et al., 1987. *Proc. ODP, Init. Repts.*, 107. College Station, TX (Ocean Drilling Program), 1013 pp.
- Kenyon N.H., Ivanov M.K., Akhmetzhanov A.M. and Akhmanov G.G. (Eds.), 2001. *Interdisciplinary Approaches to Geoscience on the North East Atlantic Margin and Mid-Atlantic Ridge*. Preliminary results of investigations during the TTR- 10 cruise of R/V *Professor Logachev*, July-August, 2000. IOC Technical Series, 60. UNESCO, 104 pp.
- Kenyon N.H., Ivanov M.K., Akhmetzhanov A.M. and Akhmanov G.G. (Eds.), 2000. *Multidisciplinary Study of Geological Processes on the North East Atlantic and Western Mediterranean Margins*. Preliminary results of geological and geophysical investigations during the TTR-9 cruise of R/V *Professor Logachev* June-July, 1999. IOC Technical Series, 56. UNESCO, 102 pp.
- Kenyon N.H., Ivanov M.K., Akhmetzhanov A.M. and Akhmanov G.G. (Eds.), 2002. *Geological Processes in the Mediterranean and Black Seas and North East Atlantic*. Preliminary results of investigations during the TTR-11 cruise of R/V *Professor Logachev*, July-September, 2001. IOC Technical Series, 62, 111 pp.
- Kenyon N.H., Ivanov M.K. and Akhmetzhanov A.M. (Eds.), 1998. Cold water carbonate mounds and sediment transport on the Northeast Atlantic margin. Preliminary results of geological and geophysical investigations during the TTR-7 cruise of R/V *Professor Logachev* in co-operation with the CORSAIRES and ENAM 2 programmes.

IOC Technical Series, 52, 178 pp.

King, E.L., Haflidason, H., Sejrup, H.P. and Loevlie, R., 1998. Glacigenic debris flows on the North Sea Trough Mouth Fan during ice stream maxima. *Marine Geology*, 152, 217-246.

Klein, B. and Siedler, G., 1989. On the origin of the Azores Current. *Journal of Geophysical Research*, 94, 6159-6168.

Kse, R. H. and Siedler, G., 1982. Meandering of the subtropical front southeast of the Azores. *Nature*, 300, 245-246.

Maldonado, A. and Comas, M. C., 1992. Geology and geophysics of the Alboran Sea: An introduction. *Geo-Marine Letters*, 12, 61-65.

Maldonado, A., Somoza, L. and Pallares, L. 1999. The Betic orogen and the Iberian-African boundary in the Gulf of Cadiz: geological evolution (Central North Atlantic). *Marine Geology*, 155, 9-43.

Marani, M. P., Gamberi, F., Casoni, L., Carrara, G., Landuzzi, V., Musacchio, M., Penitenti, D., Rossi, L. and Trua, T., 1999. New rock and hydrothermal samples from the southern Tyrrhenian Sea; the MAR-98 research cruise. Annual meeting; Italian Sedimentology Group, CNR. *Giornale di Geologia*, 61, Serie 3C, 3-24.

McClain, C. R. and Firestone, J., 1993. An investigation of Ekman Upwelling in the North Atlantic. *Journal of Geophysical Research* 98 (C7), 12327-12339.

Minniti, M. and Bonavia, F., 1984. Copper-ore grade hydrothermal mineralization discovered in a seamount in the Tyrrhenian Sea (Mediterranean); Is the mineralization related to porphyry-coppers or to base metal lodes? *Marine Geology*, 59, 271-282.

Mitchum, R.M., Vail, P.R. and Sangree, J.B., 1977. Seismic stratigraphy and global changes in sea level. Part 6. Stratigraphic interpretation of seismic reflection patterns in depositional sequences. In: C.E. Payton; P.R. Vail (Eds.), *AAPG Memoir* 26, 117-133.

Nielsen, T. and van Weering, T.C.E., 1998. Seismic stratigraphy and sedimentary processes at the Norwegian Sea margin northeast of the Faeroe Islands. *Marine Geology*, 152, 141-157.

Nielsen, T., Mathiesen, A., Stevenson, A., Hoult, R., Soerensen, A.B., Kuijpers, A. and Gillespie, E.J., 2002. Stratigraphical Development of the

Glaciated European Margin (STRATAGEM)-Regional Stratigraphy of WP2 area. EU Delivery no.19.

Perez-Belzuz, F., Alonso, B. and Ercilla, G. 1997. History of mud diapirism and trigger mechanisms in the Western Alboran Sea. *Tectonophysics*, 282, 399-422.

Riaza, C. and Martinez del Olmo, W., 1996. Depositional model of the Guadalquivir-Gulf of Cadiz Tertiary basin. In: Friend, P.F. and Dabrio, C.J., (Eds.). *Tertiary basin of Spain: the stratigraphic record of crustal kinematics*. Cambridge University Press, 330-338.

Sautkin, A., Talukder, A. R., Comas, M. C., Soto, J. I. and Alekseev, A., 2003. Mud volcanoes in the Alboran Sea: evidence from micropaleontological and geophysical data. *Marine Geology*, 195, 237-261.

Somoza, L., Diaz del Rio, V., Hernandez-Molina, F.J., Leon, R., Lobato, A., Alveirinho-Dias, J.M., Rodero, J. and TASYO team, 2000. New discovery of a mud-volcano field related to gas venting in the Gulf of Cadiz: Imagery of multibeam data and ultra-high resolution seismic. In: 3rd Symposium on Iberian Atlantic Margin Extended Abstracts. Faro, Portugal, 397-398.

Somoza, L., Ivanov M.K., Pinheiro, L., Maestro, A., Lowrie, A., Vazquez, J.T., Gardner, J., Medialdea, T. and Fernandez-Puga, M.C., 2001. Structural and tectonic control of fluid seeps and mud volcanoes in the Gulf of Cadiz. In: Akhmanov, G. and Suzyumov, A. (Eds.), *Geological processes on deep-water European margins*. IOC Workshop Report, 175, UNESCO, 41-42.

Talukder, A. R., Comas, M. C., Soto, J. I. and BASACALB cruise (TTR-9 Leg 3) Scientific Party, 2000. Diapirs and related structures in the mud volcano area of the West Alboran basin. In: Comas, M. C. and Akhmanov, G. G. (Eds.). *Geological Processes on European continental margins*, IOC Workshop Report, 168, UNESCO, 22-23.

Talukder, A. R., Comas, M. C. and Soto, J. I., In press. Pliocene to Recent mud diapirism and related mud volcanoes in the Alboran Sea (Western Mediterranean). Special publication of the Geological Society, London.


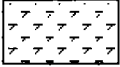
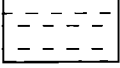

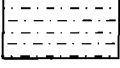



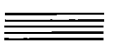



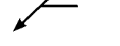
















van Weering, T.C.E., Nielsen, T., Kenyon, N.H., Akentieva, K. and Kuijpers, A.H., 1998. Sediments and sedimentation at the NE Faeroe

continental margin; contourites and large-scale sliding. *Marine Geology*, 152, 159-176.


Watts, A. B., Platt, J. P. and Buhl, P. 1993. Tectonic evolution of the Alboran Sea Basin. *Basin Research*, 5, 153-177.

Wilson, R.C.L., Hiscott, R.N., Willis M.G. and Gradstein, F.M., 1989. The Lusitanian Basin of West-Central Portugal: Mesozoic and Tertiary tectonics, stratigraphy, and subsidence history. In: Tankard, A.J., Balkwill, H.R. (Eds.), *Extensional tectonics and stratigraphy of the North Atlantic margins*. Am. Assoc. Pet. Geol. and Can. Geol. Found. AAPG Mem., 46, 111-130.

## ANNEX I. CORE LOGS

<b>LEGEND</b>	
	Foraminifera rich sediment
	marl
	mud/clay
	sand
	silt
	turbidite
	debris flow
	slump
	planar lamination
	cross lamination
	gradational boundary
	irregular boundary
	fault
	firm ground
	hard ground
	corals
	echinoderms
	gastropods
	plant debris
	shell fragments
	gas hydrate
	drop stones
	others
	<b>lithoclasts</b>
	OX oxidized layer
	DL dark layer
	flow in
	bioturbation
	burrows
	soupy sediment

## ANNEX I. CORE LOGS (LEG 1, the Faeroe Margin)


<b>R/V Professor Logachev TTR-12</b>		<b>CORE AT-358G</b>	
Location: basin floor	Date: 20/06/02		
Latitude: 62°36.002			
Longitude: 1°19.016			
Water Depth: 1640 m			
Recovery: 504 cm	<b>SUBSAMPLING CODES:</b> Sedimentology      Geochemistry 1- Collection      6- Gas      11 - T.sec 2- Grain size      7- TOC 3- Mineralogy      8- Bitum 4- X-ray      9- Pore water 5- Thin sections      10-carbonates		<b>AGE:</b> H- Holocene LP- Late Pleistocene EP- Early Pleistocene

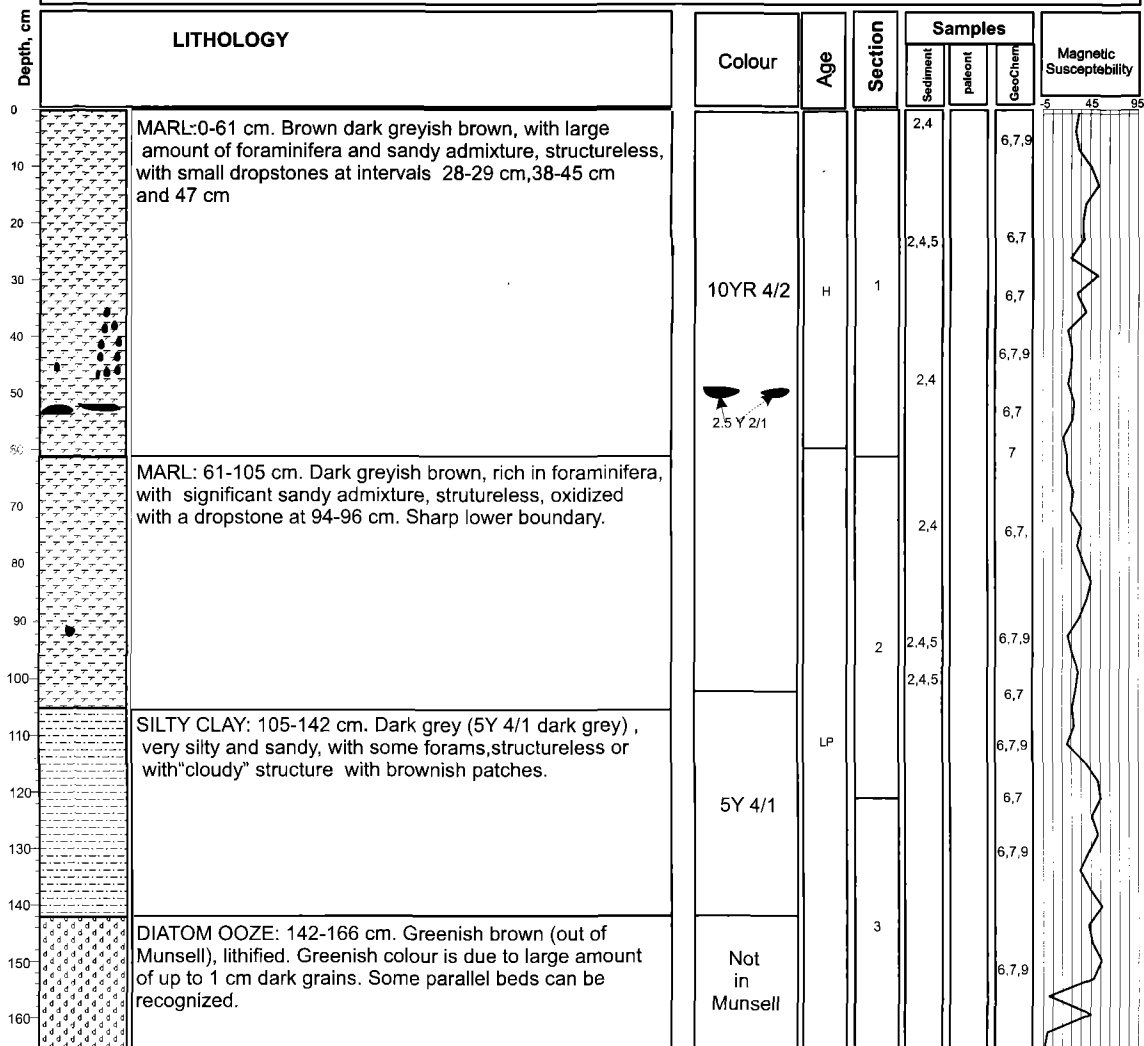
Depth, cm	LITHOLOGY	Colour	Age	Section	Samples			Magnetic susceptibility
					Sediment	palaeont	GeoChem	
0	CLAY:0 - 9 cm. Olive brown , structureless, apparently oxidized, with some foraminifera, no silty admixture. Lower boundary is sharp and planar.	2.5Y 5/4	H	1	5			
25								
50	CLAY:9 - 64cm. Dark grey structureless. At interval 36-37 cm there is 0.7 cm thick planar layer of some clay, but more silty and richer in foraminifera. At 45-46 cm interval layer of clay, but a little bit darker and more brownish, composition is the same.	5Y 4/1	H	2	5			
75								
100	CLAY:64-115 cm. Structureless, with no foraminifera, no silty admixture.	2.5Y 3/1	LP	3	5			
125								
150	SANDY CLAY:115-130 cm.very dark grey, structureless. CLAY:130 - 174 cm. Dark greyish-brown , structureless, with foraminifera. At interval 140 cm - layer across the section: 0.5 cm thick, contains sand and more foraminifera, than the rest of interval.	2.5 Y 4/2	LP	4	5			
175								
200	CLAY:174 -194 cm. Very dark grey, bioturbated, patches of dark greyish brown clay.	5Y 3/1	LP	5	5			
225								
250	CLAY: 194 - 279 cm. Brownish grey , intensively bioturbated, silt content is higher than in the above interval, lower boundary is subtle and gradual.	2.5 Y 4/21	LP	6	5			
275								
300	CLAY: 279 - 289 cm. Dark greyish brown, with foraminifera.	5Y 4/1	LP	7	5			
325								
350	SILTY CLAY: 289 - 504 cm. Dark grey, structureless, with sand admixture, scattered, with clasts 1 - 2 mm in diameter, with dropstones at 484 cm and shell fragment at 471 cm, probably debrite.	5Y 4/1	LP	8	5			
375								
400		5Y 4/1	LP	9	5			
425								
450								
475								
500								

Core log TTR-12-AT-358G



## ANNEX I. CORE LOGS (LEG 1, the Faeroe Margin)

<b>R/V Professor Logachev CRUISE TTR-12</b>		<b>CORE AT-359G</b>																					
<b>Location:</b> High backscatter patch on the southern diapiric structure	<b>Date:</b> 20/06/02																						
<b>Latitude:</b> 35°46,983'																							
<b>Longitude:</b> 7°29,355'																							
<b>Water Depth:</b> 1558 m																							
<b>Recovery:</b> 166 cm	<table border="1" style="width: 100%; border-collapse: collapse;"> <tr> <th colspan="2" style="text-align: center;">SUBSAMPLING CODES:</th> <th style="text-align: center;">AGE:</th> </tr> <tr> <td style="width: 33%;"><b>Sedimentology</b></td> <td style="width: 33%;"><b>Geochemistry</b></td> <td></td> </tr> <tr> <td>1- Collection</td> <td>6- Gas</td> <td>11 - T.sec</td> </tr> <tr> <td>2- Grain size</td> <td>7- TOC</td> <td>H- Holocene</td> </tr> <tr> <td>3- Mineralogy</td> <td>8- Bitum</td> <td>LP- Late Pleistocene</td> </tr> <tr> <td>4- X-ray</td> <td>9- Pore water</td> <td>EP- Early Pleistocene</td> </tr> <tr> <td>5- Thin sections</td> <td>10-carbonates</td> <td></td> </tr> </table>		SUBSAMPLING CODES:		AGE:	<b>Sedimentology</b>	<b>Geochemistry</b>		1- Collection	6- Gas	11 - T.sec	2- Grain size	7- TOC	H- Holocene	3- Mineralogy	8- Bitum	LP- Late Pleistocene	4- X-ray	9- Pore water	EP- Early Pleistocene	5- Thin sections	10-carbonates	
SUBSAMPLING CODES:		AGE:																					
<b>Sedimentology</b>	<b>Geochemistry</b>																						
1- Collection	6- Gas	11 - T.sec																					
2- Grain size	7- TOC	H- Holocene																					
3- Mineralogy	8- Bitum	LP- Late Pleistocene																					
4- X-ray	9- Pore water	EP- Early Pleistocene																					
5- Thin sections	10-carbonates																						



Core log TTR-12-AT-359G

## ANNEX I. CORE LOGS (LEG 1, the Faeroe Margin)

<b>R/V Professor Logachev TTR-12</b>		<b>CORE AT-360G</b>
Location:	Top of a local high on the northern diapiric structure	
Latitude:	62° 41,409'	Date: 20/06/2002
Longitude:	1° 17,145'	
Water Depth:	1548 m	
Recovery:	385 cm	
<b>SUBSAMPLING CODES:</b>		
<b>Sedimentology</b> 1- Collection 2- Grain size 3- Mineralogy 4- X-ray 5- Thin sections	<b>Geochemistry</b> 6- Gas 7- TOC 8- Bitum 9- Pore water 10-carbonates	<b>AGE:</b> H- Holocene LP- Late Pleistocene EP- Early Pleistocene

Depth, cm	LITHOLOGY	Age	Colour	Section	Samples			Magnetic Susceptibility (SI-units)
					Sediment	palaeont	GeoChem	
0	MARL: 0-35 cm. Olive brown, structureless silty clay with foraminifera and minor sandy admixture.	H	2.5 Y 4/4	1	5 2,4			
50	MARL: 35-50 cm. Olive, more water-saturated, higher silt, sand and foraminifera content than above.		5 Y 4/3		2,4,5			
50	SILTY CLAY: 50-91 cm. Very rich in silty and sandy admixture with thin sandy layers. Alternation of olive grey (5Y 4/3) and dark olive grey (5Y 3/2). Foraminifera rich. Grained admixture up to coarse sand and is very poorly sorted. More water saturated than above. Water saturation increases downcore.		5 Y 3/2	2	5 2,4			
100	CLAY: 91-149 cm. Dark grey, structureless with silty admixture and foraminifera. Less water saturated than above.		2.5 Y 4/2	3	2,4			
150	At 141 cm: Fragment of green diatom ooze (1.5 cm)	LP	5 Y 4/2		2,4,5			
150	SILTY CLAY: 149-169 cm. Many foraminifera. Small green nodules randomly distributed. Slump structures		5 Y 5/2	4	2,4			
200	CLAY: 169-228 cm. Brownish grey, structureless and rich in foraminifera. The colour changes from top to bottom. Several fragments of pale green plastic clay are present in the interval. A large fragment (2,5 cm) is found at the lower boundary.		10 YR 5/2 2.5 Y 3/3	4	2,4,5			
250	SILTY CLAY: 228- 231 cm. Dark olive brown silty clay		5 Y 5/2	5	2,4 5 2,4			
300	CLAY: 231-294 cm. Brownish grey silty, structureless and rich in foraminifera. Small and large fragments (c. 10 cm at 247 cm) of pale, green diatom ooze are present in the interval.		5 Y 5/1	5	2,4			
300	294-298 cm: More water-saturated then above. Less silty.							
300	298-380 cm: Dark grey, structureless with some silt. Small consolidated clay pebbles throughout the interval.							
350	From 323-343 cm the surface is a bit rough and contains no silt. Some dropstones present. Some foraminifera in the lower part of the layer. Overall the clay section appears to be crumbled or brecciated in places - (debrite ?)		2.5 Y 3/0	6	2,4,5 2,4			
350	380-385 cm: More consolidated than above. Minor amount of silt and foraminifera. Boundary with upper layer is sharp and sub-planar disturbed by inclined microfault.			7	2,4,5			

Core log TTR-12-AT-360G


## ANNEX I. CORE LOGS (LEG 1, the Faeroe Margin)

<b>R/V Professor Logachev TTR-12</b>		<b>CORE AT-362G</b>	
Location:	Basin floor core near the slump area	Date:	22/06/02
Latitude:	61° 47,044'		
Longitude:	3° 28,153'		
Water Depth:	1441 m		
Recovery:	428 cm		
<b>SUBSAMPLING CODES:</b> Sedimentology 1- Collection 2- Grain size 3- Mineralogy 4- X-ray 5- Thin sections		Geochemistry 6- Gas 7- TOC 8- Bitum 9- Pore water 10-carbonates	<b>AGE:</b> H- Holocene LP- Late Pleistocene EP- Early Pleistocene

Depth, cm	LITHOLOGY	Age	Colour	Section	Samples		Magnetic susceptibility
					Sediment	palaeont	
0	SILTY CLAY: 0-3 cm olive brown 2.5Y4/3 with small amount of sandy admixture. 3-6 cm olive grey 5Y4/2.	H	10Y 3/3	1	1,4		500, SI
50	SILTY SANDY CLAY: 6-20 cm dark brown with few foraminifera. Sandy admixture decreases downward.	7-2.5Y	3/2		1,4		
50	SILTY CLAY: 20-29 cm dark olive grey, water saturated.	4/2	5Y	2	1,4		
100	SILTY SANDY CLAY: 29-37 cm dark greyish brown with darker and lighter patches, with black dropstone (1x0,8x0,5 cm) at 30 cm. At 37 cm small fragment of light grey sediment. 37-46cm dark greyish brown.	LP	4/1		1,4		
100	Transitional boundary. 46-50 cm dark grey. Patchy structure. Transitional boundary. 50-63 cm dark greyish brown. Few foraminifera.		2.5Y 4/2	3	1,4		
150	SILTY CLAY: 63-69 cm grey with shell fragments. At 64-65 cm clay clast more black than the matrix. At 68-69 cm big dark clast. The lower boundary is irregular, gradational. 69-93 cm light grey brown. The lower boundary is horizontal, gradational. 93-110 cm light grey brown. At 99-101 cm darker area. The lower boundary is subhorizontal, gradational. 110-111 cm green grey brown. 111-118 cm grey brown.	10R	4/2		1,4		
150	CLAY: 118-144 cm dark greyish brown with few subrounded fragments of light green clayey diatomic ooze (0,2-0,5cm). 144-166 cm olive grey with some fine silty admixture. 166-180 cm dark greyish brown with some patches of olive grey clay in the upper part of interval.		5Y 4/2	4	1,4		
200	SILTY CLAY: 180-205 cm dark grey structureless. Upper and lower boundaries are intensively bioturbated. Burrows filled with lighter clay.		2.5Y 4/1		1,4		
200	CLAY: 205-236 cm grey, bioturbated with some silt. Burrows in the upper 5 cm are filled with dark clay. At 217 cm greenish layer. 236-249 cm dark grey. Lower boundary is bioturbated. 249-256 cm greyish brown, almost no silty admixture.		2.5Y 5/2	5	1,4		
250	SILTY CLAY: 256-265 cm dark grey, with a high silty content, rare foraminifera. The lower boundary is irregular and bioturbated. 265-279 cm lighter grey. Burrow (~1,5 cm) filled with soupy, rich in foraminifera. The boundary is irregular due to bioturbation.		5Y 5/1		1,4		
250	CLAY: 279-294 cm dark grey, bioturbated, with some patches of light grey clay. Rare foraminifera. With some silty admixture.		5Y 4/2	6	1,4		
300	SILTY CLAY: 294-304 cm dark grey. 304-307 cm very enriched in poorly sorted silty admixture. Angular dropstone (3x1x2 cm) at 305-307 cm		5Y 5/1		1,4		
300	CLAY: 307-318 cm lighter grey. 318-324 cm darker grey. 324-343 cm lighter grey. Amount of silty admixture increases downward.		5Y 4/1	7	1,4		
350	SILTY CLAY: 343-363 cm dark grey, with some mica. 363-385 cm lighter grey, with less silty admixture. 385-396 cm dark brownish grey, very silty. 396-402 cm lighter grey. 402-412 cm light grey clay, carbonate, with small amount of silty admixture. 412-428 dark grey.		5Y 5/1		1,4		
350			4/1	8	1,4		

Core log TTR-12-AT-362G

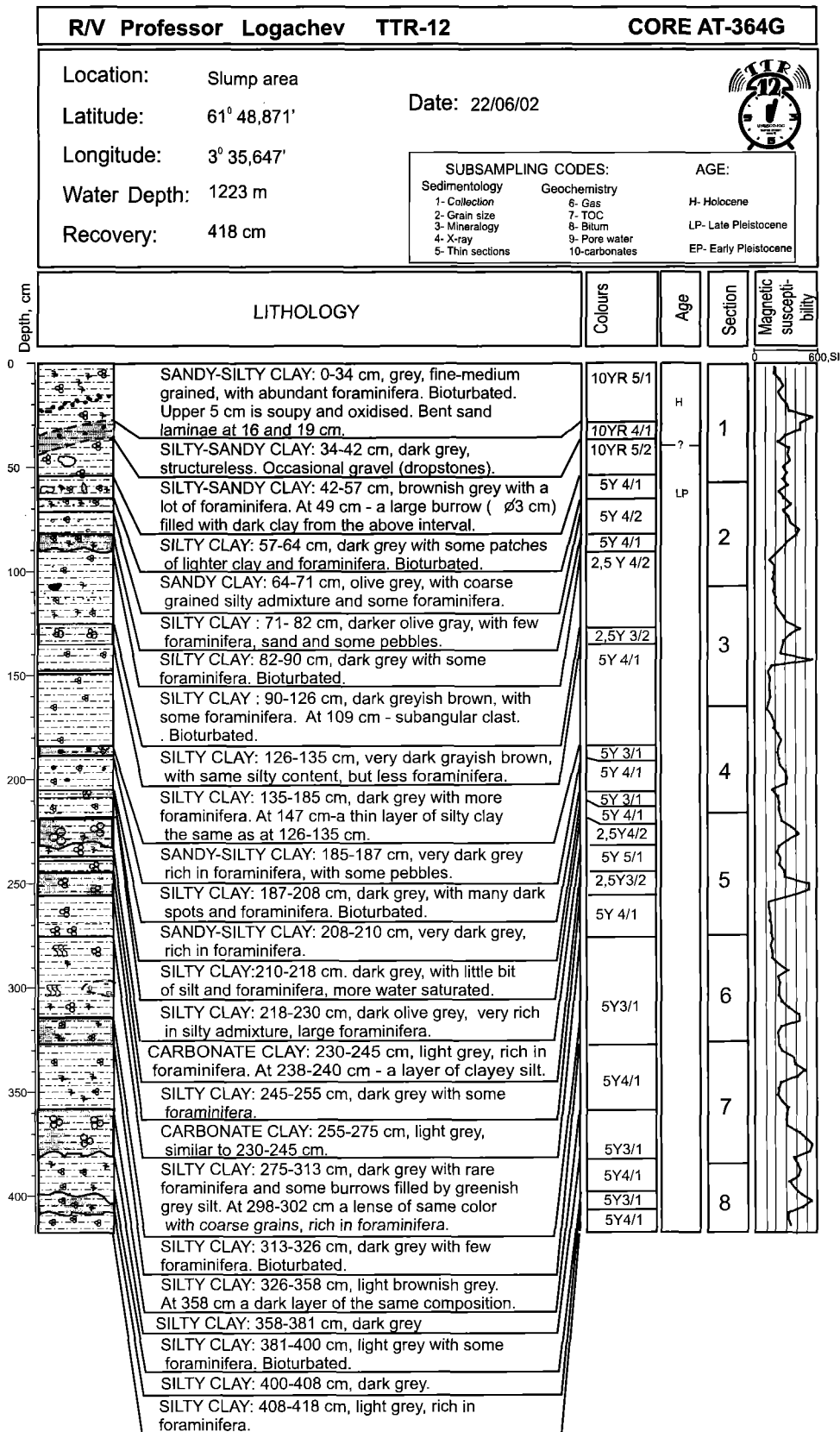
## ANNEX I. CORE LOGS (LEG 1, the Faeroe Margin)

<b>R/V Professor Logachev TTR-12</b>		<b>CORE AT-363G</b>																						
Location:	Slump area	Date:	22.06.02																					
Latitude:	61 48.774																							
Longitude:	3 35.346	<table border="1" style="width: 100%; border-collapse: collapse;"> <tr> <td colspan="3">SUBSAMPLING CODES:</td> </tr> <tr> <td style="width: 33%;">Sedimentology</td> <td style="width: 33%;">Geochemistry</td> <td style="width: 33%;">AGE:</td> </tr> <tr> <td>1- Collection</td> <td>6- Gas</td> <td>H- Holocene</td> </tr> <tr> <td>2- Grain size</td> <td>7- TOC</td> <td>LP- Late Pleistocene</td> </tr> <tr> <td>3- Mineralogy</td> <td>8- Blum</td> <td>EP- Early Pleistocene</td> </tr> <tr> <td>4- X-ray</td> <td>9- Pore water</td> <td></td> </tr> <tr> <td>5- Thin sections</td> <td>10- carbonates</td> <td></td> </tr> </table>		SUBSAMPLING CODES:			Sedimentology	Geochemistry	AGE:	1- Collection	6- Gas	H- Holocene	2- Grain size	7- TOC	LP- Late Pleistocene	3- Mineralogy	8- Blum	EP- Early Pleistocene	4- X-ray	9- Pore water		5- Thin sections	10- carbonates	
SUBSAMPLING CODES:																								
Sedimentology	Geochemistry			AGE:																				
1- Collection	6- Gas	H- Holocene																						
2- Grain size	7- TOC	LP- Late Pleistocene																						
3- Mineralogy	8- Blum	EP- Early Pleistocene																						
4- X-ray	9- Pore water																							
5- Thin sections	10- carbonates																							
Recovery:	500.5 cm																							
Water Depth:	1236 m																							

Depth, cm	LITHOLOGY	Colours	Age	Section	Samples		Magnetic susceptibility
					Sediment	paleont	
0	SILT: 0-6,5cm olive brown enriched in foraminifera with some amount of terrigenous grains.	2Y4/3	H	1	2,4	1	
	SILT: 6,5-46 light grey with less foraminifera, with mica and terrigenous grains, with burrows filled by greenish grey silt, clay content increases downwards.	2.5Y4/0			2,4,5	1	
50	SILTY CLAY: 46-73cm dark grey brown structureless more compacted than the upper sediments with little foraminifera and terrigenous grains.	5Y4/1	LP	2	2,4,5	1	
	SILTY CLAY: 73-75cm dark grey, very sandy.	2.5Y3/2			2,4,5	1	
100	SILTY CLAY: 75-97cm very dark greyish brown with some foraminifera, structureless lower part bioturbated.	2.5Y5/2			2,4	1	
	SILTY CLAY: 97-115cm olive brown structureless with sand and shell debris, 109-112cm- dark clast.	2.5Y4/2			2,4	1	
150	CLAY: 115-126cm dark greyish brown structureless with foraminifera and some silt.	5Y3/2			2,4	1	
	CLAY: 126-160m in intervals 126-145 and 145-160 cm colour changes from dark olive grey to very dark grey, structureless, water saturated, bioturbated, with foraminifera and some silt.	2.5Y4/2			2	1	
200	CLAY: 160-207cm dark greyish brown structureless with some foraminifera, the interval 201-207cm very rich in foraminifera.	2.5Y4/2			2,4	1	
	SILTY CLAY: 207-257cm dark greyish brown structureless bioturbated with some foraminifera and shell fragments, 209-211cm - clast of darker clay.	2.5Y4/2			2,4	1	
250	SILTY CLAY: 257-273cm light grey structureless	2.5Y4/0			2,4	1	
300	CLAY: 273-290cm dark grey structureless bioturbated with poorly-sorted silt, with some mica flakes and foraminifera.	2.5Y4/2	2,4	1			
	CLAY: 290-353cm olive grey structureless with silt and a little amount of foraminifera.	5Y4/2	2,4	1			
350	CLAY: 353-355cm dark grey structureless with silt and a small amount of foraminifera.	5Y4/1	7	7	2,4	1	
	CLAY: 355-368cm olive grey structureless with some foraminifera.	5Y4/2			2,4	1	
	CLAY: 368-379cm dark grey structureless with some foraminifera and terrigenous material.	5Y4/1			2,4	1	
400	CLAY: 379-415cm dark grey structureless with a small amount of foraminifera and black mineral.	5Y4/1	8	8	2,4	1	
	CLAY: 415-430cm olive grey structureless with a small amount of foraminifera and sand.	5Y4/2			2,4	1	
450	SILTY CLAY: 430-462,5cm dark grey with a small amount of foraminifera, water saturated.	5Y4/1	9	9	2,4	1	
	CLAY: 462,5-500,5cm dark grey, becoming lighter downwards, structureless with a small amount of foraminifera and sand. 469,5-473,5 - silty clay, darker and denser.	5Y4/1			2,4	1	
500					2,4	1	


Core log TTR-12-AT-363G

## ANNEX I. CORE LOGS (LEG 1, the Faeroe Margin)



Core log TTR-12-AT-364G


## ANNEX I. CORE LOGS (LEG 1, the Faeroe Margin)

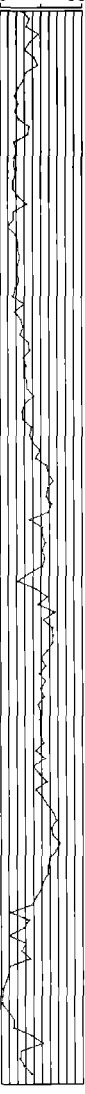
<b>R/V Professor Logachev TTR-12</b>	<b>CORE AT-365G</b>	
Location: Steep slope in the slump area	Date: 22.06.02	
Latitude: 61°50.430'		
Longitude: 3°40.123'		
Recovery: 154 cm		
Water Depth: 998 m		
<b>SUBSAMPLING CODES:</b>		
Sedimentology 1- Collection 2- Grain size 3- Mineralogy 4- X-ray 5- Thin sections	Geochemistry 6- Gas 7- TOC 8- Bitum 9- Pore water 10- carbonates	AGE: H- Holocene LP- Late Pleistocene EP- Early Pleistocene

Depth, cm	LITHOLOGY	Colors	Age	Section	Samples		Magnetic Susceptibility, SI
					Sediment	paleont	
0	SILTY SANDY CLAY: 0-8 cm olive brown, soupy.	2.5Y4/3				2,4	
	SILTY CLAYEY SAND: 8-10 cm olive grey, poorly sorted	5Y4/2				2,4,5	
	10-16cm - Interval composed of fragments of sediments, presented by: dark olive silty clay, dark grey sand poorly sorted rich in foraminifera, dark grey sandy silty clay, fragments of overlaying sediments.	5Y3/2 5Y4/1 2.5Y5/2				2,4 2,5	
	SILTY CLAY: 16-22cm greyish brown stiff with sandy patches with foraminifera..	2Y4/2		1			
	SILTY SANDY CLAY : 22-28 cm dark greyish brown.	2.5Y5/2					
	SILTY SANDY CLAY: 28-38 cm greyish brown stiff with some sandy patches with abundant foraminifera.	2.5Y4/3				4 2,4,5	
50	SILTY SANDY CLAY: 38-48 cm olive brown with sandy patches.	5Y3/2 2.5Y4/2				2,4,5	
	SILTY SANDY CLAY: 48-49 cm olive grey water saturated.	5Y3/2 2.5Y4/3					
	49-63 cm - Interval is composed of fragments of different deposits. Matrix - silty sandy clay dark greyish brown. Fragments: silty clay from upper interval olive grey water saturated, silty sandy clay dark olive grey water saturated with foraminifera, silty clayey sand olive brown with gravel grains, sandy silty clay olive brown consolidated, sandy clay dark olive with gravel and forams, 61-62 cm - drop stone 1/1 cm.	2.5Y4/2 2.5Y4/4				2,5 5	
	SILTY SANDY CLAY: 63-72 cm dark greyish brown water saturated with foraminifera and drop stone 68 cm.	2.5Y4/3 2.5Y4/2		2			
100	SILTY CLAY: 72-83 cm olive brown stiff with forams and 3 drop stones at 74-76 cm.	5Y4/2					
	SILTY CLAY: 83-90 cm dark greyish brown stiff with foraminifera.	2.5Y4/2				2,5	
	90-105cm - Interval composed of fragments of silty clay and sandy clay of different colours.	2.5Y3/2				2,4	
	SANDY CLAY: 105-111 cm dark greyish brown very soupy with foraminifera.	2.5Y4/4 2.5Y3/2					
	SILTY CLAY: 111-119 cm dark greyish brown plastic bioturbated.	5Y2.5/1		3			
	SILTY CLAY: 119-133 cm very dark greyish stiff with fragments of overlaying sediments.					2,4 2,5	
150	SILTY CLAY: 133-140 cm black very stiff.	5Y4/2 5Y3/2					
	SILTY CLAY: 140-146 cm olive grey water saturated with small fragment of silty clay from the upper layer at 143 cm.						
	SILTY CLAY: 146-154 cm very dark gray water saturated with borrows of silty clay olive grey soupy.						

Core log TTR-12-AT-365G

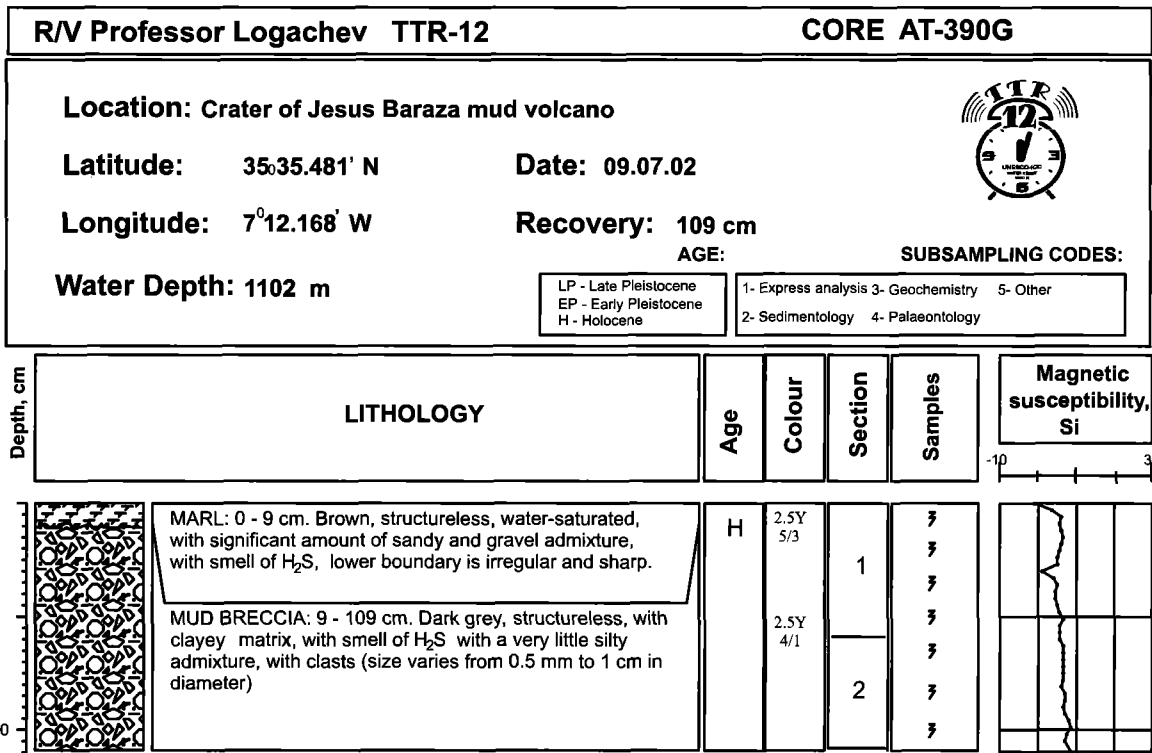
## ANNEX I. CORE LOGS (LEG 1, the Faeroe Margin)

<b>R/V Professor Logachev TTR-12</b>		<b>CORE AT-366G</b>																		
Location:	Basin floor core																			
Latitude:	66°49,775'	Date: 22/06/02																		
Longitude:	3°38,232'																			
Water Depth:	1054 m																			
Recovery:	424 cm																			
		<b>SUBSAMPLING CODES:</b> <b>AGE:</b>																		
		<table style="width: 100%; border: none;"> <tr> <td style="width: 33%;">Sedimentology</td> <td style="width: 33%;">Geochemistry</td> <td style="width: 33%;">AGE:</td> </tr> <tr> <td>1- Collection</td> <td>6- Gas</td> <td>H- Holocene</td> </tr> <tr> <td>2- Grain size</td> <td>7- TOC</td> <td>LP- Late Pleistocene</td> </tr> <tr> <td>3- Mineralogy</td> <td>8- Bitum</td> <td>EP- Early Pleistocene</td> </tr> <tr> <td>4- X-ray</td> <td>9- Pore water</td> <td></td> </tr> <tr> <td>5- Thin sections</td> <td>10-carbonates</td> <td></td> </tr> </table>	Sedimentology	Geochemistry	AGE:	1- Collection	6- Gas	H- Holocene	2- Grain size	7- TOC	LP- Late Pleistocene	3- Mineralogy	8- Bitum	EP- Early Pleistocene	4- X-ray	9- Pore water		5- Thin sections	10-carbonates	
Sedimentology	Geochemistry	AGE:																		
1- Collection	6- Gas	H- Holocene																		
2- Grain size	7- TOC	LP- Late Pleistocene																		
3- Mineralogy	8- Bitum	EP- Early Pleistocene																		
4- X-ray	9- Pore water																			
5- Thin sections	10-carbonates																			

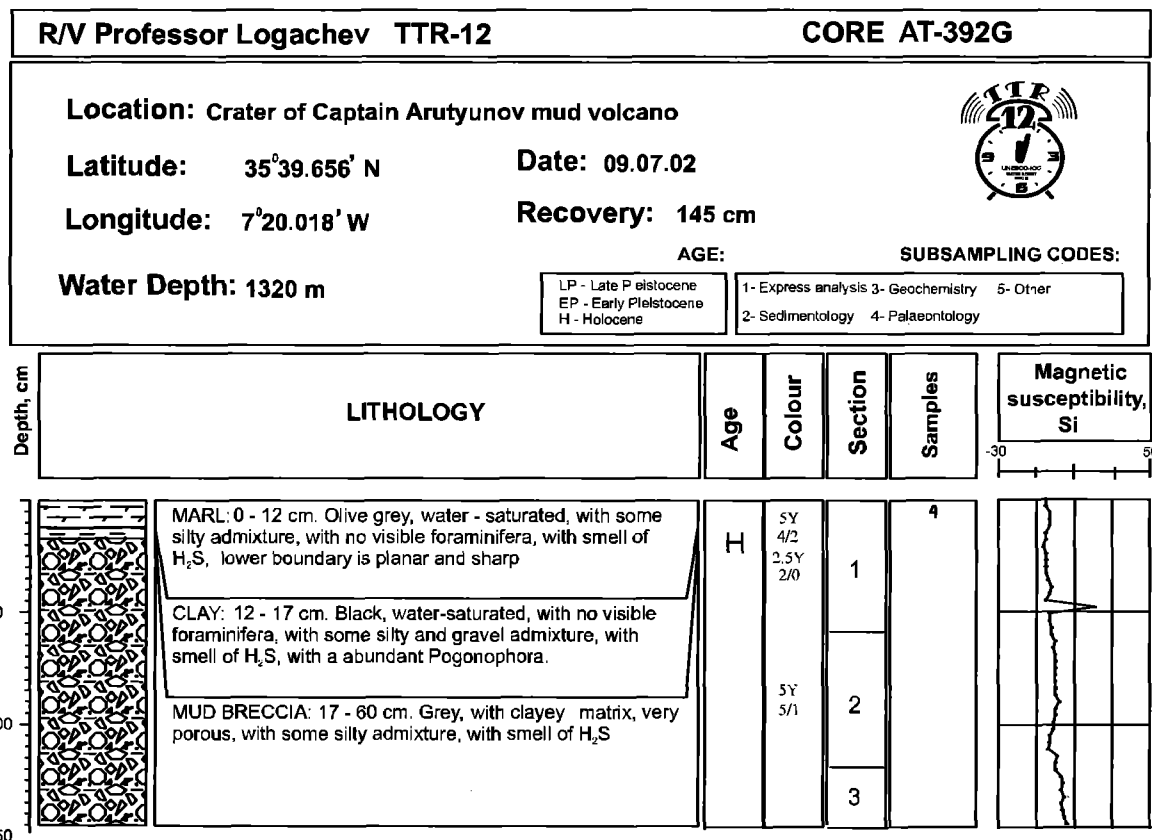
Depth, cm	LITHOLOGY	Age	Colour	Section	Samples			Magnetic susceptibility
					Sediment	palaeont	GeoChem	
0								0      500, Si
0-3	SILTY CLAY:0-3 cm. Olive brown, with sand admixture.		2.5Y4/3		2, 4			
3-7	SILTY CLAY:3-7 cm. Greyish brown, with foraminifera.							
7-14	SILTY CLAY: 7-14 cm. Brown, with silt admixture, with lens of silty clay at interval 10-14 cm. With foraminifera.	H		1	2			
14-24	SILTY CLAY:14-24cm. Dark brown, structureless, with huge amount of foraminifera, lower boundary is planar.	?	2.5Y5/3					
24-56	SILTY CLAY: 24-56 cm. Brown, with silty admixture, with foraminifera, with fragments of sediments at 32-38 cm: 1 - greyish brown silty clay, 2 - dark greyish brown silty clay stiff with small sandy content.		2.5Y4/3		5 5			
56-61	SILTY CLAY: 56-61 cm. Light brown, with silt.			2	5			
61-105	SILTY CLAY:61-105 cm. Olive brown, with foraminifera with slump structure. Silt patches at 67, 78, 96 cm.	LP	2.5Y5/2					
105-116	MARL:105-116 cm. Greyish brown, rich in foraminifera, with lense of light olive brown clay, with foraminifera and mica.		2.5Y4/2	3	2			
116-177.5	SILTY CLAY: 116-177.5 cm. Brownish-grey, with patches of silty clay at interval 122-124 cm, 124-126 cm, 138 - 140 cm.			4				
177.5 - 237.5	CLAY: 177.5 - 237.5 cm. Dark grey, with significant carbonate admixture, with foraminifera, with marl lense at 233 and dropstone at 237.5 cm.				2			
237.5 - 294.5	CLAY:237.5 - 294.5 cm. Olive grey, with dark spots At intervals 267.5-271.5, 279.5-280.5, 282.5-283.5, 287.5-288.5, 294.5-295.5 cm - lenses of more coarse silty material. With brown spots throughout the interval filled by silty clay, with large amount of foraminifera.		5Y5/1	5	2, 4			
294.5-351	SILTY CLAY: 294,5-351 cm. Dark grey, with foraminifera, with mica flakes.		5Y4/1	6	2, 4			
351-360	CLAY: 351-360 cm. Greyish brown clay, with a lot of silty admixture and foraminifera							
351-364	CLAY: 351-364 cm. Dark grey, with foraminifera and silt admixture		5Y3/2					
351-375	CLAY:351-375 cm. Light olive, with silt admixture, with foraminifera.		5Y5/2					
375-380	CLAY: 375 -380. Dark grey, with silt admixture and foraminifera.		2.5Y3/1	7	2, 4			
380-388	CLAY: 380 -388cm. Light grey, with a little content of foraminifera and silty admixture.		2.5Y5/1		2, 4			
388-402	SILTY CLAY:388-402 cm. Dark grey, with little content of foraminifera, with a little amount of black grains (probably mica).		2.5Y3/1					
402-424	CLAY: 402-424 cm. Light grey, with a little amount of foraminifera and silt admixture.		2.5Y5/1	8	2, 4			

Core log TTR-12-AT-366G

## ANNEX I. CORE LOGS (LEG 2, the Gulf of Cadiz)



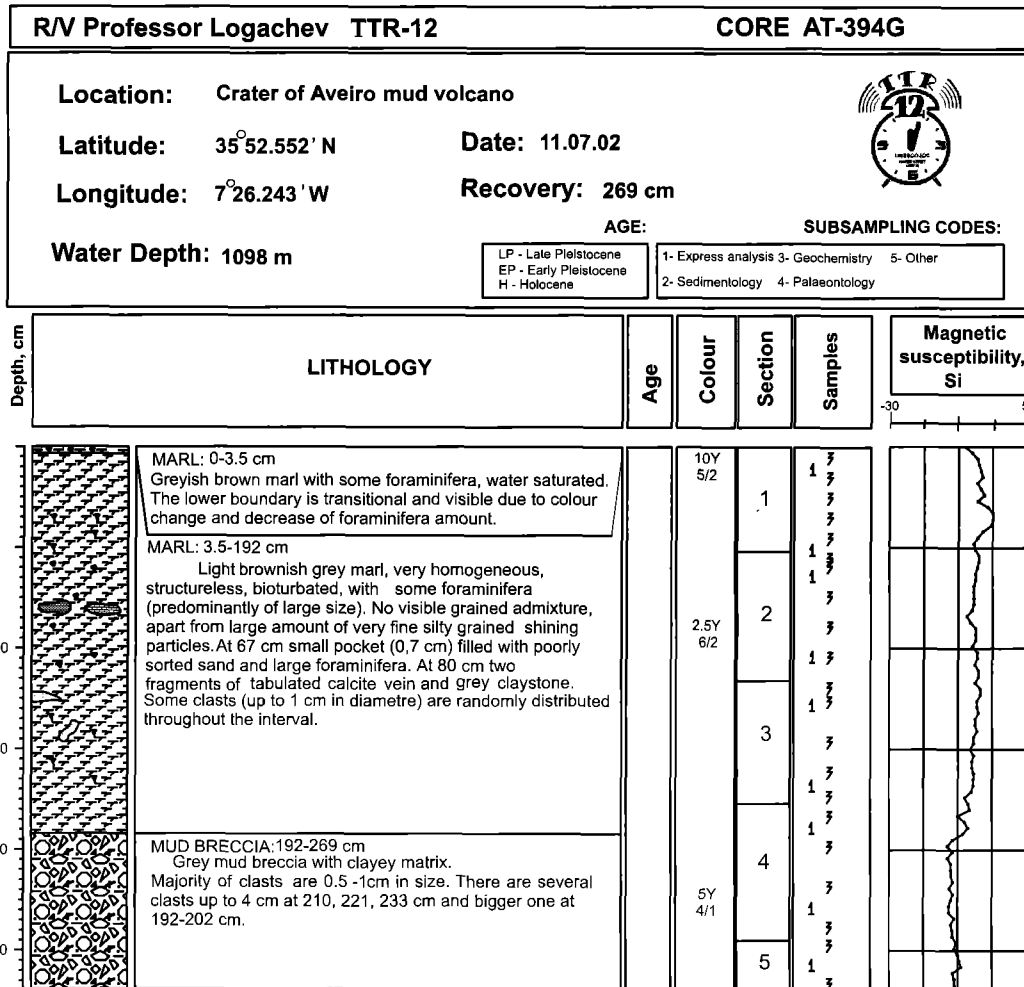
*Core log TTR-12-AT-390G*



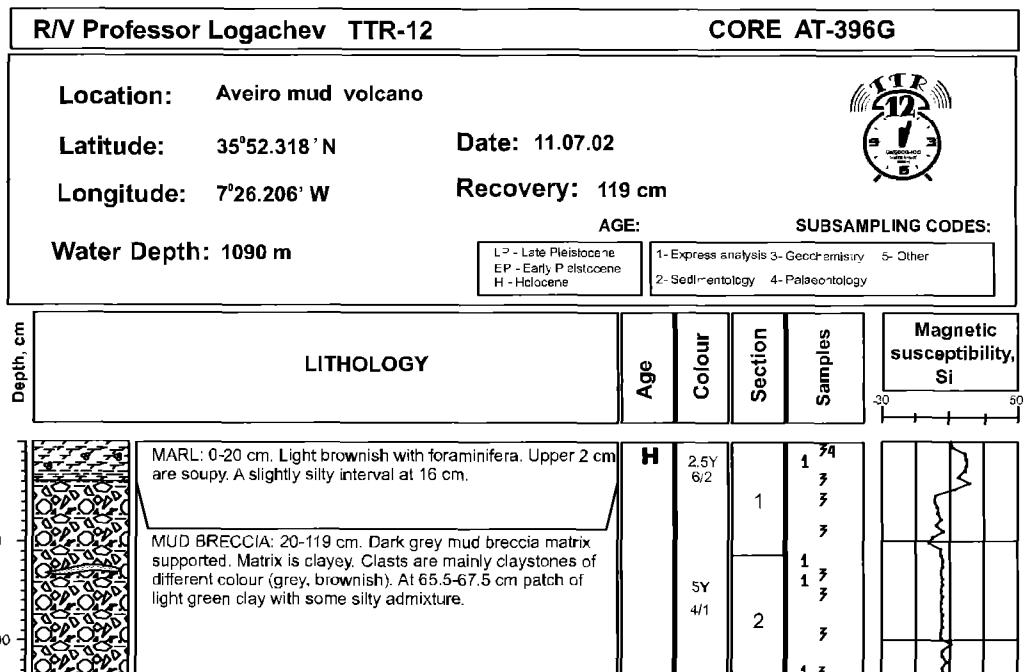
*Core log TTR-12-AT-392G*



## ANNEX I. CORE LOGS (LEG 2, the Gulf of Cadiz)

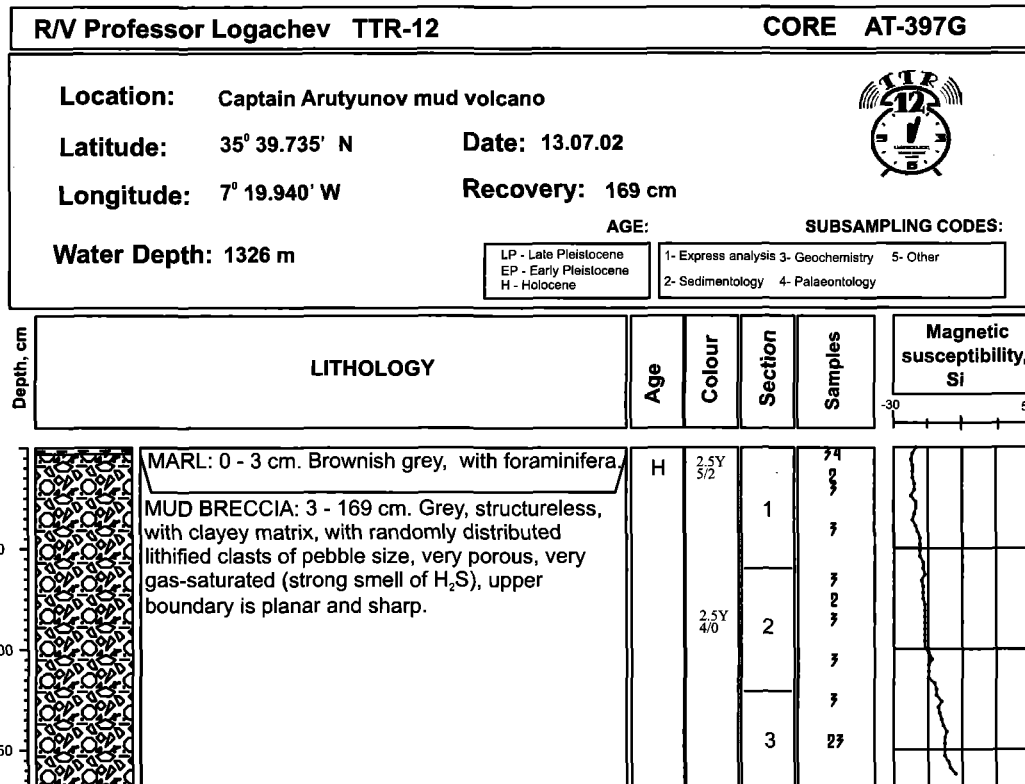


*Core log TTR-12-AT-394G*

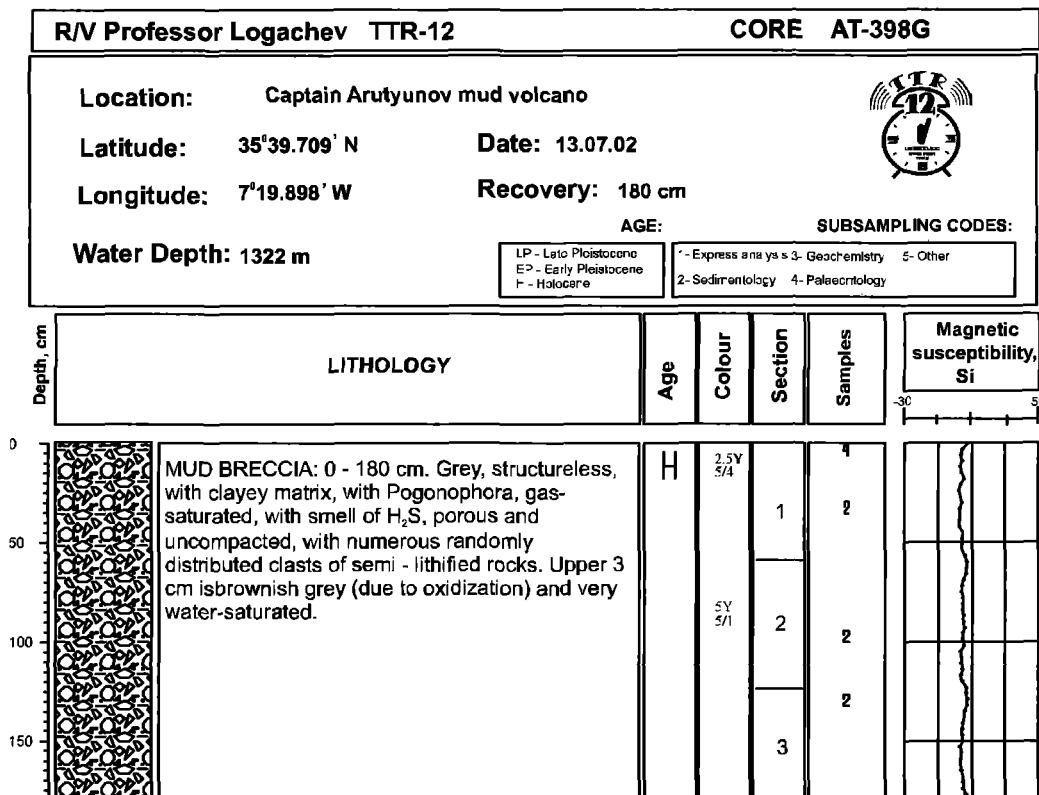


*Core log TTR-12-AT-396G*

## ANNEX I. CORE LOGS (LEG 2, the Gulf of Cadiz)




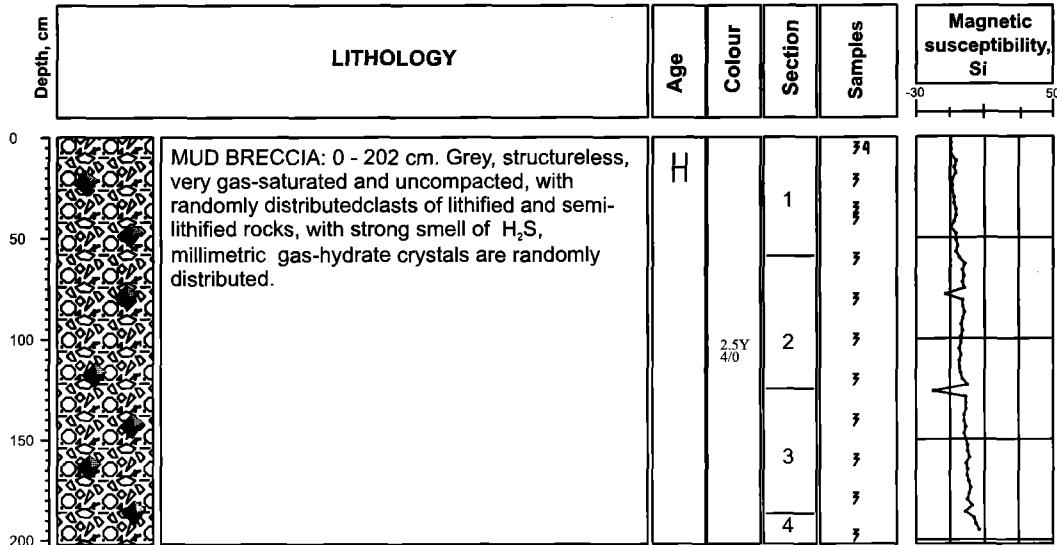
*Core log TTR-12-AT-397G*




*Core log TTR-12-AT-398G*

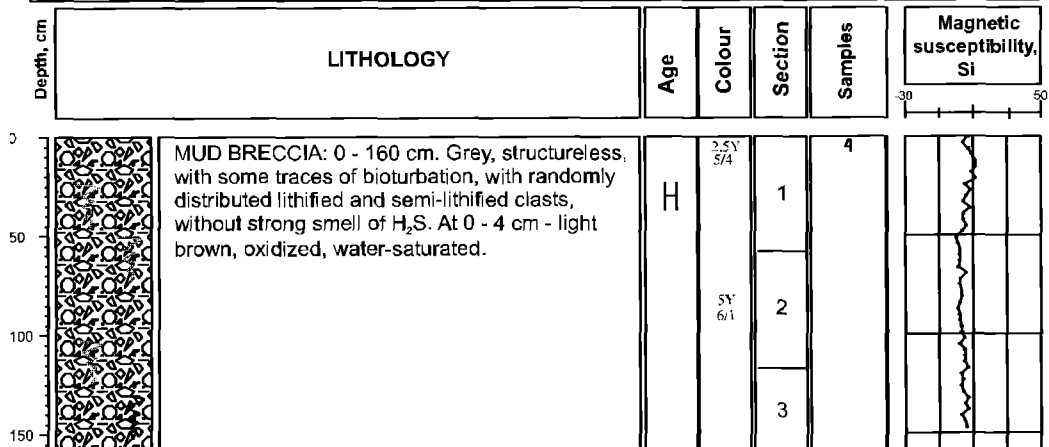
## ANNEX I. CORE LOGS (LEG 2, the Gulf of Cadiz)

<b>R/V Professor Logachev TTR-12</b>		<b>CORE AT-400G</b>	
			
<b>Location:</b> Captain Arutyunov mud volcano		<b>Date:</b> 14.07.02	
<b>Latitude:</b> 35°39.714' N	<b>Recovery:</b> 202 cm		
<b>Longitude:</b> 7°19.976' W	<b>Water Depth:</b> 1324 m		
<b>AGE:</b>		<b>SUBSAMPLING CODES:</b>	
LP - Late Pleistocene EP - Early Pleistocene H - Holocene		1- Express analysis 3- Geochemistry 5- Other 2- Sedimentology 4- Palaeontology	



*Core log TTR-12-AT-400G*

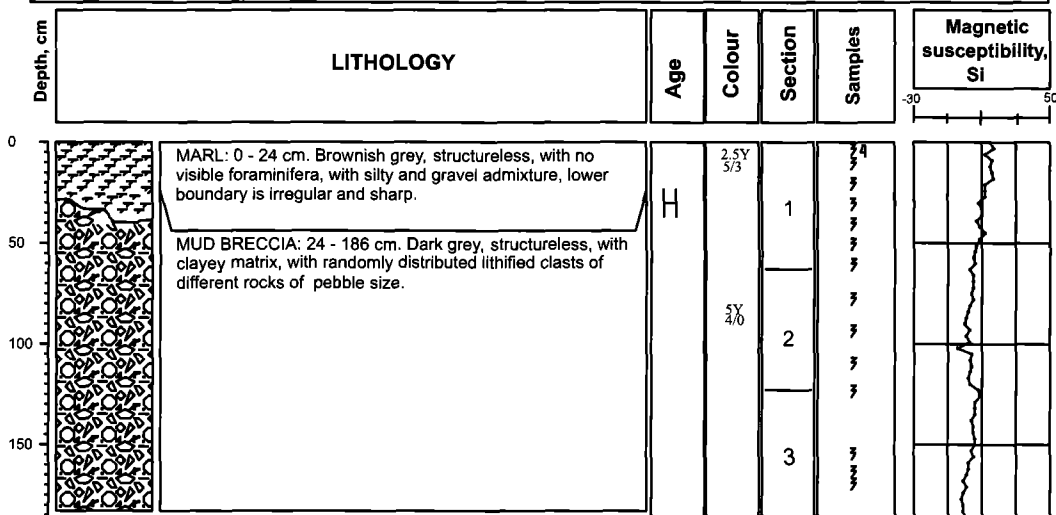
<b>R/V Professor Logachev TTR-12</b>		<b>CORE AT-401G</b>	
			
<b>Location:</b> Unnamed mud volcano on PSAT 121		<b>Date:</b> 14.07.02	
<b>Latitude:</b> 35°33.154' N	<b>Recovery:</b> 160 cm		
<b>Longitude:</b> 6°48.036' W	<b>Water Depth:</b> 794 m		
<b>AGE:</b>		<b>SUBSAMPLING CODES:</b>	
LP - Late Pleistocene EP - Early Pleistocene H - Holocene		1- Express analysis 3- Geochemistry 5- Other 2- Sedimentology 4- Palaeontology	



*Core log TTR-12-AT-401G*

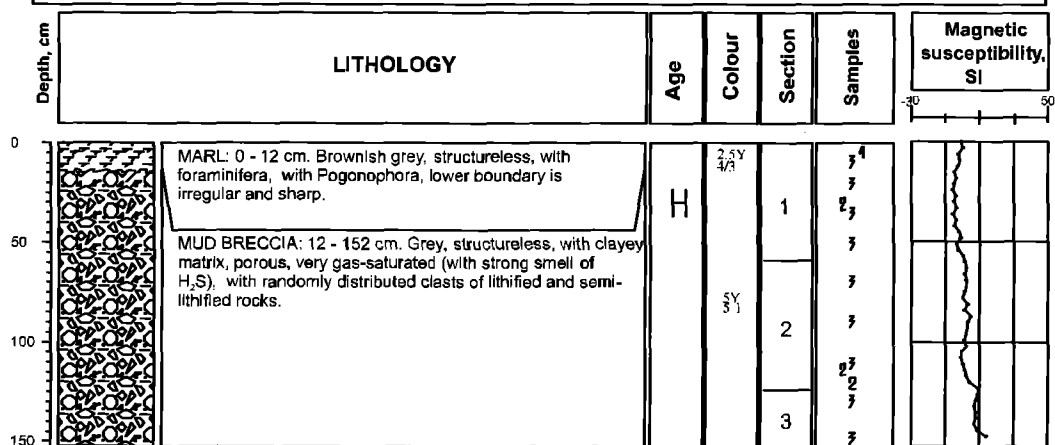
## ANNEX I. CORE LOGS (LEG 2, the Gulf of Cadiz)

<b>R/V Professor Logachev TTR-12</b>		<b>CORE AT-402G</b>	
<b>Location: Unnamed mud volcano on PSAT 122</b>			
<b>Latitude: 35°33.168' N</b>		<b>Date: 14.07.02</b>	
<b>Longitude: 6°48.105' W</b>		<b>Recovery: 186 cm</b>	
<b>Water Depth: 773 m</b>		<b>AGE:</b> LP - Late Pleistocene EP - Early Pleistocene H - Holocene	
		<b>SUBSAMPLING CODES:</b> 1- Express analysis 3- Geochemistry 5- Other 2- Sedimentology 4- Palaeontology	



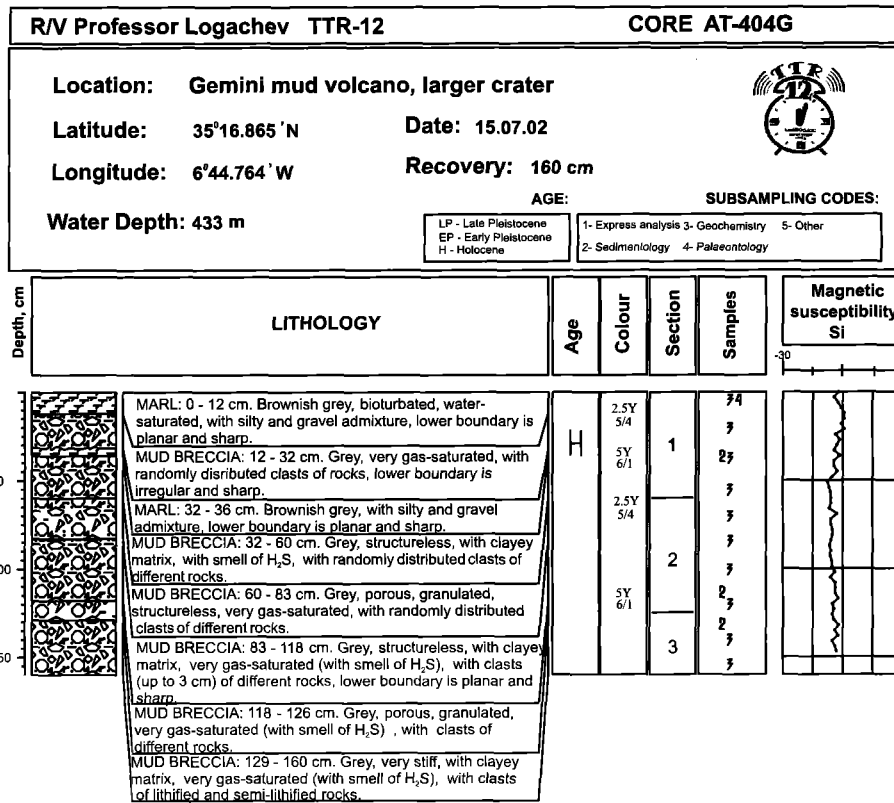
*Core log TTR-12-AT-402G*

<b>R/V Professor Logachev TTR-12</b>		<b>CORE AT-403G</b>	
<b>Location: Fuiza mud volcano</b>			
<b>Latitude: 35°15.360' N</b>		<b>Date: 15.07.02</b>	
<b>Longitude: 6°41.890' W</b>		<b>Recovery: 152 cm</b>	
<b>Water Depth: 385 m</b>		<b>AGE:</b> LP - Late Pleistocene EP - Early Pleistocene H - Holocene	
		<b>SUBSAMPLING CODES:</b> 1- Express analysis 3- Geochemistry 5- Other 2- Sedimentology 4- Palaeontology	

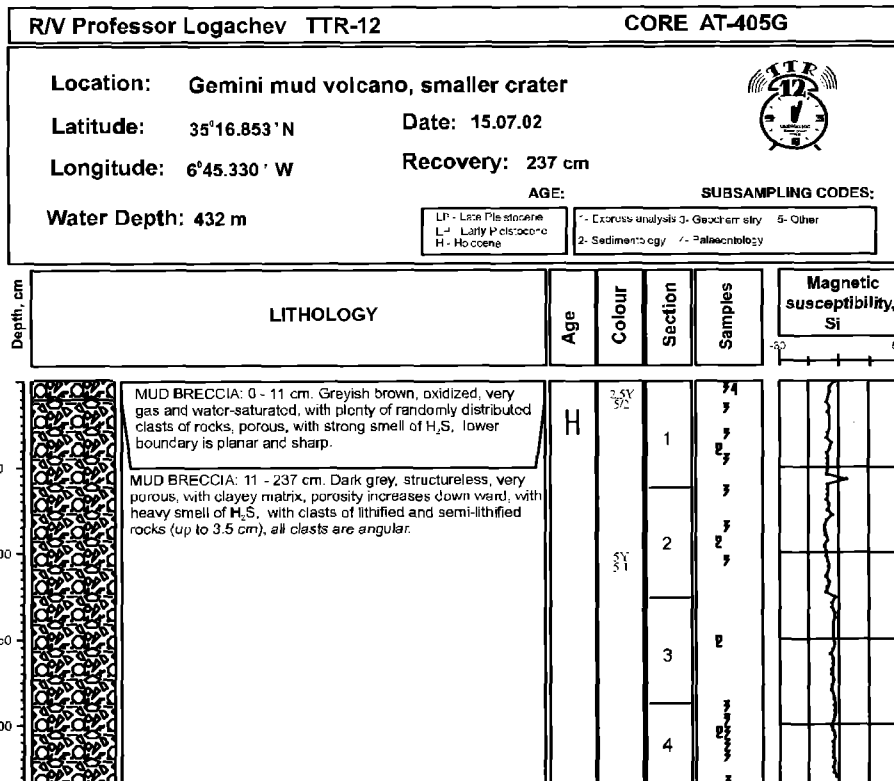


*Core log TTR-12-AT-403G*

## ANNEX I. CORE LOGS (LEG 2, the Gulf of Cadiz)

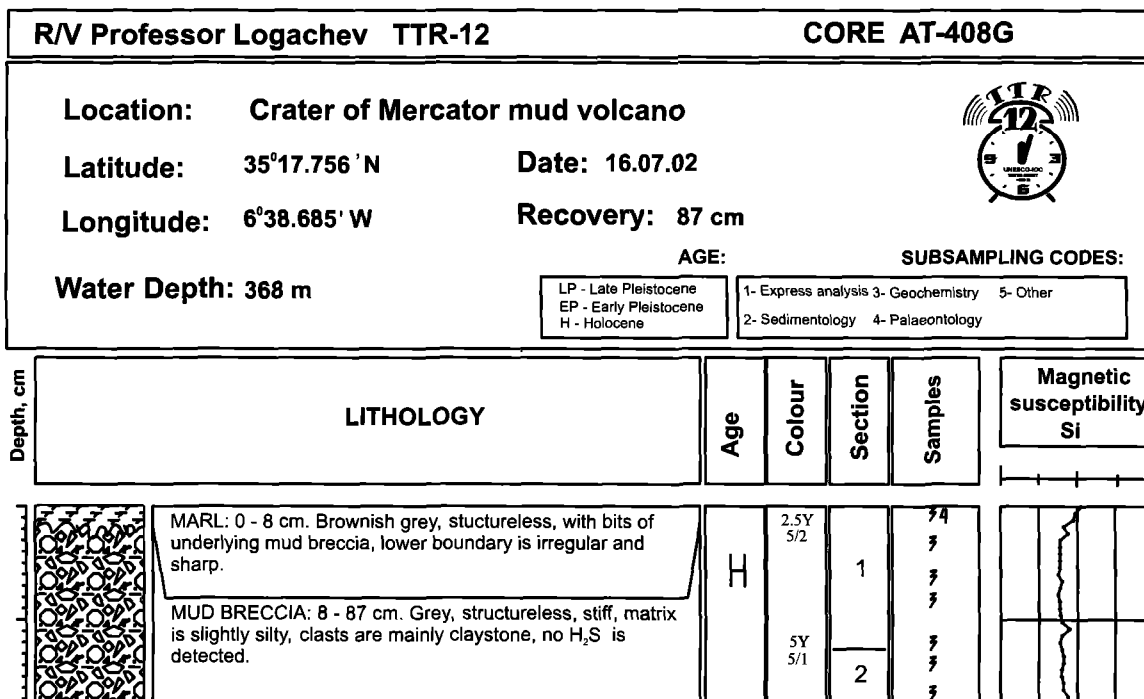


Core log TTR-12-AT-404G

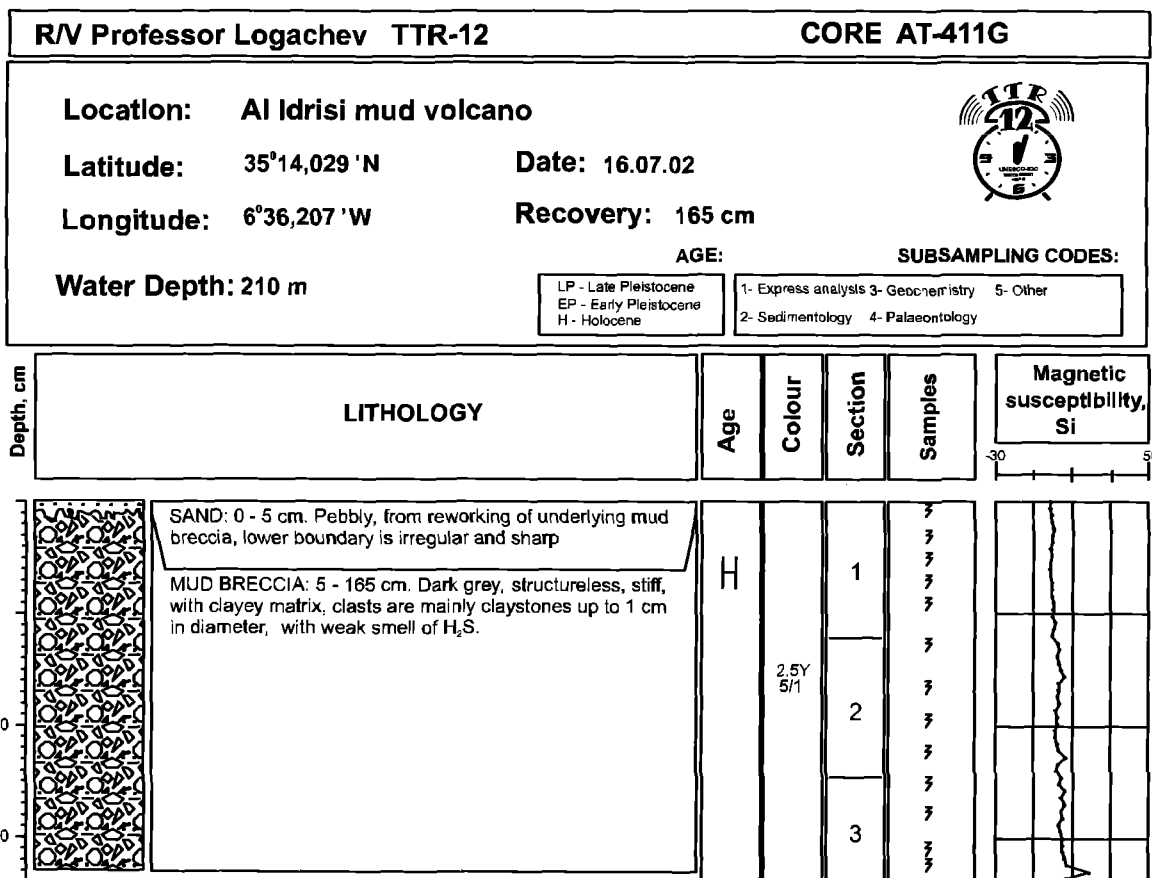


Core log TTR-12-AT-405G

## ANNEX I. CORE LOGS (LEG 2, the Gulf of Cadiz)

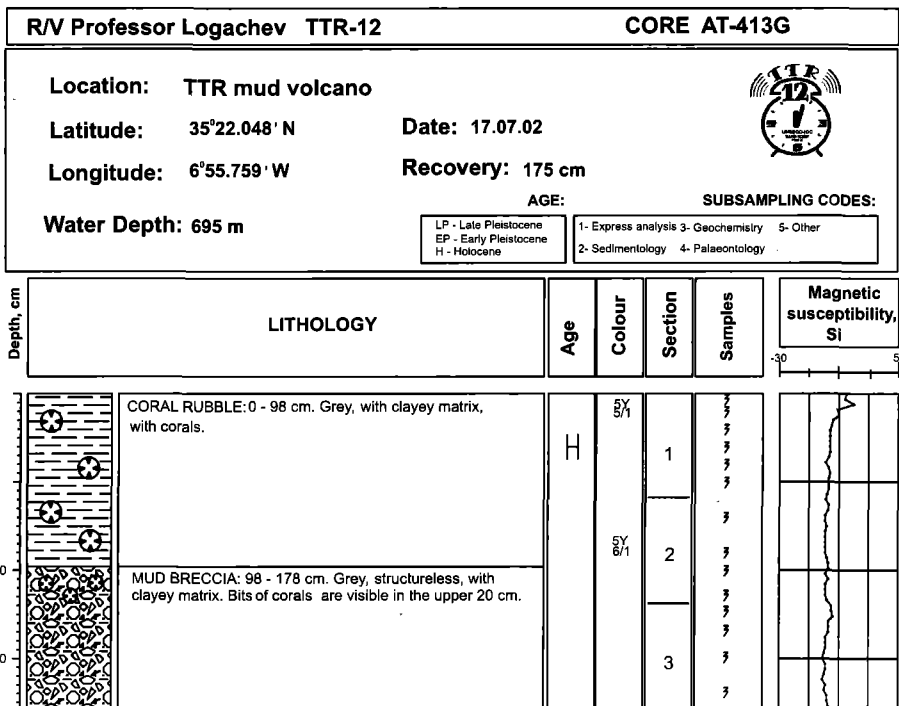


*Core log TTR-12-AT-408G*

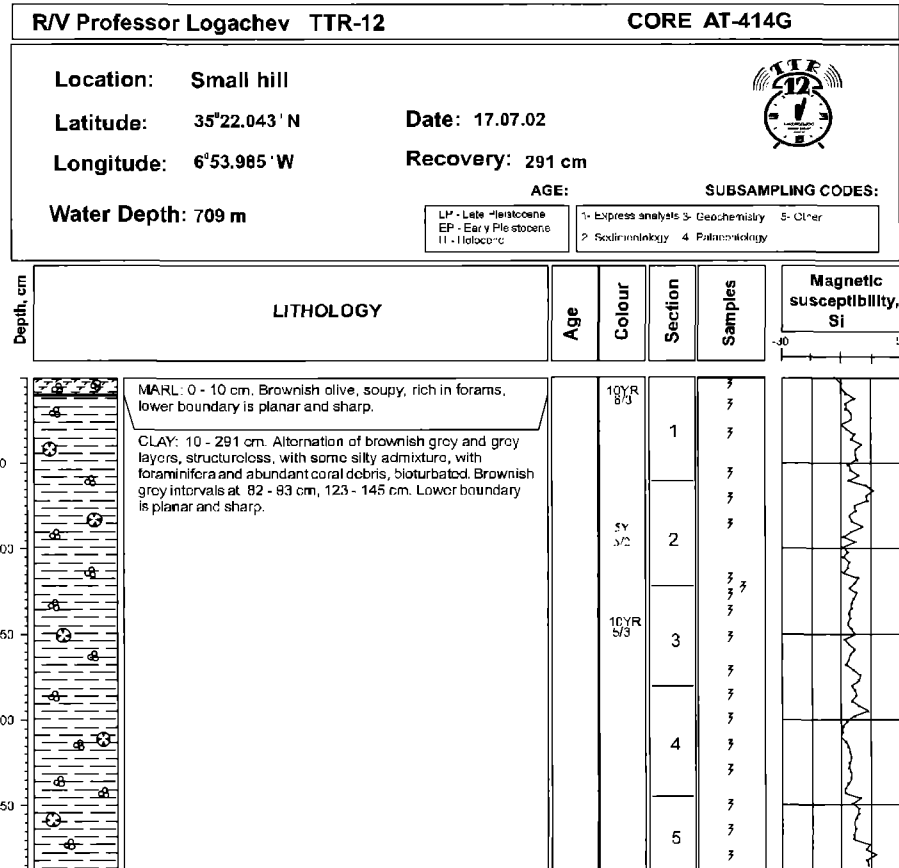


*Core log TTR-12-AT-411G*

## ANNEX I. CORE LOGS (LEG 2, the Gulf of Cadiz)




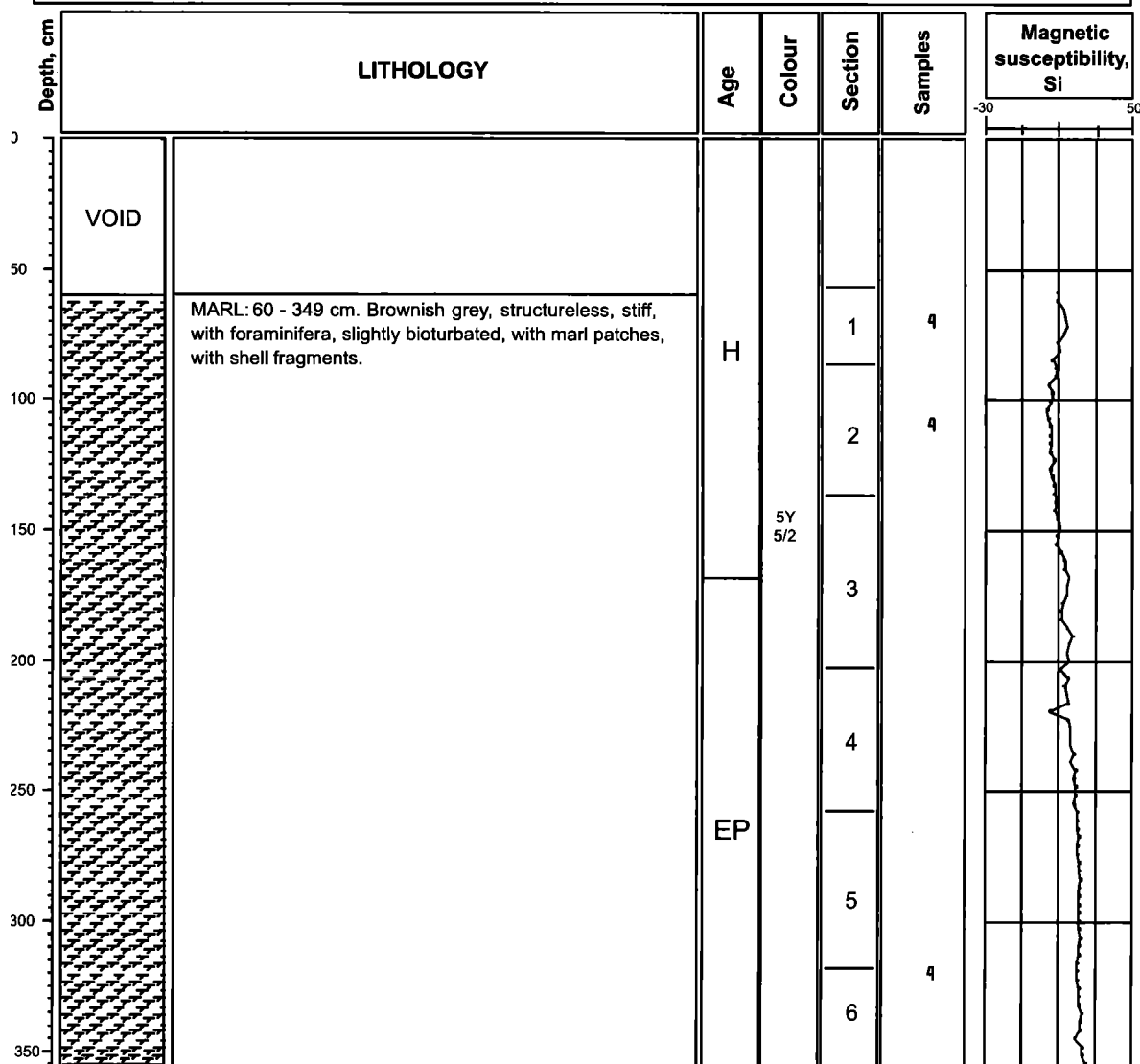
Core log TTR-12-AT-413G



Core log TTR-12-AT-414G

## ANNEX I. CORE LOGS (LEG 3, the Alboran Sea)


<b>R/V Professor Logachev TTR-12</b>		<b>CORE 279G</b>	
<div style="display: flex; justify-content: space-between; align-items: center;"> <div style="width: 60%;"> <p><b>Location: Pelagic core</b></p> <p><b>Latitude: 36°04.563' N</b></p> <p><b>Longitude: 4°59.844' W</b></p> <p><b>Date: 21.07.02</b></p> <p><b>Recovery: 289 cm</b></p> <p><b>Water Depth: 877 m</b></p> </div> <div style="width: 35%; text-align: right;">  </div> </div>			
		<b>AGE:</b>	<b>SUBSAMPLING CODES:</b>
		LP - Late Pleistocene EP - Early Pleistocene H - Holocene	1- Express analysis   3- Geochemistry   5- Other 2- Sedimentology   4- Palaeontology

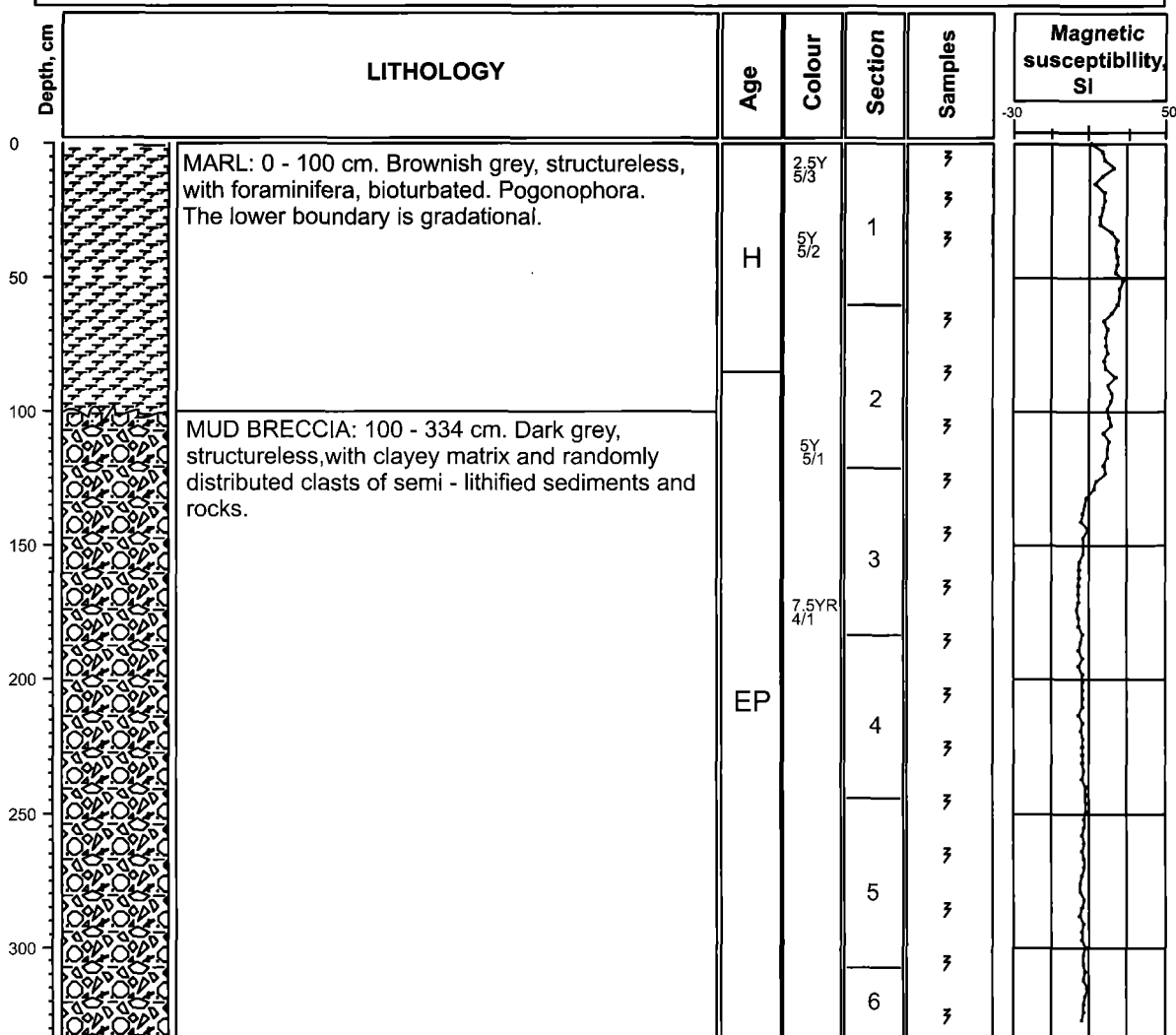


*Core log TTR-12-279G*




## ANNEX I. CORE LOGS (LEG 3, the Alboran Sea)

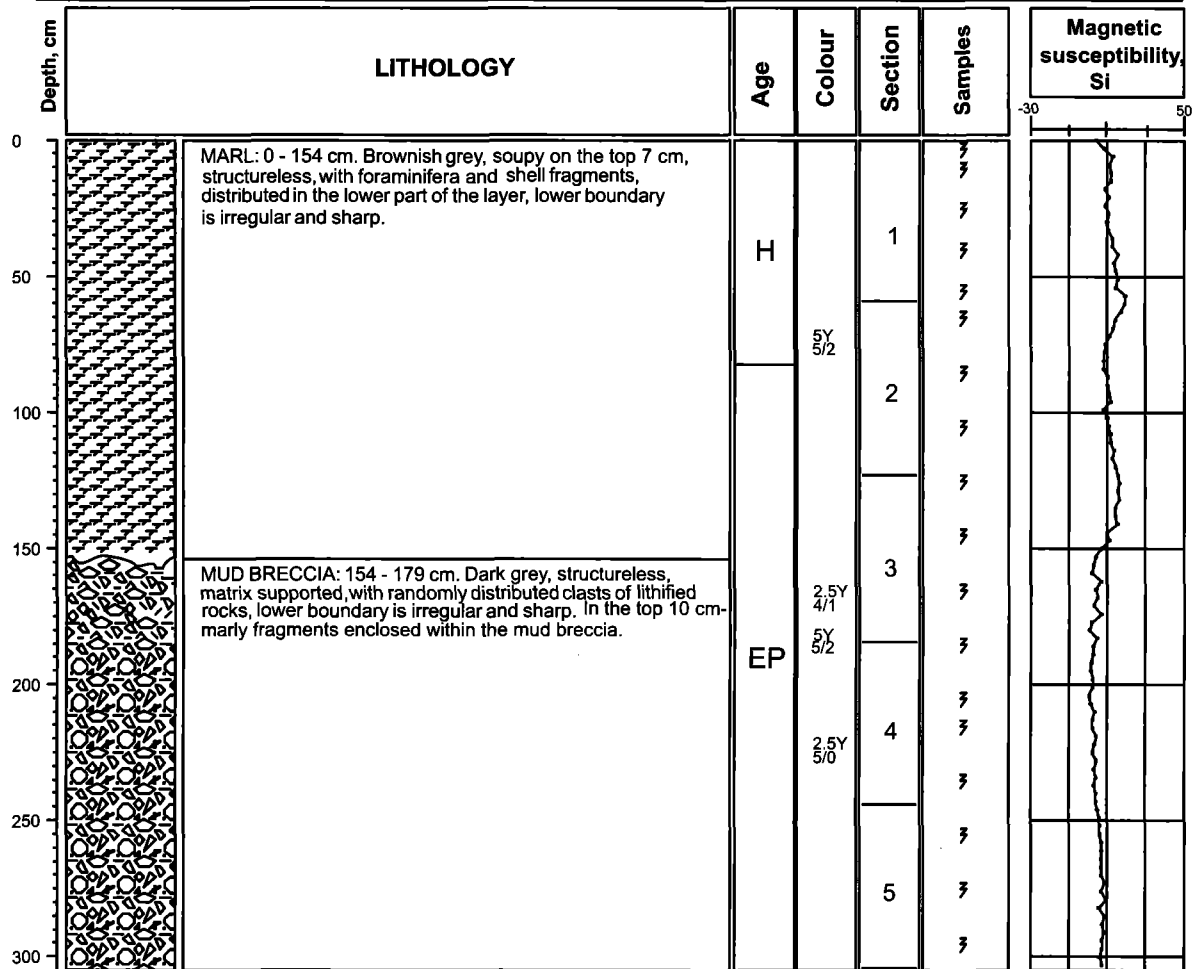
<b>R/V Professor Logachev TTR-12</b>		<b>CORE 280G</b>	
			
<b>Location:</b>	Top of Kalinin mud volcano		
<b>Latitude:</b>	36°02.828 'N	<b>Date:</b>	21.07.02
<b>Longitude:</b>	4°55.973' W	<b>Recovery:</b>	334 cm
<b>Water Depth:</b>	908 m	<b>AGE:</b>	<b>SUBSAMPLING CODES:</b>
	LP - Late Pleistocene EP - Early Pleistocene H - Holocene	1- Express analysis 3- Geochemistry 5- Other 2- Sedimentology 4- Palaeontology	



Core log TTR-12-280G


**ANNEX I. CORE LOGS (LEG 3, the Alboran Sea)**

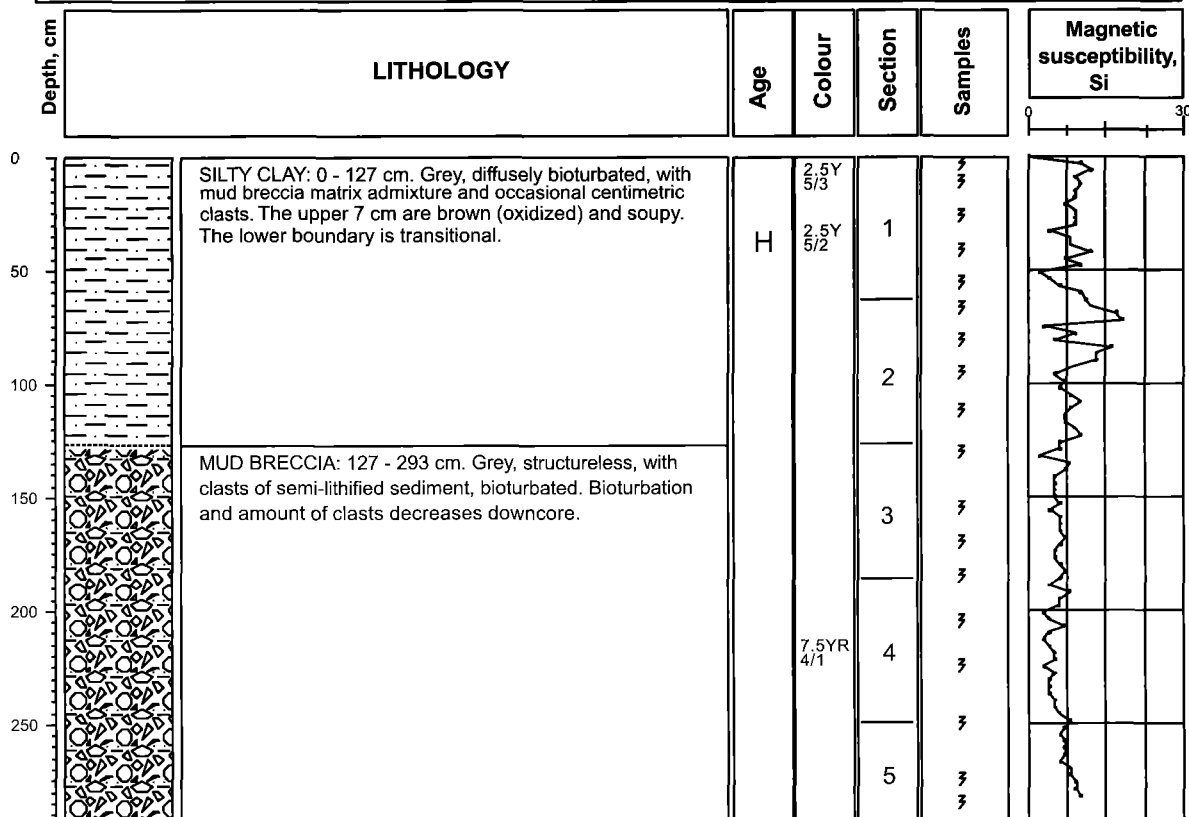
<b>R/V Professor Logachev TTR-12</b>		<b>CORE 281G</b>													
															
<b>Location:</b>	<b>Moat around Kalinin mud volcano</b>														
<b>Latitude:</b>	<b>36°02.715' N</b>	<b>Date:</b>	<b>21.07.02</b>												
<b>Longitude:</b>	<b>4°55.803' W</b>	<b>Recovery:</b>	<b>305 cm</b>												
<b>Water Depth:</b>	<b>924 m</b>	<b>AGE:</b>	<b>SUBSAMPLING CODES:</b>												
	<table border="1" style="font-size: small;"> <tr> <td>LP - Late Pleistocene</td> <td>1- Express analysis</td> <td>3- Geochemistry</td> <td>5- Other</td> </tr> <tr> <td>EP - Early Pleistocene</td> <td>2- Sedimentology</td> <td>4- Palaeontology</td> <td></td> </tr> <tr> <td>H - Holocene</td> <td></td> <td></td> <td></td> </tr> </table>	LP - Late Pleistocene	1- Express analysis	3- Geochemistry	5- Other	EP - Early Pleistocene	2- Sedimentology	4- Palaeontology		H - Holocene					
LP - Late Pleistocene	1- Express analysis	3- Geochemistry	5- Other												
EP - Early Pleistocene	2- Sedimentology	4- Palaeontology													
H - Holocene															



Core log TTR-12-281G

## ANNEX I. CORE LOGS (LEG 3, the Alboran Sea)

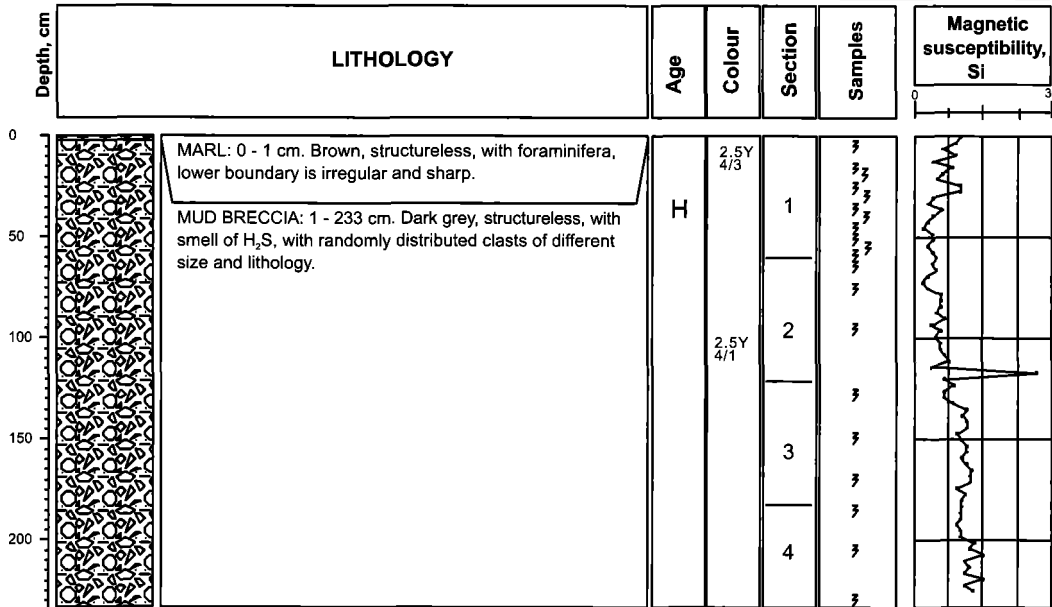
<b>R/V Professor Logachev TTR-12</b>		<b>CORE 282G</b>	
			
<b>Location:</b>	Top of Perejil mud volcano		
<b>Latitude:</b>	36°05.981' N	<b>Date:</b>	21.07.02
<b>Longitude:</b>	4°53.091' W	<b>Recovery:</b>	293 cm
<b>Water Depth:</b>	845 m	<b>AGE:</b>	<b>SUBSAMPLING CODES:</b>
	LP - Late Pleistocene EP - Early Pleistocene H - Holocene	1- Express analysis 2- Sedimentology	3- Geochemistry 4- Palaeontology 5- Other



*Core log TTR-12-282G*

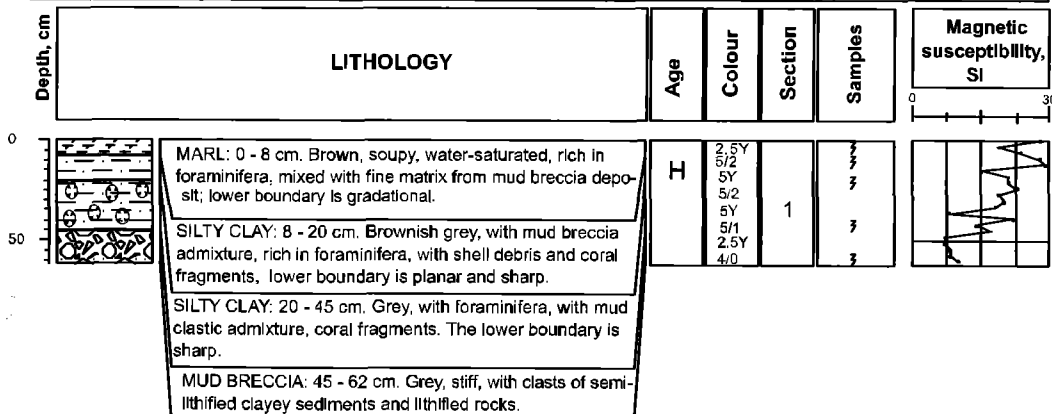
### ANNEX I. CORE LOGS (LEG 3, the Alboran Sea)

<b>R/V Professor Logachev TTR-12</b>	<b>CORE 283G</b>
<b>Location:</b> Top of Perejil mud volcano	
<b>Latitude:</b> 36°06.018' N	<b>Date:</b> 21.07.02
<b>Longitude:</b> 4°53.158' W	<b>Recovery:</b> 233 cm
<b>Water Depth:</b> 841 m	<b>AGE:</b> LP - Late Pleistocene EP - Early Pleistocene H - Holocene
	<b>SUBSAMPLING CODES:</b> 1- Express analysis   3- Geochemistry   5- Other 2- Sedimentology   4- Palaeontology



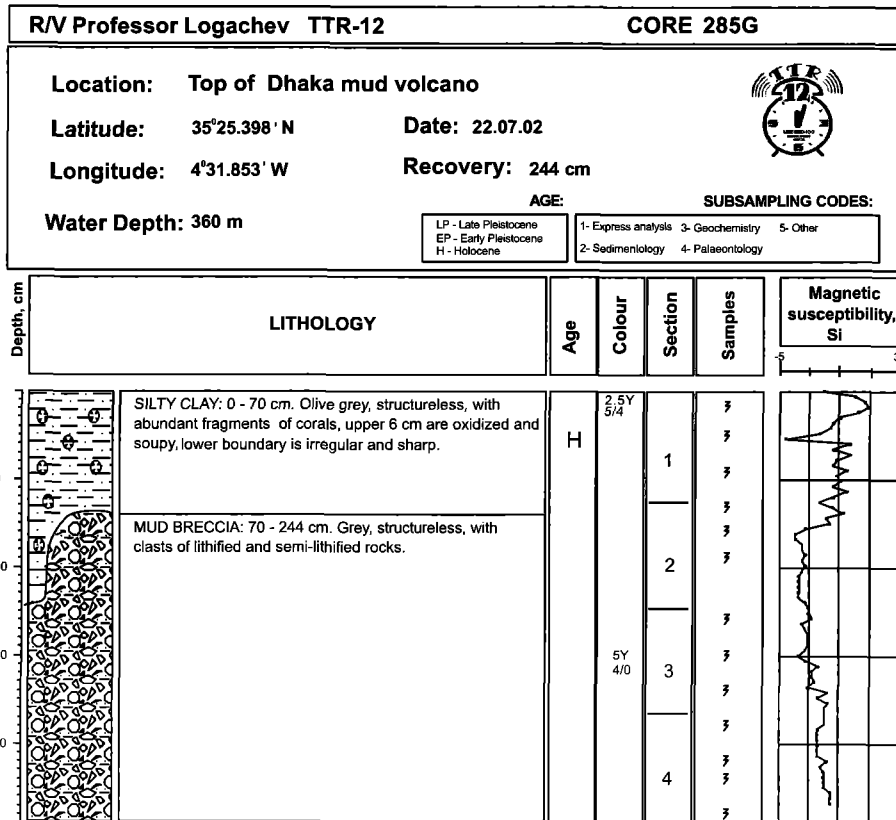
Core log TTR-12-283G

<b>R/V Professor Logachev TTR-12</b>	<b>CORE 284G</b>
<b>Location:</b> Top of Dhaka mud volcano	
<b>Latitude:</b> 35°25.400' N	<b>Date:</b> 22.07.02
<b>Longitude:</b> 4°31.854' W	<b>Recovery:</b> 62 cm
<b>Water Depth:</b> 360 m	<b>AGE:</b> LP - Late Pleistocene EP - Early Pleistocene H - Holocene
	<b>SUBSAMPLING CODES:</b> 1- Express analysis   3- Geochemistry   5- Other 2- Sedimentology   4- Palaeontology

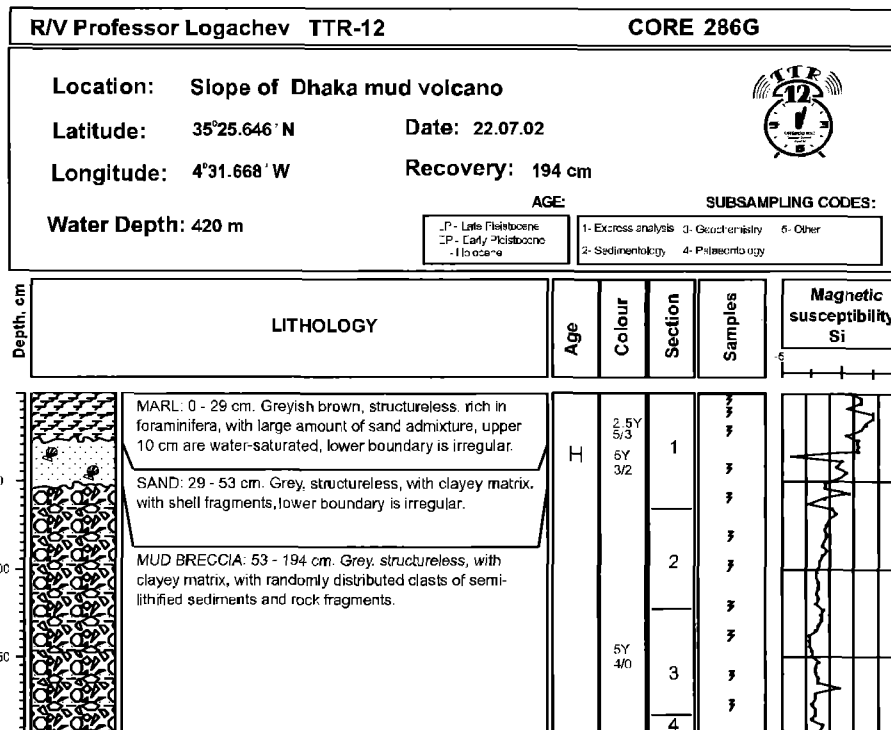


Core log TTR-12-284G

## ANNEX I. CORE LOGS (LEG 3, the Alboran Sea)

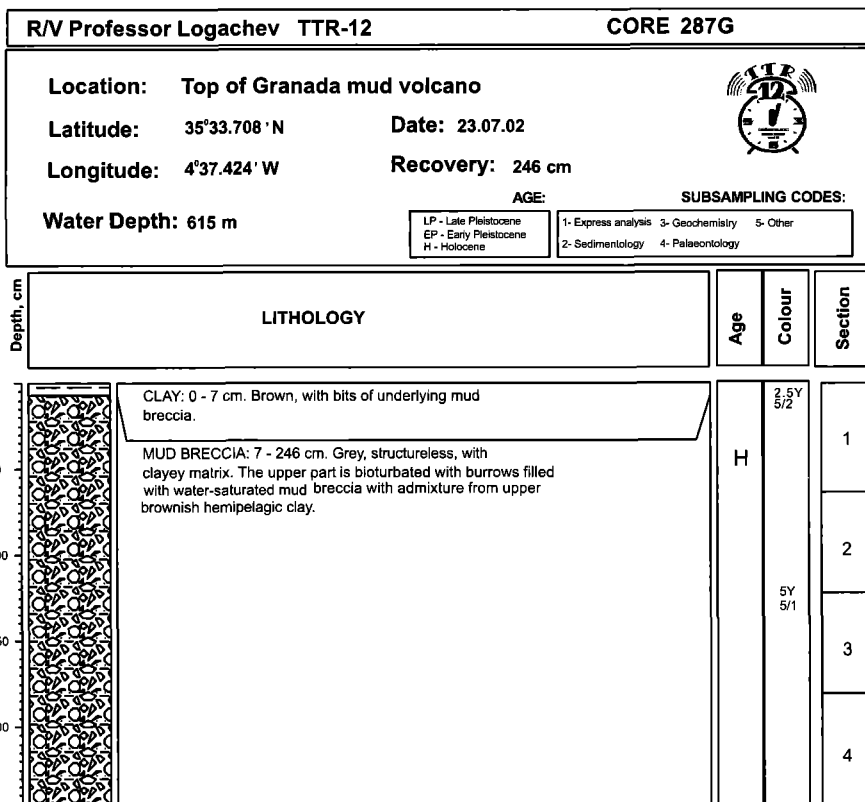


Core log TTR-12-285G

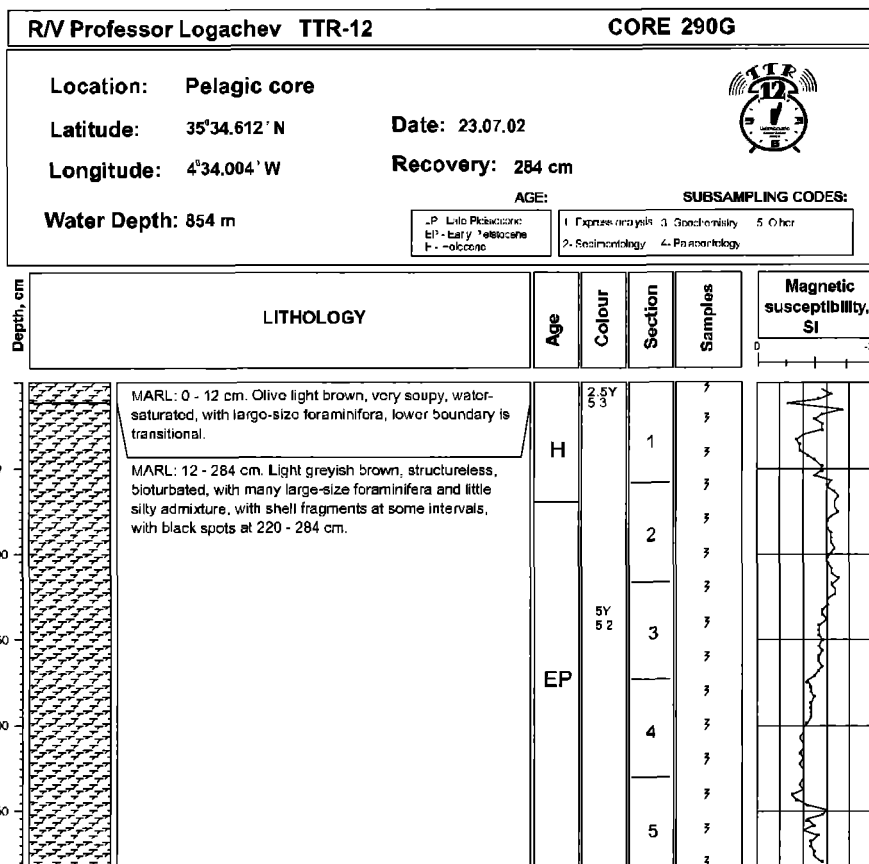


Core log TTR-12-286G

## ANNEX I. CORE LOGS (LEG 3, the Alboran Sea)




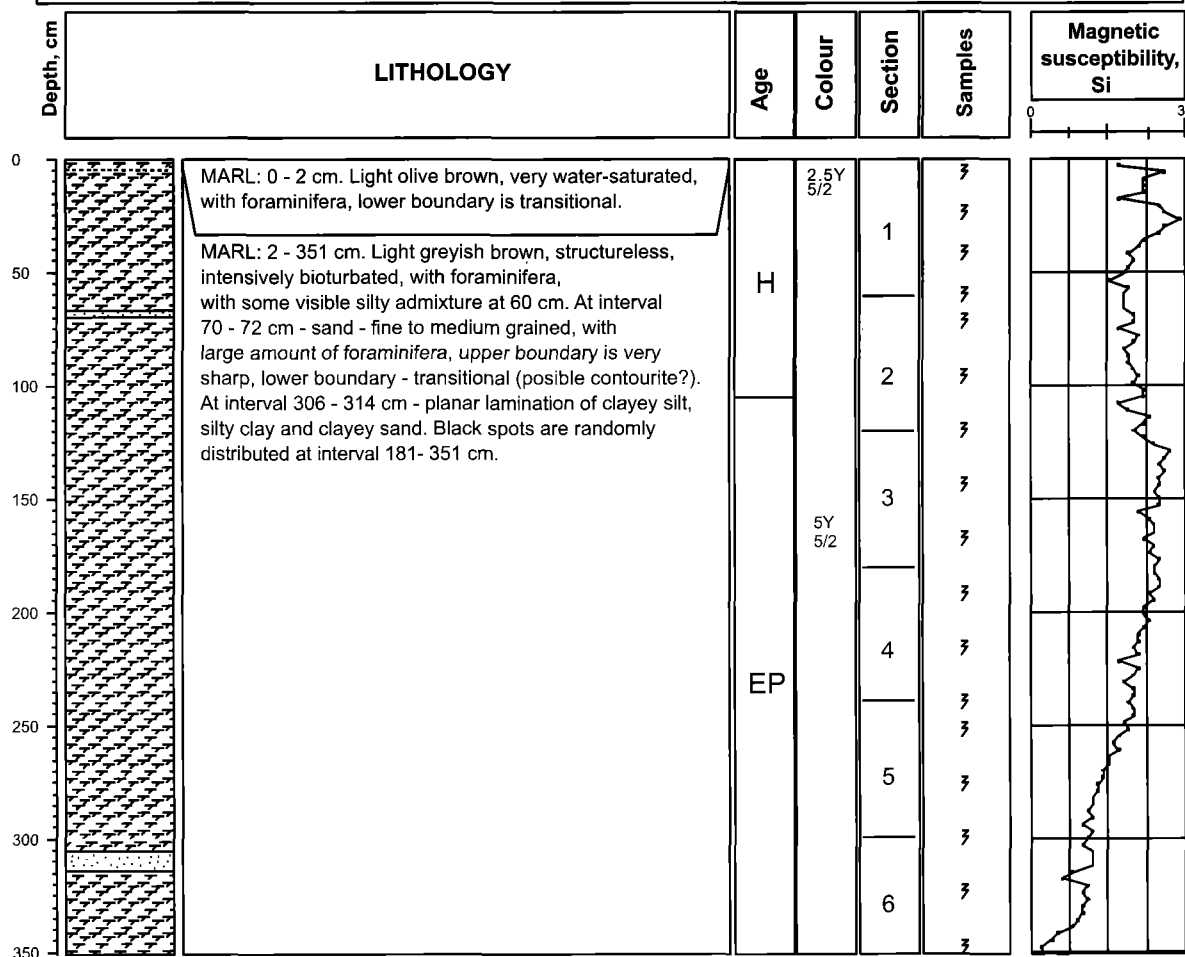
Core log TTR-12-287G



Core log TTR-12-290G


## ANNEX I. CORE LOGS (LEG 3, the Alboran Sea)

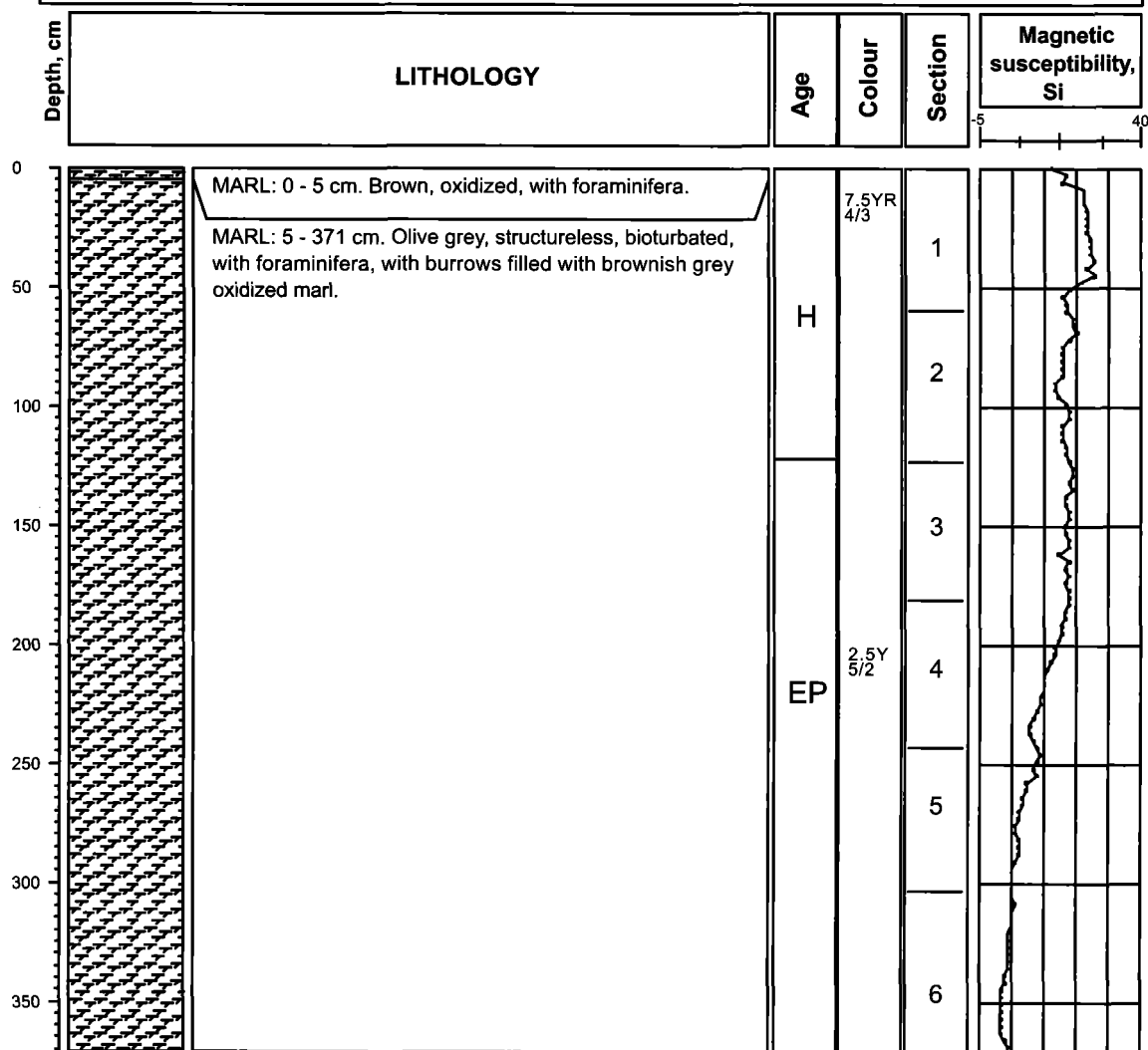
<b>R/V Professor Logachev TTR-12</b>		<b>CORE 291G</b>	
			
<b>Location:</b> Pelagic core	<b>Latitude:</b> 35°40.952' N		<b>Date:</b> 23.07.02
<b>Longitude:</b> 4°13.970' W	<b>Recovery:</b> 351 cm		
<b>Water Depth:</b> 1520 m	<b>AGE:</b>	<b>SUBSAMPLING CODES:</b>	
	LP - Late Pleistocene EP - Early Pleistocene H - Holocene	1- Express analysis 2- Sedimentology	3- Geochemistry 4- Palaeontology 5- Other



*Core log TTR-12-291G*

### ANNEX I. CORE LOGS (LEG 3, the Alboran Sea)


<b>R/V Professor Logachev TTR-12</b>		<b>CORE 292G</b>		
<b>Location:</b> Pelagic core				
<b>Latitude:</b> 35°53.850' N				<b>Date:</b> 23.07.02
<b>Longitude:</b> 3°36.330' W				<b>Recovery:</b> 371 cm
<b>Water Depth:</b> 1536 m	<b>AGE:</b>	<b>SUBSAMPLING CODES:</b>		
	LP - Late Pleistocene EP - Early Pleistocene H - Holocene	1- Express analysis 3- Geochemistry 5- Other 2- Sedimentology 4- Palaeontology		

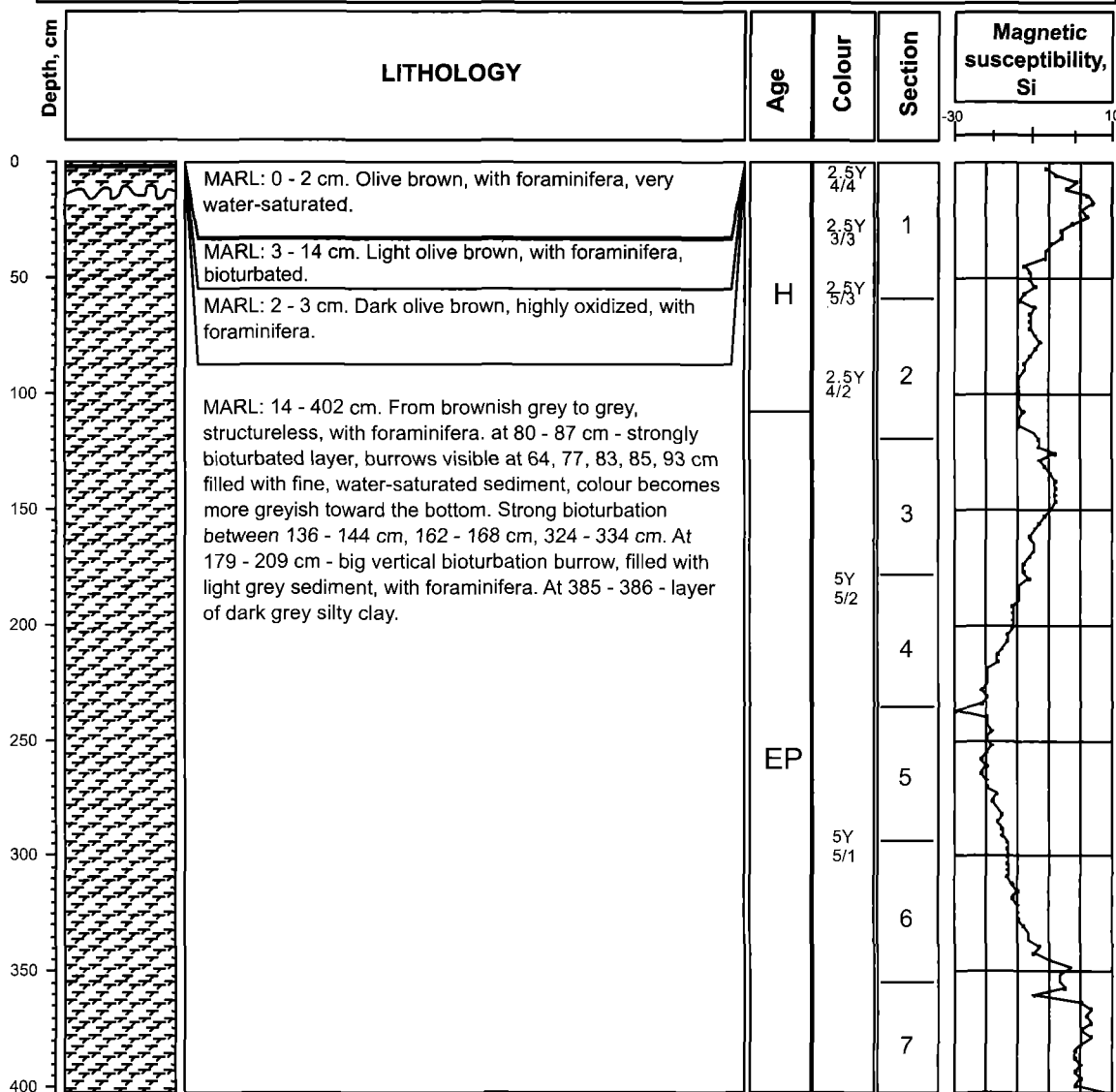


Core log TTR-12-292G



## ANNEX I. CORE LOGS (LEG 3, the Alboran Sea)

<b>R/V Professor Logachev TTR-12</b>		<b>CORE 293G</b>				
<b>Location: Pelagic core</b>						
<b>Latitude: 36°10.414' N</b>	<b>Date: 23.07.02</b>					
<b>Longitude: 2°45.280' W</b>	<b>Recovery: 402 cm</b>					
<b>Water Depth: 1840 m</b>		<table border="0" style="width: 100%;"> <tr> <td style="width: 50%;"><b>AGE:</b></td> <td style="width: 50%;"><b>SUBSAMPLING CODES:</b></td> </tr> <tr> <td>                 LP - Late Pleistocene                  EP - Early Pleistocene                  H - Holocene             </td> <td>                 1- Express analysis   3- Geochemistry   5- Other                  2- Sedimentology   4- Palaeontology             </td> </tr> </table>	<b>AGE:</b>	<b>SUBSAMPLING CODES:</b>	LP - Late Pleistocene EP - Early Pleistocene H - Holocene	1- Express analysis   3- Geochemistry   5- Other 2- Sedimentology   4- Palaeontology
<b>AGE:</b>	<b>SUBSAMPLING CODES:</b>					
LP - Late Pleistocene EP - Early Pleistocene H - Holocene	1- Express analysis   3- Geochemistry   5- Other 2- Sedimentology   4- Palaeontology					



Core log TTR-12-293G

## ANNEX I. CORE LOGS (LEG 5, the Azores Margin)

### AT 421D

Cruise: TTR 12-5 Vessel: Prof. Logachev  
Navigation System: GPS Area: Atlantis seamount

Dredge TV-Grab x

Date: 24-Aug-02

Time		Initial	End
Start Descent			8.40
Sampling		8.49	9.53
Deck Arrival			10.05

Water Depth (m):		Initial	End
Wire		614	555
Probe		614	555

Coordinates on bottom		Initial	End
Lat.	34° 00,355'		34° 00,46'
Long.	30° 10,350'		30° 10,36'



**Description:**  
Dredge collected several rock fragments - silicified basalts and carbonate crusts. Also white sponge fragments. Rocks divided into three groups.

### AT 422 GR

Cruise: TTR 12-5 Vessel: Prof. Logachev  
Navigation System: GPS Area: Atlantis seamount

Dredge TV-Grab x

Date: 24-Aug-02

Time		Initial	End
Start Descent			19.00
Sampling			19.43
Deck Arrival			19.57

Water Depth (m):		Initial	End
Wire			365
Probe			375

Coordinates on bottom		Initial	End
Lat.	34° 05,831'		
Long.	30° 11,719'		



**Description:**  
Carbonate crust. Three small fragments, largest being 8x5x3 cm. Rock description very similar to sample AT 421D / 1. The only difference is that these fragments contain carbonate cement around randomly scattered silicified basalt clasts (medium size: 3-5 mm). Individual small quartz grains are visible.

### AT 425 GR

Cruise: TTR 12-5 Vessel: Prof. Logachev  
Navigation System: GPS Area: Lucky Strike Segment

Dredge TV-Grab X

Date: 26-Aug-02

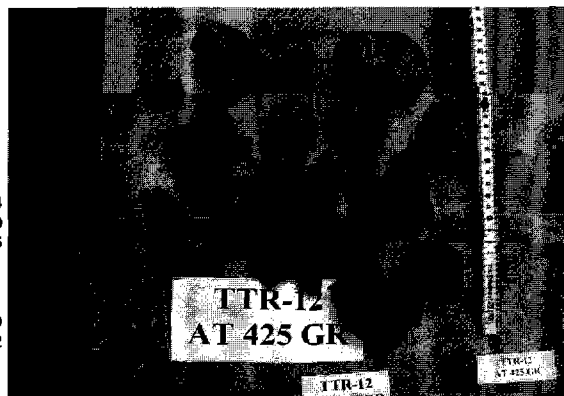
Time		Initial	End
Start Descent			11.34
Sampling			12.50
Deck Arrival			14.15

Water Depth (m):		Initial	End
Wire			2100
Probe			2072

Coordinates on bottom		Initial	End
Lat.	37° 20,265'		
Long.	32° 16,437'		

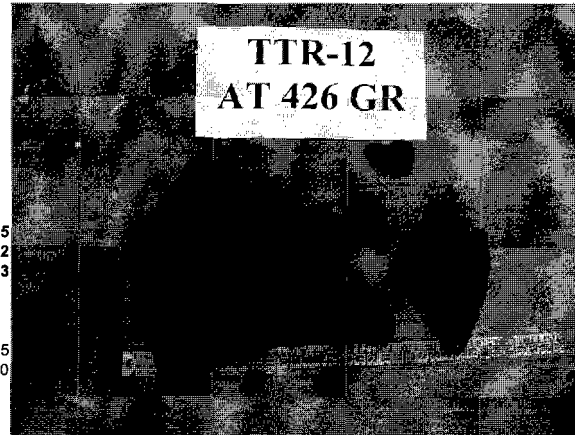


**Description:**  
Basalts - more than 30 small fragments the largest one being 8x6x4 cm and large amount of fresh volcanic glass. Avesicular basalt (occupying less than 1% of volume, rounded, with average size 1-2 mm). Very fresh. Almost all of the fragments are covered by a very thin, up to 1 mm, layer of glass; some of the glass is very fresh (black colour and very vitreous aspect) and some is completely palagonitised (opaque and brown colour). Microcrystalline matrix. Completely aphanitic in texture, with no phenocrysts; locally alternated. Grab video record shows that these fragments came from large blocks of round pillows and tubular basaltic lavas.

## ANNEX I. CORE LOGS (LEG 5, the Azores Margin)

### AT 426 GR

Cruise: **TTR 12-5** Vessel: **Prof. Logachev**  
 Navigation System: **GPS** Area: **Lucky Strike Segment**  
 Dredge  
 TV-Grab X Time  
 Date: **26-Aug-02** Start Descent Initial End  
 Sampling 14.55  
 Deck Arrival 15.52  
 16.53  
 Water Depth (m):  
 Initial End  
 Coordinates on bottom Wire 1765  
 Probe 1780  
 Initial End  
 Lat. 37° 18,922'  
 Long. 32° 16,000'

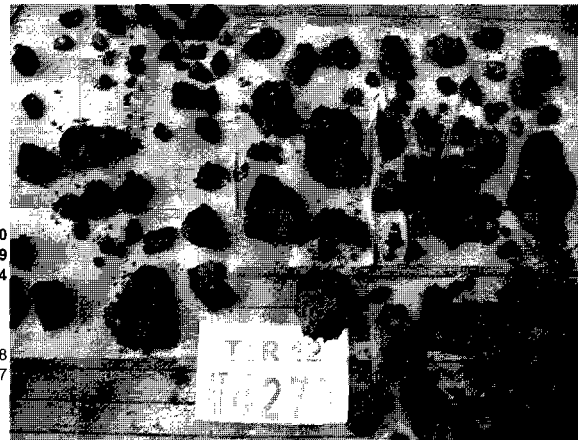


#### Description:

5 small fragments of a phyric vesicular basalt, the larger being 15x11x9 cm. The vesicles are round in shape, and distributed in an heterogeneous way in the bigger block – in some areas they make about 20% in volume but in the internal part of the fragment they could reach about 40% in volume (in this area, the diameter of the vesicles is also higher). The medium size is 1-2 mm. Plagioclase and olivine make the phenocryst assemblage. Plagioclase dominates, making 15% of the rock, subeuhedric to euhedric in habit (the last correspond to the largest crystals), very fresh, transparent (one crystal having a yellow brownish inclusion?) with seriate dimensions (< 1mm to 8 mm). The olivine has green colour, transparent, fresh and subeuhedric with elongate crystals, with 3-4 mm long. They make about 5% in volume. Glassy matrix; two mm outer layer of black fresh volcanic glass. The matrix is locally altered, with zones having brown to dark brown alteration materials (clay minerals?). The bigger block seems to be a little different from the rest of the fragments, in terms of crystals and vesicles percentage and distribution.

### AT 427 GR

Cruise: **TTR 12-5** Vessel: **Prof. Logachev**  
 Navigation System: **GPS** Area: **Lucky Strike Segment**  
 Dredge  
 TV-Grab X Time  
 Date: **26-Aug-02** Start Descent Initial End  
 Sampling 17.30  
 Deck Arrival 18.29  
 19.34  
 Water Depth (m):  
 Initial End  
 Coordinates on bottom Wire 1748  
 Probe 1747  
 Initial End  
 Lat. 37° 17,502'  
 Long. 32° 16,808'

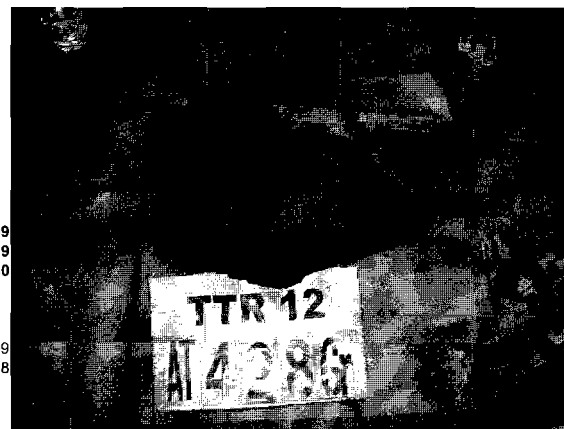


#### Description:

Large amount of basalt fragments from the lava lake (the TV grab was almost full). The basalts are very rich in volcanic glass, in the external surface; inside they are completely aphyric and avescicular. The most significant characteristic of these rocks is the extreme abundance of volcanic glass (more than 70%) which separates easily from the microcrystalline matrix of the basalt. The glass pieces have various dimensions and can be up to 30 cm long and 10 cm thick. They produce very sharp and fragile pieces and are very fresh (no palagonite visible). The external surfaces of the fragments are very irregular with ropy style. Sometimes opalescent colours are visible in the smooth rounded surfaces of the glass. The rock matrix is aphyric and avescicular – the holes seen in some fragments are not true vesicles, but small cavities, which are distributed very heterogeneously. The matrix is also mostly fresh with few brown patches of alteration.

### AT 428 GR

Cruise: **TTR 12-5** Vessel: **Prof. Logachev**  
 Navigation System: **GPS** Area: **Lucky Strike Segment**  
 Dredge  
 TV-Grab X Time  
 Date: **26-Aug-02** Start Descent Initial End  
 Sampling 20.09  
 Deck Arrival 21.19  
 22.30  
 Water Depth (m):  
 Initial End  
 Coordinates on bottom Wire 1709  
 Probe 1718  
 Initial End  
 Lat. 37° 17,289'  
 Long. 32° 16,522'



#### Description:

Large fragment (54x30x12 cm) of a hydrothermal slab. The fragment has a thin orange outer coating (sediment rich in sulfides/oxides?) some of which is soft but the majority is attached to the rock and can not be separated. Basaltic matrix is clearly visible, with a glassy texture, very vesicular and with plagioclase phenocrysts. There is evidence that the rock has been significantly altered by hydrothermal fluids rich in silica.

Plagioclase is not altered, anedric to sub euhedric (the biggest crystals are more euhedric in habit), and occupies a volume less than 10% of the sample volume; Their size can be up to 8 mm long. Some internal alteration is seen producing orange to brownish colours (could be due to palagonitisation of the glassy matrix).

## ANNEX I. CORE LOGS (LEG 5, the Azores Margin)

### AT 429D

Cruise: **TTR 12-5** Vessel: **Prof. Logachev**  
 Navigation System: **GPS** Area: **Lucky Strike Segment**  
 Dredge **X**  
 TV-Grab

Date: **26-Aug-02**

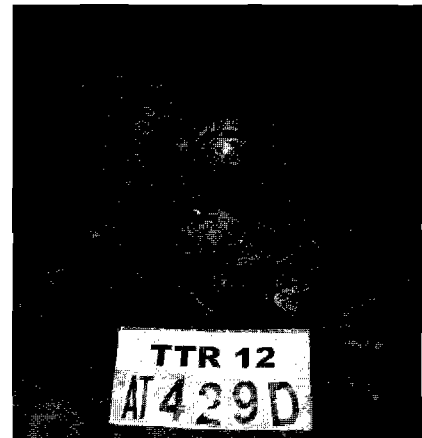
Time		Initial	End
Start Descent			23.31
Sampling		0.09	0.39
Deck Arrival			1.09

Water Depth (m):		Initial	End
Wire			
Probe		1990	1846

Coordinates on bottom			
	Initial	End	
Lat.	37° 16,850'	37° 16,795'	
Long.	32° 13,901'	32° 13,684'	



**Description:**

Samples collected occupied about 1/6 of the dredge. About 90 of the volume was made up of carbonate crust material, and the other 10% of a large amount of coral fragments and a small piece of a basaltic rock.

### AT 430 GR

Cruise: **TTR 12-5** Vessel: **Prof. Logachev**  
 Navigation System: **GPS** Area: **Lucky Strike Segment**  
 Dredge  
 TV-Grab **X**

Date: **27-Aug-02**

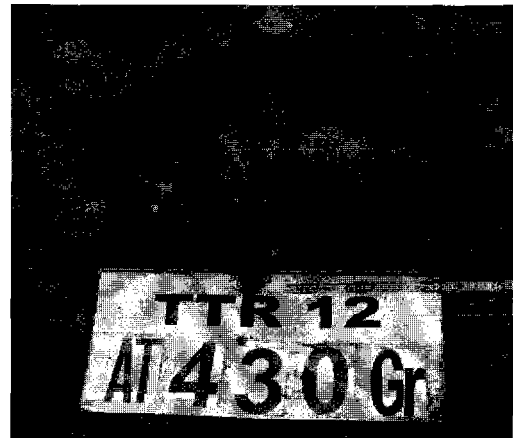
Time		Initial	End
Start Descent			15.24
Sampling			16.24
Deck Arrival			18.10

Water Depth (m):		Initial	End
Wire			1916
Probe			1916

Coordinates on bottom			
	Initial	End	
Lat.	37° 16,871'		
Long.	32° 14,579'		



**Description:**

Large pillow-lava block – 50x45x40 cm, plus two smaller blocks (30x20x15 and 15x10x10 cm). All of these blocks were fragmented. The bigger block has broken in concentric layers with thickness of 2-3 cm. The freshest part of the sample is in the innermost part. Plagioclase is the dominant phenocryst of the basalt and has uneven distribution with average dimensions around 4 mm (max up to 1,5 cm); subeuhedric to euhedric, the majority fresh, transparent aspect, but some are very altered giving a more opaque aspect, with orange/brownish colours. In the rest of the rock, plagioclase is substantially more altered. Olivine is the other phenocryst, small percentage (<1%), anedric, vitreous aspect and dimensions between 2-3 mm. Outside this unaltered area no olivine crystals were seen.

Cryptocrystalline matrix, with vesicles, occupying less than 5% of volume, and generally with rounded shapes with diameter around 1mm. In some fragments there is a regular distribution of the vesicles, with the bigger ones (2-3 mm) located in the inner parts. External outer layer contains Mn deposits and sometimes a 2 mm thick palagonite layer resulting from the volcanic glass alteration is observed. Few radial fractures are seen.

### AT 431D

Cruise: **TTR 12-5** Vessel: **Prof. Logachev**  
 Navigation System: **GPS** Area: **Lucky Strike Segment**  
 Dredge **X**  
 TV-Grab

Date: **27-Aug-02**

Time		Initial	End
Start Descent			20.13
Sampling		20.47	
Deck Arrival			22.33

Water Depth (m):		Initial	End
Wire		1791	1730
Probe		1908	1734

Coordinates on bottom			
	Initial	End	
Lat.	37° 16,438'	37° 16,358'	
Long.	32° 15,166'	32° 15,791'	



**Description:**

About 10 small fragments of basaltic lavas, the largest one being 18x13x11 cm.

## ANNEX I. CORE LOGS (LEG 5, the Azores Margin)

### AT 432 D

Cruise: **TTR 12-5** Vessel: **Prof. Logachev**  
 Navigation System: **GPS** Area: **Lucky Strike Segment**  
 Dredge **X**  
 TV-Grab  
 Date: **28-Aug-02**

Time		Initial	End
Start Descent			15.46
Sampling		16.22	17.13
Deck Arrival			17.46

Water Depth (m):		Initial	End
Wire			
Probe		2319	2205

Coordinates on bottom

	Initial	End
Lat.	37° 12,033'	37° 12,179'
Long.	32° 17,524'	32° 17,918'



**Description:**

One block of plagioclase cumulate (33x25x25 cm). Large, perfectly euhedral in habit megacrysts of plagioclase distributed all over the sample. Seriate dimensions, from 2 mm to 3 cm. The smaller ones are preferentially subeuhedral. Plagioclase makes more than 80% of the rock volume. The majority of the plagioclase megacrysts is slightly altered (yellow shadows), but some, being completely fresh, are transparent (others opaque aspect). The crystals near the external surface are clearly more altered.

External surface is very irregular due to the presence of the superficial plagioclase megacrysts, which are covered by Mn oxides; this material covers almost the entire surface, is completely black and bright and can be easily detached from the surface; it is very soft and disaggregated. Locally volcanic glass is fresh, dark and has vitreous lustre, being 1-3 mm thick, but the most part is already altered to palagonite. The palagonite is very soft and can be easily taken from the external surface (like an unconsolidated mud).

Glassy matrix, avascular, very fresh and hard. The olivine is also present as a phenocryst and as plagioclase inclusions (in the larger ones); small crystals, 2-4 mm, commonly in the border of the plagioclase megacrysts, and others inside of them. Fresh, vitreous, subeuhedral, green colour and often transparent aspect.

### AT 433 GR

Cruise: **TTR 12-5** Vessel: **Prof. Logachev**  
 Navigation System: **GPS** Area: **Lucky Strike Segment**  
 Dredge **X**  
 TV-Grab  
 Date: **28-Aug-02**

Time		Initial	End
Start Descent			23.42
Sampling			2.18
Deck Arrival			3.34

Water Depth (m):		Initial	End
Wire			1955
Probe			1957

Coordinates on bottom

	Initial	End
Lat.	37° 15,063'	
Long.	32° 17,929'	



**Description:**

Large amount of basalt fragments, the larger being 16x8x8 cm, very rich in volcanic glass. One spectacular fragment having a polychaete worm preserved by a very thin layer of volcanic glass, inside an inner cavity of the lava. The most typical feature of these fragments is the huge amount of volcanic glass, that could have 1 cm in thickness. It is very fresh, opalescence shadows in the round smooth surfaces, very hard and giving sharp corners, but easily separated from the aphyric basalt groundmass. Very irregular external surfaces, some fragments having in-folds which creates inner cavities (> 3 cm in the larger dimension). The small glass fragments make almost half of the total rock sampled. The matrix is completely aphyric, with no phenocrysts and almost avascular; the vesicles are visible, sparsely distributed (< 1% in volume, having irregular shapes and dimensions, 1-5 mm). The matrix is microcrystalline in the inner most parts of the fragments, becoming glassy to the external surface. The matrix is sometimes altered, giving orange/brownish colours, and it is more intense in the inner parts (?). Some fragments, specially the specimen AT 433 GR/A. The fragment, also contains lithified sediment that could have been hardened by high temperature lavas. Few small patches of palagonite.

## ANNEX I. CORE LOGS (LEG 5, the Azores Margin)

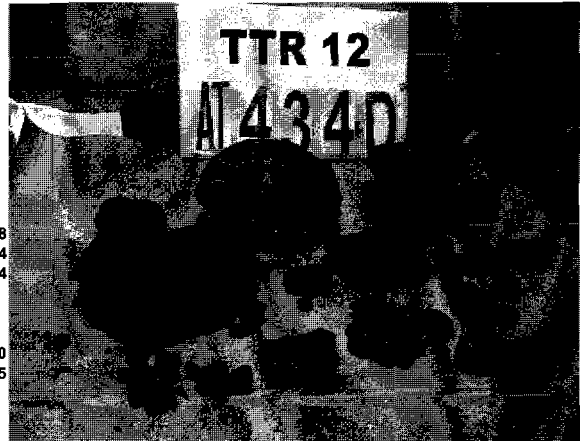
### AT 434D

Cruise: TTR 12-5 Vessel: Prof. Logachev  
Navigation System: GPS Area: Lucky Strike Segment  
Dredge X  
TV-Grab  
Date: 29-Aug-02  
Coordinates on bottom  
Lat. 37° 14,497' 37° 14,905'  
Long. 32° 16,586' 32° 16,775'

Time		Initial	End
Start Descent	-----		3.58
Sampling	-----	4.29	5.34
Deck Arrival	-----		6.04

Water Depth (m):		Initial	End
Wire		2015	1940
Probe		2030	1945



**Description:**

More than 20 fragments of aphyric basalt, seriate dimensions ranging from 1 cm3 to 24x17x12 (the largest one). Pillow-lava fragments, rounded in shape and with internal concentric zonation, and sheet-flow pieces, having external smooth surfaces (larger fragment has a ropy surface). Glass is common, but is always altered; medium thickness around 1-2 mm, brown coloured, palagonitised. The external surface is rich in Mn deposits, black colour, microgranular. This thin Mn layer covers some polychaete worm fragments present in the samples. Two fragments having small pieces of hard, cream coloured, hardened sediment. The matrix is microcrystalline to cryptocrystalline, massive in aspect, having different degrees of alteration. Predominantly aphyric rock fragments; when seen, little amount of plagioclase phenocrysts (< 1%), fresh, transparent, anedric to subeuhedric. Avesicular basalt. Fragment of an old coral attached to one lava piece.

### AT 435 D

Cruise: TTR 12-5 Vessel: Prof. Logachev  
Navigation System: GPS Area: Lucky Strike Segment  
Dredge X  
TV-Grab  
Date: 29-Aug-02  
Coordinates on bottom  
Lat. 37° 16,300' 37° 16,380'  
Long. 32° 17,068' 32° 16,540'

Time		Initial	End
Start Descent	-----		6.41
Sampling	-----	7.05	7.52
Deck Arrival	-----		8.21

Water Depth (m):		Initial	End
Wire		1770	1752
Probe		1780	1720



**Description:**

Aphyric, avescicular glass-rich basalt. Large amount of fragments, seriate dimensions, the bigger fragment being 36x20x20. Basalt fragments very similar to AT 433 GR, the only difference is in the degree of alteration which is higher in these samples. Large amount of volcanic glass presents in almost all fragments, 1-5 mm thick; locally fresh, completely black, opaque aspect, hard and with sharp corners; normally palagonitised with a general brown colour to the external surface (in some 3-4 fragments, the glass is completely altered – these may be from an older volcanic area). A great shape variety, rounded to tabular fragments. In-folds visible, ropy external surface (some more smoother appearance). Different type of matrix, microcrystalline to cryptocrystalline; near the volcanic glass, more glassy matrix. This basaltic matrix is relatively fresh, but locally seen white dusty patches of clay material (?). Fragments hard to break.

The percentage of phenocrysts is < 1%, plagioclase crystals (2-3 mm), subeuhedric, sparsely distributed through the fragments; also seen one greenish crystal of olivine, 2 mm long (just in one fragment). The majority of fragments do not have any phenocryst. Fragments with internal massive aspect, very low percentage of vesicles (<3%) of different shape and dimension.

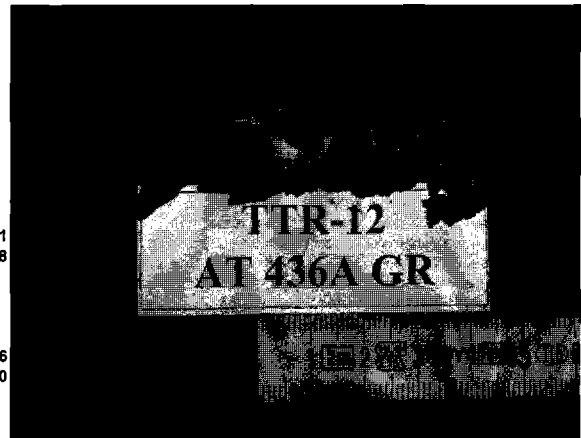
### AT 436A GR

Cruise: TTR 12-5 Vessel: Prof. Logachev  
Navigation System: GPS Area: Lucky Strike Segment  
Dredge X  
TV-Grab  
Date: 29-Aug-02  
Coordinates on bottom  
Lat. 37° 18,126'  
Long. 32° 18,000'

Time		Initial	End
Start Descent	-----		9.21
Sampling	-----		10.18
Deck Arrival	-----		

Water Depth (m):		Initial	End
Wire			1586
Probe			1580



**Description:**

Three very small pieces of volcanic glass (the largest, 4x1x1 cm), with abundant plagioclase phenocrysts in the interior, the larger ones being up to 1 cm long. The phenocrysts are subeuhedric and slightly altered. Volcanic glass is generally fresh with little amount of palagonite. Mn oxides on the external surface.

## ANNEX I. CORE LOGS (LEG 5, the Azores Margin)

### AT 436B GR

Cruise: **TTR 12-5** Vessel: **Prof. Logachev**  
 Navigation System: **GPS** Area: **Lucky Strike Segment**  
 Dredge  
 TV-Grab **X** Time  
 Date: **29-Aug-02** Start Descent Initial End 11.34  
 Sampling 13.08  
 Deck Arrival 14.11  
 Water Depth (m):  
 Initial End  
 Coordinates on bottom Wire 1706  
 Probe 1709  
 Initial End  
 Lat. 37° 17,300'  
 Long. 32° 16,563'



**Description:**

Different fragments of hydrothermal slab - more than 30, seriate dimensions, the larger being 18x13x10 cm. Three types are identified:

- 1) dark grey fragments very rich in silica material
- 2) orange/light brownish colour fragments, usually very soft, easily broken and extremely porous. Mn oxides in the external layer and a large amount of worm tubes. Very rich in anhydrite (gypsum?) and/or amorphous silica. Some of these fragments are much denser and contain volcanic glass suggesting that basalt was the original rock
- 3) tabular dark brown / black pieces that correspond to the external crust of these hydrothermal slabs, rich in Fe and Mn oxides, very soft and easy to break.

## ANNEX II. LIST OF TTR-RELATED REPORTS

- Limonov, A.F., Woodside, J.M. and Ivanov, M.K. (eds.), 1992. Geological and geophysical investigations in the Mediterranean and Black Seas. Initial results of the "Training through Research" Cruise of R/V *Gelendzhik* in the Eastern Mediterranean and the Black Sea (June-July 1991). UNESCO Reports in Marine Science, 56, 208 pp.
- Limonov, A.F., Woodside, J.M. and Ivanov, M.K. (eds.), 1993. Geological and geophysical investigations of the deep-sea fans of the Western Mediterranean Sea. Preliminary report of the 2nd cruise of the R/V *Gelendzhik* in the Western Mediterranean Sea, June-July, 1992. UNESCO Reports in Marine Science, 62, 148 pp.
- "Training-Through-Research" Opportunities Through the UNESCO/TREDMAR Programme. Report of the first post-cruise meeting of TREDMAR students. Moscow State University, 22-30 January, 1993. MARINF, 91, UNESCO, 1993.
- Limonov, A.F., Woodside, J.M. and Ivanov, M.K. (eds.), 1994. Mud volcanism in the Mediterranean and Black Seas and Shallow Structure of the Eratosthenes Seamount. Initial results of the geological and geophysical investigations during the Third UNESCO-ESF "Training-through-Research" Cruise of R/V *Gelendzhik* (June-July 1993). UNESCO Reports in Marine Science, 64, 173 pp.
- Recent Marine Geological Research in the Mediterranean and Black Seas through the UNESCO/TREDMAR programme and its "Floating University" project, Free University, Amsterdam, 31 January-4 February 1994. Abstracts. MARINF, 94, UNESCO, 1994.
- Limonov, A.F., Kenyon, N.H., Ivanov, M.K. and Woodside J.M. (eds.), 1995. Deep sea depositional systems of the Western Mediterranean and mud volcanism on the Mediterranean Ridge. Initial results of geological and geophysical investigations during the Fourth UNESCO-ESF "Training through Research" Cruise of R/V *Gelendzhik* (June-July 1994). UNESCO Reports in Marine Science, 67, 171 pp.
- Deep-sea depositional systems and mud volcanism in the Mediterranean and Black Seas. 3rd post-cruise meeting, Cardiff, 30 January - 3 February 1995. Abstracts. MARINF, 99, UNESCO, 1995.
- Ivanov, M.K., Limonov, A.F. and Cronin, B.T. (eds.), 1996. Mud volcanism and fluid venting in the eastern part of the Mediterranean Ridge. Initial results of geological, geophysical and geochemical investigations during the 5th Training-through-Research Cruise of R/V *Professor Logachev* (July-September 1995). UNESCO Reports in Marine Science, 68, 127pp.
- Sedimentary basins of the Mediterranean and Black Seas. 4th Post-Cruise Meeting, Training-through-research Programme. Moscow and Zvenigorod, Russia, 29 January-3 February. Abstracts. MARINF, 100, UNESCO, 1996.
- Woodside, J.M., Ivanov, M.K. and Limonov, A.F. (eds.), 1997. Neotectonics and Fluid Flow through Seafloor Sediments in the Eastern Mediterranean and Black Seas. Preliminary results of geological and geophysical investigations during the ANAXIPROBE/TTR-6 cruise of R/V *Gelendzhik*, July-August 1996. Vols. 1, 2. IOC Technical Series, 48, UNESCO, 226 pp.
- Gas and Fluids in Marine Sediments: Gas Hydrates, Mud Volcanoes, Tectonics, Sedimentology and Geochemistry in Mediterranean and Black Seas. Fifth Post-cruise Meeting of the Training-through-research Programme and International Congress, Amsterdam, The Netherlands, 27-29 January 1997. IOC Workshop Reports, 129, UNESCO, 1997.
- Geosphere-biosphere coupling: Carbonate Mud Mounds and Cold Water Reefs. International Conference and Sixth Post-Cruise Meeting of the Training-through-Research Programme, Gent, Belgium, 7-11 February 1998. IOC Workshop Reports, 143, UNESCO, 1998.
- Kenyon, N.H., Ivanov, M.K. and Akhmetzhanov, A.M. (eds.), 1998. Cold water carbonate mounds and sediment transport on the Northeast Atlantic Margin. IOC Technical Series, 52, UNESCO, 178 pp.
- Kenyon, N.H., Ivanov, M.K. and Akhmetzhanov, A.M. (eds.), 1999. Geological Processes on the Northeast Atlantic Margin. IOC Technical Series, 54, UNESCO, 141 pp.
- Geological Processes on European Continental Margins. International Conference and Eighth Post-cruise Meeting of the Training-Through-Research Programme, University of Granada, Spain, 31 January - 3 February 2000. IOC Workshop Reports, 168, UNESCO, 2000.



Kenyon, N.H., Ivanov, M.K., Akhmetzhanov, A.M. and Akhmanov, G.G., (eds), 2000, Multidisciplinary study of geological processes on the Northeast Atlantic and Western Mediterranean margins. IOC Technical Series, 56, UNESCO, 119 pp.

Geological processes on deep-sea European margins. International Conference and Ninth Post-Cruise Meeting of the Training-through-Research Programme. Moscow/Mozhenka, Russia, 28 January - 3 February 2001. IOC Workshop Reports, 175. UNESCO, 2001, 76 pp.

Kenyon, N.H., Ivanov, M. K., Akhmetzhanov, A. and Akhmanov, G. G. (eds), 2001. Interdisciplinary Approaches to Geoscience on the North East Atlantic Margin and Mid-Atlantic Ridge. IOC Technical Series, 60, UNESCO, 134 pp.

Geosphere/Biosphere/Hydrosphere Coupling Processes, Fluid Escape Structures and Tectonics at Continental Margins and Ocean Ridges. International Conference and Tenth Post-Cruise Meeting of the Training-through-Research Programme. Aveiro, Portugal, 30 January - 2 February 2002. IOC Workshop Reports, 183. UNESCO, 2002, 50 pp.

Kenyon, N.H., Ivanov, M. K., Akhmetzhanov, A. and Akhmanov, G. G. (eds), 2002. Interdisciplinary studies of geological processes in the Mediterranean and Black Seas and North East Atlantic. IOC Technical Series, 62, UNESCO, 134 pp.

Geological and biological processes at deep-sea European margins and oceanic basins. International Conference and Eleventh Post-Cruise Meeting of the Training-through-Research Programme. Bologna, Italy, February 2-6, 2003. IOC Workshop Reports, 187. UNESCO, 2003, 32 pp.